Titre: Title:	A Multi-Sector Planning Support Model for en Route Air Traffic Control
Auteur: Author:	Mohamed Ossama Hassan
Date:	2017
Type:	Mémoire ou thèse / Dissertation or Thesis
Référence: Citation:	Hassan, M. O. (2017). A Multi-Sector Planning Support Model for en Route Air Traffic Control [Thèse de doctorat, École Polytechnique de Montréal]. PolyPublie. https://publications.polymtl.ca/2941/

UNIVERSITÉ DE MONTRÉAL

A MULTI-SECTOR PLANNING SUPPORT MODEL FOR EN ROUTE AIR TRAFFIC CONTROL

MOHAMED OSSAMA HASSAN
DÉPARTEMENT DE MATHÉMATIQUES ET DE GÉNIE INDUSTRIEL
ÉCOLE POLYTECHNIQUE DE MONTRÉAL

THÈSE PRÉSENTÉE EN VUE DE L'OBTENTION
DU DIPLÔME DE PHILOSOPHIÆ DOCTOR
(GÉNIE INDUSTRIEL)
DÉCEMBRE 2017

UNIVERSITÉ DE MONTRÉAL

ÉCOLE POLYTECHNIQUE DE MONTRÉAL

Cette thèse intitulée :

A MULTI-SECTOR PLANNING SUPPORT MODEL FOR EN ROUTE AIR TRAFFIC CONTROL

présentée par : HASSAN Mohamed Ossama
en vue de l'obtention du diplôme de : Philosophiæ Doctor
a été dûment acceptée par le jury d'examen constitué de :

M. SOUMIS François, Ph. D., président
M. SAUCIER Antoine, Ph. D., membre et directeur de recherche
Mme YACOUT Soumaya, D. Sc., membre et codirectrice de recherche
M. DESAULNIERS Guy, Ph. D., membre
M. DELAHAYE Daniel, Doctorat, membre externe

DEDICATION

To the memory of my grandmother Fawkia El Maraghy,
who taught me the true meaning of perseverance
and that there is no excuse for not learning ...

ACKNOWLEDGEMENTS

I wish to express my heartfelt gratitude and appreciation to my director Professor Antoine Saucier for his continuous guidance, thorough remarks and availability, which enabled me to complete and present this work. Throughout my Ph.D. program, he was an example for the professor I wish to be.

I also wish to thank my co-director Professor Soumaya Yacout for both her moral and scientific support. She always pushed me and encouraged me to do my best. She shared with me her knowledge and experience, her advices on both my work and my life were always of a great help. For her I will always be grateful.

I owe Professor François Soumis special thanks as he was the one who advised me to look into the topic of this work.

Many thanks also goes to my colleagues Wissem Maazoun and Ahmed Ragab for their help and advices that improved this work.

I also thank the Thales group, RAAS and Air Canada companies as well as the NSERC and CRIAQ funds who financially supported this project.

I would like to extend my thanks to the jury members Professor François Soumis, Professor Guy Desaulniers and Professor Daniel Delahaye to take the time to evaluate this work.

Last but not least, my sincere appreciation to my mother and my father who have been my role models throughout my life, there are no words who can describe my gratitude to them. My utmost gratitude to my beloved wife for her unconditional support, comprehension and patience throughout the years I took to finish this work.

RÉSUMÉ

Le concept de planification multisectorielle (PM) a été récemment introduit dans le contrôle du trafic aérien. Ce concept consiste à remplacer le contrôleur de planification par un planificateur multisectoriel (PrM). Le PrM est responsable des tâches de planification dans un ensemble de secteurs adjacents. L'objectif principal du PrM est de minimiser et d'équilibrer la charge de travail des contrôleurs entre les secteurs. Le PrM a besoin d'outils d'aide à la décision pour l'aider à accomplir ses tâches. L'objectif de cette thèse est de fournir au PrM un modèle d'aide à la décision qui minimise et équilibre la charge de travail des contrôleurs dans un ensemble de secteurs en route sur un horizon de temps moyen, soit 20 à 90 minutes. On propose une définition complète du problème de la résolution de la complexité, qui est une mesure de la charge de travail, dans le contexte de la PM. On représente la charge de travail des contrôleurs par le nombre de conflits. Pour obtenir des solutions optimales rapidement pour des problèmes impliquant de nombreux avions (par exemple 200), nous avons choisi d'utiliser un modèle de programmation linéaire mixte. Notre modèle minimise et équilibre le nombre des conflits de croisement et de rattrapage avec le nombre minimum de trajectoires modifiées. Nous présentons une formulation linéaire pour la détection et la résolution des conflits de croisement et de rattrapage. Notre formulation repose sur une transformation des distances de séparation en temps de séparation, et consiste à examiner ces temps en utilisant des contraintes linéaires. Nous avons aussi proposé une première méthode permettant d'équilibrer le nombre de conflits entre les secteurs.

Notre modèle permet l'utilisation de changements de vitesse, de cap et d'altitude. Nous avons formulé le modèle de telle sorte que toutes les combinaisons de ces trois manœuvres puissent être utilisées ou empêchées. Nous avons défini les trois manœuvres pour obtenir des changements minimes du temps de parcours des trajectoires modifiées. Notre modèle ne modifie pas les points d'arrivée et de sortie des avions dans les secteurs.

Pour un ensemble de problèmes étalons de détection-résolution de conflits, notre modèle a éliminé 100% des conflits dans des problèmes impliquant 25 avions et 300 conflits simultanés. Ces résultats ont été obtenus en moins d'une seconde de calculs. Pour un ensemble de problèmes de résolution de complexité générés aléatoirement et impliquant jusqu'à 200 avions, notre modèle a éliminé tous les conflits en modifiant moins de 30% des trajectoires. Le retard moyen par trajectoire modifiée était inférieur à 2,5% du temps de parcours.

Nous concluons que notre modèle est un outil efficace pour réduire le nombre de conflits dans un ensemble de secteurs adjacents tout en minimisant le nombre de trajectoires modifiées. Notre modèle permet de calculer des solutions avec le nombre minimum de conflits dans un

temps raisonnable (<10 minutes). Nous avons montré que l'ajout des changements de cap et d'altitude aux changements de vitesse permet de réduire significativement le nombre de conflits non résolus et le nombre de trajectoires modifiées. Nous avons aussi montré que notre méthode d'équilibrage des conflits entre les secteurs permet d'éviter de surcharger l'un des secteurs sans augmenter significativement le nombre total de conflits.

ABSTRACT

The concept of multi-sector planning (MSP) was recently introduced into air traffic control to accommodate the continuous growth of air traffic. This concept consists in replacing the planner controller by a multi-sector planner (MSPr). The MSPr is responsible for the planning tasks in a set of adjacent sectors. The primary aim of the MSPr is to minimize and balance the workload among sectors. The MSPr needs advisory tools and models to help him fulfil his tasks. The main objective of this thesis is to develop a MSP support model that minimizes and balances controllers workload in a set of adjacent en route sectors over a medium time horizon, i.e. 20 to 90 minutes.

We introduce a complete definition of the complexity resolution problem in a MSP context. The complexity is a measure for controllers workload. We choose to measure the controllers workload by the number of conflicts. Since the MSPr deals with many aircraft and requires relatively fast solutions, we formulate our model using a mixed integer linear program. Our model minimizes and balances the crossing and trailing conflicts with the minimum number of modified trajectories. We introduce a linear formulation for the detection and resolution of crossing and trailing conflicts. Our formulation relies on the transformation of safe separation distances into safe separation times and on the examination of the separation times between aircraft using linear constraints. We also propose a first method to take into account workload balancing in the complexity resolution problem.

Our model enables the use of speed, heading and altitude changes. We formulated the model so that any combination of these three manoeuvres can be used or prevented. We defined the three manoeuvres so that the model ensures minimal changes in the travel duration of the modified trajectories. Our model also ensures spatial trajectory recovery.

For a set of conflict detection and resolution benchmark problems, our model eliminates 100% of the conflicts in problems that involve up to 25 aircraft and 300 simultaneous conflicts. The solutions are obtained in less than one second. For a set of randomly generated complexity resolution problems, our model eliminates all the conflicts in problems that involve up to 200 aircraft by modifying less than 30% of the trajectories. The average delay per modified trajectory is less than 2.5% of the travel duration through the multi-sector area.

We conclude that our model is an efficient tool to decrease and balance the total number of conflicts in a set of adjacent sectors using the minimum number of modified trajectories. Our model is able to obtain solutions with the minimum number of conflicts in a reasonable amount of time (<10 minutes). In comparison with the use of only speed changes, the introduction of the heading and altitude changes can reduce significantly the number of

unresolved conflicts and the number of modified trajectories. We also found that our workload balancing method prevents overloading one of the sectors without a significant increase of the total number of conflicts.

TABLE OF CONTENTS

LIST OF TABLES

LIST OF FIGURES

LIST OF SYMBOLS AND ABBREVIATIONS

α the maximum percentage of aircraft trajectories that can be modified using speed changes.

β the maximum percentage of aircraft trajectories that can be modified using altitude changes.

γ the maximum allowed percentage of modified trajectories.

$\bar{\gamma}$ the minimum value of γ that resolves most conflicts.

λ the workload balancing multiplier $= \dfrac{\text{Maximum allowed workload per sector}}{\text{Average workload in all sectors}}$.

$\theta_{i,j}$ intersection angle between flight plans i and j.

$\bar{\theta}_{i,j}$ the angle between two consecutive common flight segments between flight plans i and j.

ϕ Turn angle of the heading change manoeuvres.

A the number of aircraft.

$\bar{\mathcal{A}}$ the number of trajectories.

A_p
- 1 if the aircraft following the first flight plan, i, of the p^{th} flight plan pair in E arrives at the intersection point before the aircraft following the second flight plan, j, and they are safely separated;
- 0 otherwise.

B_p
- 1 if the aircraft following the second flight plan, i, of the p^{th} flight plan pair in E arrives at the intersection point before the aircraft following the first flight plan, j, and they are safely separated;
- 0 otherwise.

C_p
- 1 if a conflict is predicted to happen between the p^{th} flight plan pair in E;
- 0 otherwise.

C_g^1
- 1 if the aircraft following the g^{th} plan pair in $\bar{E}$ lose separation at the beginning of the CFS,
- 0 otherwise.

C_g^2 $\begin{cases} 1 \text{ if the aircraft following the } g^{th} \text{ plan pair in } \bar{E} \text{ lose separation} \\ \quad \text{at the end of the CFS,} \\ 0 \text{ otherwise.} \end{cases}$

$\bar{C}_g$ $\begin{cases} 1 \text{ if a trailing conflict is predicted to happen for the } g^{th} \text{ plan pair} \\ \quad \text{in } \bar{E}, \\ 0 \text{ otherwise.} \end{cases}$

D Safe horizontal separation distance (=5NM).

$D_i(m)$ the distance between waypoints m and $m+1$ of flight plan i

d Separation distance between alternative flight plans, i.e. heading change manoeuvres.

$d_{i,j}(\theta_{i,j})$ The separation distance between the aircraft following flight plans i and j with and intersection angle equals $\theta_{i,j}$.

$d_i(w)$ the euclidean distance between the the w^{th} intersection point of the flight plan i and the previous waypoint.

$\bar{d}_1(g,\ell)$ the euclidean distance between waypoint m and the first point in the CFS,

$\bar{d}_2(g,\ell)$ the euclidean distance between waypoint m and the end point in the CFS.

E the set of all flight plan pairs that are at risk of a pairwise crossing conflict.

$\bar{E}$ the set of flight plan pairs at risk of a trailing conflict.

$H_p(k)$ $\begin{cases} 0 \text{ if both flight plans of the } p^{th} \text{ pair in } E \text{ use flight level } k \text{ at their} \\ \quad \text{intersection point;} \\ 1 \text{ otherwise.} \end{cases}$

$\bar{H}_g(k)$ $\begin{cases} 0 \text{ if both flight plans of the } g^{th} \text{ pair in } \bar{E} \text{ use flight level } k \text{ at the CFS;} \\ 1 \text{ otherwise.} \end{cases}$

$I_a(i)$ $\begin{cases} 1 \text{ if aircraft } a \text{ can use flight plan } i; \\ 0 \text{ otherwise.} \end{cases}$

I_p^s $\begin{cases} 1 \text{ if the intersection point of the } p^{th} \text{ flight plan pair in } E \text{ is located} \\ \quad \text{in sector } s\,; \\ 0 \text{ otherwise.} \end{cases}$

$\bar{I}_g^s$ $\begin{cases} 1 \text{ if the beginning of the CFS for the } g^{th} \text{ flight plan pair in } \bar{E} \text{ is} \\ \quad \text{located in sector } s\,; \\ 0 \text{ otherwise.} \end{cases}$

$\mathcal{I}_s(i)$ $\begin{cases} 1 \text{ if flight plan } i \text{ includes a speed change manoeuvre;} \\ 0 \text{ otherwise.} \end{cases}$

$\mathcal{I}_h(a)$ $\begin{cases} 1 \text{ if aircraft } a \text{ undergoes a heading change manoeuvre;} \\ 0 \text{ otherwise.} \end{cases}$

$\mathcal{I}_l(i)$ $\begin{cases} 1 \text{ if flight plan } i \text{ includes an altitude modification;} \\ 0 \text{ otherwise.} \end{cases}$

$\mathcal{I}(a)$ $\begin{cases} 1 \text{ if the trajectory of aircraft } a \text{ undergoes any modifications;} \\ 0 \text{ otherwise.} \end{cases}$

$i(p)$ the first flight plan of the p^{th} flight plan pair in E.

$\bar{i}(g)$ the first flight plan of the g^{th} flight plan pair in $\bar{E}$.

J the number of possible flight plans.

$j(p)$ the second flight plan of the p^{th} flight plan pair in E.

$\bar{j}(g)$ the second flight plan of the g^{th} flight plan pair in $\bar{E}$.

K the number of flight levels.

$L(i)$ the number of flight level changes in the original flight plan i.

$L_i(m,k)$ $\begin{cases} 1 \text{ if flight plan } i \text{ includes flying between waypoints } m \text{ and } m+1 \\ \quad \text{on flight level } k; \\ 0 \text{ otherwise.} \end{cases}$

$N(i)$ the number of waypoints in flight plan i.

$\mathcal{N}$ The total number of conflicts in a problem

$P(i)$ $\begin{cases} 1 \text{ if there is an aircraft using flight plan } i; \\ 0 \text{ otherwise.} \end{cases}$

R_g $\begin{cases} 1 \text{ if the aircraft following flight plan } \bar{i}(g) \text{ arrives to the CFS before} \\ \quad \text{the aircraft following flight plan } \bar{j}(g), \\ 0 \text{ otherwise.} \end{cases}$

$\dot{S}_{i,j}$ the minimum separation time at the intersection point between flight plans i and j at fixed speeds.

$S_{i,j}$ the minimum separation time at the intersection point between flight plans i and j

S_p the minimum separation time at the intersection point between the p^{th} flight plan pair in E

$\bar{S}_{i,j}$ the minimum separation time at the beginning and the end of the CFS between flight plans i and j

$\bar{S}_g$ the minimum separation time at the beginning and the end of the CFS between the g^{th} flight plan pair in $\bar{E}$

$T_i(m)$ the time taken by an aircraft following flight plan i to pass from waypoint m to waypoint $m+1$.

$t_i(m)$ the planned time at which an aircraft that uses flight plan i passes by its m^{th} waypoint

$t'_i(m)$ the actual time at which an aircraft that uses flight plan i passes by its m^{th} waypoint

$t_i^+(m)$ the maximum possible time at which an aircraft following flight plan i can reach its m^{th} waypoint.

$t_i^-(m)$ the minimum possible time at which an aircraft following flight plan i can reach its m^{th} waypoint.

$\bar{t}_1(g,\ell)$ the passage time at the first point of the CFS for the ℓ^{th} flight plan of the g^{th} flight plan pair in $\bar{E}$.

$\bar{t}_2(g,\ell)$ the passage time at the end point of the CFS for the ℓ^{th} flight plan of the g^{th} flight plan pair in $\bar{E}$.

$\bar{t}_1^-(g,\ell)$ the minimum passage time at the first point in the CFS for the ℓ^{th} flight plan of the g^{th} flight plan pair in $\bar{E}$.

$\bar{t}_1^+(g,\ell)$ the maximum passage time at the first point in the CFS for the ℓ^{th} flight plan of the g^{th} flight plan pair in $\bar{E}$.

$\bar{t}_2^-(g,\ell)$ the minimum passage time at the end point in the CFS for the ℓ^{th} flight plan of the g^{th} flight plan pair in $\bar{E}$.

$\bar{t}_2^+(g,\ell)$ the maximum passage time at the end point in the CFS for the ℓ^{th} flight plan of the g^{th} flight plan pair in $\bar{E}$.

$\hat{t}_i(w)$ the passage time of the w^{th} intersection point of the modified flight plan i.

$\hat{t}_i^+(w)$ the maximum possible time at which an aircraft following flight plan i can reach the w^{th} intersection point.

$\hat{t}_i^-(w)$ the minimum possible time at which an aircraft following flight plan i can reach the w^{th} intersection point.

$U_i(m,k)$ $\begin{cases} 0 \text{ if flight plan } i \text{ uses flight level } k \text{ at the waypoints } m \text{ and } m+1 \\ 1 \text{ otherwise.} \end{cases}$

$\bar{v}_a$ the cruising speed for aircraft a

v_a^+	the maximum allowed speed for aircraft a
v_a^-	the minimum allowed speed for aircraft a
$X_i(m)$	the X coordinate of the m^{th} waypoint in flight plan i.
$Y_i(m)$	the Y coordinate of the m^{th} waypoint in flight plan i.
$Z_i(m)$	the flight level index at the m^{th} waypoint in flight plan i.
$W(i)$	the number of intersection point in flight plan i.

ATC :	Air Traffic Control
ATCO :	Air Traffic Control Officer
ATM :	Air Traffic Management
CFS :	Common Flight Segment
CDR :	Conflict Detection and Resolution
FMS :	Flight Management System
ICAO :	International Civil Aviation Organization
IDEF0 :	Integrated definition of function modelling
MILP :	Mixed Integer Linear Program
MINLP :	Mixed Integer Non Linear Program
MSA :	Multi-Sector Area
MSP :	Multi-Sector Planning
MSPr :	Multi-Sector Planner
MSP-H/C :	Multi-sector planning support model using heading changes for crossing conflicts
MSP-S/C :	Multi-Sector Planning support model using Speed changes for crossing conflicts
MSP-SH/C :	Multi-Sector Planning support model using Speed and Heading changes for Crossing conflicts
MSP-A/CT :	Multi-Sector Planning support model using Altitude changes for Crossing and Trailing conflicts
MSP-H/CT :	Multi-Sector Planning support model using Heading changes for Crossing and Trailing conflicts
MSP-S/CT :	Multi-Sector Planning support model using Speed and changes for Crossing and Trailing conflicts
MSP-SH/CT :	Multi-Sector Planning support model using Speed and Heading changes for Crossing and Trailing conflicts
MSP-SHA/CT :	Multi-Sector Planning support model using Speed, Heading and Altitude changes for Crossing and Trailing conflicts
NextGen :	The next generation air transportation system
NM :	Nautical Mile, 1 NM $\approx$ 1.852 Km
PHARE :	Program for Harmonized ATM Research in EUROCONTROL
PC :	Planner Controller
SESAR :	Single European Sky ATM Research project
TC :	Tactical Controller
TFM :	Traffic Flow Management

LIST OF APPENDICES

CHAPTER 1 INTRODUCTION

Since the beginning of the commercial use of planes, the growth of air traffic always results into the evolution of Air Traffic Control (ATC). Due to the current growth rate, such an evolution is imperative. One of the recently developed concepts introduced to the ATC to answer this need is the Multi-Sector Planning (MSP). It relies on expanding the role of the planner controller to be responsible of a set of adjacent sectors instead of only one. The application of this concept is attributed to the advancement in the flight management and communication systems. The MSP entails the need for tools and models to help the Multi-Sector Planner (MSPr) fulfilling his new tasks efficiently.
A brief review of the air traffic control system, the multi-sector planning concept, the motivation of the presented work, the objectives, the approach followed and an overview of the dissertation will be presented in the following sections.

1.1 Air traffic control

The airspace and the runways can be seen as limited resources that have to be shared between the aircraft. Each aircraft uses these resources to optimize several factors such as fuel consumption, punctuality and passenger comfort. Air Traffic Management (ATM) is the process, procedure and resources that are used to coordinate the aircraft to enable safe and efficient aircraft operations, both in air and on ground. According to the European organization for the safety of air navigation (EUROCONTROL), the ATM system is composed of three subsystems (EUROCONTROL, 2012) :

- Airspace management that is responsible for the design of the airspace (sectors and routes).
- Traffic Flow Management (TFM) that is responsible for ensuring that the planned aircraft trajectories do not lead to exceeding the airspace or the airports capacities.
- ATC that is responsible for monitoring the aircraft in real time and ensure that they maintain safe separation distances between each other.

In the current ATM system, the airspace can be seen as a set of flight levels and routes forming a network designed to simplify the control of air traffic. The flight levels are horizontal plans separated by 1000 ft, where each flight level is characterized by a constant atmospheric pressure using a sea level pressure datum of 29.92 inches of mercury. This design ensures that two aircraft flying at different levels can never be in conflict.
The safe separation distances between aircraft are specified by the International Civil Aviation

Organization (ICAO). The horizontal separation distance en route is normally 5 NM and the vertical separation distance is 1000 ft for altitudes lower than 29,000 ft and 2000 ft for altitudes higher than 29,000 ft (Prandini et al., 2000). ICAO changed these norms by applying the reduced vertical separation minima rule that is now implemented in almost all countries. The reduced vertical separation minima rule reduces the vertical separation distance to 1000 ft for the altitudes between 29,000 ft and 41,000 ft and requires the equipment of aircraft using these altitudes with a certified altimeter (ICAO, 2002).

Two or more aircraft are considered in conflict when their separation distances are below these norms. There are three types of possible conflicts between flights : crossing, trailing and head-to-head conflicts, Figure 1.1. The design of the airspace and flight trajectories prevents the occurrence of head-to-head conflicts. The semicircular rule is applied worldwide : a single flight direction (eastbound or westbound) is assigned to each flight level. The flight direction assignment is done alternatively. For example, for flight levels below 29,000 ft (FL290), the eastbound flights are assigned to odd flight levels (FL270, FL250,..) whereas the westbound flights are assigned to even flight levels (FL280, FL260,...),Figure 1.2.

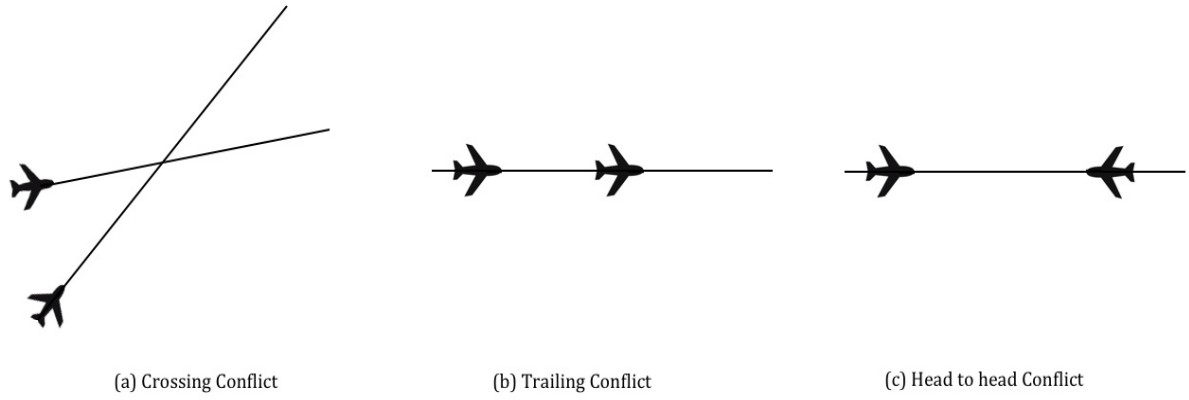

Figure 1.1 Conflict types

It is the task of the ATC to predict the occurrence of conflicts over a short time horizon (10-15 min) and to devise a solution to ensure the separation of aircraft (Whiteley, 1999a). A solution consists in giving instructions (clearances) to one or more of the aircraft in conflict to undergo a change in the trajectory. Clearances can indicate changes of speed, heading and/or altitude.

Nowadays, the controlled airspace is divided into space volumes called sectors. Each sector has a distinct radio frequency for communication with aircraft. A terminal sector is a sector that includes an airport. Otherwise, it is called an en route sector. A team of 2-3 Air Traffic

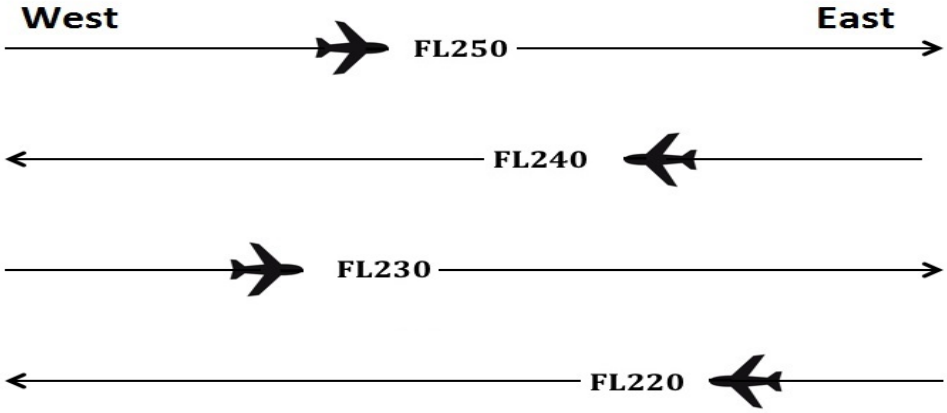

Figure 1.2 The semicircular rule

Control Officer (ATCO) is responsible for the ATC tasks in a sector. These tasks can be classified in two main tasks (Conversy et al., 2011) :

1. Receiving/handing off the aircraft from/to adjacent sectors (hello, goodbye, negotiating exit conditions and change of radio frequency)
2. Ensuring the separation of the aircraft. That includes detecting the conflicts and solving them :
   — Detecting possible conflicts within the sector.
   — Finding a feasible solution to the detected conflicts.
   — Transmitting the instructions to the pilots.
   — Ensuring that the pilots follow the instructions.

According to EUROCONTROL (2014), the number of aircraft that a team of ATCO can handle depends on several factors such as the location of the sector, the complexity of the traffic flows and the day. Each sector has a capacity expressed in the current ATM system by the number of aircraft entering the sector per hour. Most commonly in Europe, this capacity is between 40 and 60 entries per hour.
The latest reports from EUROCONTROL in 2013 (EUROCONTROL, 2013a,b) lowered the predicted annual growth rate of air traffic in medium and long terms to (0.7-2.6%) from the previous 2010 predicted growth rate of (1.6-3.9%) (EUROCONTROL, 2010, 2011). Even with these lower predicted rates, the air traffic is anticipated to undergo an increase of 20-80% in the next 20 years. This growth of air traffic in the already congested air space shows the need of increasing the efficiency of the ATM system and air space capacity while ensuring the safety of flights and minimizing delays. In the current ATM system, the increase in air traffic is handled by grouping or splitting the sectors to keep the controllers workload within

a reasonable range. However, this method is attaining its limit. The sectors are becoming so small that aircraft pass by them in a few minutes. This indicates that by further decreasing sectors size, the hand off and communication task would be more frequent and would form a burden on the controllers (Whiteley, 1999a; Conversy et al., 2011). As a result, the Single European Sky ATM Research project (SESAR) in Europe and the Next Generation air transportation system (NextGen) project in the USA were launched to address the challenges inherited from the predicted air traffic increase.

Many attempts were made to reduce the amount of work required from the controllers. These were motivated by the fact that the ATCO workload is one of the main factors limiting the capacity of the sectors, subsequently limiting the capacity of the airspace (Whiteley, 1999a; Rey et al., 2012; Prandini et al., 2011, 2010a; Herr et al., 2005). These attempts include introducing new communication systems, advancements in the Flight Management System (FMS), introducing new tools for the controllers, automating the ATC tasks and presenting new ATC operational structure (e.g. Multi-sector planning). In the next sections some of these attempts are briefly presented along with a detailed review on the introduction of the multi-sector planning concept.

1.1.1 Digital communication

Nowadays, most of the communication and the exchange of information between pilots and controllers are done using voice radio communication. This is done on high, very high and ultra high frequencies. Whenever a pilot enters a new sector, he is given a radio frequency to perform his communication (Nolan, 2010). This system suffers from several drawbacks (Zingale et al.; Omer, 2013) :

- The amount of exchanged information is limited and needs to be concise.
- The controller can receive information from only one pilot at a time.
- The exchange of information requires time, which limits the number of the aircraft that a controller can handle.

A support communication system to overcome the disadvantages of the voice system is based on exchanging the information on digital form through a data link system (Zingale et al.; Omer, 2013; Yun-sheng et al., 2016; ICAO, 2013). A data link system would allow the pilot and the controllers to exchange detailed information such as the local weather condition, the status of the aircraft and the latest weather prediction. Data link is supposed to reduce the amount of time taken by the controller in communication and reduce the voice channel congestion (ICAO, 2013). It is an essential tool in the future of ATM.

1.1.2 Flight management system

The FMS is a computerized system for aircraft navigation, flight planning and en route guidance. It is installed on a large number of aircraft. The FMS takes as input the flight plan, the current position of the aircraft and gathers information from aircraft systems such as the engine and the fuel systems and the surveillance system. Using this information, the FMS determines the optimal trajectory for the aircraft according to a cost function. This cost function is based on the fuel consumption and flight time related costs. The FMS updates its information during the flight and serves as an en route guidance system that delivers instructions to the pilot (or the autopilot) to follow the flight plan (Walter, 2000; Gawinowski et al., 2007).

The FMS can help to improve the efficiency of the ATM system in many ways. It gathers detailed information about the aircraft and the flight status. Coupled with a data link system, the FMS will allow to quickly exchange this information with ground control. The FMS serves as a guidance system for the autopilot en route. This implies that aircraft trajectories obtained by following the autopilot are not subject to human decisions and consequently are more predictable. In other words, the FMS should improve the predictability of aircraft positions in the future, which is a key enabler to improve the ATM system (Omer, 2013; Gawinowski et al., 2007).

Mueller and Sandy (2007) found that the FMS coupled with a data link system is able to correct periodically the lateral deviation from the planned trajectory. They also found using simulation that an integration of the current FMS version along with a data link system is able to ensure the following of required time of arrival at waypoints and allows the implementation of the trajectory based operations. In addition, new versions of the FMS do not only provide tracking of the flight plan in 3D (space), but they can also ensure the following of a 4D flight plan (space and time) (Walter, 2000; Wichman et al., 2001). This means ensuring that aircraft follow their flight plans precisely both in space and time. Such a system will also improve the predictability of the aircraft position over a long time horizon.

1.1.3 New air traffic control tools

One of the projects proposed by EUROCONRTOL was the Multi Actor Man Machine Interface (MAMMI) that aimed at introducing a new layout and new tools for the control center (Vales et al., 2007). The proposed control center (Conversy et al., 2011; Vales et al., 2007) was designed to increase the collaboration between the controllers in the same team, subsequently redistributing the workload and increasing the ability of the team to handle a greater number of aircraft.

1.1.4 Automatic air traffic control

While ATC tasks are still being performed manually by controllers monitoring a radar screen, devising solutions and communicating instructions to pilots (Cafieri and Durand, 2014), the automation of the ATC is considered as a requirement for improving the ATM system (SESAR, 2007). So, much research work proposed new methods and tools for automatic Conflict Detection and Resolution (CDR). These methods and tools are aimed to be included in the ATC system to reduce controller workload (Kuchar and Yang, 2000a; Omer and Farges, 2012). This direction of research is motivated by the fact that while the number of aircraft per sector (traffic density) is a significant factor for ATCO workload, it is not the only one. Other important factors include the number and the complexity of the conflicts. Varying these factors can have a high impact on the number of tasks required from the controllers.
The En Route Air traffic Soft Management Ultimate System (ERASMUS), part of the SESAR project (Gawinowski et al., 2007; Drogoul et al., 2009), proposed a framework to solve conflicts over a time horizon of 30 minutes based only on minor speed adjustments. The results of ERASMUS encouraged other researchers (Rey et al., 2012, 2015; Vela et al., 2009; Chaloulos et al., 2010) to investigate the potential of using only speed regulations for CDR and to decrease the number of conflicts over a long time horizon. The CDR problem and a set of different models proposed to solve it are discussed in details in the next chapter.

1.1.5 Multi-sector planning

The standard ATC team structure includes two controllers for each sector. One is the Planner Controller (PC) and the other one is the tactical controller (TC), also called the executive controller. The main tasks of the PC are :

- Conflict detection over a medium time horizon. This includes observing the aircraft that are intended to enter the sector and predict if any of these aircraft will be involved in a conflict in the sector.
- Planning out the aircraft trajectories. This comprises determining the entry and exit conditions of the aircraft to prevent predicted conflicts from occurring, if possible.
- Co-ordination with adjacent sectors and centers. This incorporates the negotiation of the entry and exit conditions with adjacent sectors as they may have contradicting conditions.

The main tasks of the TC are :

- Supervision of the traffic within the sector. This includes monitoring the progress of the aircraft in the sector to ensure that each aircraft does not deviate from its flight plan and that it leaves the sector at the planned time and position.

— Conflict detection over a short time horizon (15 min) by predicting the loss of safe separation between the aircraft within the sector.
— Conflict resolution. This incorporates the planning of a solution for the predicted conflicts, transmitting the clearances to the pilots through radio communication and verifying it is followed.
— Updating the flight plan of the aircraft whether it has deviated due to controller intervention or by accident.
— Handover of the aircraft to adjacent sectors.

The standard operational structure (one PC - one TC per sector) is not the best structure to handle the predicted increase in air traffic. The continuous process of redesigning the sectors and the subsequent change in resources allocation requires an operational structure that is more flexible (Vales et al., 2007; Whiteley, 1999a; SESAR, 2013a). This signifies the need of new ATC concepts and team structures to answer to the new challenges in the future ATM system. These challenges include the need for increasing the airspace capacity and providing a new solution to handling the expected increase in demand other than the redesigning of the sectors.

As an answer to this need, the Program for Harmonized ATM Research in EUROCONTROL (PHARE) was the first to introduce the concept of MSP (Whiteley, 1999a; Latron et al., 1997). PHARE is a European research program, launched in 1989 and completed in 1999, to investigate the future of ATM concepts. The general idea of MSP is to add a new controller position called the MSPr, who is responsible for the planning of aircraft trajectories in a set of adjacent sectors (Multi-sector area) over a medium time horizon. The aim of the MSPr is to reduce and balance the workload of the sectors controllers in a Multi-Sector Area (MSA) (Figure 1.3) in order to increase the global capacity (Ehrmanntraut and McMillan, 2007; Prevot et al., 2010a). The application of the MSP concept shall decrease the uncertainties in controllers decisions which are regarded as the main source of error in the prediction of aircraft trajectories (Swierstra and Green, 2003; Herr et al., 2005).

The original concept presented in PHARE (Whiteley, 1999a; Latron et al., 1997) suggested the introduction of the MSPr to the ATC operational structure in addition to the original positions of the planner and tactical controllers. The tasks of the PC and TC shall remain the same as in the standard structure. In the new structure proposed by PHARE, the MSPr shall be responsible for detecting complex situations in a set of adjacent sectors over a medium time horizon (10-40 min). He shall be also responsible for finding solutions to avoid the occurrence of these complex situations. The aim of introducing the MSPr was to reduce the complexity of situations encountered by the sector controllers in order to reduce the required planning tasks.

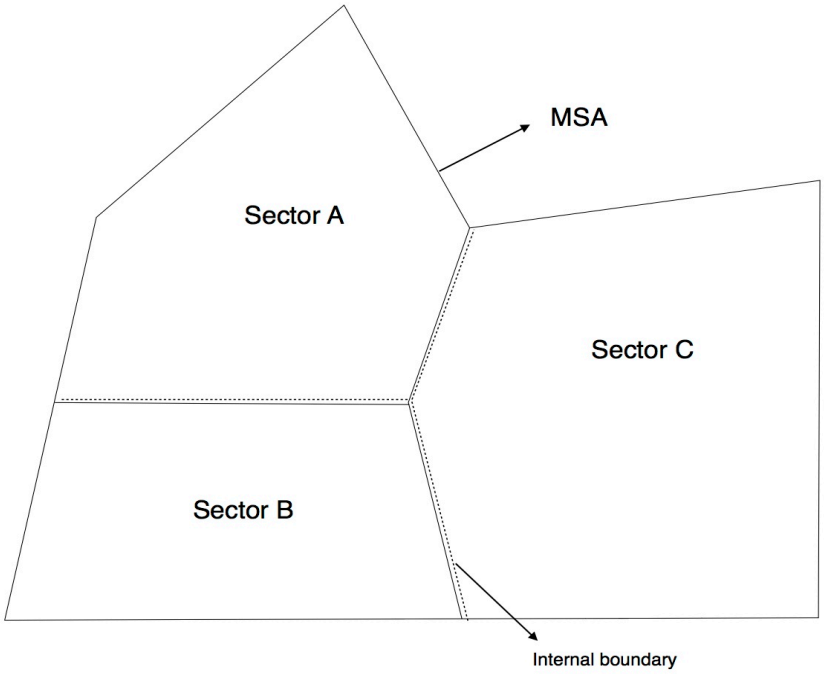

Figure 1.3 Example of a multi-sector area

To test this concept, a new complexity measure was developed in PHARE to quantify the expected workload in a sector. In addition, different tools such as the tactical load smoother software (a tool to calculate the predicted complexity over a medium time horizon) were developed as part of PHARE to help the MSPr perform his tasks. The application of the concept was tested via simulation by controllers using different scenarios (Whiteley, 1999a; Latron et al., 1997) and proved the feasibility of the concept. During the simulations, it was found that the controllers tend to use tactical load smoother to check if their solutions to conflicts would decrease the complexity of the situation in medium term. It was also found that the MSPr can decrease MSA complexity without the need to solve any conflict through his interventions at the MSA level. For example, in one case the MSPr imposed several route changes from the beginning to spread horizontally a flow of traffic and by this he reduced the MSA complexity.

One of the conclusions in PHARE was the need for validation of the multi-sector planning concept and the need for the definition of the working procedure of the ATC under this concept. It suggested that further studies have to be done to define precisely the tasks of the controllers in a multi-sector planning structure.

As part of the Gate-to-Gate project, launched by EUROCONTROL to validate the new ATM concepts, the MSP concept was tested and validated (Herr et al., 2005; EUROCONTROL, 2006). Herr et al. (2005) suggested three operational configurations for the ATC under the

multi-sector planning concept. One of these configurations was tested and validated using real time simulations. This configuration (MSP configuration) implies that the MSPr performs, with the aid of different tools, the tasks of the PC in several adjacent sectors and that the tasks of TC remain the same as in the standard configuration. Table 2.1 shows a comparison between the standard and the MSP configuration from the tasks assignment point of view.

Table 1.1 Tasks assignment in the traditional and multi-sector planning configurations

	Conflict detection (Medium term)	Planning out the trajectories (Entry/exit conditions)	Supervision of the aircraft (within the sector)	Conflict detection (Short term)	Conflict resolution	Updating flight plan	Coordination tasks	Handover the flights
Standard Configuration	PC	PC	TC	TC	TC	TC	PC	TC
MSP Configuration	Software	MSPr	TC	TC	TC	TC	MSPr	TC

The MSP configuration was incorporated in the SESAR project (SESAR, 2013a). The configuration was introduced and tested for a MSA of two sectors and it was labeled as 1P-2T configuration (one PC for two TC). The MSPr was responsible for the planning tasks in two adjacent sectors. In SESAR, the MSPr main goal is to avoid conflicts by determining conflict free trajectories to decrease the workload of the tactical controllers. The 1P-2T configuration was validated using simulations and the findings of this study pointed out that the configuration is applicable, provides better flexibility in managing the controllers and leads to comfortable level of workload for the controllers. The 1P-2T configuration was considered in SESAR as the first step for the application of the multi-sector planning concept (1P-nT) that will be later investigated.

The multi-sector planning concept was also introduced in NextGen. It was presented as a new controllers operational structure (Willems et al., 2005; Corker et al., 2006; Williams et al., 2007; Celio, 2007). This new structure comprises a controller for each sector and a strategic controller responsible for a set of adjacent sectors. The role of the strategic controller is slightly different than that of the MSP as introduced in SESAR. In addition to generating solutions based on a global view of the assigned sectors, the strategic controller is to help sector controllers in their tasks whenever the sector workload increases. Celio (2007) stated that the controllers in NextGen will respond to conflicts by checking a set of automatically generated

solutions and deciding which one to apply instead of generating the solutions themselves. Also, it was said that due to the improvement in the accuracy of predicting the position of aircraft and the use of automatic prediction of conflicts, the controllers in many cases would solve conflicts that are predicted to happen in adjacent sectors. This means that the resolution of the conflicts will be done and the correcting clearances will be issued in a sector prior to the one where the conflict is predicted to occur.

In the context of NextGen project, different operational structures for the MSP were investigated (Willems et al., 2005; Corker et al., 2006; Smith et al., 2010) mainly to study the difference between incorporating the MSPr as a coordinator in addition to traditional operational structure and replacing the PC of multiple sectors. The work of Willems et al. (2005) and Corker et al. (2006) showed the feasibility of the MSP concept. Williams et al. (2007) also demonstrated that the application of the MSP concept improves the utilization of controllers. A series of human-in-the-loop simulations were conducted in (Smith et al., 2010; Prevot et al., 2010a) to evaluate the feasibility and determine the best operational structure for the MSP concept in the United States national airspace. In these simulations, real controllers took the roles of MSPr and sector controllers for a simulated MSA. The results demonstrated the ability of the MSPr to reduce the workload of the controllers, sector complexity and number of conflicts with all the tested operational structures.

As the magnitude of the planning tasks required from the MSPr exceeds that of the PC, the necessity for tools and models to help the MSPr fulfill his tasks increases. Prevot et al. (2010b) presented the results of an extensive study, using human-in-the-loop simulations, for the assessment of a set of tools designed to help the MSPr. One of these tools allows the MSPr to test and filter the traffic to help him focus on a specific criterion (e.g. flight level or time domain). Another tool predicts the number of aircraft per sector and the sector complexity by predicting flights trajectories. One of the important tested tools tests the solutions proposed by the MSPr before its application. The results showed the importance of such tools for the application of the MSP concept.

A model or a tool to generate solutions that decrease and balance the workload in a MSA is essential for the application of the MSP concept. As a part of the continuous work of EUROCONTROL on the multi-sector planning concept, Flener et al. (2007a,b) presented a constraint programming method for complexity resolution in a multi-sector planning ATC environment. This method aims at modifying flights trajectories to reduce the predicted complexity measure over a medium time horizon (20-90 min) for a set of adjacent sectors. The method also aims at balancing complexities between sectors. Recently, Hong et al. (2016) presented a two level hierarchical architecture for the resolution of conflicts in a designated sector in a multi-sector planning framework. In a first step, a mixed integer linear program

(MILP) is used to minimize the complexity in the neighbour sectors. Aircraft trajectories are modified using speed or heading changes. The complexity is measured by the magnitude of the deviation from the original flight plans. In a second step, another MILP is used to solve conflicts in the designated sector while using the solutions generated in the first step as entry/exit conditions on the flights that pass through the sectors. Both the models of Flener et al. (2007a,b) and Hong et al. (2016) will be discussed in details in the next chapter. While the importance of such models for the MSPr seems to be essential, to our knowledge the work of Flener et al. (2007a,b) and Hong et al. (2016) remain the only reported literature in this research area.

1.2 Motivation

The SESAR and NextGen projects that represent the future of the ATM systems in Europe and in the United States of America promote a new ATC system. This system promotes the control of aircraft and the resolution of conflicts based on medium time horizon prediction to reduce the controllers' workload. The availability of such an ATC system is attributed to the advancement in communication and flight support systems that have increased the precision of aircraft position prediction.

Both SESAR and NextGen adopted the multi-sector planning concept. The concept introduces a new controller position (MSPr). The MSPr will be responsible for the planning tasks in a set of adjacent sectors (MSA) taking into account the traffic situation in each sector within the MSA. The main objective of the MSPr is to balance and reduce the workload of the sector controllers. One of the main benefits of applying the MSP is the responsive management of the traffic by redistributing the workload at sector level.

The multi-sector planning concept brought out the need for tools to help the MSPr to fulfil his tasks. Such tools must be able to :

- Evaluate the workload of the controllers and indicate the complex areas in the MSA.
- Predict the position of the aircraft and predict the possible conflicts over a medium time horizon.
- Propose a set of solutions that solve the conflicts, minimize and balance the workload of the sectors controllers.

The work proposed here addresses this need. It aims at presenting a support tool for the MSPr that evaluates the workload of the controllers, predicts and solves conflicts over a medium time horizon and provides a set of optimal solutions while taking into consideration the difference between the MSP and the traditional CDR problem. Such a tool requires the definition of the complexity resolution problem in a multi-sector planning framework and its

solution in an appropriate time frame.

1.3 Objectives

The objectives of this work can be summarized as follows :

— Define precisely the complexity resolution problem in a multi-sector planning framework. The problem definition shall include the detection of both crossing and trailing conflicts. It shall also incorporate the ability of the MSPr to modify an aircraft trajectory using all types of manoeuvres (speed, heading and altitude changes).

— Develop an approach to modify aircraft trajectories (with minimal changes) to reduce and balance the predicted complexities of a set of adjacent sectors (MSA) over a medium time horizon (20 – 90 minutes). This approach shall be able to provide a set of different solutions to the complexity resolution problem in a reasonable amount of time while balancing the workload amongst the sectors.

— Validate and test the feasibility and efficiency of our approach.

— Test and compare the effect of multiple manoeuvres combinations on different air traffic scenarios to suggest the best combination for each scenario.

1.4 Research approach

Due to the complexity of that problem and in order to achieve the research objectives, we broke down the project into the following steps :

1. Present a precise definition of the complexity resolution problem in a MSP framework, including the choice of the complexity measure that will be used in this work.
2. Formulate a model to solve the complexity resolution problem as defined in the first step using only speed and heading manoeuvres. This model shall be able to predict aircraft position and handle only crossing conflicts.
3. Validate and test the model using randomly generated problems. Test the effect of the workload balancing and different manoeuvres combinations on the generated solutions.
4. Modify the model to include the detection and solution of trailing conflicts.
5. Test the effect of trailing conflicts on the model efficiency and the tested manoeuvres combinations using different air traffic scenarios.
6. Reformulate the model to include altitude change manoeuvres.
7. Test the new possible manoeuvres combinations on different air traffic scenarios.

1.5 Thesis outline

The thesis is presented in six chapters. Chapter 2 presents a review of the related literature highlighting the research gaps in the complexity resolution problem under the MSP context. This chapter includes also a review on the complexity measures and the conflict detection and resolution problem. Chapter 3 covers the first three research steps. It introduces the definition of complexity resolution problem under the MSP concept and presents the formulation of the mathematical model to address the problem using only speed and heading manoeuvres. Several randomly generated problems are used to evaluate the benefits of the developed model and to test different manoeuvres combinations. Chapter 4 covers the next two research steps. It presents a detailed description of the modification of the MSP support model to handle trailing conflicts in addition to crossing conflicts. Randomly generated problems are used to assess the efficiency of the model including the count of the trailing conflicts. Different air traffic scenarios are also used to test the different combinations of manoeuvres. Chapter 5 covers the last two research steps. It presents the full model including all three types of manoeuvres and the tests used to assess its efficiency. Finally, the summary and main conclusions are presented in Chapter 6.

CHAPTER 2 LITERATURE REVIEW

Multi-sector planning is a new ATC concept that aims at reducing and balancing controllers workload in a set of adjacent sectors. This objective is achieved through the introduction of a new ATC position called multi-sector planner (MSPr). Tools and models to help the MSPr fulfill his tasks are essential to the application of the MSP. These tools must be able to analyze air traffic situations and devise solutions that reduce and balance the controllers workload.

The complexity resolution problem targets the modification of flights trajectories to reduce a measure that represents controllers workload over a predetermined time period for a set of sectors. Solving this problem while trying to balance the complexity measure, which represents controllers workload, is fundamental to the MSP support tools.

In this chapter, we present a detailed review of the approaches used to solve the complexity resolution problem in a MSP context. We also introduce a brief review on the complexity measure formulation with the aim of identifying an appropriate measure. Finally, we present a review on the conflict detection and resolution problem to determine an approach to solve the complexity resolution problem in a MSP framework.

2.1 Complexity resolution problem

The MSP was first introduced as part of the PHARE project (Whiteley, 1999a; Latron et al., 1997) to increase airspace capacity. In PHARE, the term complexity resolution was defined as the task of determining the complex areas in a MSA and finding a solution that resolves these problematic areas by solving the predicted conflicts (Latron et al., 1997). Several ATC support tools were introduced in PHARE to help the controllers including the MSPr.

One of these tools is the tactical load smoother (TLS). It is intended to help the MSPr by predicting the complexity in a MSA over a 40 min time horizon. The complexity measure used in the TLS depends on the number of aircraft in the sector, position of each aircraft, number and type of conflicts and the number of trajectory changes. The TLS uses these factors along with the uncertainty in aircraft position and the conflict probability to calculate a global complexity measure. The TLS presents a map of the MSA that highlights the problematic zones with high complexity measure. It displays this map along with the number of aircraft and the number of conflicts per sector. This information is supposed to be used by the MSPr to devise a solution using other support tools.

PHARE also presented a set of tools to help the MSPr to devise solutions for different air

traffic situations. These tools include a conflict detection tool called conflict probe (Kremer et al., 1999). It aims at comparing flight plans and trajectories with each other to detect possible conflicts while taking into account restricted flight zones. Another tool, problem solver, was presented in PHARE to help solving the conflicts (Whiteley, 1999b). This tool does not propose any solutions to solve the conflicts but gives the controller a geometric view of the conflict and enables him to modify the trajectories graphically and test his solutions.
The tools developed in PHARE were tested using human-in-loop simulations where controllers took the roles of MSPr and sector controllers in a simulated air traffic situation. The tools were found to be helpful from the controllers point of view. The MSPr controllers used the TLS to identify the zones with high workload (complexity measure). Then they reduced its complexity using classic deconfliction manoeuvres (i.e. speed, heading and altitude manoeuvres) for the conflicts. Having a global view of the MSA, the MSPr were also able to avoid high complexity zones by spreading the flow horizontally. Note that in the latter case, the MSPr did not target the resolution of conflicts. A traditional planner controller would not be able to devise such a solution. The controllers used the suggested support tools to test their solutions and ensure their efficiency (Whiteley, 1999a; Kremer et al., 1999; Whiteley, 1999b).
The work of Flener et al. (2007a,b,c) as part of the ongoing work of EUROCONTROL on the MSP concept targeted the complexity resolution problem. The main objective of this work was to develop a model that minimizes and balances the complexities in a set of adjacent upper airspace sectors.
Flener et al. defined the complexity of a sector s at a given moment m as

$$C(s,m) = N_{sec}(s,m) + N_{nsb}(s,m) + N_{cd}(s,m) \tag{2.1}$$

where $N_{sec}(s,m)$ is the number of aircraft in sector s at moment m, $N_{nsb}(s,m)$ is the number of aircraft near the borders of sector s (< 2 min flight) at moment m and $N_{cd}(s,m)$ is the number of climbing and descending aircraft in sector s at moment m.
This measure takes the same form of the one introduced in PHARE (Whiteley, 1999a). Flener et al. decided not to include a term related to aircraft equipments due to the lack of data. They also decided to exclude the number of flight pairs in potential conflicts arguing that it was not strongly correlated to another complexity measure developed by EUROCONTROL as part of the complexity and capacity project (Hilburn, 2004; Flynn et al., 2003).
Such a measure gives an instantaneous read on air traffic complexity and is subject to sudden rises and falls. As a result, Flener et al. redefined the sector complexity as the average of the

instantaneous complexity at the beginning, middle and end of a 7 minutes time period using

$$\mathcal{C}(s,m) = \frac{\sum_{i=0}^{2} C(s, m+3.5i)}{3}. \tag{2.2}$$

Flener et al. (2007a) stated that the average time to pass a European upper airspace sector is 8 minutes. So choosing a sampling interval that is $\approx 44\%$ of the average time to pass a sector can neglect important information regarding the air traffic situation. For example, an Airbus A320 has a nominal climb rate of ≈ 1200 feet per minute (over FL300), hence it can climb two flight levels (2000 feet) in less than two minutes. Such a climb can be neglected if it occurs between two sampling points. This means that a solution that minimizes (2.2) can include high unaccounted complexities between sampling points.

Flener et al. (2007a,c) defined the complexity resolution problem as follows. Given a MSA S and the flight plans of the aircraft planned to pass through S during a given time period of 20 to 90 minutes, find a modification of the flight trajectories such that a minimum of $f\%$ of these flights pass through S during this time period and such that the sum of sectors complexities as measured in (2.2) is minimized.

The minimum percentage $f\%$ was introduced to prevent the resolution algorithm from rerouting all the flights outside the MSA. Imposing such a constraint is necessary if the solutions can involve large changes in the aircraft trajectories. Such changes, if applicable, are costly and raise the problem of equity among the flights. While the value of f has a major impact on the output solution, Flener et al. did not present an approach to properly determine its value nor did they present results using different values other than 90%.

To solve the complexity resolution problem, Flener et al. proposed three types of modifications for aircraft trajectories. The first type is a change of take off time. This type allows the modification of aircraft take off time by multiples of 5 minutes. Although this change can represent a powerful tool, there is no guarantee that the imposed solution will comply with airports or other MSA capacities. As the change of take off time remains always within the authority of the central flow management unit and beyond the responsibility of the MSPr (Whiteley, 1999a; Barnier and Allignol, 2012), there is no guarantee that the solution will be applicable.

The second type of modification suggested by Flener et al. (2007a,b,c) was changing the time at which the aircraft enters the MSA. This change was constrained to be in the range of -2 to +1 minutes per 20 minutes of flight time. This modification is implemented by changing the aircraft speed within two sectors around the MSA. Such a change requires the MSPr to negotiate new entry conditions with neighbouring sectors to validate it. There are no guarantees on the feasibility of the implied changes.

The third and last type of modification is flight level change. Flener et al. (2007a,b,c) suggested that the flight level change per minute does not exceed 30 flight levels down or 10 flight levels up if it is a jet and does not exceed 10 flight level up or down if it is a turbo-prop. They also stated that one of their main assumptions is that a flight level change has to be small. As the difference between flight levels is 1000 ft, a change of $+10^4$ ft (+10 flight levels) is not a small change. Also a climb rate $+10^4$ ft/min is not even feasible for most aircraft type. So we think that the authors meant -3000/+1000 and -1000/+1000 ft/min, which represents small and feasible change.

Flener et al. (2007a,c) formulated the problem using constraint programming. The model objective was to minimize

$$z = \sum_{s \in S} \sum_{i \in I} \mathcal{C}(s, i), \tag{2.3}$$

where S is a set of the sectors in the MSA, I is a set of all the sampling moments indices and $\mathcal{C}(s, i)$ is the complexity measure defined by (2.2).

In the model of Flener et al. (2007a,c) constraints were used to enforce the changes limits and to calculate the sector complexities. Although the authors stated in the problem definition that the complexities shall be ideally better balanced, there was no constraint to enforce balancing. To solve the constraint program, Flener et al. used a non linear model. The model was then tested on flight profiles that were planned to pass through five adjacent en route upper airspace sectors during a 15 hours time period. The results showed the model ability to decrease the sectors complexity by $\sim 50\%$. Although the authors stated that the model was able to balance complexities, no proof or results about complexity balancing were presented.

Recently, Hong et al. (2016) proposed an approach for conflict detection and resolution in a MSP context. This approach aims at detecting and solving conflicts in a sector using either speed or heading changes while minimizing complexities in adjacent sectors. The complexity resolution problem in Hong et al. (2016) can be seen as follows. Given a designated sector $\bar{s}$, a set of adjacent sectors S and the flight plans of the flights planned to pass through S and $\bar{s}$, find the entry/exit conditions of each flight passing through $\bar{s}$ such that it is conflict free and such that the complexities in S are minimized. Hong et al. defined the complexity in a sector $s \in S$ as the sum of the magnitude of the manoeuvres required to solve any conflict in s caused by a flight exiting $\bar{s}$ and entering s.

Hong et al. assumed that the time required to change the speed or the heading of an aircraft is negligible, either speed or heading changes are instantaneous and that aircraft follows straight lines at constant speed between waypoints. They also assumed that all aircraft have the same speed.

The approach of Hong et al. consists in a two level hierarchical architecture to solve the

problem under the previous assumptions. It solves the problem for each single aircraft moving between two sectors. So for an aircraft moving from sector A to sector B, the first level involves the solution of a CDR problem, either by speed or heading changes, for sector B at each possible entry situation for the aircraft (Figure 2.1).

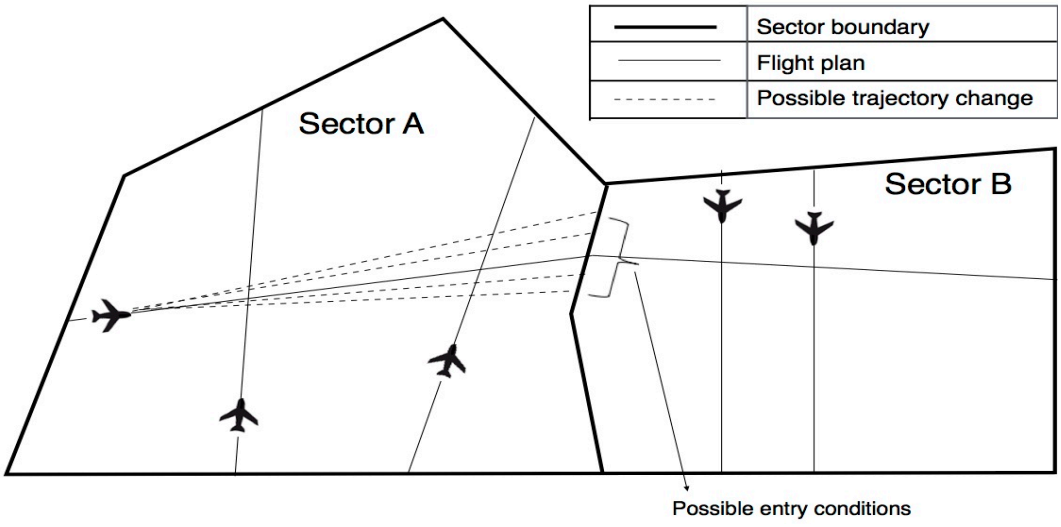

Figure 2.1 Example of a CDR problem in two sectors using heading changes

More precisely, the solution of the first level gives the possible heading angles θ and speeds v that lead to no additional conflicts in sector B. In other words, the solution determines all possible exit conditions for sector A that will not lead to a workload increase in sector B.
On the second level of this proposed architecture, the CDR problem is solved for the originating sector A, while taking as a constraint the set of exit/entry conditions that resulted from the first level solution. The application of the CDR problem on this level consists in searching for the exit condition that solves conflicts in sector A among a set of exit conditions that do not lead to conflicts in sector B.
Hong et al. (2016) used the two MILP models developed by Pallottino et al. (2002) to solve CDR problems. The first model solves the CDR problem using only speed changes and the other solves it using only heading changes. Both models will be discussed in details in section 2.3. Hong et al. tested their approach on a set of 50 randomly generated problems. To prove the merits of their approach, they solved the problems first using only the CDR model without considering neighbour sector. Second, they solved the problem using their proposed approach. Comparing the two results, the number of aircraft involved in a conflict avoidance manoeuvre was decreased by 17-55 % using speed change model and by 33-81% using the heading change model. Also the complexity measure decreased by 15-50% using the speed change model and by 15-82% using the heading change model.

The MILP model for CDR using only speed changes adopted by Hong et al. (2016) suffers from two major problems. The first one is the null denominator problem reported by Pallottino et al. (2002), where a null denominator appears in conflict detection constraints when

$$v_i \cos(\theta_i) = v_j \cos(\theta_j), \tag{2.4}$$

where v_i, v_j are respectively the optimal speeds of aircraft i and j, and θ_i, θ_j are respectively the angles between the x-axis and the direction of aircraft i and j. A solution to this problem was suggested by Pallottino et al. (2002) and was applied by Alonso-Ayuso et al. (2011). Hong et al. (2016) did not solve this problem and instead they assumed in their model that $v_i \cos(\theta_i) \neq v_j \cos(\theta_j)$. For their test problems they set all aircraft velocities to the same value and avoided using heading angles (θ_i, θ_j) that satisfy (2.4).

The second major problem in the MILP developed by Pallottino et al. (2002) and used by Hong et al. (2016) was reported by Alonso-Ayuso et al. (2011). This problem relies on the geometrical construction of the conflict detection constraints. It leads to false conflict detection in situations where two aircraft are flying away from each other and are not at risk of losing separation. This problem leads to unnecessary speed changes to satisfy the separation constraints.

The two level hierarchical architecture proposed by Hong et al. (2016) depends on the CDR algorithm and can lead to an explosion in the computation time in the case of multiple aircraft leaving the sector. This problem is attributed to the fact that this approach requires solving the CDR model multiple times, i.e. once for each possible entry/exit condition. In the example involving only one leaving aircraft solved by Hong et al. (2016), the speed only MILP and the heading change only MILP were solved respectively 172 and 83 times. For example, if two flights leave the sector towards the same adjacent sector, the number of different possible entry/exit conditions is $172^2 \simeq 3 \times 10^4$. If the computation time of the MILP is one second, then it follows that the solution of the complete problem will take more than eight hours.

Hong et al. (2016) considered the problem of solving conflicts in a sector while minimizing the complexities in adjacent sectors. In their approach, they assumed that there always exists an entry/exit condition that does not lead to any conflict in the adjacent sectors. In other words, they assumed that the complexity in the adjacent sectors can always be zero. They argued that in the case of an infeasible problem, for which no entry condition will solve the conflict, they must choose the solution that leads to the minimum complexity measure in the adjacent sector. They did not propose a model for such a case, nor did they state a possible modification to the MILP model used in the second level. Moreover, they did not present a method for dealing with multiple adjacent sectors. Their work neglected the fact that all flights in the originating sector will finally reach an adjacent sector and can be involved in

conflicts in it. A solution that minimizes the complexity of an adjacent sector can increase the complexity of another one.

2.2 Complexity measures

The research in complexity measures aims at identifying measures to quantify the complexity of air situations. Such measures are to be used as an indicator of the controller workload and to identify a complex situation before its occurrence. This line of research is motivated by the fact that the number of aircraft in a sector is not an adequate measure of difficulty of the air traffic situation (Delahaye and Puechmorel, 2000; Masalonis et al., 2003). The benefit of using an appropriate complexity measure is the ability to predict situations that exceed the controllers ability to detect and solve conflicts.

Laudeman et al. (1998) introduced the dynamic density metric as a measure of air traffic complexity. The proposed measure is the weighted sum of air traffic density, number of aircraft with headings change, number of aircraft with speed changes, number of aircraft with altitude changes, number of aircraft in conflict, and number of predicted conflicts in short, medium and long term. They compared the dynamic density with traffic density and found that the dynamic density is more strongly correlated to the controllers workload than the traffic density. They used multiple regression analysis to determine the values of the weights. The analysis results showed the insignificance of four terms : the number of aircraft changing altitude, the number of aircraft changing speed, the number of aircraft with the closest distance to another aircraft is less than 5 NM and the number of aircraft in conflict in a short term (<25 NM). Nevertheless, the authors did not exclude these factors, as further tests were required in different traffic situations.

Delahaye and Puechmorel (2000) presented two different approaches to quantify the complexity of an air traffic situation. Their first approach makes use of the relative distances and speeds between aircraft. The authors defined three metrics upon which the airspace complexity depends : density (that depends on the relative distances between aircraft), divergence/convergence (a measure of how fast two aircraft move away from/towards each other) and sensitivity (a measure of the rate of variation of the relative distances or conflict durations between the aircraft with respect to a change in trajectory). The second approach is a dynamical approach in which the history of aircraft trajectories is considered and the complexity of the system is defined as the topological entropy. The dynamical approach defines the complexity measure based on the complexity of the geometry of the traffic depending on the interactions of the traffic flows and not the actual conflicts. The authors did not present a way to interpret the values of their measures nor did they present any experiments or

comparison to justify the importance of these metrics.

Lee et al. (2007) proposed a new approach, called input-output approach, to evaluate the complexity of any space region. This approach implied the application of a CDR algorithm. In a given airspace, an additional aircraft is introduced with given location and has to fly in a straight line using a constant speed. At every possible location and at every possible speed value, the CDR algorithm is applied to eliminate conflicts. The difference between the original trajectories and the corrected trajectories after CDR is used to define a complexity measure. The complexity is measured as the sum of the maneuvers (heading angles and speeds) required to solve the conflicts resulting from the introduced aircraft. A broad range of possible locations and velocities of the additional aircraft must be considered. This approach resulted in a complexity map that highlights the positions from which an entering aircraft can lead to complex situations. The major shortcoming of this method is that it depends on the CDR algorithm used, as a result the complexity of the same air traffic situations varies with the use of different CDR algorithms. It is also predicted to be time consuming.

A complexity measure that takes into account the uncertainty of the prediction of aircraft positions was proposed by Prandini et al. (2010a,b). They defined the air traffic complexity at a point X in a three dimensional space as the probability that a region surrounding X is occupied by a given number of aircraft (threshold) within a time period. The aircraft position was calculated using a modified version of the two dimensional model presented by Prandini et al. (2000). The uncertainty in the position of an aircraft was modeled as a 3D Brownian motion added to the nominal position. To measure the complexity of a space region, the authors proposed to calculate two complexity measures, C1 and C2, at every point in this region. C1 is the probability that at least one aircraft occupies a given region. C2 is the probability that this region is occupied by at least two aircraft. The regions with high C2 correspond to possible congested areas. They also presented a single complexity measure that incorporates both C1 and C2. This measure represents the minimum separation distance between the aircraft at a given probability.

Prevot and Lee (2011) introduced a trajectory-based complexity measure designed to be implemented in NextGen. The general idea of this measure is to determine an ideal condition (weather condition, number of conflicts, number of headings change etc.) for which the air traffic density is a representative measure of the ATCO workload. Upon the determination of the ideal condition parameters, one searches for adjusting factors to correct the deviation from the ideal parameters. These factors are used to adjust the air traffic density to account for the changes. The main advantage of such a measure is that it can be calculated in real time and that it can be easily interpreted by controllers. Later Lee and Prevot (2012) conducted a human in loop simulation experiment proving the merits of using this metric

instead of the aircraft count in situations including a mix of aircraft equipped with Data link and other using traditional radio frequency. Although the proposed measure was better than traditional aircraft count, it was found that the adjusting factors need to be tuned to reflect adequately controllers workload.

From this brief review, it can be clearly seen that a comprehensive measure that incorporates several terms can be more representative of the controllers workload than traffic density. However, such comprehensive measures require controllers surveys and simulations to properly set the weights and parameters of each term. Such a study is beyond the scope and the objectives of this work that does not target the development of an accurate complexity measure. Also, comprehensive measures are not easily interpreted by the controllers (Prevot and Lee, 2011) and may increase the difficulty of analysing and explaining the results of our work.

On the other hand, traffic density is a simple measure that is already being used by the controllers. Yet, it does not reflect directly the predicted conflicts which can limit its use as a complexity measure in a MSP context. First, one of the main tasks of the MSPr as defined in SESAR (2013a,b) is trying to avoid conflicts through the planning of flight trajectories in a MSA. Second, using traffic density as the objective function to be minimized may lead to solutions with a good distribution of aircraft among sectors but at the same time it could generate complex unsolvable conflicts. So, we think that using a complexity measure that is directly related to air traffic conflicts is essential for a MSPr support model to address the objectives of the MSP.

We think that the number of predicted conflicts in a sector is an appropriate complexity measure regarding the scope and objectives of this work. This choice is motivated by several reasons. First, the number of predicted conflicts in a sector gives an insight on the predicted air traffic complexity. Second, it is a simple objective measure that can be used to identify the complex regions within a sector. Also, while it is not the most accurate measure of controllers workload, it can be easily interpreted by controllers. Finally, for most of the comprehensive complexity measures, the term related to conflicts is the most difficult one to calculate due to the non linearity of the equations used to detect conflicts. So a model that uses the number of conflicts as a complexity measure can be easily modified to take into account other factors.

2.3 Conflict detection and resolution

Developing automation tools to detect air conflicts and solve them is a topic that has been extensively studied recently. These studies aim at introducing automation to ATC to reduce controllers' workload and help them to handle the expected increase in air traffic. An automated CDR method should detect automatically conflicts and present a solution or a set of

solutions for the predicted air traffic situation. A comprehensive review on CDR models can be found in Kuchar and Yang (2000b). The literature concerning CDR can be classified into two main categories :

— CDR methods in a deterministic environment where the prediction of aircraft position is assumed to be exact (Rey et al., 2012; Omer and Farges, 2012; Pallottino et al., 2002; Constans et al., 2006; Omer and Farges, 2013; Omer, 2015; Lehouillier et al., 2017a).

— CDR methods that take into account the uncertainty in the prediction of aircraft position, usually attributed to the effect of the uncertainty on wind speed (Prandini et al., 2000; Irvine, 2002, 2003; Al Basman and Hu, 2012; Lehouillier et al., 2017b).

As in this thesis we decided to use the number of conflicts as the complexity measure, we need an appropriate CDR approach. Such an approach must be able to detect and generate solutions for conflicts. Solutions include the use of speed, heading and altitude changes. Also, it must be able to find these solutions within a reasonable amount of time for a large number of aircraft.

On the one hand, the most realistic CDR models use an optimal control approach (Omer, 2015). The work of Bicchi and Pallottino (2000), Hu et al. (2002) and Raghunathan et al. (2004) are good examples of such models. On the other hand, such models do not provide fast solutions and analytical solutions were provided only for small problem instances. Since computation time is a very important factor for the application of a CDR method, many researchers tackled the problem using a Mixed Integer Linear Program (MILP) model.

Pallottino et al. (2002) presented two MILP for CDR at a single flight level. The first model uses only speed changes and the other one uses only heading changes manoeuvres. The objective of these models was to solve all predicted conflicts while minimizing the sum of manoeuvres magnitudes. The authors formulated the conflict detection constraints as linear constraints using the geometry of conflict situations. They regarded each aircraft as a moving disk with a diameter equal to the safety distance. Then, they used the non-intersection conditions of moving disks as the conflict detection constraints. It was formulated in the speed changes model as

$$\begin{aligned} &\tfrac{v_i \sin(\theta_i) - v_j \sin(\theta_j)}{v_i \cos(\theta_i) - v_j \cos(\theta_j)} \geq \tan(l_{ij}), \\ &\text{or} \\ &\tfrac{v_i \sin(\theta_i) - v_j \sin(\theta_j)}{v_i \cos(\theta_i) - v_j \cos(\theta_j)} \leq \tan(r_{ij}), \end{aligned} \tag{2.5}$$

where v_i, v_j are respectively the optimal speeds of aircraft i and j, and $\theta_i, \theta_j, l_{ij}$ and r_{ij} are the conflict geometry angles as shown in Figure 2.2.

The decision variable in the speed model is the aircraft speed (v_i), hence the conflict constraints

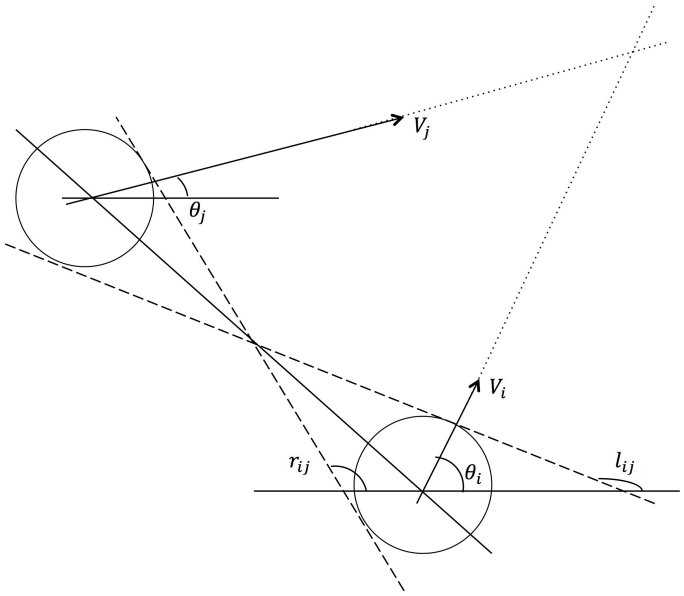

Figure 2.2 Geometrical construction of conflict constraints for two aircraft

as written in (2.5) are not linear. Pallottino et al. linearized (2.5) by multiplying it by the denominator, thus creating two different cases. One when

$$v_i \cos(\theta_i) - v_j \cos(\theta_j) < 0$$

and another one when

$$v_i \cos(\theta_i) - v_j \cos(\theta_j) > 0.$$

In case of a null denominator, the authors suggested rotating the axis to avoid it. The rotation of the axis for every possible case where $v_i \cos(\theta_i) = v_j \cos(\theta_j)$ is not straightforward. Alonso-Ayuso et al. (2011) tried to reformulate the model to include the axis rotation but were able to apply it only to special cases.

Alonso-Ayuso et al. (2011) also reported that the speed change model of Pallottino et al. (2002) falsely detect conflicts between aircraft pairs which are not at risk of conflicts. This false detection happens when two aircraft are flying away from each other as in Figure 2.3. In this case, such a pair will undergo a speed change according to (2.5), while in fact this pair will never lose safe separation distance.

Pallottino et al. (2002) solved a randomized problem set following both models using CPLEX and were able to reach optimal solutions for problems incorporating up to 17 aircraft in less than 16 seconds.

Richards and How (2002) developed a MILP to solve the CDR in 2D. The considered model

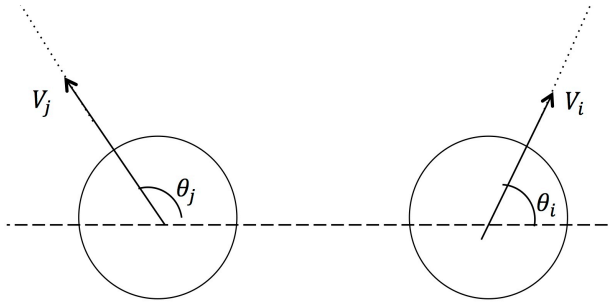

Figure 2.3 False detection example

assumes that the aircraft must cover a set of waypoints in any order in 2D, using constant speed between waypoints, and with a limit on the turning angle. Each aircraft position is checked at a predefined time step to ensure separation. The model tries to minimize the sum of the flight time. They solved three problems involving 1-3 aircraft using CPLEX. The results showed that the model tends to force the aircraft to follow its maximum speed except at turns where the limits on the acting forces limit the allowed velocity. The main contribution of Richards and How (2002) is the linearisation of the constraints that enforce speed limits and forces acting on the aircraft.

Vela et al. (2010) proposed a MILP for CDR using speed and heading changes. The authors modified the speed changes model presented by Pallottino et al. (2002) to minimize fuel consumption and the deviation from planned trajectories. Vela et al. assumed that the planned trajectory for each aircraft is the direct line between the initial position and the destination with a constant given speed. The model seeks the generation of conflict free trajectories by assigning to each aircraft a new heading and speed. As the model does not include a method for an aircraft to return to its planned destination, the model penalizes the deviation from the destination position. The authors also assumed that heading or speed changes are instantaneous. They argued that the time needed to apply a change in speed or heading is insignificant compared to the time to conflict.

The main contribution of Vela et al. (2010) was the derivation of a linear cost function for fuel consumption. It was based on the BADA performance model. The authors tested their model on a set of randomly generated problems. The results showed that CPLEX was able to reach solutions 0.01-0.05% away from the optimal solution within a few seconds for scenarios involving 15 aircraft.

Vela et al. (2009) presented another MILP for CDR using speed changes and flight level assignment. The model assumes that each aircraft follows a set of waypoints with direct routes between them. In this model, the authors described a potential conflict as the intersection of the trajectories of two aircraft where they are predicted to lose the safe separation distance.

Assuming that aircraft fly in straight lines near intersection points as shown in Figure 2.4, the authors used

$$\hat{S}_{ij} = \frac{D}{v_i v_j |\sin(\theta_{ij})|} \sqrt{v_i^2 + v_j^2 - 2v_i v_j \cos(\theta_{i,j})}, \tag{2.6}$$

to calculate the minimum separation time between two aircraft to ensure safe separation distance, where v_i, v_j are the speeds of aircraft i and j respectively, $\theta_{i,j}$ is the angle between aircraft trajectories and D is the minimum separation distance between two aircraft (usually 5 NM). This formulation was first introduced by Carlier et al. (2002) in a disjunctive scheduling approach to determine the order by which aircraft shall maneuver to solve a conflict. The main advantage of this formulation is that it transforms the conflict detection problem to the time domain, where separation is ensured by only respecting the minimum separation time at the intersection points.

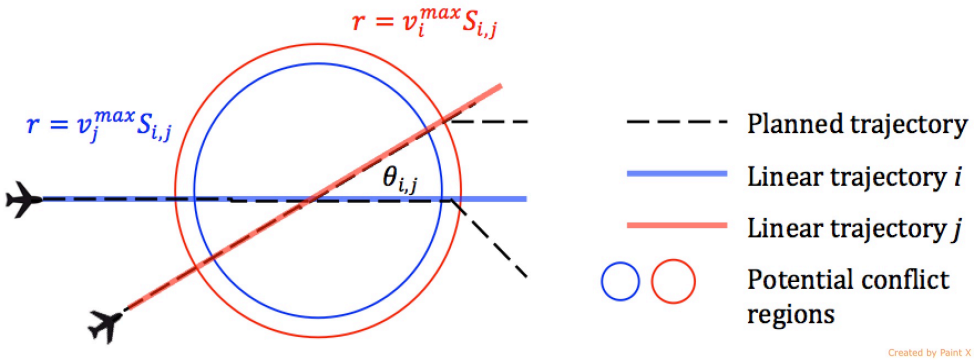

Figure 2.4 Intersection point of two flight plans

An upper bound on the minimum separation time is calculated using the limits on aircraft speeds as

$$S_{ij} = \max\{\hat{S}_{ij} : v_i \in [v_i^{min}, v_i^{max}], v_j \in [v_j^{min}, v_j^{max}]\}.$$

The objective of Vela et al. model was to minimize fuel consumption while ensuring aircraft separation. The model allows to change the arrival time of an aircraft to the controlled airspace, the travelling time between waypoints and also changing the flight level (at most once) at the entry of the controlled airspace. As (2.6) is not defined in the case of a trailing conflict ($\theta_{i,j} = 0$), Vela et al. defined two sets of aircraft pairs. The first one I^x that includes

all aircraft pairs that are at risk of a crossing conflict and are subject to

$$\left.\begin{array}{l} T_{i,m} + S_{ij} \leq T_{j,n} \\ \text{or} \\ T_{j,n} + S_{ij} \leq T_{i,m} \end{array}\right\} \qquad (i,j) \in I^x, \tag{2.7}$$

to ensure safe separation, where m and n are the indices of the waypoints at which flight i and j intersect, $T_{i,m}$ is the time at which aircraft i pass by waypoint m and $S_{i,j}$ is the minimum separation time between flights i and j. The constraint (2.7) ensures that the difference between the passage times of a flight plan pair in I^x at the intersection point between their trajectories is bigger than S_{ij}. The other set I^T includes all aircraft pairs that follow exactly the same spatial trajectory. These pairs are at risk of a trailing conflict. They are subject to

$$\left.\begin{array}{l} T_{i,m} - \dfrac{D_s}{D_{i,m}} t_{im} \geq T_{j,n} \\ \text{or} \\ T_{j,n} - \dfrac{D_s}{D_{j,n}} t_{jn} \geq T_{i,m} \end{array}\right\} \qquad (i,j) \in I^T, \tag{2.8}$$

where D_s is the minimum separation distance, $D_{i,m}$ is the distance between waypoints $m-1$ and m in the flight plan of aircraft i, and t_{im} is the travel duration between waypoints $m-1$ and m. The constraint (2.8) ensures that the difference between the passage times of a flight plan pair in I^T at each waypoint is larger than the time needed for the trailing aircraft to fly a distance equal to D_s.

Vela et al. tested their model using a set of scenarios that models realistic air traffic situations in an en route sector in the United States of America national airspace system. The set of scenarios included simulated high-density air traffic flow (60-300 aircraft/hour per flight level). The model was solved using CPLEX with a solution time limit of 10 minutes. It was able to provide conflict free trajectories for all aircraft even in high density scenarios, for which flight level assignment was used.

A possible drawback in the formulation of Vela et al. (2009) lies in the definition of I^x and I^T. First, the set I^x was defined to include all aircraft pairs that can possibly reach the intersection point between their trajectories at the same time. This means that if a pair of aircraft can arrive at the intersection point with a time difference less than S_{ij} but can not arrive at the same time, then it will not be included in I^x. It can be clearly seen that such a pair is in fact at risk of losing safe separation. Second, I^T was defined in a way that a pair of aircraft $(i,j) \in I^T$ if and only if both aircraft follow exactly the same set of waypoints (all trajectory). However, two aircraft can only share some waypoints (part of the trajectory) and

be at risk of having a trailing conflict. This means that this formulation can lead to solutions that contain undetected crossing and trailing conflicts.

Rey et al. (2012) introduced a MILP to solve CDR problems using only speed regulations. Their model detects and solves both crossing and trailing conflicts while minimizing the sum of conflict durations. The authors argued that the conflict duration is proportional to its severity. They used a formulation for the crossing conflict detection similar to that of Vela et al. (2009) to detect crossing conflicts. The model was tested using problems for which flights speeds have a $\pm 5\%$ uncertainty. They applied a sliding time horizon approach where the problem is solved at fixed time intervals. At each interval, the locations of the aircraft are updated using uncertain speeds. The conflicts predicted to happen in the current time interval are given more weight in the objective function. The test problems included simulated air traffic trajectories over the European airspace during one day. Rey et al. used two different speed changes limits as used in the project ERASMUS (Drogoul et al., 2009). The first limit of -6% to $+3\%$ of the cruise speed represents small speed changes. The second is of -12% to $+6\%$ of the cruise speed and represents large speed changes. The model was able to reduce the duration of conflicts by 60-80%. The results showed the robustness of the solutions to a 6% error in the speed prediction. The results also showed that the small speed change interval gives solutions closely similar ($1 - 3\%$ difference) to that with the large speed limits. Recently, Rey et al. (2015) modified the model they presented in (Rey et al., 2012) to minimize the number of conflicts. They tested and compared both models using randomly generated problems including up to 30 aircraft. Both models were able to minimize the duration and number of conflicts significantly in a small computation time. They proved the efficiency of both models with uncertain speed predictions using the same approach used in (Rey et al., 2012). It is worth mentioning that as both models do not have a constraint on the number of modifications, the resulting trajectories showed unnecessary speed modifications : they obtained trajectories with more than five enforced speed changes and one trajectory with 13 changes.

Cobano et al. (2012) presented a two step heuristic to solve the CDR problem using only speed changes. The model depends on a discretization of space into cubic cells and each trajectory is defined by the cells they pass through. A conflict is detected if two aircraft pass by cells that violate the minimum separation distance at the same time. The first step consists in detecting conflict zones in space and then generating all possible aircraft arrivals order to the conflict zones. The generation of possible orders continues until a feasible order that eliminates all conflicts is reached. The second step consists in solving a quadratic program model that minimizes the sum of the magnitudes of speed changes following the aircraft arrival order found in the first step. The heuristic was able to reach a feasible solution for

problems involving up to 10 aircraft in a reasonable amount of time (<350 s). The solution of the suggested heuristic was validated using simulation. The main contribution of Cobano et al. (2012) is to consider non linear trajectories with multiple speed changes.

Cafieri and Durand (2014) proposed a Mixed Integer Non Linear Program (MINLP) to solve CDR problems using only speed changes. They presented two different formulations. The first one involves changing aircraft speeds at time 0 and maintain the modified speeds on the whole trajectory. The second formulation allows the change of aircraft speed to occur within a given time interval. The duration of this time interval is minimized along with the magnitude of speed changes. Both formulations were modeled as MINLP and were used to solve a set of randomly generated problems using an exact MINLP solver. The solver was able to reach optimal solutions for small problems (up to five aircraft) in a reasonable amount of time. It took the solver more than 14 hours to reach the optimal solution of a problem involving six aircraft. Cafieri and Durand suggested the use of a decomposition heuristic to solve problems with more than four aircraft. While the suggested heuristic was able to solve the six aircraft problem in less than two minutes, its performance was inconsistent. For a problem involving seven aircraft and four conflicts, it took 40 minutes to reach a feasible solution. Another problem involving seven aircraft and six conflicts was solved in 14 seconds. The authors did not provide any explanation for this inconsistency.

Alonso-Ayuso et al. (2011) presented a MILP to solve CDR problems using speed and altitude changes. This model is a modified version of the speed changes model introduced by Pallottino et al. (2002). In their model, Alons-Ayuso et al. were able to solve the false detection problem and also suggested a solution for the null denominator problem that appears in the model of Pallottino et al. (2002). They also added to their model the altitude changes, detection and solution of trailing and head-to-head conflicts. In the case of trailing or head-to-head conflicts, the aircraft are separated vertically through the assignment of different flight levels for each aircraft. As the model does not include a method to return to the original trajectory, Alonso-Ayuso et al. penalized the changes from the original flight plans. They used CPLEX to solve randomly generated problems with 20 to 50 aircraft and 5 to 10 flight levels. CPLEX was able to reach optimal solutions in less than 3 seconds.

In order to solve the null denominator problem, Alonso-Ayuso et al. suggested turning the axis by π for each aircraft pair where the difference between the abscissa is less than the safe distance. While such a solution solves the problem for a number of cases, it does not cover all possible situations for which a null denominator can appear. A null denominator appears when $v_i \cos(\theta_i) = v_j \cos(\theta_j)$ regardless of the difference between the abscissa of the aircraft positions. They extended this model in (Alonso-Ayuso et al., 2014) to consider the conflicts that can occur at the intermediate flight levels for an aircraft changing its altitude by more

than one level. Alonso-Ayuso et al. (2014) also considered solving the conflicts that involve aircraft near the border of the sector but not within its perimeter. Such a solution requires the coordination of the controllers with adjacent sectors. CPLEX was able to reach optimal solutions in less than five seconds for problems involving up to 50 aircraft and 10 flight levels. Alonso-Ayuso et al. (2012) presented another modified version of the speed changes MILP of Pallottino et al. (2002). The modified model targets the solution of the CDR problem using only speed changes but without the assumption of instantaneous speed changes found in (Pallottino et al., 2002). The new model also deals with piecewise linear trajectories compared to linear trajectories in (Pallottino et al., 2002). Alonso-Ayuso et al. used a discretized time domain in their formulation. They assumed that if a new modified speed is to be used during a time period, then an aircraft has to reach the new speed using a constant acceleration during the previous period. The modified model is a MINLP because of the constraints dealing with acceleration. The model minimizes the sum of the absolute value of the acceleration changes. To solve the model in a reasonable amount of time, Alonso-Ayuso et al. proposed a sequential mixed integer linear heuristic for which the non linear terms of the constraints are linearised using Taylor polynomials. The linearised model is solved iteratively. At each iteration, an approximated linear model is solved using fixed parameter values (speed, acceleration and position). These values are updated at each iteration. The values change depending on the sum of the absolute value of the error in aircraft travelled distance. The iterations stop when the error in aircraft travelled distance reaches below a given threshold. The suggested heuristic was able to reach feasible solutions for problems up to 30 aircraft in approximately one minute.

Alonso-Ayuso et al. (2015) presented a MINLP to solve the CDR problem using speed, heading and altitude changes. The model is based on the geometrical construction of the conflict constraints presented in (Pallottino et al., 2002). The main contributions in (Alonso-Ayuso et al., 2015) are the consideration of the three types of changes simultaneously and the solution of relatively large problem instances. They proposed a new solution for the null denominator problem of the MILP of Pallottino et al. (2002), other than that which they presented in (Alonso-Ayuso et al., 2011). Again, this solution covers only a set of cases where the null denominator problem appears. The model also does not ensure trajectory recovery. Using a MINLP solver, the model was able to solve problems involving up to 10 aircraft in a reasonable time. A major part of the work presented in Alonso-Ayuso et al. (2015) lies in the construction and comparison of different objective function formulations minimizing the magnitude of the changes. The results showed that the fitness of the solution and the computational time are highly sensitive to the weights used in the objective function. The authors argued that the weights have to be determined by experts. Alonso-Ayuso et al. (2016)

presented a linearised model of this MINLP. In the new linearised model, they discretised the possible heading angle range and considered only a set of possible angles. They proposed then a sequential mixed integer linear approach where the linearised model is solved sequentially and the angle range gets smaller at each iteration. The proposed heuristic was able to reach solutions that are 3% far from that found using the MINLP in less than 25 seconds. Also, it was able to reach feasible solutions for problems instances that the MINLP was not able to solve in less than one hour.

Omer (2015) presented a MILP to solve the CDR problem using speed and heading changes. The formulation of this MILP included a model of aircraft dynamics which permits the consideration of more realistic manoeuvres. The model assumed continuous speed change using constant acceleration but with constant speed around trajectories intersection points. The heading change is assumed to follow the maximum yaw rate. The MILP minimizes fuel consumption and delays while ensuring spatial trajectory recovery. The crossing conflict model is an extension of the model presented by Vela et al. (2009). The model restricts speed and heading manoeuvres to two predefined forms that permit the relaxation of the instantaneous changes assumption usually taken in the MILP formulation for CDR. The heading changes are limited to a predetermined finite set of possible heading angles. Omer (2015) stated that the model did not include altitude change to reduce model complexity and that such a manoeuvre is more appropriate for a medium term conflict detection approach.

In order to summarize the literature concerning CDR reported in this section, the models along with their main characteristics are presented in Table 2.1. The models are characterized by their formulation, the main assumptions, the types of allowed manoeuvres, and the types of conflicts solved. In Table 2.1, *instantaneous changes* means that the time to apply the manoeuvres is considered to be negligible. *Linear trajectory* means that the model assumes that an aircraft trajectory is a straight line. *Piecewise linear trajectory* means that an aircraft is assumed to follow direct lines between waypoints with instantaneous heading changes at waypoints. *Constant speed* means that the model assumes that aircraft use constant speed between waypoints. *Trajectory recovery* means that the model forces the aircraft to return to its original destination (trajectory) after the trajectory changing manoeuvre.

From Table 2.1, it can be noticed that only few works tried to solve the CDR problem using speed, heading and altitude changes simultaneously using a MILP formulation. Only Alonso-Ayuso et al. (2016) was able to tackle such problem but through an approximated MILP sequential heuristic. Most of the works targeted the detection and the solution of only crossing conflicts. When the trailing conflict was tackled in (Alonso-Ayuso et al., 2011, 2014, 2015, 2016), the aircraft were to be separated vertically even if it uses speeds that may avoid the conflict. A solution for the trailing conflict using speed and altitude changes was presented

Table 2.1 Summary of the reported literature on the CDR problem

	Formulation	Speed changes	Heading changes	Altitude changes	Crossing conflict	Trailing conflict	Head-to-head conflict	2D	3D	Instantaneous changes	Constant speed	Linear trajectory	Piecewise Linear trajectory	Trajectory recovery
Pallottino et al. (2002)	MILP	✓			✓			✓		✓	✓	✓		
	MILP		✓		✓			✓		✓	✓	✓		
Vela et al. (2010)	MILP	✓	✓		✓			✓		✓	✓	✓		
Vela et al. (2009)	MILP	✓		✓	✓	✓			✓	✓	✓		✓	
Rey et al. (2012)	MILP	✓			✓	✓		✓		✓	✓		✓	- [a]
Cobano et al. (2012)	QP [b]	✓			✓	✓		✓		✓	✓		✓	✓
Cafieri and Durand (2014)	MINLP	✓			✓			✓		✓	✓	✓		
Alonso-Ayuso et al. (2011)	MILP	✓		✓	✓	✓ [c]	✓		✓	✓	✓	✓		
Alonso-Ayuso et al. (2014)	MILP	✓		✓	✓	✓ [c]	✓		✓	✓	✓	✓		
Alonso-Ayuso et al. (2012)	MINLP	✓			✓			✓					✓	✓
Alonso-Ayuso et al. (2015)	MINLP	✓	✓	✓	✓	✓ [c]	✓		✓	✓	✓	✓		
Alonso-Ayuso et al. (2016)	MILP [d]	✓	✓	✓	✓	✓ [c]	✓		✓	✓	✓	✓		
Omer (2015)	MILP	✓	✓		✓	✓	✓	✓			- [e]	✓ [f]		✓

a. Minimal trajectory change. The speed change was limited to -6%-+3%
b. Quadratic programming
c. Each aircraft pair at risk of trailing was forced to use different flight levels
d. Approximated sequential mixed integer linear program
e. Constant speed around the conflict zones
f. The original trajectory is linear but the resolved trajectory can include a heading change

by Vela et al. (2009). Most of the work reported in Table 2.1 assumed that the time required to apply the changes is negligible and that the changes are instantaneous. Another common assumption is that the aircraft follow direct trajectories between waypoints using constant speed. The assumption of instantaneous changes was not taken in (Alonso-Ayuso et al., 2012), for which the model became non linear and was only solved for small size problems.

2.4 Concluding remarks

There exist many research issues and gaps in the complexity resolution problem in a MSP context. In our opinion some of these issues are the following :

- To our knowledge, no work to date handled the complexity resolution problem in MSP while considering speed, heading and altitude changes simultaneously. Flener et al. (2007a,b,c) tackled the problem using speed and altitude changes. Hong et al. (2016) solved the complexity resolution problem in adjacent sectors using either speed or heading changes.
- The detection and solution of trailing conflicts was not considered in the solution of the complexity resolution problem. Hong et al. (2016) considered only the detection and solution of the crossing conflicts. Flener et al. (2007a,b,c) did not take into consideration the detection of any type of conflict.
- While the solution of the complexity resolution problem involves the modification of aircraft trajectories, no work presented a model that ensures trajectory recovery or even minimal modifications.
- A key feature in the MSP concept is workload balancing among the sectors in the MSA through the MSPr. To our knowledge, no work to date considered the balancing of the complexity measure while solving the complexity resolution problem. Neglecting such a characteristic in any tool designed for the MSPr may limit the ability to analyse its efficiency or its applicability. While Flener et al. (2007a,b,c) included workload balancing in their problem definition, neither the results nor the model reported in their work included anything related to it. Hong et al. (2016) tackled the workload minimization in only one adjacent sector so there was no mention of workload balancing.

In conclusion, there is a need for a model to solve the complexity resolution problem in a MSP context that covers the above-mentioned shortcomings. Such a model has to be able to modify aircraft trajectories through speed, heading and altitude manoeuvres while ensuring trajectory recovery. This model has also to be able to ensure workload balancing among sectors in the MSA. We propose a model with such characteristics in this thesis.

After a brief review of the complexity measure literature, we decided that the number of conflicts is a suitable measure of controllers workload in the context of the objectives and scope of this thesis. The literature on the CDR problem is vast and includes many different approaches. From this literature, we decided to focus on the work that used a MILP approach. The models using MILP are characterized by small computational time and the ability to handle large numbers of aircraft. Both features are fundamental to the complexity resolution problem.

In the CDR literature, we noticed that the MILP formulation of Pallottino et al. (2002) was adopted and modified more than once (Vela et al., 2010; Alonso-Ayuso et al., 2011, 2014, 2012, 2015, 2016). This formulation enables the linearisation of the separation constraints through a simple geometrical formulation of the conflicts. The model of Pallottino et al. (2002) suffers from two limitations, first the null denominator problem as reported by Pallottino et al. (2002) and the other one is the false conflict detection reported by Alonso-Ayuso et al. (2011). The false detection problem was solved by Alonso-Ayuso et al. (2011) but the null denominator was only partially solved by Alonso-Ayuso et al. (2011, 2015). Another formulation which used also a geometrical construction of the conflict was presented by Vela et al. (2009). This formulation enables the transformation of the separation constraints into the time domain where safe separation can be ensured by checking the passage time at the intersection point between aircraft trajectories. In Vela et al. (2009), the definition of aircraft pairs that are predicted to lose separation, both for crossing and trailing conflict, is not complete because it does not include all possible cases. The set of flights pairs at risk of crossing conflicts needs to include the pairs that can lose the safe separation distance with a minimum separation distance larger than 0. The set of flights pairs at risk of a trailing conflict needs to include the flights pairs that share only a part of their trajectories.

While the model of Pallottino et al. (2002) includes both angle and speed in the separation constraints and requires the handling of the null denominator problem, the model presented by Vela et al. (2009) uses only the passage time in the separation constraints and requires only the redefinition of the aircraft pair sets. In this thesis, we propose the solution of the complexity resolution problem in a MSP context based on a modified formulation of the MILP presented in Vela et al. (2009).

Following our research approach, in the next chapter we introduce a full definition of the complexity resolution problem in a MSP context, followed by a mixed integer linear programming model to solve the problem for only the crossing conflicts using speed and heading changes.

CHAPTER 3 MULTI-SECTOR PLANNING FOR CROSSING CONFLICTS

In this chapter we propose a definition of the complexity resolution problem in a MSP framework. The definition includes a description of the context where the model is applied, the assumptions under which the problem is tackled and the types of allowed trajectory changes. Following the problem definition, we introduce a MILP model to solve the problem using only speed and predefined heading changes. Next, we present in details a problem example and solve it with our model. Later, we use different sets of randomly generated problems to test the efficiency of the CDR algorithm and to test the effect of different manoeuvres combinations on the solutions fitness. Finally, we test and prove the efficiency of our workload balancing method via numerical experiments.

3.1 Problem definition

The complexity resolution problem in a multi-sector planning context consists in minimizing and balancing controllers workload in a set of adjacent sectors over a medium time horizon. This is achieved by performing suitable modifications of aircraft trajectories. Solving this problem is the main task of the MSPr. A tool that can solve this problem should be essential for the MSPr in MSA management. In this work, we chose to use the number of conflicts in a sector as a measure of the controllers workload.

We present in this chapter such a model to be applied in the following scenario : at a given time t_{now}, the MSPr wants to plan the trajectories of all aircraft that are scheduled to pass through a designated MSA in a period of 20 to 90 minutes after t_{now}. The model provides the MSPr with a set of possible solutions that minimizes and balances the predicted number of conflicts in the MSA. It is then the task of the MSPr to choose one of these solutions. The time period of 20 to 90 minutes was suggested in the work of Eurocontrol on the MSP concept by Flener et al. (2007a) as an appropriate time horizon to solve the complexity resolution problem in a MSP context. It ensures that there is enough time to solve the problem and apply the solution while avoiding large error in the prediction of aircraft trajectories. It gives 10 minutes to solve the problem and another 10 minutes to apply the modifications.

A schematic of the information flow in such a system is presented in Figure 3.1. The model gathers information from the MSA (e.g. geometry, common routes, flight plans), aircraft (e.g. current mass, speed, wind speed) and sector controllers (e.g. tactical manoeuvres, predicted conflicts). The model uses this information along with solution parameters imposed by the MSPr to generate a set of possible solutions. The MSPr then chooses a solution from this set

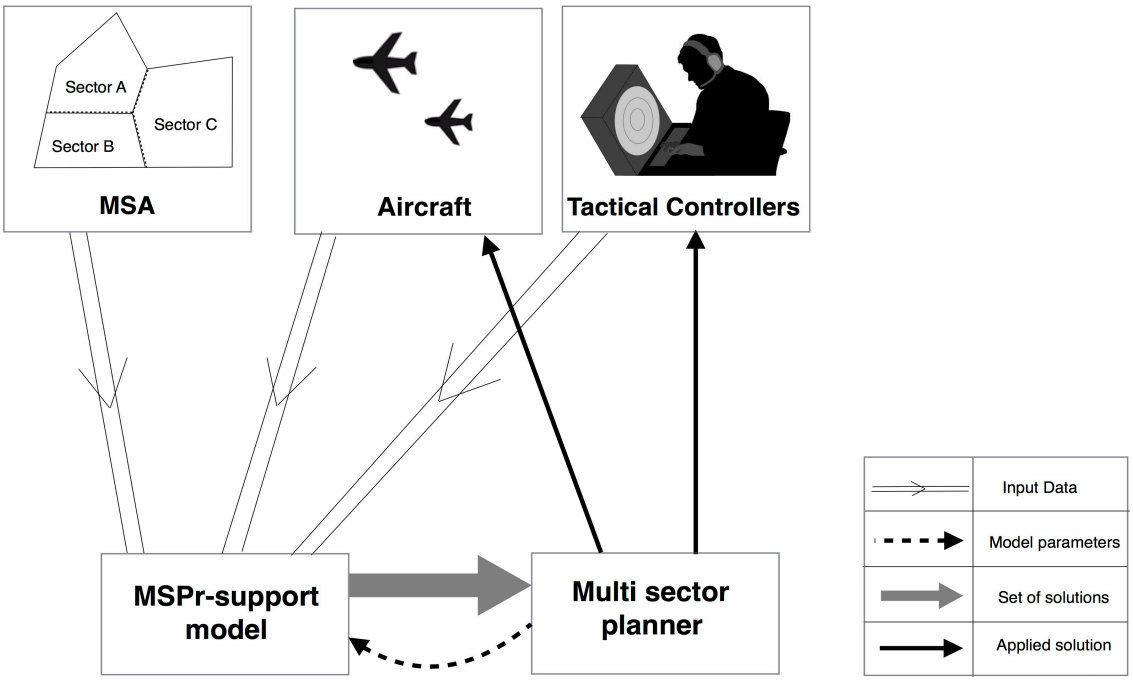

Figure 3.1 MSPr support model application scenario.

based on his analysis, transmits it to the controllers and applies it to the aircraft.

3.1.1 Trajectory modification

A solution to the complexity resolution problem is a set of trajectory modifications for one or several aircraft. These modifications are only applied to aircraft that pass through the MSA within the prediction time horizon. The trajectory modifications that we consider in this chapter are speed changes and heading manoeuvre changes.

Speed changes

A flight plan is expressed by a set of waypoints. Each waypoint is defined by space coordinates and the time at which the aircraft is planned to pass by this point. In this work, we represent a change of an aircraft speed by a change of its waypoints passage times. In aeronautics, there are several expressions for an aircraft speed, some of which are airspeed and ground speed. The airspeed is the speed of the aircraft relative to the air, while the ground speed is the speed of the aircraft relative to the ground. As the air traffic control speed adjustments are for the airspeed, in the rest of this thesis the term speed will indicate an aircraft airspeed. Following the work of Rey et al. (2012, 2015) on CDR using small speed changes, we consider in this work two different limits for speed changes :

— Small speed changes : $\Delta v \in [-0.06\ v_c,\ 0.03\ v_c]$, where Δv denotes the value of the airspeed change and v_c denotes the original cruise airspeed.
— Large speed changes : $\Delta v \in [-0.12\ v_c,\ 0.06\ v_c]$.

The speed change limits respect the fact that in general an aircraft uses a speed that is near its maximum limit. Being close to its maximum speed, the aircraft has a small window to increase its speed. However, the window for decreasing its speed is larger.
Since the speed changes that we consider in this work are small, we may assume that they happen instantaneously at waypoints. The aircraft follows the new speed indicated at each waypoint until the next point. In our work, we do not allow for a change in the MSA entry point. We made this choice because a change in the MSA entry point requires a negotiation with the neighbouring MSA, and in general there is no guarantee that such a change would be approved.

Heading changes

A heading change manoeuvre is a change in aircraft direction from that indicated in its flight plan. The manoeuvre can also include a return to the original trajectory, as in figure 3.2. In our model, we only allow for a set of predefined heading manoeuvres.

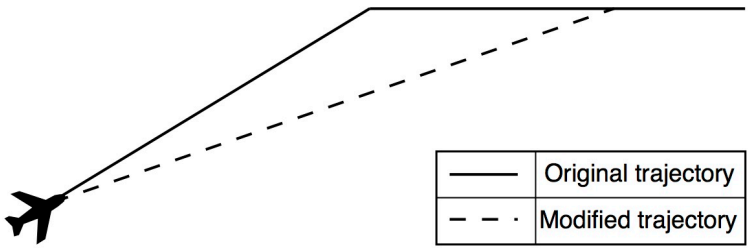

Figure 3.2 Example of a heading change manoeuvre.

For each aircraft, we will assign a set of alternative flight plans. Each alternative flight plan is a modified trajectory using one of the predefined heading manoeuvres. Similarly to the speed changes, the heading change in the heading manoeuvre has to be small so that we can assume instantaneous changes in directions. For the sake of simplicity, we use only three alternative flight plans for each flight. The first one is the original trajectory. The second one is obtained by enforcing an instantaneous turn to the right of $\phi = 8°$ at the MSA entry point until the aircraft reaches a distance $d = 5$ NM away from the original flight plan. Then the aircraft follows a trajectory parallel to the original path until the final segment in the MSA. At this point, the aircraft makes a $\phi = 8°$ turn to the left to reach the spatial exit point

defined in the original flight plan (Figure 3.3-a).

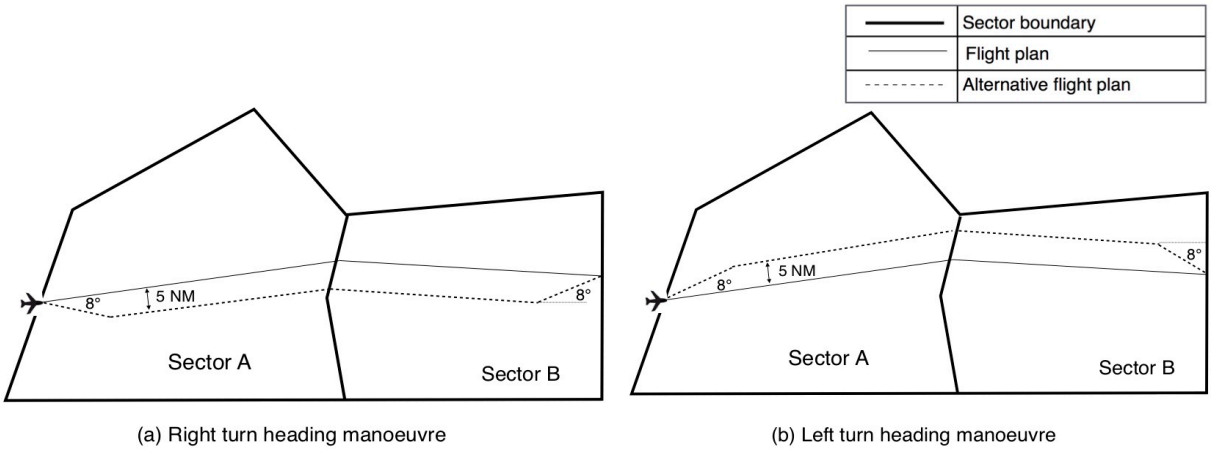

Figure 3.3 Predefined heading changes.

The third and last flight plan that we consider in this work is similar to the second one : the aircraft starts this manoeuvre with a left turn of $\phi = 8°$ at the MSA entry point until the aircraft reaches a distance of $d = 5$ NM away from the original flight plan. The aircraft then follows a trajectory parallel to the original one. At the final segment of the trajectory, the aircraft performs an $8°$ right turn to reach the original exit point (Figure 3.3-b). In other words, for each flight plan we consider two parallel alternatives : the first one is 5 NM to the right and the second one is 5 NM to the left, and both use the same MSA entry waypoint and exit spatial point (the exit times may differ). We chose a turn angle $\phi = 8°$ to minimize the magnitude of trajectories changes. In the case of multiple aircraft following the exact same spatial trajectory, our heading manoeuvre allows to put them on parallel trajectories that are safely separated.

Since we model heading change manoeuvres as alternative flight plans, there is no constraint on the definition of the manoeuvres. A complex manoeuvre including multiple heading changes can be also considered as an alternative flight plan. A MSPr can define alternative trajectories for the most common routes in his designated MSA and use them as heading manoeuvres.

3.1.2 Assumptions

Following the definition of the complexity resolution problem of Flener et al. (2007a,c), we define the complexity resolution problem in a multi-sector planning framework as follows : given a set S of adjacent sectors and a moment of time t_{now}, determine a modification of

the trajectories of the A aircraft that are planned to be inside S within the time interval $[t_{now} + 20, t_{now} + 90]$ minutes such that the complexity measure representing the controllers workload of all the sectors in S is minimized and balanced. In Flener et al. (2007a,c), the problem definition did not include the workload balancing and included enforcing a predetermined fraction of the aircraft to remain in the MSA.

In this thesis, we use the number of conflicts along the prediction time horizon as a complexity measure. In this chapter, we allow for trajectory modifications consisting of speed and/or heading changes, as previously described. We study the problem under the following assumptions :

1. The problem addresses en route controlled sectors and not the terminals.
2. The problem addresses the flights in the upper airspace only (flights in low flight levels are not considered). This assumption was made because aircraft at high altitudes represent most of the controllers workload and are the main target of the multi-sector planning concept.
3. The detection and resolution of conflicts comprises both the trailing and crossing conflicts.
4. The problem does not cover the detection of head-to-head conflicts. This type of conflicts is avoided in the design of aircraft trajectories using the semicircular rule.
5. The flight plans are defined by a set of waypoints between which the aircraft fly in straight lines at constant speed with instantaneous change in directions and speed at waypoints.
6. We assume that exact knowledge of aircraft position in real time is available. In a controlled airspace, all aircraft are monitored using radars and their actual positions are known.
7. We assume that the manoeuvres approved by controllers and transferred to pilots are known at all moments. Tools and technologies that enable such an assumption are part of the SESAR project.
8. We assume that the wind perturbations effect are small and can be neglected, as a result the prediction of aircraft positions is deterministic. We made this assumption because the future application of 4D FMS and Data link will significantly reduce the uncertainty on the prediction of aircraft positions.
9. We assume that there are no changes in the MSA entry and exit waypoints spatial coordinates. We made this assumption to ensure the feasibility of the generated solutions.

10. The magnitude of trajectory changes has to be small. We made this assumption to minimize the effect of trajectory modifications on the neighbouring MSA. This assumption is imposed via the definition of the allowed trajectory modifications.

In the following section, we propose a multi-sector planning support model using speed and heading changes for crossing conflicts (MSP-SH/C). MSP-SH/C is a mixed integer linear model we use to solve the complexity resolution problem as previously defined. This model considers only crossing conflicts and uses speed and heading changes.

3.2 Multi-sector planning support model using speed and heading changes

A model to solve the conflict resolution problem, as we defined in this thesis, requires the detection and resolution of conflicts in a MSP context. The MSP context means that the problem has to be solved for multiple sectors with a high traffic density. It also means that the number of conflicts has to be balanced among sectors.

To detect and solve conflicts, we decided to adopt a modelling approach similar to that of Carlier et al. (2002) and Vela et al. (2009). This approach relies on setting a lower bound on the difference between the passage times of two aircraft at the intersection point between their trajectories. This lower bound is defined to ensure safe separation between the two aircraft and it assumes that both aircraft use a constant speed around the intersection point. Two aircraft i and j flying at airspeeds v_i and v_j respectively with an intersection angle $\theta_{i,j}$ between their trajectories remain separated by a distance larger than D at all time if the magnitude of the difference between their passage times at the intersection point is greater than a threshold $\dot{S}_{i,j}$ given by

$$\dot{S}_{i,j} = \frac{D}{v_i v_j |\sin(\theta_{i,j})|} \sqrt{v_i^2 + v_j^2 - 2 v_i v_j \cos(\theta_{i,j})}, \tag{3.1}$$

where $\theta_{i,j} \in]0, \pi[\cup]\pi, 2\pi[$ and is defined as in Figure 3.4. In the rest of this thesis we use $D = 5$ NM ~ 9.2 km. Note that (3.1) is not defined in the case of a trailing conflict ($\theta_{i,j} = 0$ or 2π), nor is it defined in the case of a head to head conflict ($\theta_{i,j} = \pi$). The justification of (3.1) is given in Appendix A.

Safe separation between a pair of aircraft is guaranteed if the difference between the passage time at the intersection point is greater than $\dot{S}_{i,j}$ for all allowed speeds $v_i \in [v_i^-, v_i^+]$ and $v_j \in [v_j^-, v_j^+]$, where v_i^- and v_i^+ denote the minimum and maximum allowed airspeeds for aircraft i respectively. Rey et al. (2012) proved that $S_{i,j}$ defined as

$$S_{i,j} = \max\left(\frac{D\, \Omega_{i,j}}{v_i^- |\sin(\theta_{i,j})|}, \frac{D\, \Omega_{j,i}}{v_j^- |\sin(\theta_{i,j})|} \right), \tag{3.2}$$

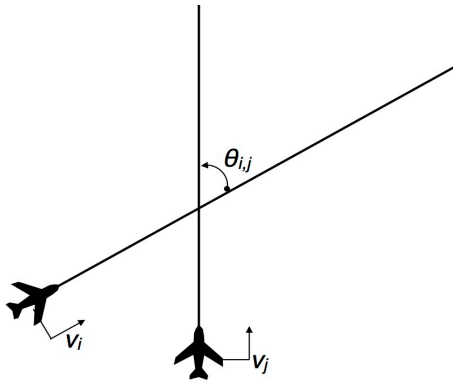

Figure 3.4 The intersection angle $\theta_{i,j}$ between two aircraft.

is an upper bound to $\dot{S}_{i,j}$ within the allowed speed limits, where $\Omega_{i,j}$ is defined as

$$\Omega_{i,j} = \max\left(\sqrt{(\frac{v_i^+}{v_j^-})^2 - \frac{2\,v_i^+\,\cos(\theta_{i,j})}{v_j^-} + 1}, \sqrt{(\frac{v_i^-}{v_j^+})^2 - \frac{2\,v_i^-\,\cos(\theta_{i,j})}{v_j^+} + 1}\right).$$

In our model we will use $S_{i,j}$ as defined in (3.2) to determine the minimum separation time at an intersection point that ensures no conflict. In order to study the change in $S_{i,j}$ for different conflict situations, we calculated its value for two aircraft having the same minimum speed of 456 knots and the same maximum speed of 513 knots for different values of $\theta_{i,j}$. Figure 3.5 displays the value of $S_{i,j}$ as a function of $\theta_{i,j}$ for $\theta_{i,j} \in [0.5°,\ \ 179.5°]$. We see that $S_{i,j}$ takes small values ($<$ 3 minutes) for most intersection angles, i.e. $\theta_{i,j} \in [2°$ - $160°]$. The time $S_{i,j}$ takes relatively large values for very small intersection angles ($\theta_{i,j} < 2°$) and takes much larger values for large intersection angles ($\theta_{i,j} \geq 160°$). This is due to the fact that (3.2) ensures safe separation for all times assuming that both aircraft use a constant speed and direction. For very small values of $\theta_{i,j}$, the aircraft configuration takes the form of a trailing conflict and therefore the safe time difference has to be relatively large to avoid conflict. For large $\theta_{i,j}$, i.e. $\theta_{i,j} \geq 175°$, the aircraft configuration resembles the form of a head-to-head conflict. In this case, the value of $S_{i,j}$ increases significantly as the intersection angle increases until it reaches $+\infty$ at 180°, where no safe separation can be reached. Since the aircraft maintain linear trajectories before and after the intersection point, we can see from Figures 3.6 and 3.7 that in both cases the distance between the trajectories is small and $S_{i,j}$ must be large to maintain a safe distance between the aircraft.

Note that a large intersection angle ($\theta_{i,j} > 165°$) represents a head to head conflict which is avoided in the design of aircraft trajectories using the semi-circular rule. Small intersection angles ($\theta_{i,j} < 2°$) represent the case of trailing conflicts that we solve in chapter 4.

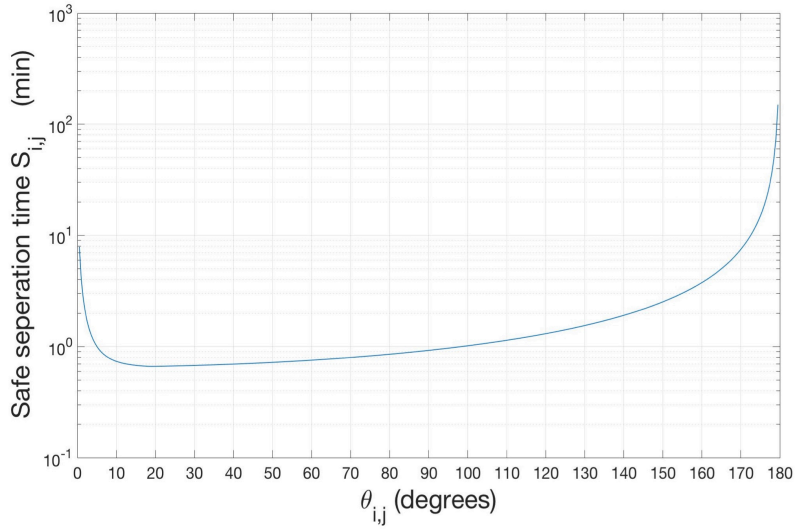

Figure 3.5 The minimum separation time for different intersection angles.

In the rest of this section, we propose a MILP formulation (MSP-SH/C model) based on $S_{i,j}$ to solve the complexity resolution problem. The objective is to minimize the number of crossing conflicts in a MSA over a time horizon of 20 to 90 minutes while ensuring that the number of conflicts is balanced among sectors.

3.2.1 Input data

The input data is the information that we need to solve the complexity resolution problem. This information is related to aircraft, flight plans and sectors. We assume that these data are given and known in advance.

Aircraft information

Regarding the aircraft information, we will use the index $a \in \{1, ..., A\}$ to represent each aircraft, where A is the total number of aircraft that are planned to pass inside S within the time interval $[t_{now} + 20, t_{now} + 90]$. For each aircraft a, the maximum allowed speed v_a^+, the minimum allowed speed v_a^- and the cruising speed $\bar{v}_a$ are known.

Flight plans information

Following the problem definition and our formulation of the heading change manoeuvre, each aircraft is given a set of possible flight plans that it can use. Let $i \in \{1, ..., J\}$ denote the flight plan index, where J is the total number of possible flight plans for all aircraft. We

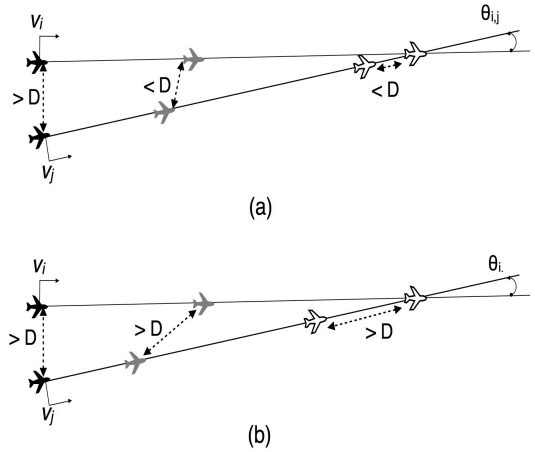

Figure 3.6 Crossing conflict with small $\theta_{i,j}$: (a) Separation time $< S_{i,j}$; (b) Separation time $> S_{i,j}$.

define the indicator $I_a(i)$ as

$$I_a(i) = \begin{cases} 1 \text{ if aircraft } a \text{ can use the flight plan } i\,; \\ 0 \text{ otherwise.} \end{cases}$$

A flight plan is assigned to only one aircraft, we can express this as

$$\sum_{a=1}^{A} I_a(i) = 1, \qquad i = \{1, 2, ..., J\}.$$

Regarding the flight plans data, we define a flight plan $\mathcal{P}_i$ by a set of $N(i)$ waypoints between which the aircraft flies in straight lines at constant speed, performing instantaneous changes in direction and speed at waypoints. Each waypoint of index $m \in \mathbb{N}$ is defined by its spatial coordinates $(x_i(m), y_i(m), z_i(m)) \in \mathbb{R}^3$ and its planned time of passage $t_i(m) \in \mathbb{R}^+$ at waypoint m. The variables $x_i(m)$ and $y_i(m)$ are the coordinates of the waypoint m in the horizontal plane and $z_i(m)$ is the flight level (altitude) used between waypoints m and $m+1$. To summarize, a flight plan is defined by the set

$$\mathcal{P}_i = \{\, (x_i(m), y_i(m), z_i(m), t_i(m)),\, m \in \{1, 2, ..., N(i)\}\,\}\,.$$

As the control of the multi-sector planner starts when an aircraft enters the multi-sector area S, the waypoint at which an aircraft enters S is not controllable. As a result, all the flight plans assigned to a given aircraft a share the same starting point. We express this condition

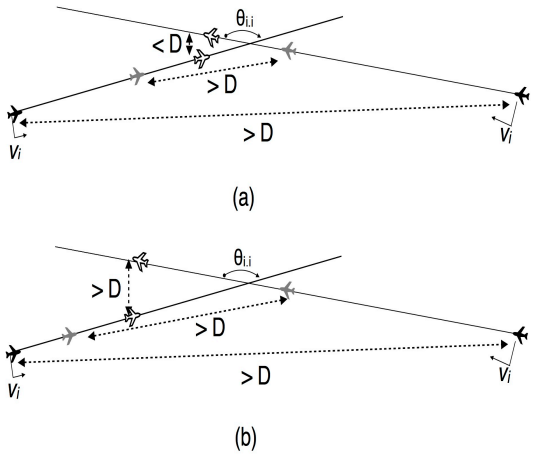

Figure 3.7 Crossing conflict with large $\theta_{i,j}$: (a) Separation time $< S_{i,j}$; (b) Separation time $> S_{i,j}$.

with the following set of identities : for $a \in \{1, 2, ..., A\}$,

$$\begin{cases} (x_i(1), y_i(1), z_i(1), t_i(1)) = (x_j(1), y_j(1), z_j(1), t_j(1)), \\ (i, j) \in \{1, 2, ..., J\}^2 : I_a(i) = I_a(j) = 1. \end{cases} \tag{3.3}$$

Note that the start waypoint is not a variable and is given by the original trajectory. The equation (3.3) is used to generate the alternative flight plans in a preprocessing stage.
Our formulation consists in predicting the conflicts by examining the times at which the aircraft pass at the intersection point of their trajectories, if this intersection exists. This examination requires the calculation of the minimum separation time $S_{i,j}$ with (3.2) for each pair of flight plans that have an intersection point, and then checking if the difference of passage time is less than $S_{i,j}$ or not. However, as noted by Vela et al. (2009), not all of these pairs can lead to a conflict. In some cases, the occurrence of a conflict is impossible because of time and speed constraints. For example, let us consider two aircraft having an intersection point between their trajectories. The first aircraft can arrive at the intersection in the time interval [90 min, 100 min], and the other one can reach it in the time interval [10 min, 20 min]. The minimum separation time is $S_{i,j} = 1$ min. Since the difference between the arrival times of the two aircraft is always larger than $S_{i,j}$, then it is impossible to have a conflict between these two aircraft at this intersection. This implies that there is no need to check the separation between these two aircraft.
This observation led Vela et al. (2009) to define a set of flight plan pairs at risk of a crossing conflict. A crossing conflict can happen between two aircraft if the passage time at the intersection of their trajectories is less than the minimum separation time $S_{i,j}$. The definition

of Vela et al. was not complete and did not include all the pairs at risk of a crossing conflict. They only included the pairs for which both aircraft can reach the intersection point at the same time. Since the speeds of aircraft are variable, each aircraft has a possible arrival time window at the intersection point w which we denote $[\hat{t}_i^-(w),\, \hat{t}_i^+(w)]$, where $\hat{t}_i^-(w)$ and $\hat{t}_i^+(w)$ are the minimum and maximum possible times at which an aircraft following flight plan i can reach the intersection point w respectively. Figure 3.8 illustrates all the possible cases of the arrival time windows that can lead to a crossing conflict. In Figure 3.8, w_1 and w_2 denote the indices of the intersection point in flight plans i and j respectively. Figure 3.8-a displays the case where there is an intersection between the arrival time windows, which means that both aircraft can arrive at the intersection at the same time. The Figures 3.8-b and 3.8-c represent the case where there is no intersection between the time windows but the difference between the minimum and the maximum possible arrival times of both aircraft is less than $S_{i,j}$. The definition of Vela et al. covers only the first case and consequently can lead to undetected conflicts. In the following, we propose to solve this problem by defining a set E that overcomes this shortcoming.

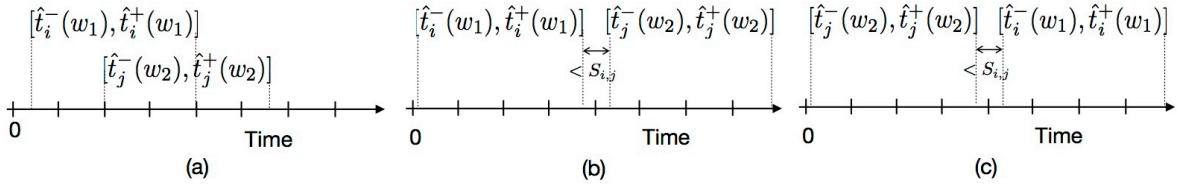

Figure 3.8 Time windows leading to a crossing conflict : (a) intersecting time windows ; (b) and (c) disjoint time windows.

The set E contains all distinct flight plan pairs having an intersection point that can be reached with a time difference less than $S_{i,j}$. We define $\hat{\mathcal{P}}_i$ as flight plan i with the waypoints defined only in 2D (X and Y coordinates), i.e.

$$\hat{\mathcal{P}}_i = \{\, (x_i(m), y_i(m)),\, m \in \{1, 2, ..., N(i)\}\,\}\,.$$

A pair (i, j) of flight plans belongs to E if and only if there exists an intersection between i and j that satisfies

$$\hat{\mathcal{P}}_i \neq \hat{\mathcal{P}}_j, \tag{3.4}$$

and

$$\begin{cases} \hat{t}_i^-(w_1) \leq \hat{t}_j^+(w_2) + S_{i,j}, \\ \hat{t}_j^-(w_2) \leq \hat{t}_i^+(w_1) + S_{i,j}, \end{cases} \tag{3.5}$$

where w_1 and w_2 denote the intersection point in flight plans i and j respectively.
If (3.4) and (3.5) are satisfied for a pair of flight plans, then this pair is at risk of a crossing conflict. Equation (3.4) ensures that E includes only flight plan pairs that have an intersection point while not following the same spatial trajectory all along the MSA. It excludes the flight plans that follow exactly the same spatial trajectory as they are at risk of a trailing conflict and not of a crossing conflict. The inequalities (3.5) cover the three cases in Figure 3.8. The inequalities (3.5) check if there is an intersection between the time windows $[\hat{t}_i^-(w_1), \hat{t}_i^+(w_1) + S_{i,j}]$ and $[\hat{t}_j^-(w_2), \hat{t}_j^+(w_2) + S_{i,j}]$.
Each pair in E is assigned an index $p \in \{1, 2, ..., |E|\}$. The flight plan pair of index p will be denoted by $(i(p), j(p))$, where $i(p)$ and $j(p)$ are the corresponding flight plan indices. We introduce the simplified notation

$$S_p := S_{i(p),j(p)}.$$

Sectors information

We specify the location of each intersection point in the MSA with the indicator matrix I_p^s, that we define as

$$I_p^s = \begin{cases} 1 \text{ if the intersection point of the } p^{th} \text{ flight plan pair in } E \text{ is located in sector } s\,; \\ 0 \text{ otherwise.} \end{cases}$$

For the MSP-SH/C model, we use a preprocessing stage to prepare the input data. It takes as input the MSA sectors geometry and the flight plans and provides as output E, S_p and I_p^s. The preprocessing stage will be discussed in details in section 3.2.5.

3.2.2 Decision variables

In the MSP-SH/C model, we define two sets of decision variables, each of which represents one of the possible modifications of the planned aircraft trajectories. The first set of decision variables represents the heading change manoeuvre modification. The heading manoeuvre is achieved by selecting one of the possible flight plans assigned to an aircraft. As by definition a flight plan i can be used by only one aircraft, we simply need a variable to indicate whether flight plan i is used or not. We denote this variable by $P(i)$ and define it as

$$P(i) = \begin{cases} 1 \text{ if flight plan } i \text{ is used;} \\ 0 \text{ otherwise,} \end{cases} \qquad i \in \{1, 2, ..., J\}.$$

We define a second set of decision variables that represents the speed up and speed down modifications. The speed modifications are achieved by changing travel durations between waypoints. The time lapse between waypoints m and $m+1$ for flight plan i will be denoted by $T_i(m)$. Note that $T_i(N(i))$ does not exist, so the total number of variables $T_i(m)$ is $\sum_{i=1}^{J}(N(i)-1)$. The total number of decision variables, i.e. both $P(i)$ and $T_i(m)$, is $J+\sum_{i=1}^{J}(N(i)-1)=\sum_{i=1}^{J}N(i)$.

3.2.3 Objective function

The objective of our formulation is to minimize the total number of predicted conflicts in S. In our model, a crossing conflict can happen only for a pair of flight plans that belongs to E. Therefore, we represent a crossing conflict for the p^{th} flight plan pair in E by the indicator C_p, defined as

$$C_p = \begin{cases} 1 \text{ if a conflict is predicted to happen for the } p^{th} \text{ flight plan pair in } E, \\ 0 \text{ otherwise.} \end{cases}$$

We define the objective function to be minimized as

$$Z = \sum_{p=1}^{|E|} C_p. \tag{3.6}$$

3.2.4 Constraints

The output of our method is a set of modified flight plans. The modified flight plans information include the modified waypoints passage times. Since the geographical position of each waypoint is fixed, the modified flight plans are given by

$$\mathcal{P}'_i = \{\, (x_i(m), y_i(m), z_i(m), t'_i(m)),\ m \in \{1,2,...,N(i)\},\ i \in \{1,2,...,J\} \,\},$$

where $t'_i(m)$ is the modified passage time of the m^{th} waypoint of flight plan i.

Heading change constraints

The heading change constraints ensure that an aircraft is assigned to one and only one of its possible flight plans. To do so, we use the equality constraint

$$\sum_{i=1}^{J} I_a(i)P(i) = 1, \qquad a \in \{1,...,A\}, \tag{3.7}$$

which ensures that a flight plan is assigned to an aircraft if this flight plan is one of the aircraft possible choices. Note that the constraint (3.7) is linear in the decision variables $P(i)$.

Speed change constraints

In this model, we represent a speed change by a change in waypoints passage times. For a flight plan i, the modified passage time of the m^{th} waypoint is denoted by $t'_i(m)$, and it is given by

$$t'_i(m) = t_i(1) + \sum_{w=1}^{m-1} T_i(w), \qquad m \in \{2, 3, ..., N(i)\}, \quad i \in \{1, 2, ..., J\}. \tag{3.8}$$

Remember that the MSA entry time is fixed, i.e.

$$t'_i(1) = t_i(1), \qquad i \in \{1, 2, ..., J\}. \tag{3.9}$$

As each aircraft has its own speed limits, we impose these limits with the inequality constraints

$$\sum_{a=1}^{A} \frac{I_a(i)}{v_a^+} \;\leq\; \frac{T_i(m)}{D_i(m)} \;\leq\; \sum_{a=1}^{A} \frac{I_a(i)}{v_a^-}, \quad i \in \{1, ..., J\}, \quad m \in \{1, 2, ..., N(i) - 1\}, \tag{3.10}$$

where $D_i(m)$ is the distance between the waypoints m and $m + 1$ of flight plan i. We chose $\frac{T_i(m)}{D_i(m)}$ instead of $\frac{D_i(m)}{T_i(m)}$ to maintain the model linearity with respect to the decision variables.

Constraints on the number of modified trajectories constraints

For a single air traffic situation there may exist multiple solutions to eliminate the conflicts each with a different number of modifications. From a practical point of view, if two solutions eliminate the same number of conflicts then the one with less modifications is the better. The solution with fewer modifications leads to less workload on the controller. In our model, the number of modifications is not minimized as it is not included in the objective function. As a result, if the number of modifications is not limited, we may obtain solutions that include a large number of modifications while there may exist solutions with less modifications. In the following we define a set of constraints to limit the number of modified trajectories. First, we introduce a set of constraints to evaluate if each aircraft undergoes speed and/or heading

modification. For the speed change, we introduce a new binary variable $\mathcal{I}_s(i)$ defined as

$$\mathcal{I}_s(i) = \begin{cases} 1 \text{ if flight plan } i \text{ includes a speed change manoeuvre;} \\ 0 \text{ otherwise.} \end{cases}$$

To set the value of $\mathcal{I}_s(i)$ to 1 if the difference between the modified and original passage times is other than 0 (i.e. $t_i'(m) \neq t_i(m)$), we use the following set of inequalities :
for $i \in \{1, 2, ..., J\},\ m \in \{1, 2, ..., N(i)\}$,

$$\begin{cases} t_i'(m) - t_i(m) \leq \mathcal{I}_s(i)\ (t_i^+(m) - t_i(m) + 1), \\ \\ t_i(m) - t_i'(m) \leq \mathcal{I}_s(i)\ (t_i(m) - t_i^-(m) + 1), \end{cases} \tag{3.11}$$

where $t_i^-(m)$ and $t_i^+(m)$ are the minimum and maximum possible times at which an aircraft following flight plan i can reach waypoint m.
We limit the number of speed modifications using

$$\sum_{i=1}^{J} \mathcal{I}_s(i) \leq \alpha\ A, \tag{3.12}$$

where α is the maximum allowed percentage of speed modified flight plans.
For the heading manoeuvre changes, we introduce the variable $\mathcal{I}_h(a)$ defined as

$$\mathcal{I}_h(a) = \begin{cases} 1 \text{ if aircraft } a \text{ undergoes a heading change manoeuvre;} \\ 0 \text{ otherwise.} \end{cases}$$

For each aircraft we assign three possible flight plans. All the flight plans are indexed such that the indices of the flight plans assigned to aircraft a are $3a-2, 3a-1$ and $3a$. The original trajectory takes the index $3a-2$ and the other two indices are for heading change manoeuvres. Consequently we use

$$\mathcal{I}_h(a) = 1 - P(3a-2), \qquad a \in \{1, 2, ..., A\}, \tag{3.13}$$

to set the value $\mathcal{I}_h(a)$.
The final variable we introduce in the model to count the number of trajectory modifications is $\mathcal{I}(a)$ defined as

$$\mathcal{I}(a) = \begin{cases} 1 \text{ if the trajectory of aircraft } a \text{ undergoes any modifications;} \\ 0 \text{ otherwise.} \end{cases}$$

To set the value of $\mathcal{I}(a)$ to 1 if aircraft a undergoes a speed and/or a heading modification, i.e. $\sum_{i=1}^{J} I_a(i)\ \mathcal{I}_s(i) = 1$ and/or $\mathcal{I}_h(a) = 1$, and 0 otherwise, we use the following set of inequalities : for $a \in \{1, 2, ..., A\}$,

$$\begin{cases} \mathcal{I}_h(a) + \sum_{i=1}^{J} I_a(i)\ \mathcal{I}_s(i) \leq 2\ \mathcal{I}(a), \\ \mathcal{I}_h(a) + \sum_{i=1}^{J} I_a(i)\ \mathcal{I}_s(i) \geq 2\ (\mathcal{I}(a) - 0.9). \end{cases} \tag{3.14}$$

Finally, we bound the percentage of modified trajectories using

$$\sum_{a=1}^{A} \mathcal{I}(a) \leq \gamma\ A, \tag{3.15}$$

where γ is the maximum allowed percentage of modified trajectories.

Conflict prediction constraints

We use the following set of constraints to predict the conflicts and set the values of the conflict indicator C_p. A conflict is predicted at the intersection of two flight plans $(i, j) \in E$ if all the following conditions are met :

1. there are two aircraft using the flight plans ;
2. both aircraft are using the same flight level at the intersection point ;
3. the difference between their passage times at the intersection point is smaller than S_p.

The first condition can be verified by checking the values of $P(i)$ and $P(j)$. If both variables equal 1 then both flight plans are used. As for the second condition, we want to verify the use of the same flight level at the intersection point. First we introduce a new indicator $L_i(m, k)$, defined as

$$L_i(m, k) = \begin{cases} 1 \text{ if flight plan } i \text{ uses flight level } k \text{ between waypoints } m \text{ and } m+1, \\ 0 \text{ otherwise.} \end{cases}$$

The MSP-SH/C model does not include flight level changes, so in the preprocessing stage we set the value of $L_i(m, k)$ using

$$L_i(m, k) = \begin{cases} 1 & \text{if } z_i(m) = k, \\ 0 & \text{otherwise,} \end{cases} \qquad i \in \{1, 2, ..., J\},\ m \in \{1, 2, ..., N(i)\},\ k \in \{1, 2, ..., K\},$$

where K is the total number of flight levels in the MSA.
The information regarding whether both flight plans use the same level at the intersection

point or not is given by the indicator $H_p(k)$ that we define as

$$H_p(k) = \begin{cases} 0 \text{ if both flight plans of the } p^{th} \text{ pair in } E \text{ use flight level } k \text{ at the intersection} \\ \quad \text{point;} \\ 1 \text{ otherwise.} \end{cases}$$

Since the flight levels of the aircraft are predefined, then the value of $H_p(k)$ can be determined in a preprocessing stage. In chapter 5, we allow for flight level changes. In such a case, $H_p(k)$ becomes a variable and we can set $H_p(k) = 0$ if $L_{i(p)}(m,k) = 1$ and $L_{j(p)}(n,k) = 1$ and $H_p(k) = 1$ otherwise by using the following set of inequalities : for $p \in \{1,2,...,|E|\}$ and $k \in \{1,2,...,K\}$

$$\begin{cases} L_{i(p)}(m,k) + L_{j(p)}(n,k) \leq 2 - H_p(k), \\ L_{i(p)}(m,k) + L_{j(p)}(n,k) \geq 1.1 - 2\ H_p(k), \end{cases} \tag{3.16}$$

where m, n are the indices of the waypoints after which the flight plans $i(p)$ and $j(p)$ intersect respectively.

As for the third condition, we want to know if the difference between the passage times of the intersection point of the two modified flight plans is greater than the safe limit or not. As the intersection point is generally not a waypoint, we determine the passage time $\hat{t}_i(w)$ at intersection point w with

$$\hat{t}_i(w) = t'_i(m) + \frac{T_i(m)}{D_i(m)}\ d_i(w), \qquad i \in \{1,...,J\}, \quad w \in \{1,2,...,W(i)\}, \tag{3.17}$$

where m is the waypoint after which the intersection point w exists, $D_i(m)$ is the euclidean distance between waypoints m and $m+1$ of flight plan i, $d_i(w)$ is the euclidean distance between the w^{th} intersection point of the modified flight plan i and the previous waypoint m, and $W(i)$ is the total number of intersection points in flight plan i (Figure 3.9). Note that although the existence of multiple intersection points between a pair of trajectories is not common in high flight levels, our model is able to handle such a case.

The third condition for a crossing conflict between flight plans i and j can be expressed as

$$|\hat{t}_{i(p)}(w_1) - \hat{t}_{j(p)}(w_2)| < S_p, \qquad p \in \{1,2,...,|E|\}, \tag{3.18}$$

where w_1 and w_2 are the indices of the intersection point in flight plans i and j respectively. Constraint (3.18) is not linear because of the absolute term. To linearise (3.18), we will introduce a binary variable along with a set of linear equations for each of the two possible

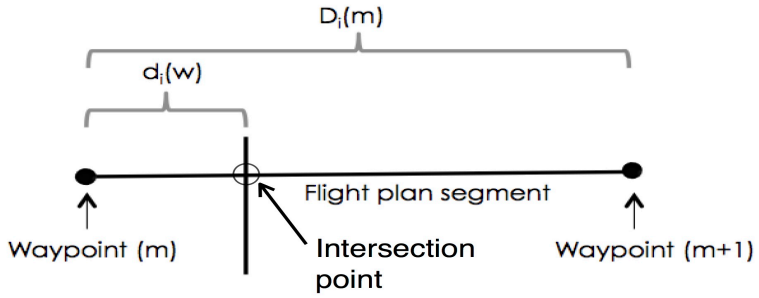

Figure 3.9 Example of an intersection of two flight plans.

order of arrivals. First, we introduce two binary variables A_p and B_p defined as

$$A_p = \begin{cases} 1 \text{ if the aircraft following the first flight plan, } i, \text{ of the } p^{th} \text{ flight plan pair in } E \\ \quad \text{arrives at the intersection point before the aircraft following the second flight} \\ \quad \text{plan, } j, \text{ and they are safely separated,} \\ 0 \text{ otherwise}; \end{cases}$$

$$B_p = \begin{cases} 1 \text{ if the aircraft following the second flight plan, } j, \text{ of the } p^{th} \text{ flight plan pair in } E \\ \quad \text{arrives at the intersection point before the aircraft following the first flight} \\ \quad \text{plan, } i, \text{ and they are safely separated,} \\ 0 \text{ otherwise.} \end{cases}$$

To have $A_p = 1$ if $\hat{t}_{j(p)}(w_2) - \hat{t}_{i(p)}(w_1) > S_p$ and $A_p = 0$ otherwise, we use the following system of inequalities : for $p \in \{1, 2, ..., |E|\}$,

$$\begin{cases} \hat{t}_{i(p)}(w_1) - \hat{t}_{j(p)}(w_2) + S_p \leq (1 - A_p)\ M_p^1, \\ \hat{t}_{i(p)}(w_1) - \hat{t}_{j(p)}(w_2) + S_p \geq -A_p\ M_p^1, \end{cases} \tag{3.19}$$

where M_p^1 is a relatively large positive number. We evaluate M_p^1 using the following equation

$$M_p^1 = \hat{t}^+_{i(p)}(w_1) - \hat{t}^-_{j(p)}(w_2) + S_p + 0.1, \qquad p \in \{1, 2, ..., |E|\}. \tag{3.20}$$

We chose this value of M_p^1 because in a big-M formulation such as (3.19), the value of M has to be as small as possible to minimize the computational time (Türkay and Grossmann, 1996; Appa et al., 2006).

Similarly, to have $B_p = 1$ if $\hat{t}_{i(p)}(w_1) - \hat{t}_{j(p)}(w_2) > S_p$ and $B_p = 0$ otherwise, we use the

following system of inequalities : for $p \in \{1, 2, ..., |E|\}$,

$$\begin{cases} \hat{t}_{j(p)}(w_2) - \hat{t}_{i(p)}(w_1) + S_p \leq (1 - B_p)\ M_p^2, \\ \hat{t}_{j(p)}(w_2) - \hat{t}_{i(p)}(w_1) + S_p \geq -B_p\ M_p^2, \end{cases} \tag{3.21}$$

where M_p^2 is evaluated using

$$M_p^2 = \hat{t}^+_{j(p)}(w_2) - \hat{t}^-_{i(p)}(w_1) + S_p + 0.1, \qquad p \in \{1, 2, ..., |E|\}. \tag{3.22}$$

Using the new variables, we can formulate the three conditions for a crossing conflict between the p^{th} flight plan pair in E as follows :

1. $P(i(p)) = 1$ and $P(j(p)) = 1$, hence there are two aircraft using flight plans $i(p)$ and $j(p)$.
2. $\sum_{k=1}^{K} H_p(k) = K - 1$, which means that the flight plans i and j use the same flight level at the intersection point.
3. $A_p = B_p = 0$, which means that the difference between the passage times at the intersection point is smaller than S_p.

Finally, to have $C_p = 1$ if all these three conditions are met and $C_p = 0$ otherwise, we use the following system of inequalities :

$$A_p + B_p + \sum_{k=1}^{K} H_p(k) - P(i(p)) - P(j(p)) + 2 - K \geq -5\ C_p, \quad p \in \{1, 2, ..., |E|\}, \tag{3.23}$$

$$A_p + B_p + \sum_{k=1}^{K} H_p(k) - P(i(p)) - P(j(p)) + 2 - K \leq 5\ (1 - C_p), \quad p \in \{1, 2, ..., |E|\}. \tag{3.24}$$

A verification of the constraints (3.23) and (3.24) is presented in Appendix B.

Balancing constraint

The last constraint we present in this model is used to balance the number of predicted conflicts among the sectors in a MSA. Our formulation for the balancing constraint relies on preventing the number of conflicts predicted to happen in sector s, given by $\sum_{p=1}^{|E|} C_p\, I_p^s$, from exceeding λ times the average number of conflicts in all the sectors. This constraint takes the form

$$\sum_{p=1}^{|E|} C_p\, I_p^s \leq \lambda\ \frac{\sum_{p=1}^{|E|} C_p}{|S|}, \qquad s \in \{1, ..., |S|\}, \tag{3.25}$$

where λ is the workload balancing multiplier defined as the ratio between the maximum allowed workload per sector and the average workload in all sectors (e.g. = 1.5), and $|S|$

is the number of sectors in the MSA. If $\lambda = 1$, then (3.25) will ensure that the number of conflicts is the same in all sectors. If $\lambda = |S|$, then (3.25) is relaxed and there is no balancing of the conflicts. In section 3.5.7 we will determine experimentally the values of λ for high and low density air traffic.

3.2.5 MSP-SH/C formulation

To be concise, we define $\mathcal{A} := \{1, 2, ..., A\}$, $\mathcal{J} := \{1, 2, ..., J\}$, $\mathcal{M}_i := \{1, 2, ..., N(i)\}$, $\bar{\mathcal{M}}_i := \{1, 2, ..., N(i) - 1\}$, $\mathcal{K} := \{1, 2, ..., K\}$ and $\mathcal{P} := \{1, 2, ..., |E|\}$. The complete model takes the following form :

$$\min_{P(i),T_i(m)} \sum_{p=1}^{|E|} C_p \tag{3.26}$$

subject to

Heading changes constraint :

$\sum_{i=1}^{J} I_a(i)P(i) = 1, \qquad a \in \mathcal{A}$

Speed changes constraints :

$t'_i(m) = t_i(1) + \sum_{w=1}^{m-1} T_i(w), \qquad m \in \mathcal{M}_i - \{1\},\ i \in \mathcal{J},$

$t'_i(1) = t_i(1), \qquad i \in \mathcal{J},$

$\sum_{a=1}^{A} \frac{I_a(i)}{v_a^+} \leq \frac{T_i(m)}{D_i(m)} \leq \sum_{a=1}^{A} \frac{I_a(i)}{v_a^-}, \qquad i \in \mathcal{J},\ m \in \bar{\mathcal{M}}_i,$

Number of modified trajectories constraints :

$t'_i(m) - t_i(m) \leq \mathcal{I}_s(i)\ (t_i^+(m) - t_i(m) + 1), \qquad i \in \mathcal{J},\ m \in \mathcal{M}_i,$

$t_i(m) - t'_i(m) \leq \mathcal{I}_s(i)\ (t_i(m) - t_i^-(m) + 1), \qquad i \in \mathcal{J},\ m \in \mathcal{M}_i,$

$\sum_{i=1}^{J} \mathcal{I}_s(i) \leq \alpha\ A,$

$\mathcal{I}_h(a) = 1 - P(3a - 2), \qquad a \in \mathcal{A},$

$\mathcal{I}_h(a) + \sum_{i=1}^{J} I_a(i)\ \mathcal{I}_s(i) \leq 2\ \mathcal{I}(a), \qquad a \in \mathcal{A},$

$\mathcal{I}_h(a) + \sum_{i=1}^{J} I_a(i)\ \mathcal{I}_s(i) \geq 2\ (\mathcal{I}(a) - 0.9), \qquad a \in \mathcal{A},$

$\sum_{a=1}^{A} \mathcal{I}(a) \leq \gamma\ A,$

Conflict detection constraints :

$L_{i(p)}(m, k) + L_{j(p)}(n, k) \leq 2 - H_p(k), \qquad p \in \mathcal{P},\ \ k \in \mathcal{K},$

$L_{i(p)}(m, k) + L_{j(p)}(n, k) \geq 1.1 - 2\ H_p(k), \qquad p \in \mathcal{P},\ \ k \in \mathcal{K},$

$\hat{t}_i(w) = t'_i(m) + \dfrac{T_i(m)}{D_i(m)}\ d_i(w), \qquad i \in \mathcal{J},\ w \in \{1, 2, ..., W(i)\},$

$\hat{t}_{i(p)}(w_1) + S_p - \hat{t}_{j(p)}(w_2) \leq (1 - A_p)\ M_p^1, \qquad p \in \mathcal{P},$

$\hat{t}_{i(p)}(w_1) + S_p - \hat{t}_{j(p)}(w_2) \geq -A_p\ M_p^1, \qquad p \in \mathcal{P},$

$\hat{t}_{j(p)}(w_2) + S_p - \hat{t}_{i(p)}(w_1) \leq (1 - B_p)\ M_p^2, \qquad p \in \mathcal{P},$

$\hat{t}_{j(p)}(w_2) + S_p - \hat{t}_{i(p)}(w_1) \geq -B_p\ M_p^2, \qquad p \in \mathcal{P},$

$A_p + B_p + \sum_{k=1}^{K} H_p(k) - P(i(p)) - P(j(p)) + 2 - K \geq -5\ C_p, \quad p \in \mathcal{P},$

$A_p + B_p + \sum_{k=1}^{K} H_p(k) - P(i(p)) - P(j(p)) + 2 - K \leq 5\ (1 - C_p), \quad p \in \mathcal{P},$

Balancing constraints :

$\sum_{p=1}^{|E|} C_p\, I_p^s \leq \lambda\ \frac{\sum_{p=1}^{|E|} C_p}{|S|}, \qquad s \in \{1, ..., |S|\},$

Integrality and nonnegativity constraints :

$C_p,\ A_p,\ B_p,\ H_p(k) \in \{0, 1\}, \qquad p \in \mathcal{P},\ k \in \mathcal{K},$

$\mathcal{I}_h(a),\ \mathcal{I}(a) \in \{0, 1\}, \qquad a \in \mathcal{A},$

$P(i),\ \mathcal{I}_s(i) \in \{0, 1\}, \qquad i \in \mathcal{J},$

$T_i(m) \in \mathbb{R}^+, \qquad i \in \mathcal{J},\ m \in \bar{\mathcal{M}}_i$

$t'_i(m),\ \hat{t}_i(w) \in \mathbb{R}^+, \qquad i \in \mathcal{J},\ m \in \mathcal{M}_i,\ w \in \{1, 2, ...W(i)\}.$

This model can be solved optimally using a commercial solver such as Gurobi, Cplex or Lingo. Note that the model input parameters are $\alpha, \gamma, \lambda, A, D_i(m), |E|, I_a(i), J, K, L_i(m, k), M_p^1, M_p^2, N(i), S_p, t_i(m), t_i^-(m), t_i^+(m), v_a^-, v_a^+$ and $W(i)$. If we use $\lambda = |S|$, i.e. no balancing, a feasible solution always exists because the original trajectories are part of the search space and satisfy all the constraints. The lower bound of the objective function is 0 while the upper bound is $|E|$. Following that there exists at least one feasible solution, in case of no balancing, and that the objective function is bounded, there exists at least one optimal solution. For an air traffic situations there may exist multiple different solutions that lead to the same reduction in the number of conflicts. For example, for a simple situation with only two aircraft in conflict there may exist two optimal solutions leading to eliminate the conflict. The first is to modify the trajectory of one of the aircraft and the other solution is to modify the other trajectory.

In this work we use Gurobi 6.5.0 solver and we set it to try to find one proven optimal solution. The input data has to pass by a preprocessing stage to generate the input data in the suitable format, i.e. model parameters, after which the problem is solved to generate the modified trajectories. An integrated definition of function modelling (IDEF0) model of the MSP-SH/C is presented in Figure 3.10. In Figure 3.10, we see that the preprocessing stage takes as input the flight plans of all aircraft that pass through the MSA over a time horizon of 20 to 90 minutes. It takes also aircraft related data i.e. the cruising, maximum and minimum speeds. Finally, it takes information related to the sectors geometry i.e. the coordinates of the sector boundaries. The output of this stage includes the alternative flight plans as a result of the heading change manoeuvres, the set E of flight plan pairs that are at risk of a crossing conflict, the safe separation time S_p for each pair and the sector indicator matrix I_p^s. The output also includes information regarding the intersection points for each flight plan $(W(i), d_i(w), D_i(m))$ and the values of M_p^1 and M_p^2 that are needed for (3.19) and (3.21). We programmed the preprocessing stage using MATLAB 8.4. In the solution stage, a commercial solver takes the data from the preprocessing stage along with the allowed per-

centages of modification α and γ, the balancing factor λ and generates the optimal solution.

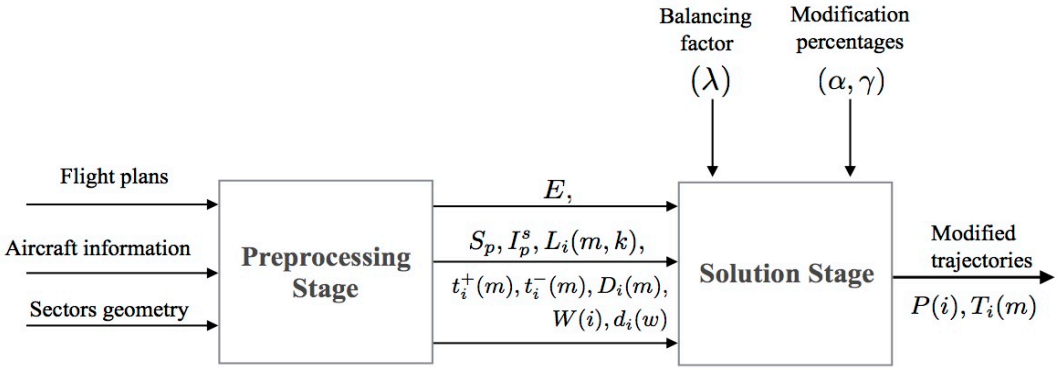

Figure 3.10 IDEF0 for the MSP-SH/C model.

In the following section, we present an example detailing the input data, the output of the preprocessing stage and an optimal solution.

3.3 Detailed example

In this section we present an example that consists of eight aircraft that are planned to pass through a designated MSA within a time interval of 20 to 90 minutes. This MSA is composed of four square adjacent sectors of 200 km side (Figure 3.11).

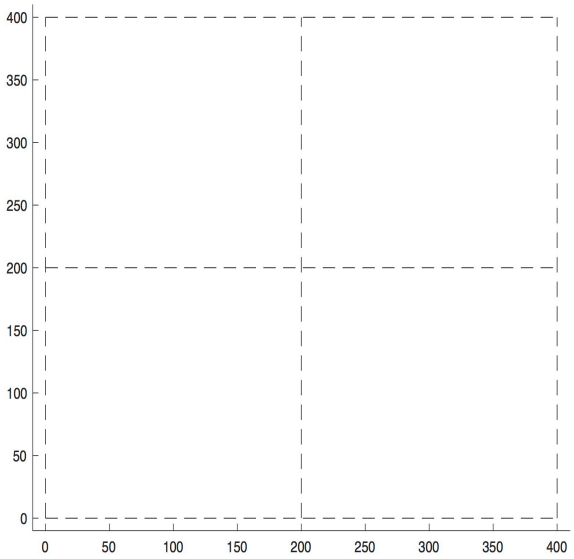

Figure 3.11 The multi-sector area of the detailed example.

We assume that all aircraft use a cruise speed of 485 knots ($\simeq$ 900 km/h) with a minimum allowed speed of 456 knots ($\simeq$ 850 km/h) and a maximum allowed speed of 513 knots ($\simeq$ 950 km/h). We will use these limits for the allowed speed modifications, which represent $\pm 6\%$ of the cruise speed.

The trajectory of each aircraft according to the original plans is illustrated in Figure 3.12-a, where $*$ represents a waypoint and $\bigcirc$ represents a conflict. We chose these trajectories so that they present the following cases :

- an aircraft is involved in two conflicts in two different sectors (aircraft 1), to show the model ability to solve two conflicts in different sectors using one trajectory modification,
- three aircraft are involved in a three-way conflict (aircraft 4, 5 and 6), to show that the model can be used to solve large problems and not only pairwise conflicts,
- a conflict between two aircraft that cannot be resolved by using only speed changes (aircraft 7 and 8), to force the model to use a heading change manoeuvre.

Following our definition of the heading change manoeuvres, we introduce two additional flight plans for each aircraft as shown in Figure 3.3. The detailed data of the original and alternative flight plans are presented in Table 3.1. Note that in Table 3.1 the waypoint data are given in km and minute and that flight plans 1, 4, 7, ... are the original flight plans, i.e. input for the preprocessing stage, and that the rest are the result of the preprocessing stage. Using Table 3.1, it can be shown that if all aircraft follow their original trajectories then the conflict cases mentioned above are present.

In the preprocessing stage, we check all intersecting flight plan pairs to determine whether they are at risk of a crossing conflict or not. After applying the preprocessing stage, there are 88 different pairs of flight plans that satisfy the conditions (3.4) and (3.5), i.e. that belong to E. Note that E includes also the alternative flight plans and not only the original trajectories. Table 3.2 shows the indices $i(p)$ and $j(p)$ of each flight plan pair p in E along with the minimum separation time S_p in seconds. For example we can see in Table 3.2 for the first three pairs, that flight plan 1, which is the original flight plan of aircraft 1, is at risk of a conflict with flight plans 4, 5 and 6 that correspond to aircraft 2. Also, we can see that the minimum separation time S_p for these three pairs is 53.9 seconds.

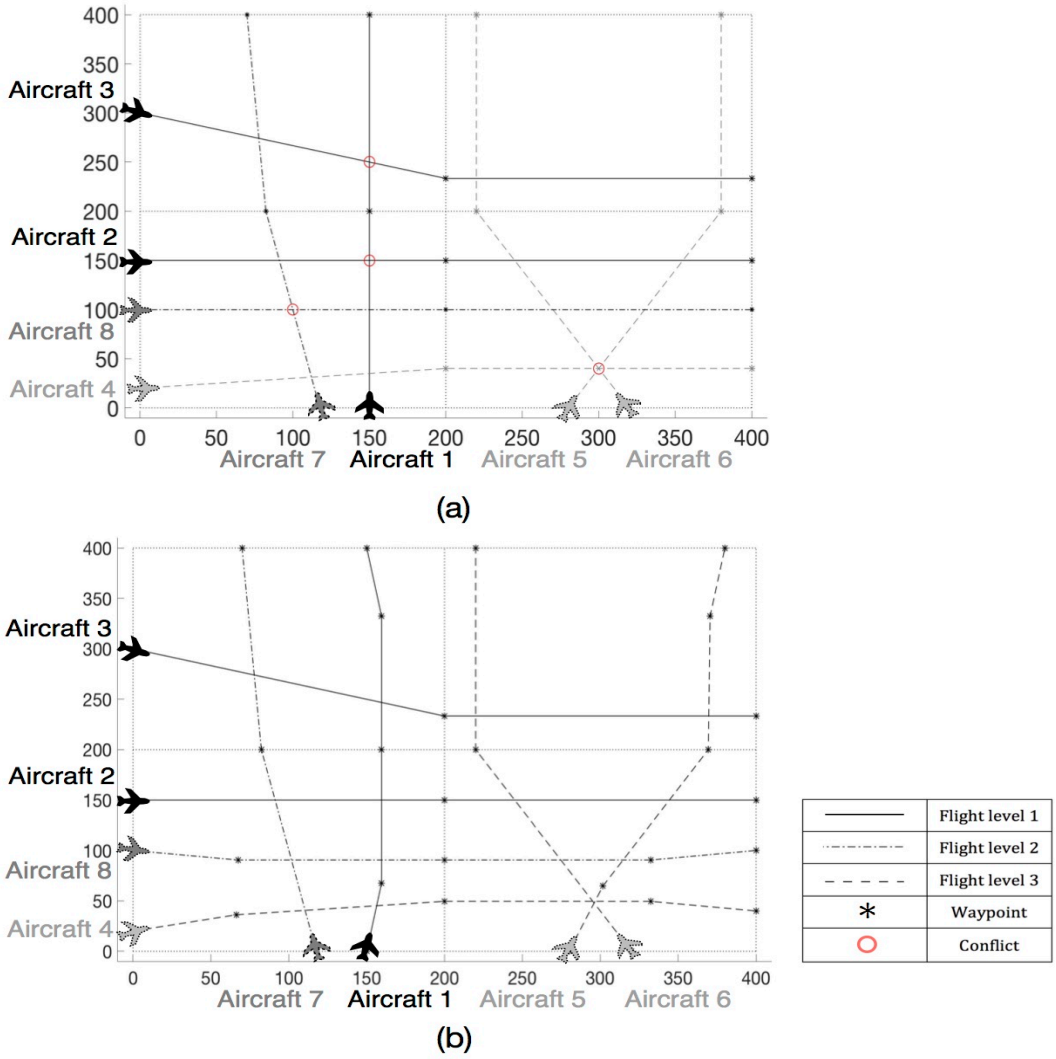

Figure 3.12 Aircraft trajectories for the detailed example : (a) original trajectories ; (b) modified trajectories.

Table 3.1 Flight plans for the detailed example, (x, y) in km and $t_i(m)$ in minutes

Aircraft index (a)	**Flight plan (i)**	**Waypoint 1**		**Waypoint 2**		**Waypoint 3**		**Waypoint 4**		**Waypoint 5**		$N(i)$
		(x, y, z)	$t_i(1)$	(x, y, z)	$t_i(2)$	(x, y, z)	$t_i(3)$	(x, y, z)	$t_i(4)$	(x, y, z)	$t_i(5)$	
1	1	(150,0,1)	24.8	(150,200,1)	38.13	(150,400,1)	51.46	-	-	-	-	3
1	2	(150,0,1)	24.8	(159.5,67.6,1)	29.35	(159.5,200,1)	38.18	(159.5,332.4,1)	47	(150,400,1)	51.56	5
1	3	(150,0,1)	24.8	(140.5,67.6,1)	29.35	(140.5,200,1)	38.18	(140.5,332.4,1)	47	(150,400,1)	51.56	5
2	4	(0,150,1)	25	(200,150,1)	38.33	(400,150,1)	51.67	-	-	-	-	3
2	5	(0,150,1)	25	(67.6,140.5,1)	29.55	(200,140.5,1)	38.38	(332.4,140.5,1)	47.21	(400,150,1)	51.76	5
2	6	(0,150,1)	25	(67.6,159.5,1)	29.55	(200,159.5,1)	38.38	(332.4,159.5,1)	47.21	(400,150,1)	51.76	5
3	7	(0,300,1)	30.53	(200,233.3,1)	44.58	(400,233.3,1)	57.91	-	-	-	-	3
3	8	(0,300,1)	30.53	(61.1,269.6,1)	35.08	(200,223.3,1)	44.84	(332.4,223.8,1)	53.66	(400,233.3,1)	58.2	5
3	9	(0,300,1,)	30.53	(67.1,287.6,1)	35.08	(200,243.3,1)	44.41	(332.4,242.8,1)	53.24	(400,233.3,1)	57.79	5
4	10	(0,20,2)	21	(200,40,2)	34.4	(400,40,2)	47.7	-	-	-	-	3
4	11	(0,20,2)	21	(68.2,17.3,2)	25.55	(200,30.5,2)	34.38	(332.4,30.5,2)	43.21	(400,40,2)	47.76	5
4	12	(0,20,2)	21	(66.3,36.2,2)	25.55	(200,49.6,2)	34.51	(332.4,49.5,2)	43.33	(400,40,2)	47.89	5
5	13	(280,0,2)	38.39	(380,200,2)	53.29	(380,400,2)	66.63	-	-	-	-	3
5	14	(280,0,2)	38.39	(318.7,56.2,2)	42.94	(390.6,200,2)	53.65	(389.5,332.4,2)	62.48	(380,400,2)	67.03	5
5	15	(280,0,2)	38.39	(301.73,64.71,2)	42.94	(369.38,200,2)	53.02	(370.5,332.4,2)	61.85	(380,400,2)	66.4	5
6	16	(320,0,2)	38.7	(220,200,2)	53.61	(220,400,2)	66.94	-	-	-	-	3
6	17	(320,0,2)	38.7	(298.3,64.7,2)	43.25	(230.62,200,2)	53.34	(229.5,332.4,2)	62.16	(220,400,2)	66.71	5
6	18	(320,0,2)	38.7	(281.3,56.2,2)	43.25	(209.4,200,2)	53.97	(210.5,332.4,2)	62.8	(220,400,2)	67.35	5
7	19	(117.6,0,3)	24.8	(82.4,200,3)	38.34	(70,400,3)	51.7	-	-	-	-	3
7	20	(117.6,0,3)	24.8	(115.2,68.2,3)	29.35	(92,200,3)	38.27	(83.7,333.1,3)	47.16	(70,400,3)	51.71	5
7	21	(117.6,0,3)	24.8	(96.5,64.9,3)	29.35	(72.7,200,3)	38.5	(64.7,331.9,3)	47.31	(70,400,3)	51.86	5
8	22	(0,100,3)	24.9	(200,100,3)	38.23	(400,100,3)	51.57	-	-	-	-	3
8	23	(0,100,3)	24.9	(67.6,90.5,3)	29.45	(200,90.5,3)	38.28	(332.4,90.5,3)	47.11	(400,100,3)	51.66	5
8	24	(0,100,3)	24.9	(67.6,109.5,3)	29.45	(200,109.5,3)	38.28	(332.4,109.5,3)	47.11	(400,100,3)	51.66	5

We solved this example optimally in less than 0.5 seconds using Gurobi 6.5.0 on a MacBook pro having 16.0 GB of RAM supported by an Intel® Core i7 running at 2.6GHz with a 6MB cache size, operated with OS X 10.12.1. For this example, the model has 1263 binary variables, 240 continuous variables and 2361 constraints. The example was solved while allowing for 50% of the trajectories to be modified ($\alpha = 0.5, \gamma = 0.5$) and with equal balancing among sectors ($\lambda = 1$).

Our model was able to eliminate all six conflicts by modifying only four aircraft trajectories. The values of the decision variables $P(i)$ and $T_i(m)$ in the optimal solution are presented in Table 3.3. Notice that the values of the decision variables determine the values of all the model variables and subsequently the modified trajectory of each aircraft. The aircraft trajectories in the solution are illustrated in Figure 3.12-b and presented in details in Table 3.4. Note that as the predefined heading changes are modelled as different possible flight plans, there is no need to repeat the spatial coordinates of the waypoints and only the new passage times in minutes are presented in Table 3.4. Note that the index of the original trajectory of aircraft a is $3a - 2$. For example we can see in Table 3.4 that aircraft 1 follows flight plan 2, thus it undergoes a heading change manoeuvre. Also, by comparing the waypoint passage time to that in Table 3.1, we can see that aircraft 1 also undergoes a speed up change that results in decreasing the passage time of its last waypoint by approximately 1 minute.

From these results we can see that by applying a heading and a speed change on the trajectory of aircraft 1, two conflicts were avoided in two different sectors. We can also notice that MSP-SH/C was able to solve a conflict involving three aircraft (4, 5 and 6). The model considers a three-way conflict as three pairwise conflicts. The model solved these conflicts by modifying the trajectories of aircraft 4 and 5 as shown in Figure 3.12-b. Finally, as the conflict between aircraft 7 and 8 cannot be avoided through speed modifications, the model enforces a heading change on aircraft 8.

In the following section, we test the capacity of MSP-SH/C to detect and solve crossing conflicts using a set of known CDR benchmark test problems.

3.4 Conflict detection and resolution for the circle problem

In real air traffic situations, the complexity and the solution of a CDR problem depends on many parameters other than the number and speed of aircraft. Such parameters include the sector geometry, location and number of conflicts and original aircraft trajectories. As a result, researchers in the CDR domain turned to unrealistic standardized problems. These problems have a complexity that depends only on the number of aircraft.

One of the most used benchmark test problems in the CDR literature is the circle problem.

Table 3.2 Flight pairs at risk of a crossing conflict - E

p	1	2	3	4	5	6	7	8	9	10	11	12	13	14	15	16
i(p)	1	1	1	1	1	1	2	2	2	2	2	2	3	3	3	3
j(p)	4	5	6	7	8	9	4	5	6	7	8	9	4	5	6	7
S_p	53.9	53.9	53.9	65.2	65.2	65.2	53.9	53.9	53.9	65.2	65.2	65.2	53.9	53.9	53.9	65.2

p	17	18	19	20	21	22	23	24	25	26	27	28	29	30	31	32
i(p)	3	3	4	4	4	5	5	5	6	6	6	7	7	7	8	8
j(p)	8	9	13	14	15	13	14	15	13	14	15	13	14	15	13	14
S_p	65.2	65.2	44.8	44.8	44.8	43.1	43.1	43.1	46.9	46.9	46.9	53.9	54.1	53.7	50.5	50.7

p	33	34	35	36	37	38	39	40	41	42	43	44	45	46	47	48
i(p)	8	9	9	9	10	10	10	10	10	10	10	11	11	11	11	11
j(p)	15	13	14	15	21	13	14	15	16	17	18	13	14	15	16	17
S_p	50.3	58.1	58.4	57.8	60.8	44.8	43.1	46.9	72.5	65.3	82.0	44.8	43.1	46.9	72.5	65.3

p	49	50	51	52	53	54	55	56	57	58	59	60	61	62	63	64
i(p)	11	12	12	12	12	12	12	12	12	12	13	13	13	13	13	13
j(p)	18	19	20	21	13	14	15	16	17	18	16	17	18	22	23	24
S_p	81.9	56.0	52.2	60.8	44.8	43.1	47.0	72.5	65.3	82.0	42.6	41.3	44.3	44.8	44.8	46.9

p	65	66	67	68	69	70	71	72	73	74	75	76	77	78	79	80
i(p)	14	14	14	14	14	14	15	15	15	15	15	15	16	17	17	19
j(p)	16	17	18	22	23	24	16	17	18	22	23	24	23	22	23	22
S_p	44.3	42.6	46.3	44.8	43.1	46.9	41.3	40.2	42.6	44.8	44.8	44.8	72.5	72.5	72.5	59.3

p	81	82	83	84	85	86	87	88
i(p)	19	19	20	20	20	21	21	21
j(p)	23	24	22	23	24	22	23	24
S_p	59.3	59.3	59.3	59.3	59.3	59.3	59.3	59.3

Table 3.3 The values of the decision variables for the optimal solution of the detailed example- $T_i(m)$ in minutes

i	1	2	3	4	5	6	7	8	9	10	11	12
$\boldsymbol{P(i)}$	0	1	0	1	0	0	1	0	0	0	0	1
$\boldsymbol{T_i(1)}$	13.33	4.37	4.55	13.33	4.55	4.55	14.06	4.55	4.55	13.4	4.55	4.54
$\boldsymbol{T_i(2)}$	13.33	8.48	8.83	13.33	8.83	8.83	13.33	9.76	9.34	13.34	8.83	8.94
$\boldsymbol{T_i(3)}$	0	8.48	8.83	0	8.83	8.82	0	8.83	8.83	0	8.82	8.81
$\boldsymbol{T_i(4)}$	0	4.37	4.55	0	4.55	4.55	0	4.55	4.55	0	4.55	4.54

i	13	14	15	16	17	18	19	20	21	22	23	24
$\boldsymbol{P(i)}$	0	0	1	1	0	0	1	0	0	0	1	0
$\boldsymbol{T_i(1)}$	14.91	4.55	4.32	14.91	4.55	4.55	13.54	4.55	4.55	13.33	4.82	4.55
$\boldsymbol{T_i(2)}$	13.33	10.72	10.1	13.33	10.08	10.72	13.36	8.92	9.14	13.33	8.52	8.83
$\boldsymbol{T_i(3)}$	0	8.83	8.36	0	8.83	8.83	0	8.89	8.81	0	8.36	8.83
$\boldsymbol{T_i(4)}$	0	4.55	4.82	0	4.55	4.55	0	4.55	4.55	0	4.31	4.55

Table 3.4 Optimal solution of the detailed example - modified trajectories

Aircraft index (a)	**Flight plan (i)**	**Waypoint 1** $t_i(1)$	**Waypoint 2** $t_i(2)$	**Waypoint 3** $t_i(3)$	**Waypoint 4** $t_i(4)$	**Waypoint 5** $t_i(5)$
1	2	24.8	29.171	37.65	46.128	50.499
2	4	25	38.333	51.667	-	-
3	7	30.526	44.58	57.914	-	-
4	12	21	25.54	34.479	43.287	47.829
5	15	38.385	42.704	52.808	61.171	65.989
6	16	38.7	53.607	66.94	-	-
7	19	24.8	38.339	51.698	-	-
8	23	24.903	29.721	38.242	46.605	50.916

In this problem, a number A of aircraft are evenly distributed on a circle of a radius r and are all flying with the same speed v in a direct line towards the circle centre as shown in Figure 3.13. This problem was first introduced by Durand et al. (1996) to test a genetic algorithm to solve the CDR problem. The number of conflicts $\mathcal{N}$ is given by $\mathcal{N} = A(A-1)/2$. The circle problem was used to test the ability of CDR models to solve complicated conflicts (Durand and Alliot, 2009; Omer and Farges, 2012; Rey et al., 2015; Alonso-Ayuso et al., 2015, 2016).

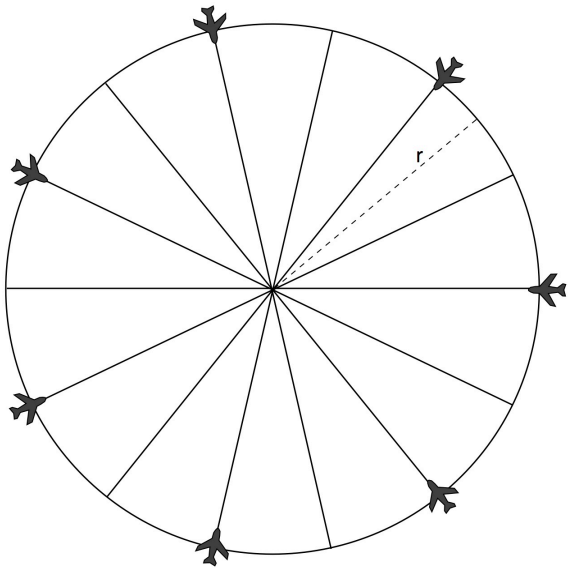

Figure 3.13 Example of a 7 aircraft circle problem.

To assess the ability of our model MSP-SH/C to detect and solve crossing conflicts in a reasonable amount of time, we tested it using a set of circle problems. For each problem, MSP-SH/C considers the circle as a single sector. We considered the safe separation distance $D = 5$ NM, the cruise speed for all aircraft is constant and equals to 485 knots and the circle radius is $r = 200$ km(≈ 108 NM). The allowed speed change is of $\pm 6\%$. We first solved the problem for the MSP-SH/C model using a heading change of $\phi = 8°$ turning angle and a separation distance between the alternative flight plans $d = 5$ NM as presented in section

3.1.1. We limited solution time to 10 minutes. If the solver, i.e. Gurobi, is not able to determine the optimal solution in less than 10 minutes, then it will return the best solution found.
The results for solving a set of circle problems using $\alpha = 1$ and $\gamma = 1$ are presented in Table 3.5. We chose an odd number of aircraft to avoid the head-to-head conflicts that are present if this number is even. The optimal solution was obtained for problems with up to 9 aircraft in a small amount of time (≤ 17 seconds). In these problems, the model was able to generate conflict free solution. For the problem involving 11 aircraft, the model was not able to find a solution with no conflicts in less than 10 minutes. The solution found after 10 minutes includes 4 unresolved conflicts. By allowing the model to run for 13.8 minutes, we were able to determine that this is in fact the optimal solution.

For the circle problem, Durand et al. (1996) stated that the conflict free solutions include the turning of all aircraft in the same direction. We observed a similar behaviour for the problems solved in Table 3.5. Figure 3.14 shows the original and modified trajectories for the circle problem involving 5 aircraft. We observe that all the aircraft took a heading change to the left.

As the allowed heading change manoeuvres have a limited magnitude, we thought that by allowing larger heading changes the model would be able to reach conflict free solutions for larger problems. So we tested the model with a second set of circle problems where we increased the turning angle to $\phi = 12°$ and used larger values for the separation distance d. The results of this second test are given in Table 3.6. For a separation distance between the alternative plans $d = 15$ NM, the conflict free optimal solution for problems involving up to 21 aircraft were obtained in less than one second. For the problem involving 23 aircraft and 253 conflicts, the optimal solution was obtained in more than 10 minutes and it includes one unresolved conflict (Figure 3.15). By increasing the value of d to 20 NM, we were able to reach conflict free solutions for problems with up to 25 aircraft and 300 conflicts in less than a second. We concluded that all conflicts can be resolved by allowing larger trajectories modifications.

Table 3.5 Performance of MSP-SH/C on the circle problem with $\phi = 8°$

A	$\mathcal{N}$	**number of unsolved conflicts**	**Reduction of the number of conflicts (%)**	**Computational time (s)**
5	10	0	100	0.02
7	21	0	100	0.24
9	36	0	100	17.03
11	55	4	92.7	600

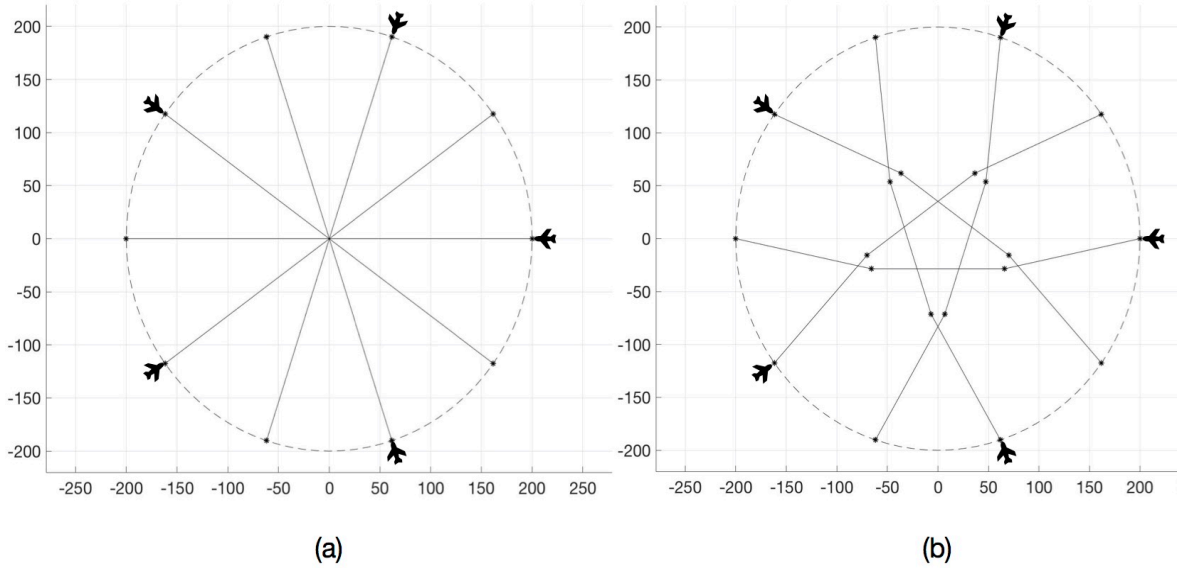

Figure 3.14 Example of a 5 aircraft circle problem : (a) original trajectories; (b) modified trajectories.

Table 3.6 Performance of MSP-SH/C on the circle problem with $\phi = 12°$

A	$\mathcal{N}$	d (NM)	**number of unsolved conflicts**	**Reduction of the number of conflicts (%)**	**Computational time (s)**
5	10	15	0	100	0.01
7	21	15	0	100	0.04
9	36	15	0	100	0.06
11	55	15	0	100	0.06
13	78	15	0	100	0.1
15	105	15	0	100	0.14
17	136	15	0	100	0.29
19	171	15	0	100	1.39
21	210	15	1	99.5	600
21	210	20	0	100	0.31
23	253	20	0	100	0.48
25	300	20	0	100	0.55

3.5 Numerical experiments

In this section, we conduct three different sets of experiments on the MSP-SH/C model. In the first set, we solve a large number of randomly generated problems with varying number of conflicts using MSP-SH/C. The problems will be solved using different combinations of manoeuvres to test and assess the model capacity to solve a large number of conflicts in a reasonable amount of time. In the second set, we test the performance of our model while varying the allowed percentage of modified trajectories γ. In the third set of tests, we solve randomly generated problems with different balancing levels to demonstrate the potential benefits of considering workload balancing.

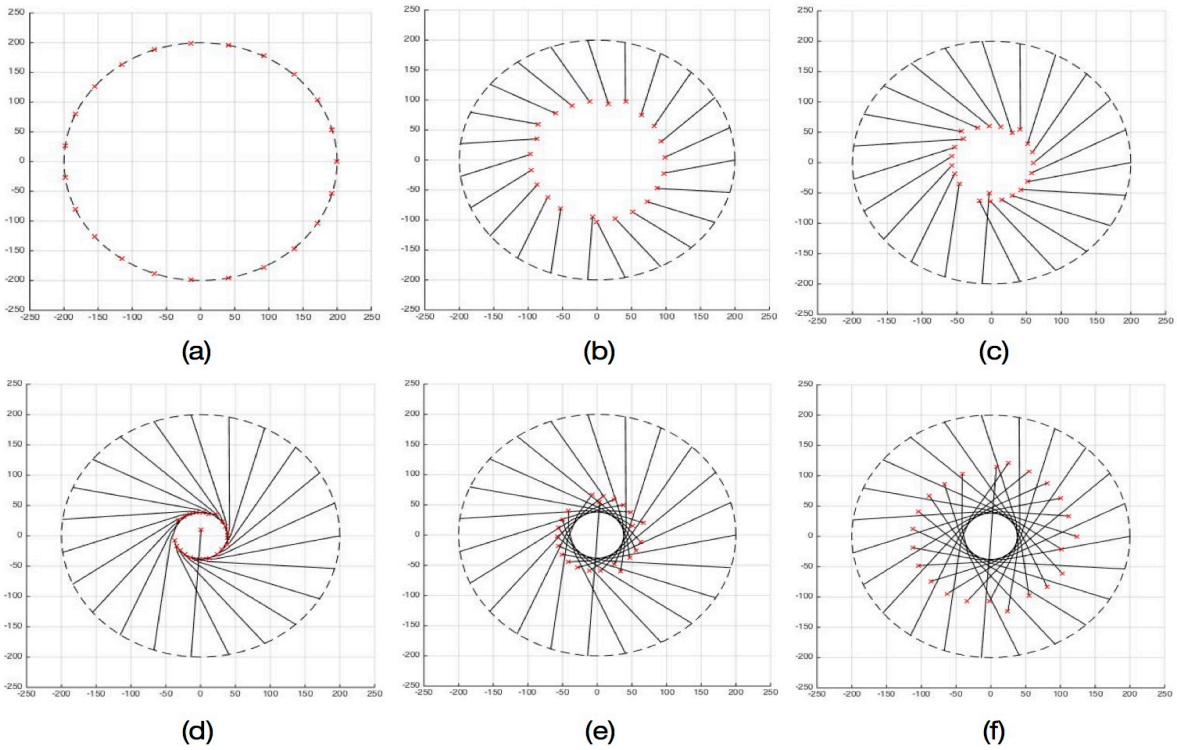

Figure 3.15 Solution of a circle problem with 23 aircraft at : (a) time=0 ; (b) time= 7 min, (c) time= 10 min ; (d) time= 14 min ; (e) time= 17 min ; (f) time = 21 min.

3.5.1 Experimental design

In the tests presented in the following sections, we solve randomly generated problems using different combinations of allowed manoeuvres. In this section, we present first the different model variants used to solve the problems then the complete description of the problems.

Model variants

For this chapter we have four different model variants. The first variant uses only speed changes limited to $[-0.06\ \bar{v}_a, 0.03\ \bar{v}_a]$. The second uses large speed changes in the range of $[-0.12\ \bar{v}_a, 0.06\ \bar{v}_a]$. The third allows for only heading changes. The last variant solves the problems using a combination of small speed changes and heading changes.
Solving the complexity resolution problems using only speed changes requires the introduction of the constraint :

$$P(3a-2) = 1, \qquad a \in \{1, 2, ..., A\}, \tag{3.27}$$

to prevent heading changes. This constraint enforces the use of the original spatial waypoints but still permits speed change. This variant of the model will be denoted by MSP-S/C, which stands for *Multi-Sector Planning support model using Speed changes for Crossing conflicts*. It is formulated as

$$\begin{cases} \min\limits_{P(i),T_i(m)} \sum\limits_{p=1}^{|E|} C_p, \\ \text{subject to} \\ (3.7)-(3.17),\ (3.19), (3.21), (3.23)-(3.25) \text{ and } (3.27) \\ C_p,\ P(i),\ \mathcal{I}_s(i),\ \mathcal{I}_h(a),\ \mathcal{I}(a),\ H_p(k),\ A_p,\ B_p \in \{0,1\} \quad p \in \{1,2,...,|E|\}, \\ \ i \in \{1,2,...,J\},\ a \in \{1,2,...,A\},\ k \in \{1,2,...,K\}, \\ T_i(m) \in \mathbb{R}^+, \qquad i \in \{1,2,...,J\},\ m \in \{1,2,...,N(i)-1\} \\ t'_i(m),\ \hat{t}_i(w) \in \mathbb{R}^+, \qquad i \in \{1,2,...,J\},\ m \in \{1,2,...,N(i)\},\ w \in \{1,2,...W(i)\}. \end{cases} \tag{3.28}$$

The only difference between MSP-SH/C (3.26) and MSP-S/C (3.28) is the introduction of the constraint (3.27).

Solving the problem by allowing only heading changes can be easily done by setting the percentage of speed modified trajectories α to 0 in MSP-SH/C. This is a new variant of our model that we will denote by MSP-H/C, which stands for *Multi-Sector Planning support model using Heading changes for Crossing conflicts*.

Randomly generated problems

All the randomly generated problems in this chapter consider a number A of aircraft passing through a MSA composed of four square adjacent sectors of 300 km side. The aircraft use four different flight levels which are all part of the MSA. The MSA in these problems takes the same shape as in the detailed example of section 3.3. The aircraft trajectories are randomly generated in such a way that all aircraft are either flying from bottom to upper MSA borders, or from left to right borders. Taking the origin at the bottom left corner of the MSA, the distance between the first waypoint and the origin is randomly generated using the uniform distribution U[75 km, 595 km]. The first waypoint is located on either the bottom or the left MSA border. We forbid the generation of the first waypoint to be in the regions $(X = 0, Y \in [0, 75])$ and $(X \in [0, 75], Y = 0)$ to avoid unsolvable conflicts. If a conflict is to happen in the bottom left 75 km $\times$ 75 km square, then this means that the aircraft will be in conflict just after their entry to the MSA. Consequently, there is not enough space or time to avoid such a conflict. The remaining of the waypoints are generated along the opposing sector borders

following a uniform distribution.
The cruise speeds of the aircraft are randomly generated using the uniform distribution U[458 knots, 506 knots]. The minimum and maximum speed, which are used to evaluate the minimum separation time S_p with (3.2), are set to -12% and $+6\%$ of the cruise speed. In real air traffic situations, these limits shall be set to the minimum and maximum allowed speed for each aircraft. We emphasize that these limits generally differ from the limits on allowed speed change manoeuvre in (3.10). In these problems, the allowed speed change limits are bounded to $[-6\%, +3\%]$ of the cruising speed for small speed changes and $[-12\%, +6\%]$ of the cruising speed for large speed changes.
The time at which the aircraft enters the MSA follows the uniform distribution U[20 min, 90 min]. The flight level used for each trajectory is randomly generated following a discrete uniform distribution U$\{1, K\}$. 90% of the aircraft use a single flight level along their trajectory in the MSA. The remaining 10% undergoes one flight level change at the internal boundary. For these aircraft, the second flight level is also randomly generated using U$\{1, K\}$ while excluding the flight level followed in the first sector.
The problems will be identified by the number A of aircraft passing through the MSA. As the trajectories are generated randomly, the number of conflicts for a given value of A is also random. Following Orth et al. (2012), we plotted in Figure 3.16 the average number of conflicts $\bar{\mathcal{N}}$ as a function of the number of problem replications n to determine an appropriate number of replications for the tests. In Figure 3.16, we observe that a fairly accurate estimate of $\bar{\mathcal{N}}$ is obtained for $n = 50$, i.e. the standard deviation of $\bar{\mathcal{N}}$ is less than 5% of $\bar{\mathcal{N}}$ except for $A = 20$ problems (=17%). We think that $n = 50$ represents a good compromise between the precision and computation time. We solved the problems using Gurobi 6.5.0 on a MacBook pro having 16.0 GB of RAM supported by an Intel® Core i7 running at 2.6GHz with a 6MB cache size, operated with OS X 10.12.1.

3.5.2 Computational time

In this section we compare the computational times of the four model variants : MSP-S/C (large), MSP-S/C (small), MSP-H/C and MSP-SH/C. The time for each model variant to find an optimal solution for problems involving up to 150 aircraft, using $\alpha = 0.5$, $\gamma = 0.5$ and $\lambda = 4$, is displayed in Table 3.7. The column avg gives the average time and the column SD gives the standard deviation. The computational time results show the merits of choosing the MILP formulation. The average solution time for problems involving 150 aircraft is less than 3.5 seconds with a standard deviation less than 23% of the average. Raising the magnitude or the number of manoeuvres increases the search space, which increases the computational time. For small (A=20) and medium (A=50 or 70) size problems, the optimal solution is

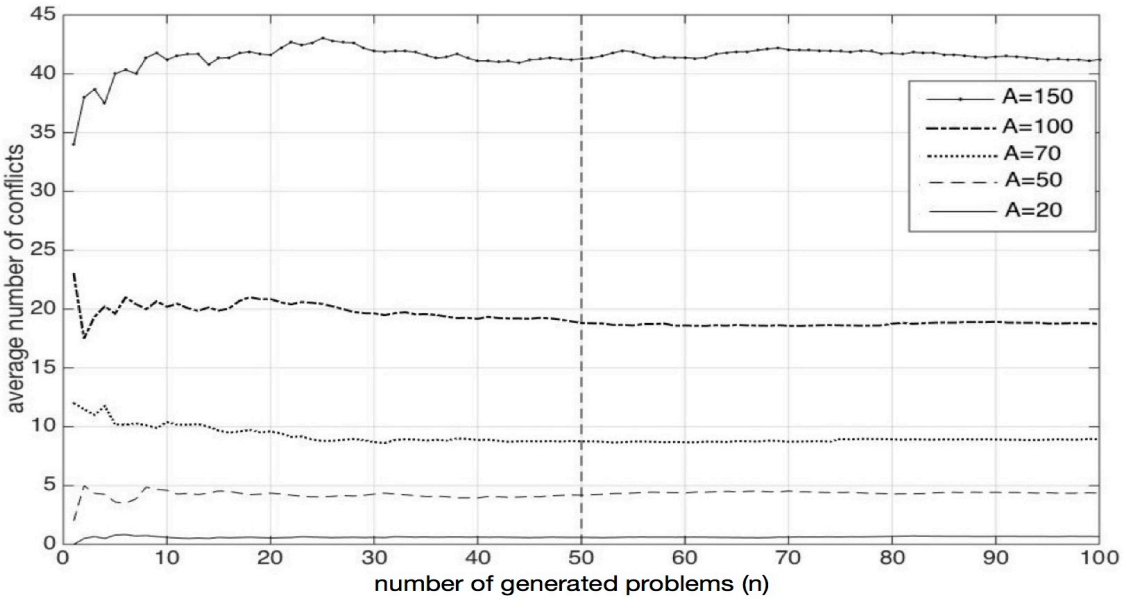

Figure 3.16 Average number of conflicts as a function of the number of problems.

found almost instantaneously with any model variant. For larger problems (A=100 or 150), using only small speed changes or only heading changes gives an optimal solution in less than a second. Using large speed changes or a combination of small speed and heading changes increases this time by 0.5-2.5 seconds on average.

3.5.3 Comparison between the performance of each manoeuvre

Each of the three model variants : MSP-S/C (large), MSP-S/C (small) and MSP-H/C represent the use of only one type of manoeuvre separately. In this section we compare the capacity of each of the three manoeuvres, i.e. large speed changes, small speed changes and heading changes, to solve crossing conflicts by comparing the performance of these model variants. The performance results of the three variants in solving problems involving up to 150 aircraft, using $\alpha = 0.5$, $\gamma = 0.5$ and $\lambda = 4$, are displayed in Table 3.8. In Table 3.8, the column $\bar{\mathcal{N}}$ gives the average number of conflicts before solutions, the column avg (%)

Table 3.7 Computational time in seconds - $\alpha, \gamma = 0.5$ and $\lambda = 4$

Number of aircraft A	**MSP-S/C (large)**		**MSP-S/C (small)**		**MSP-H/C**		**MSP-SH/C**	
	avg	SD	avg	SD	avg	SD	avg	SD
20	0.02	0.004	0.01	0.002	0.008	0	0.04	0.007
50	0.09	0.02	0.06	0.01	0.04	0.006	0.19	0.04
70	0.19	0.04	0.13	0.02	0.08	0.008	0.45	0.08
100	0.51	0.09	0.3	0.04	0.17	0.02	1.16	0.24
150	1.57	0.2	0.88	0.15	0.41	0.04	3.5	0.77

gives the mean percentage of resolved conflicts and the column SD (%) gives the standard deviation.

The results in Table 3.8 show that using any of the three manoeuvres separately solves most of the predicted crossing conflicts. The performances of the three manoeuvres are similar in situations that involve a small number of aircraft. For problems involving 20 aircraft, the average percentages of resolved conflicts are 96%, 91.7% and 95.8% for large speed, small speed and heading changes respectively. The similarity in the performance in these cases is due to the small number of conflicts and aircraft. As the number of aircraft decreases, the probability of having an aircraft involved in more than one conflicts decreases. With few conflicts, small manoeuvres can eliminate most of the conflicts. The large speed change manoeuvre variant shows an expected slight advantage in situations involving a larger number of aircraft. For example, for the problems involving 100 aircraft MSP-S/C (large) eliminated 97.4% of the conflicts, while the MSP-S/C (small) and MSP-H/C resolved 91.1% and 82.2% of the conflicts respectively. Even if the magnitude of heading changes is small, the MSP-H/C reduces the number of crossing conflicts by more than 80%, even in high density situations.

In Table 3.8, we see that the standard deviation is relatively small for all model variants, except for $A = 20$ and $A = 50$ problems. For these problems, the number of conflicts is small and varies between 0 and 3. For some problems there may be only one conflict, and it is not solvable with the allowed manoeuvres. This means that the percentage of resolved conflicts is 0%, which increases the standard deviation. For example, for problems with $A = 20$ while using MSP-S/C (large), we found only two problems from the 50 tested problems with one unsolvable conflict. The model found conflict free solutions for the remaining 48 problems. These two unresolved conflicts lead to a standard deviation of 19.8%.

3.5.4 Comparison between the performance of MSP-S/C (large speed) and MSP-SH/C

In this section we present a comparison between the performance of MSP-S/C (large) and MSP-SH/C. Note that the allowed manoeuvres for MSP-SH/C are small speed changes and heading changes. Table 3.9 displays the results of using both model variants in solving pro-

Table 3.8 Percentage of resolved conflicts using different model variants- $\alpha, \gamma = 0.5$ and $\lambda = 4$

Number of aircraft A	$\bar{\mathcal{N}}$	**MSP-S/C (large)**		**MSP-S/C (small)**		**MSP-H/C**	
		avg (%)	SD (%)	avg (%)	SD (%)	avg (%)	SD (%)
20	1.25	96	19.8	91.7	28	95.8	20.4
50	4.27	98.6	6.7	95.3	10	91.3	18.1
70	8.76	98.7	4.1	94.2	7.8	86.9	10.5
100	18.82	97.4	3.2	91.1	6.5	82.2	9.1
150	41.28	97.8	2.5	91.8	3.9	82.5	5.7

blems up to 150 aircraft. Note that the column *confidence interval* gives the confidence interval with a confidence level of 95%. In Table 3.9, we see that MSP-SH/C eliminated 99%-100% of the conflicts for all problem sizes. For the problem with $A = 100$, the percentage of resolved conflicts using MSP-S/C (large) is in the range $[96.5, 98.2]$ with a confidence level of 95%. For the same problem, the percentage of resolved conflicts using MSP-SH/C is in the range $[98.6, 99.75]$. These results show that the performance of the MSP-SH/C on the average is significantly better than that of MSP-S/C (large) for the problems with $A = 100$. By comparing the confidence intervals of both model variants for the problem with $A = 150$, we conclude also that the performance of the MSP-SH/C on the average is significantly better than that of MSP-S/C (large) for the problems with $A = 150$.

The number of unresolved conflicts for each problem instance for $A = 100$ and $A = 150$ problems using both variants are presented in Figure 3.17. In this figure, we see that MSP-SH/C gives the same or a lower number of conflicts than MSP-S/C (large) for each problem instance and not only on the average.

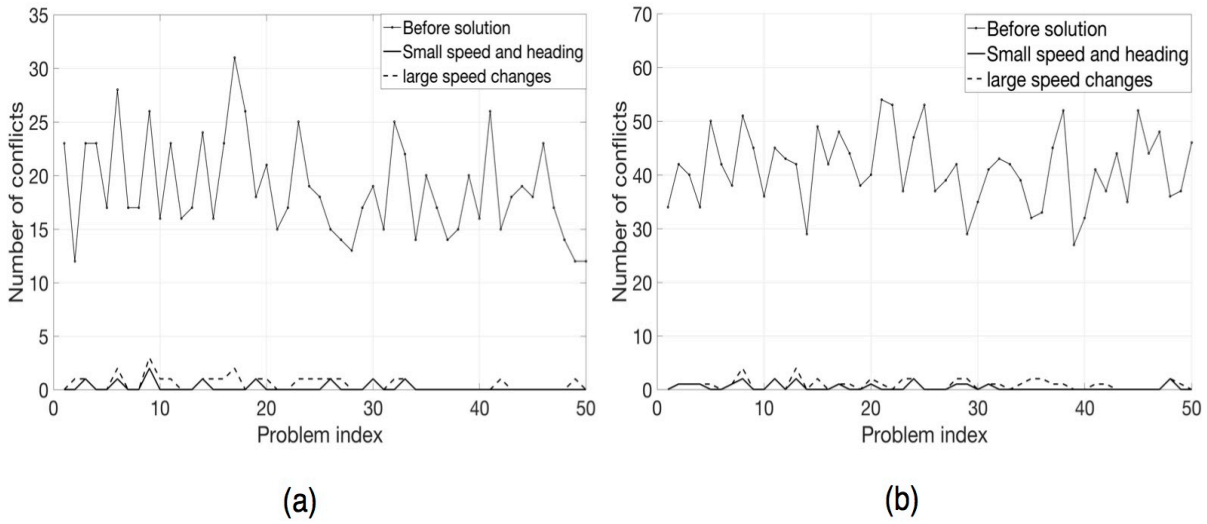

Figure 3.17 Number of unresolved conflicts using MSP-S/C (large speed) and MSP-SH/C for : (a) A=100 ; (b) A=150.

Table 3.9 Percentage of resolved conflicts using MSP-S/C (large) and MSP-SH/C- $\alpha, \gamma = 0.5$ and $\lambda = 4$

Number of aircraft A	$\bar{\mathcal{N}}$	**MSP-S/C (large)**			**MSP-SH/C**		
		avg (%)	SD (%)	confidence interval	avg (%)	SD (%)	confidence interval
20	1.25	96	19.8	[90.5, 100]	100	0	[100, 100]
50	4.27	98.6	6.7	[96.7 100]	100	0	[100 100]
70	8.76	98.7	4.1	[97.5, 99.8]	99.6	1.8	[99.1, 100]
100	18.82	97.4	3.2	[96.5, 98.2]	99.2	2	[98.6, 99.75]
150	41.28	97.8	2.5	[97.1, 98.4]	99.1	1.6	[98.6, 99.5]

Although we used $\gamma = 0.5$, allowing for 50% of the trajectories to be modified, some of the conflicts in a few cases remain unsolved using MSP-S/C (large). By examining the solutions of these cases using MSP-SH/C, we found that the model was able to find conflict free solutions for some of these cases but not in all of them. By investigating each case, we found that the unsolved conflicts occur either just after the aircraft entry into the MSA, as in Figure 3.18-a, or when both the intersection angle $\theta_{i,j}$ and the separation time at the intersection point are small, as in Figure 3.18-b. Such special case conflicts cannot be solved using only speed changes. For some cases there may exist a solution via heading changes as the solution shown in Figure 3.19. We observe that the heading change solution increases the distance travelled before the intersection, which enlarges the effect of any difference in aircraft speeds on the separation time. The heading change cannot solve all these cases as the existence of a solution depends also on the speed limits and the time difference in the original trajectories. In real air traffic situations, if these cases of unsolvable conflicts exists, then it will be the task of sector controllers to solve them on a tactical level with modifications with a larger magnitude.

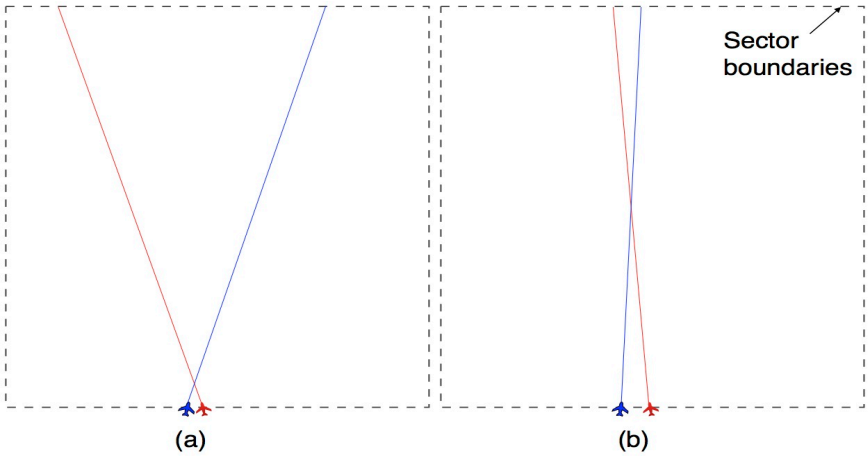

Figure 3.18 Unsolvable conflicts examples : (a) near borders ; (b) small angle.

3.5.5 Travel time results

It is important to study the change in the travel duration for the modified trajectories. A large change in the travel duration may be unacceptable. In this section, we measure this change by the percentage of delay per modified trajectory defined as

$$\Delta T = \frac{100}{\sum_{a=1}^{A} \mathcal{I}(a)} \sum_{i:\sum_{a=1}^{A} P(i)\ I_a(i)\ \mathcal{I}(a)=1} \frac{|t'_i(N(i)) - t_i(N(i))|}{t_i(N(i)) - t_i(1)}. \tag{3.29}$$

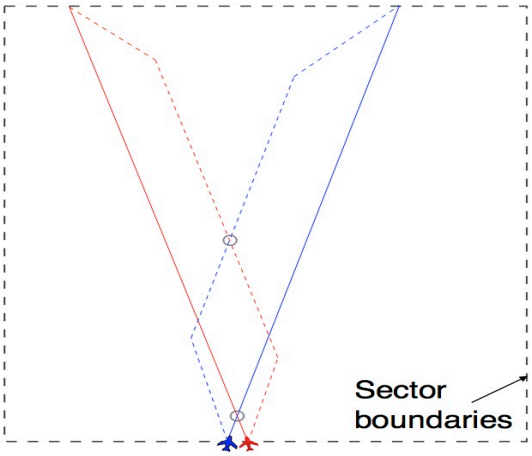

Figure 3.19 Heading manoeuvre to solve near border conflict.

In equation (3.29), the term $|t_i'(N(i)) - t_i(N(i))|$ is the delay in flight plan i, $t_i(N(i)) - t_i(1)$ is the travel duration in the MSA for flight plan i, and $\sum_{a=1}^{A} \mathcal{I}(a)$ is the number of modified trajectories. The summation is performed on modified trajectories used by an aircraft.
The delay percentage results of each model variant in solving problems involving up to 150 aircraft, using $\alpha = 0.5$, $\gamma = 0.5$ and $\lambda = 4$, is displayed in Table 3.10. In Table 3.10, the column *avg* gives the average of ΔT and the columns *max* gives the maximum value of ΔT for all problem instances. Comparing the average ΔT of all the model variants, the large speed change manoeuvre has the largest effect on the travel duration of the modified trajectories with an average ΔT varying between 2.7% and 3.24%. The heading change manoeuvre has the smallest effect on the travel durations with an average $\Delta T \leq 0.73\%$ for all problem sizes. The changes of the travel durations using MSP-S/C (small) and MSP-SH/C are comparable. These results show that the model variant MSP-SH/C reduced the number of conflicts by 99%-100% with an average change in the travel duration of the modified trajectories less than 2%. We conclude that the time delays caused by our trajectory modifications are minimal.

Table 3.10 Average delay percentage per modified trajectory

Number of	**MSP-S/C (large)**		**MSP-S/C (small)**		**MSP-H/C**		**MSP-SH/C**	
aircraft A	avg	max	avg	max	avg	max	avg	max
20	3.24	7.56	1.57	4	0.52	0.89	1.67	3.88
50	3.5	9.55	2.02	5.67	0.69	1.67	1.97	5.03
70	3.25	10.78	1.87	5.56	0.68	1.74	1.9	5.6
100	2.81	9.86	1.72	5.88	0.73	1.86	1.63	5.1
150	2.69	10.72	1.65	6	0.73	1.9	1.6	5.6

3.5.6 Effect of the allowed percentage of modified trajectories

To study the effect of the allowed percentage of modified trajectories γ on the performance of the MSP-SH/C model, we chose to solve the large size problems $A = 100$ and $A = 150$ for different values of γ varying from 0.01 to 1. The Figures 3.20-a and 3.20-b display the average number of unresolved conflicts as function of γ for problems involving 100 and 150 aircraft respectively. In these figures we see that conflict free solutions are obtained by modifying approximately 20% and 30% of the trajectories for problems involving 100 and 150 aircraft respectively.

By examining individually the problem instances, we observed that if we use

$$\gamma = \gamma^* := \frac{\mathcal{N}}{A},$$

then the model resolves most of the conflicts. Using $\gamma = \gamma^*$ means that we allow the modification of a number of trajectories that equals the number of conflicts in a problem. Usually the modification of only one trajectory is sufficient to solve a conflict, hence $\gamma = \gamma^*$ allows the solution of most conflicts. This observation can be noticed in the average results of all instances. With $\bar{\mathcal{N}}$ equals to 18.82 and 41.28 for $A = 100$ and $A = 150$ respectively, the value of $\frac{\bar{\mathcal{N}}}{A}$ equals 18.8% and 27.5% for the two problems respectively. These values corresponds to the values of γ, i.e. 20% and 30%, that produced conflict free solutions.

The average computational times for the problems with $A = 100$ and $A = 150$ as a function of γ are displayed in the Figures 3.20-c and 3.20-d respectively. In these figures, we observe that the average computational time is always less than 5.5 seconds for $A = 100$ and less than 30 seconds for $A = 150$. We also observe that the computational time is maximum for $\gamma \approx \gamma^*$ in both problems. A local maximum in the computational time is also observed for $\gamma \approx 0$. By further examining these cases, we observed that usually the solver reaches the optimal solution in an early stage and that most of the computational time is used to determine the optimality of the solution. For $\gamma \approx \gamma^*$ and $\gamma \approx 0$, the optimal solution is not conflict free. Also there exist multiple optimal solutions with different trajectory modification scenarios. Even if the solver reaches an optimal solution, it will take more time to determine its optimality, i.e. that there is not a solution with a lower objective value. When the value of $\gamma >> \gamma^*$, the model can eliminate all conflicts. Since the objective function (3.6) has a 0 lower bound, the solver stops as soon as it reaches a conflict free solution.

The actual percentage of modified trajectories as a function of γ for problems with $A = 100$ and $A = 150$ is displayed in Figures 3.21-a and 3.21-b respectively. In these figures we observe that the percentage of modified trajectories equals, on the average, the value of γ. This implies that if we use a value of γ larger than the smallest value needed to eliminate all conflicts,

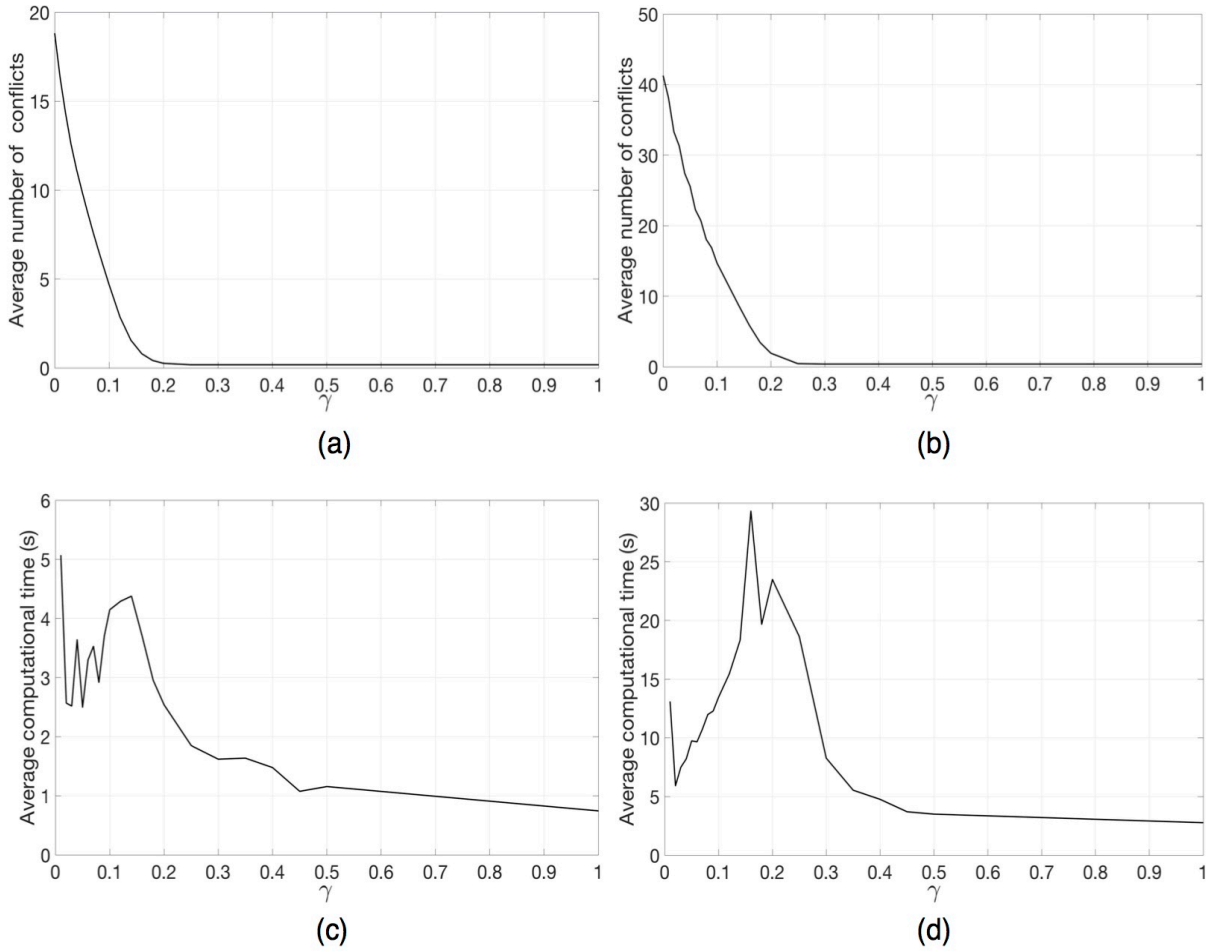

Figure 3.20 Testing the effect of γ on the performance of MSP-SH/C : (a) number of unresolved conflicts for $A = 100$; (b) number of unresolved conflicts for $A = 150$; (c) average computational time for $A = 100$; (d) average computational time for $A = 150$.

then we may get a solution with unnecessary trajectory modifications. For example, let us consider one of the problems with $A = 100$ that has 31 conflicts. The percentage of modified trajectories and the number of resolved conflict as a function of γ are displayed in Figure 3.22. In this figure, we see that the modification of 24% of the trajectories is sufficient to eliminate all conflicts. Also, we see that using a larger value of γ, e.g. 0.4, causes 40% of the trajectories to be modified. This means that the number of modifications has increased by 14% without any need. This problem of unnecessary modifications results from the fact that the number of modifications is not optimized in our model, i.e. it is not part of the objective function. For our model, a solution with 20 modifications is as good as a solution with only one modification as long as both solutions eliminate the same number of conflicts.

As described in our problem definition, the scenario in which the MSP-SH/C is used relies on generating alternative solutions using different model parameters (e.g. only heading changes,

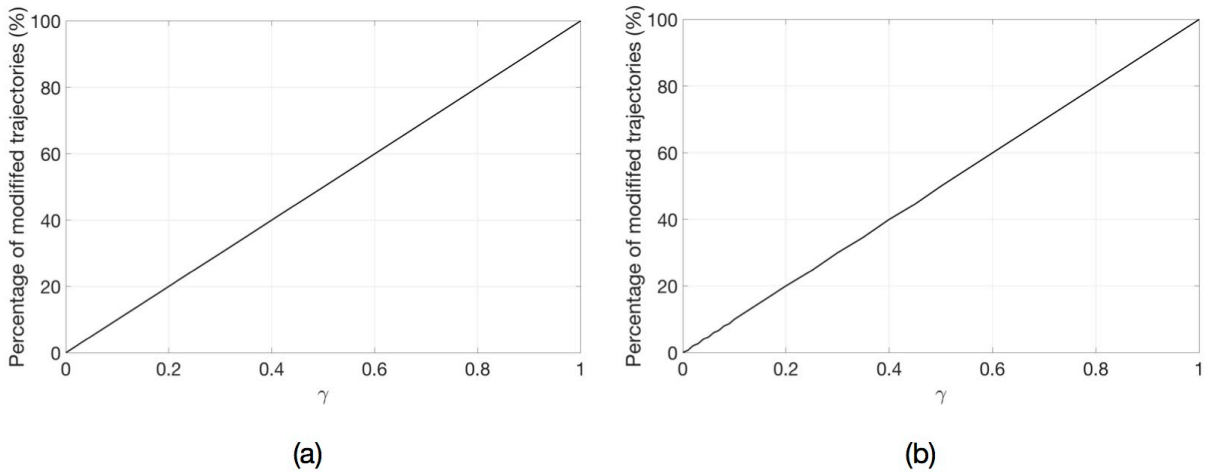

Figure 3.21 The actual percentage of modified trajectories for : (a) $A = 100$; (b) $A = 150$.

large speed changes, different γ values). Although the computational time remains relatively small and far from the limit of 10 minutes imposed by our problem definition, the results suggest that few alternative solutions shall use a value of γ close to γ^* or 0 to avoid high computational times. We also suggest the use of $\gamma = 0.1$ because this value allowed the elimination of 75% and 64% of the average number of conflicts for $A = 100$ and $A = 150$ problems respectively. To eliminate the rest of the solvable conflicts, γ has to be increased to 0.25 and 0.3. This means that the gain from increasing the value γ decreases after 0.1.

3.5.7 Workload balancing tests

In the previous tests, we used $\lambda = 4$, which means that no workload balancing was imposed. This was done to allow us to study solely the model performance and the effect of varying γ. In this section, we want to study the effect of varying the workload balancing factor λ on the solution. The workload balancing problem is most relevant in cases where a large number of conflicts exists. Consequently, we chose to test the workload balancing on the large size problems $A = 100$ and $A = 150$ and solve them using $\alpha = \gamma = 0.1$. Indeed, small size problems with $A \leq 70$ include only a small number of conflicts that can be completely eliminated with few modifications. In such case, there will be no meaning in testing the balancing on a solution with no conflicts. We chose $\alpha = \gamma = 0.1$ because for these values we found that 25-35% of the conflicts remain unresolved which will allow us to observe the effect of workload balancing.

When we solved small size problems with values of λ near 1, i.e. equally balanced, the model returned with no feasible solutions for some of the problems. For some other problems, the

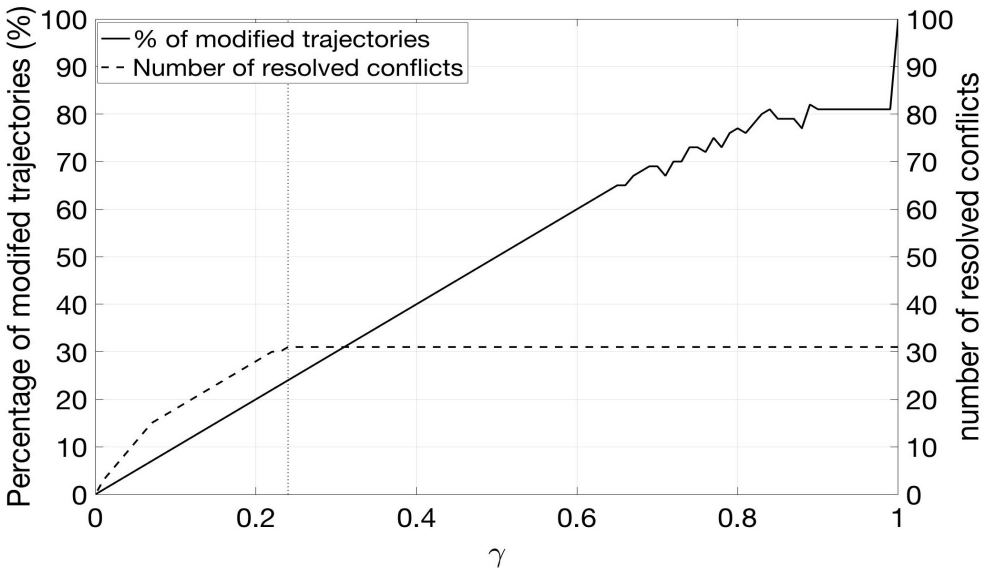

Figure 3.22 A comparison between the percentage of modified trajectories and number of resolved conflicts for a problem with $A = 100$.

optimal solution created conflicts in sectors where there were no conflicts. This is mostly the result of the unsolvable conflicts. For example, let us consider an air traffic situation where a sector has an unsolvable conflict while the remaining sectors have no conflict. If we use our model to solve this case while enforcing equal loading of conflicts, then it may end up with creating conflicts in the rest of the sectors. If it is not possible to create a conflict in one of the sectors, which happens usually in low traffic situations, then the model will return with no feasible solutions.

The average number of unresolved conflicts as a function of λ for $A = 100$ and $A = 150$ is displayed in the Figures 3.23 and 3.24 respectively. These figures also display the average number of conflicts per sector for each problem, where the sectors are indexed, only in these figures, in such a way that sector 1 is the sector with the most unresolved conflicts and sector 4 is the sector with the least number of unresolved conflicts. Note that $\lambda = 1$ means that sectors have to be equally loaded, whereas $\lambda = 4$ (i.e. number of sectors) means no workload balancing. In these figures, we see that the minimum number of conflicts is obtained for $\lambda = 4$. As λ decreases, i.e. enforcing more workload balance, we observe that the total number of conflicts increases. We observe that the difference between the no balancing and equal balancing solutions is on the average 1.78 and 2.88 conflicts for $A = 100$ and $A = 150$ problems respectively. From these results we conclude that in comparison with the no balancing solution, enforcing equal distribution of conflicts among the sectors did not lead to a significant increase in the total number of conflicts.

In the Figures 3.23 and 3.24, we see that in the case of no balancing, i.e. $\lambda = 4$, there is one sector that has a higher number of conflicts than the others. As λ decreases, the average number of conflicts in the highest loaded sector decreases as conflicts are redistributed among the sectors until $\lambda = 1$ where all the sectors have the same number of conflicts. This means that for $\lambda \approx |S|$, the total number of conflicts is minimized at the expense of overloading a single sector.

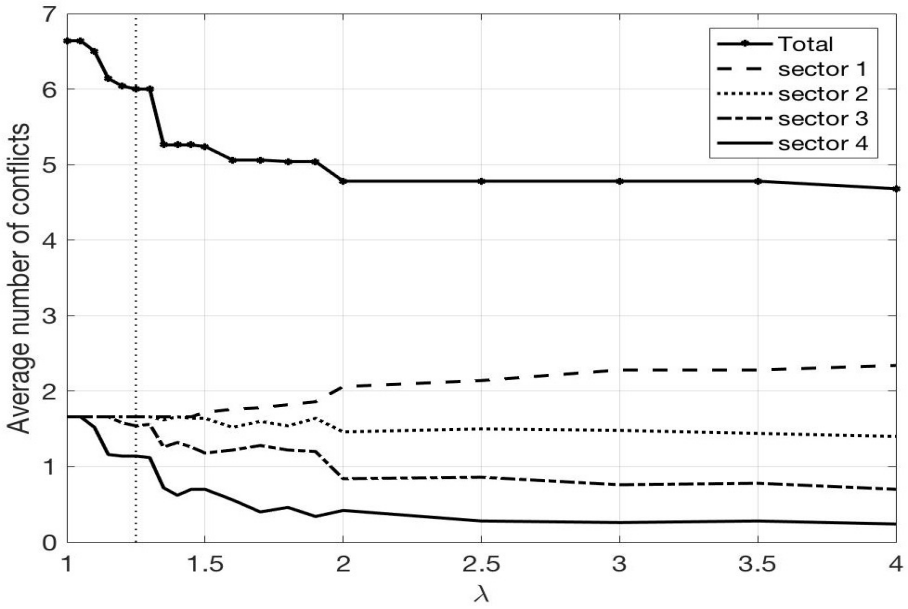

Figure 3.23 Workload balancing results for problems involving 100 aircraft.

To demonstrate in details the effect of the workload balancing constraint, the number of conflicts in each sector for one problem instance is plotted for $\lambda = 4, 1.5$ and 1 in Figure 3.25. In the case of no workload balancing, i.e. $\lambda = 4$, we see in Figure 3.25-a that the $A = 100$ problem has $4 + 2 + 1 + 1 = 8$ conflicts and that sector 1 has the highest workload. Similarly, we see in Figure 3.25-d that the $A = 150$ problem has $3 + 6 + 5 + 3 = 17$ conflicts and sectors 2 and 3 have a higher workload than the others. Decreasing the value of λ causes our model to redistribute the conflicts among sectors. Comparing Figures 3.25-a and 3.25-b, we observe that one of the conflicts in sector 1 was solved at the expense of adding a conflict to sector 2. A similar effect can be observed in Figures 3.25-d and 3.25-e.

As mentioned before, using a value of $\lambda = 1$ enforces equal workload in all the sectors. Comparing Figures 3.25-b and 3.25-c, we observe that the model eliminated a conflict from sectors 1 and 2 and added one conflict in each of the remaining two sectors. For the problem with $A = 100$, by comparing the no balancing and equal balancing solutions we see that the model equally balanced the workload without leading to any additional conflict. This was

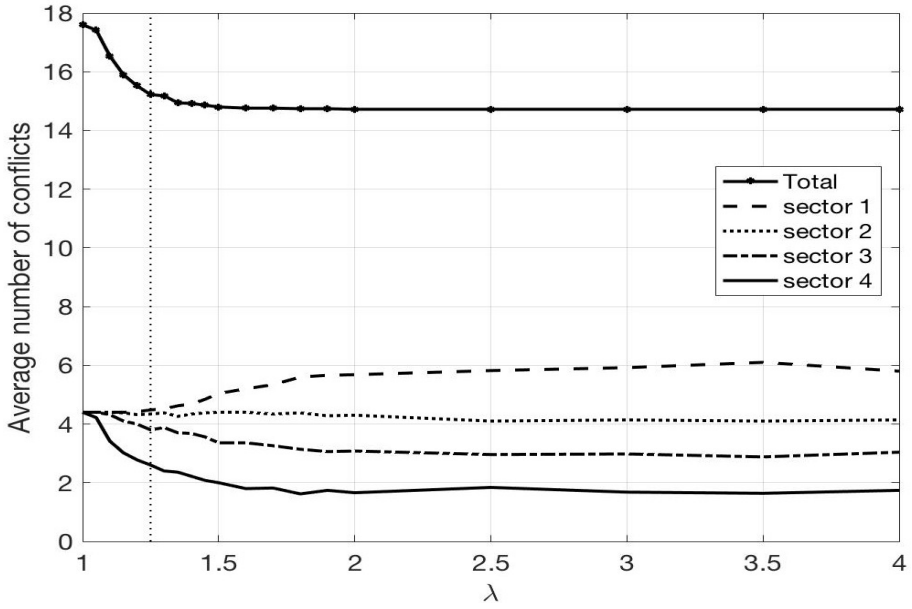

Figure 3.24 Workload balancing results for problems involving 150 aircraft.

not the case for the $A = 150$ problem. In Figure 3.25-f, we see that each of the four sectors has 5 conflicts with a total number of conflicts that equals to 20. This means that forcing equal workload in this problem leads to an additional 3 conflicts. This increase is caused by the fact that the number of conflicts in the no balancing case, that equals 17, is not divisible by 4. So, as the equal balancing is a special case of the no balancing then there is no feasible solution with a number of conflicts less than 17.

We conclude that minimizing the total number of conflicts and balancing the workload are two competing objectives. On the one hand, if we do not enforce any workload balance then we will end up with the minimum total number of conflicts but with unbalanced distribution of conflicts. On the other hand, if we enforce equal workload distributions then we will ensure that each sector has the same number of conflicts but we may end up with a higher total number of conflicts in comparison with the no balancing solution. In Figures 3.23 and 3.24, we see that $\lambda = 1.25$ produces a good compromise between the two competing objectives. At this value of λ the workload is better distributed among the sectors with only a small increase in the total number of conflicts in comparison to the no balancing solution.

As a conclusion, we can say that while the workload balancing constraint is very important in the solution of high traffic MSA, it has to be taken with some consideration in the solution of situations with low traffic. In the latter, the MSPr has to look carefully first at the solution with no balancing and compare it to that with the enforced workload balancing. He has to compare the balanced solution to the original situation to verify that it has not led to an

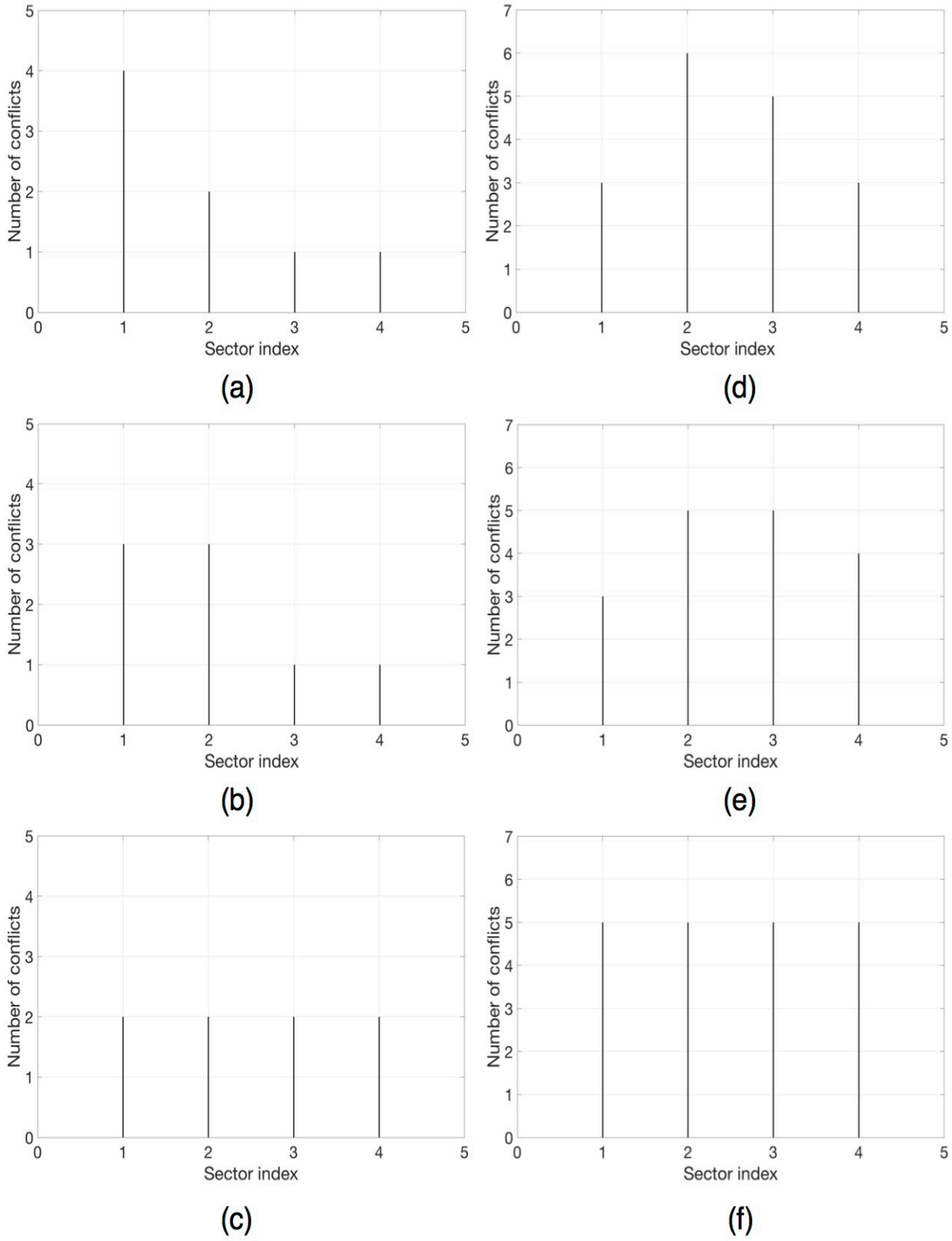

Figure 3.25 Number of conflicts per sector for : (a) $A = 100,\ \lambda = 4$; (b) $A = 100,\ \lambda = 1.5$; (c) $A = 100,\ \lambda = 1$; (d) $A = 150,\ \lambda = 4$; (e) $A = 150,\ \lambda = 1.5$; (f) $A = 150,\ \lambda = 1$.

increase in the number of conflicts.

3.6 Concluding remarks

In this chapter, we introduced a complete definition of the complexity resolution problem in a multi-sector planning context. The problem aims at minimizing and balancing the number of crossing conflicts in a set of adjacent sectors using speed and heading modifications. To solve the problem optimally, we proposed a MILP model (MSP-SH/C) in which a linear formulation of the separation constraint between aircraft was used. Our model was able to solve complex conflicts that involve more than 2 aircraft and use both types of modifications simultaneously, if needed, as shown in the detailed example of section 3.3. The MSP-SH/C model detects and solves conflicts efficiently and in a small computational time as it was able to solve the circle problem with 25 aircraft and 300 simultaneous conflicts in less than a second.

In a multi-sector planning environment, solving the MSP-SH/C model reduces the number of crossing conflicts significantly. For different sets of randomly generated problems involving up to 150 aircraft, MSP-SH/C reduced the number of crossing conflicts by 99% in less than 4 seconds. This reduction in the number of conflicts was attained while causing minimal effect on the travel duration of the modified trajectories. The average delay per modified trajectory was 1.67%-3.24% of the flight duration in the MSA in the test problems. The introduction of the heading changes was proven to be important because the use of a combination of heading changes and small speed changes (-6%,+3%) outperforms the use of only large speed changes (-12%,+6%).

As the value of γ increases, the solution of MSP-SH/C converges to a conflict free solution. The highest computational time occurs for $\gamma \approx \gamma^*$ and $\gamma \approx 0$. We found that enforcing workload balancing in the solution of high traffic situations is very beneficial : it prevents assigning a large number of conflicts in one of the sectors without a significant increase in the total number of conflicts. For low traffic situations, enforcing the workload balance can be delicate : the model can return no feasible solution or a solution with a higher number of conflicts.

In the next chapter, we will reformulate MSP-SH/C to include the detection and solution of trailing conflicts. We will also present a reformulation of the objective function to avoid the unnecessary trajectory modification that we encountered in the solution of some of the problems.

CHAPTER 4 MULTI-SECTOR PLANNING FOR CROSSING AND TRAILING CONFLICTS

In this chapter, we present a reformulation of the multi-sector planning support model using speed and heading changes for crossing conflict (MSP-SH/C) that we developed in chapter 3. The model MSP-SH/C targets the minimization and balancing of the number of crossing conflicts. The reformulation that we propose in this chapter aims at introducing the detection and resolution of trailing and crossing conflicts. We also propose a reformulation of the objective function to avoid unnecessary trajectory modifications. Firstly, we present the reformulated model, which we call the *Multi-Sector Planning support model using Speed and Heading changes for Crossing and Trailing conflicts* (MSP-SH/CT). Secondly, we solve a detailed example to demonstrate the model ability to solve trailing conflicts. Finally, we compare the model performance for different manoeuvre combinations in different traffic situations on randomly generated problems.

4.1 Multi-sector planning support model using speed and heading changes for crossing and trailing conflicts

If two aircraft lose minimum separation distance, then they are considered to be in conflict. The possible types of air traffic conflicts are crossing, trailing and head-to-head conflicts. While the occurrence of the latter is rare and avoided in the design of flight plans, the first two types are considered more common. A tool or a model for the planning of aircraft trajectories has to be able to detect both types. If this is not the case, then the model can solve one type of conflict at the expense of creating the other type.

In chapter 3, we presented the MSP-SH/C model for the solution of the complexity resolution problem in a MSP environment. While MSP-SH/C is an efficient tool for the detection and resolution of crossing conflicts in a MSP context, it did not include a method for the detection of trailing conflicts (section 3.2). This limits its use in real air traffic situations. The MSP-SH/C model relies on the linear formulation of the minimum separation time to replace the minimum separation distance (3.1). In this formulation, the denominator is multiplied by $\sin(\theta_{i,j})$. Since $\theta_{i,j} = 0$ for a trailing conflict, this formulation is not defined for trailing conflicts and cannot be used to detect them. In this section we introduce a new formulation for the detection of trailing conflicts.

Two aircraft are at risk of a trailing conflict if they share a part of their trajectories in which both aircraft use the same flight level. A trailing conflict will occur if the trailing aircraft

uses a speed v_j higher than the speed v_i of the leading aircraft. In such a case, if the shared flight segment is long enough, then they can lose their safe separation distance as shown in Figure 4.1.

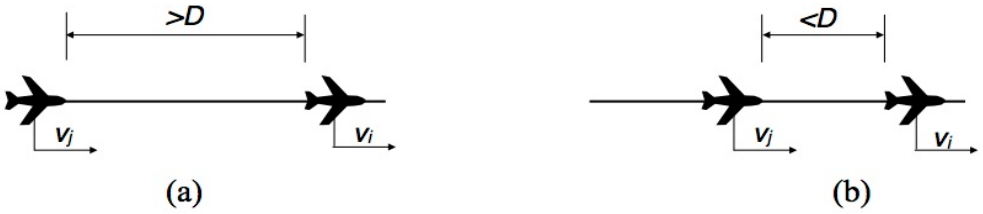

Figure 4.1 Example of a trailing conflict at : (a) T_1, where the aircraft are safely separated ; (b) $T_2 > T_1$, where the distance between the aircraft is less than the safe separation distance D.

In our reformulated model MSP-SH/CT, we want to transform the safe separation distance between two aircraft at risk of a trailing conflict into a safe separation time $\bar{S}_{i,j}$. We chose this formulation because all variables in the original model MSP-SH/C depend on time and not on distance.

Suppose that two aircraft following flight plans i and j are flying at the same flight level and are at risk of a trailing conflict between two points P_1 and P_2 as in Figure 4.2. As previously discussed in section 3.1.2, we assume that aircraft speed is constant between the waypoints. Consequently, if the leading aircraft remains in the lead between P_1 and P_2, then the minimum separation distance between the aircraft occurs either when the trailing aircraft is at P_1 or when the leading aircraft is at P_2. Following this, we conclude that, under the condition that the leading aircraft remains in lead, a pair of trailing aircraft are not in conflict between P_1 and P_2 if they maintain the safe separation distance between them at point P_1 and point P_2 as shown in Figures 4.3. If the leading aircraft does not remain in lead, then this pair is involved in a trailing conflict. We verify the leading aircraft condition and determine accordingly the occurrence of a conflict via the model constraints that we will discuss in section 4.1.4.

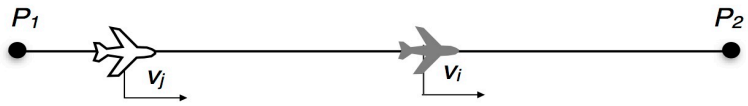

Figure 4.2 Illustration of a trailing conflict between two points.

Assuming that the aircraft following flight plan i arrives first at P_1, the distance between the aircraft following flight plans i and j when the trailing aircraft is at point P_1 is $v_i\ \Delta t_1$, where

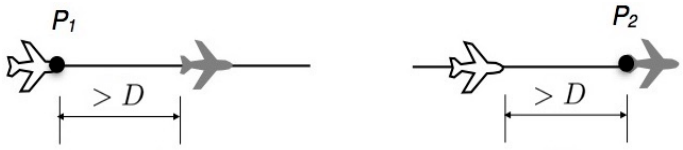

Figure 4.3 Conflict free condition for a trailing conflict.

Δt_1 is the difference between the passage time of the pair of aircraft at point P_1. The pair of aircraft is safely separated when the trailing aircraft is at P_1 if

$$v_i \, \Delta t_1 \geq D. \tag{4.1}$$

As $v_i \in [v_{a_1}^-, \, v_{a_1}^+]$, safe separation is guaranteed at P_1 if

$$\Delta t_1 \geq \frac{D}{v_{a_1}^-}, \tag{4.2}$$

where a_1 is the index of the aircraft following flight plan i. Assuming also that the aircraft following flight plan i arrives first at P_2, safe separation is guaranteed when the leading aircraft is at P_2 if

$$\Delta t_2 \geq \frac{D}{v_{a_2}^-}, \tag{4.3}$$

where Δt_2 is the difference between the passage time of the pair of aircraft at point P_2, and a_2 is the index of the aircraft following flight plan j. In summary, a pair of aircraft following flight plans i and j are safely separated between P_1 and P_2 if the aircraft following flight plan i arrives first at P_1 and P_2 and (4.2)-(4.3) are satisfied.

The aircraft arrival times at waypoints are not predetermined because the aircraft speeds are model variables. For most pairs of aircraft at risk of a trailing conflict, there is a possibility that any of the two aircraft arrives first at the common flight segment $\overline{P_1P_2}$ (CFS). Consequently, we define $\bar{S}_{i,j}$ as the minimum separation time at the beginning and the end of the CFS that guarantees no trailing conflict for a pair of aircraft following flight plans i and j. This time is given by

$$\bar{S}_{i,j} = \max\left\{\frac{D}{v_{a_1}^-}, \; \frac{D}{v_{a_2}^-}\right\}, \tag{4.4}$$

where a_1 and a_2 are the aircraft that can follow flight plans i and j respectively.

If the leading aircraft condition is satisfied, then maintaining a separation time greater than $\bar{S}_{i,j}$ at P_1 and P_2 ensures safe separation when the two trailing aircraft are both flying along the CFS. This does not ensure safe separation between a pair of trailing aircraft at all times. For example, consider two aircraft following a pair of flight plans (i, j) that shares

the same spatial coordinates. In this case, each flight segment of these two flight plans is a CFS. Figure 4.4 displays two consecutive flight segments for this example. If the difference between the passage times of the aircraft is greater than $\bar{S}_{i,j}$ at n_1, n_2 and n_3, then both aircraft are safely separated when they are both on the same CFS, i.e. either between n_1 and n_2 or between n_2 and n_3. However, there is no guarantee that the aircraft remain separated when one of the aircraft is on a flight segment, e.g. between n_1 and n_2, and the other one is on the next flight segment, e.g. between n_2 and n_3.

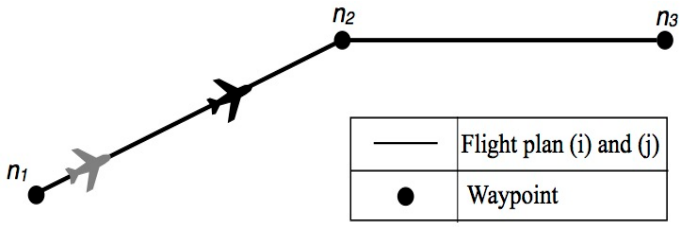

Figure 4.4 Consecutive flight segments for two trailing aircraft.

When two trailing aircraft are on two consecutive flight segments, the situation resembles a crossing conflict with an intersection point at the common waypoint of the flight segments, e.g. n_2 in Figure 4.5. To ensure safe separation in these cases, we decided to add all the flight plan pairs with the same spatial coordinates to the set E of flight plan pairs at risk of a crossing conflict. Each pair of flight plans (i, j) that belongs to E is defined by an intersection point and an intersection angle $\theta_{i,j}$. For the pairs of trailing aircraft that belong to E, we consider each waypoint as an intersection point except for the first and last waypoints. We set the corresponding value of $\theta_{i,j}$ to the angle between the consecutive flight segments $\bar{\theta}_{i,j}$ as defined in Figure 4.5.

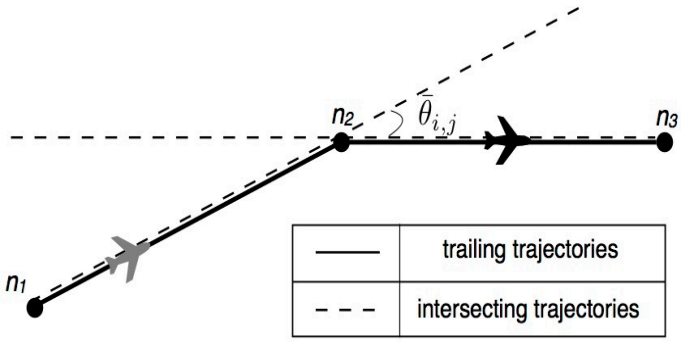

Figure 4.5 Trailing aircraft on consecutive flight segments.

For each pair p of flight plans in E, we calculate the minimum safe separation time S_p. If the difference between the passage times at the intersection point is larger than S_p, then

a pair of aircraft that follows the intersection trajectories, i.e. the dashed lines in Figure 4.5, are safely separated for all times and all speeds. From section 3.2 we know that S_p is large for small values of $\theta_{i(p),j(p)}$. These large values of S_p are caused by the fact that S_p ensures safe separation along the whole trajectories before and after the intersection point. A pair of trailing aircraft on consecutive flight segments acts as if they follow the intersecting trajectories only after the arrival of the leading aircraft to the common waypoint, e.g. n_2 in Figure 4.5, and until the arrival of the trailing aircraft to the common waypoint. Consequently, using $\bar{\theta}_{i,j}$ to evaluate S_p overestimates the safe separation time for small values of $\bar{\theta}_{i,j}$. In the following, we intend to find a smaller upper bound for the safe separation time for two trailing aircraft on consecutive flight segments.

Note that the work in this thesis deals with en route high altitude sectors where a sudden change in the direction of an aircraft with an angle $\bar{\theta}_{i,j} > 90°$ is not common. Let us consider two trailing aircraft on two consecutive flight segments as shown in Figure 4.6. The distance $d_{i,j}(\bar{\theta}_{i,j})$ between the two aircraft is given by

$$d_{i,j}(\bar{\theta}_{i,j}) = \sqrt{d_1^2 + d_2^2 + 2d_1 d_2 \cos \bar{\theta}_{i,j}}, \tag{4.5}$$

where d_1 and d_2 are the distances between the aircraft and the common waypoint n_2. We observe that for fixed values of d_1 and d_2, we have

$$d_{i,j}(\bar{\theta}_{i,j}) \geq d_{i,j}(90) \quad \text{for all } \bar{\theta}_{i,j} \in \{0°, 90°\}. \tag{4.6}$$

Let us denote S_p evaluated at $\bar{\theta}_{i,j}$ as $S_p(\bar{\theta}_{i,j})$. By definition of S_p, if the difference between the passage times of the aircraft at point n_2 is larger than $S_p(90)$, then

$$d_{i,j}(90) \geq D$$

for all times and all speeds, which implies via (4.6) that

$$d_{i,j}(\bar{\theta}_{i,j}) > D \quad \text{for all } \bar{\theta}_{i,j} \in \{0°, 90°\}$$

and safe separation is ensured.

In summary, we handle trailing conflicts as follows. For all pairs of trailing aircraft with at least one CFS, we calculate the corresponding safe separation time $\bar{S}_{i,j}$ that guarantees safe separation along the CFS. For a pair of aircraft that shares consecutive CFSs, in addition to calculating $\bar{S}_{i,j}$, we also add this pair to the set E. Such a pair is handled as a pair at risk of a crossing conflict with a minimum separation time of $S_p(\bar{\theta}_{i,j})$. For $\bar{\theta}_{i,j} < 90°$, we use a

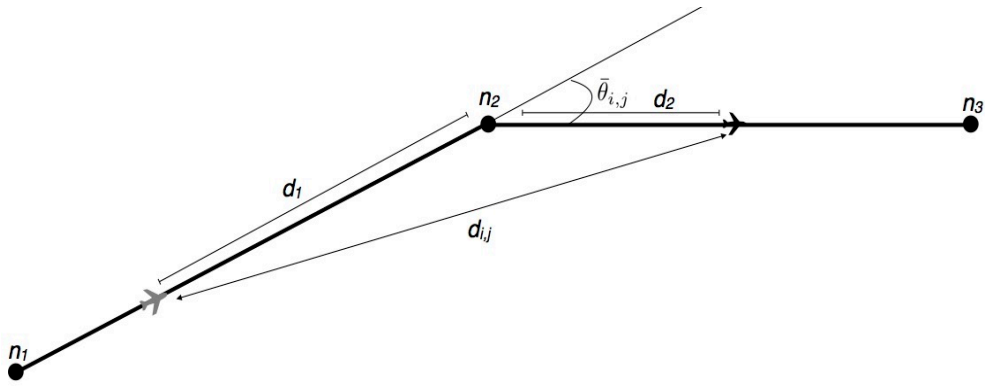

Figure 4.6 Separation distance between two trailing aircraft on consecutive flight segments.

minimum separation time that equals $S_p(90)$. Note that although $\bar{\theta}_{i,j} > 90°$ is not common in our context, our formulation handles such case by using $S_p(\bar{\theta}_{i,j})$ as the safe separation time.

4.1.1 Input data

All the input data of the model MSP-SH/C are needed for the model MSP-SH/CT but we also need complementary data related to trailing conflicts. As for the case of crossing conflicts, not all flight plans pairs that share a CFS are at risk of a trailing conflict. Consequently, we introduce $\bar{E}$ as the set of flight plan pairs at risk of a trailing conflict. A pair of flight plans is at risk of a trailing conflict if and only if they share a CFS and :

— the separation time between the arrival time windows at the beginning or the end of the CFS is less than $\bar{S}_{i,j}$,
and/or
— one of the two aircraft can reach the beginning of the CFS first but can also arrive last at the end of the CFS.

We formulated these conditions as follows. A pair (i, j) of flight plans belongs to $\bar{E}$ if they share a CFS and satisfy at least one of the following :

$$\begin{cases} t_i^-(m_1) \leq t_j^+(n_1) + \bar{S}_{i,j}, \\ t_i^+(m_1) \geq t_j^-(n_1) - \bar{S}_{i,j}, \end{cases} \tag{4.7}$$

or

$$\begin{cases} t_i^-(m_2) \leq t_j^+(n_2) + \bar{S}_{i,j}, \\ t_i^+(m_2) \geq t_j^-(n_2) - \bar{S}_{i,j}, \end{cases} \tag{4.8}$$

or

$$\begin{cases} t_i^-(m_1) \leq t_j^+(n_1), \\ t_i^+(m_2) \geq t_j^-(n_2), \end{cases} \tag{4.9}$$

or

$$\begin{cases} t_j^-(n_1) \leq t_i^+(m_1), \\ t_j^+(n_2) \geq t_i^-(m_2), \end{cases} \tag{4.10}$$

where m_1 and m_2 are the waypoints in flight plan i that represent the start and the end of the CFS. Similarly, n_1 and n_2 are the waypoints at the start and the end of the CFS for flight plan j.

If the inequalities (4.7) are satisfied, then there is an intersection between the time windows $[t_i^-(m_1), t_i^+(m_1) + \bar{S}_{i,j}]$ and $[t_j^-(n_1), t_j^+(n_1) + \bar{S}_{i,j}]$. This means that both aircraft can arrive at the start of the CFS with a time difference less than $\bar{S}_{i,j}$. Similarly, the inequalities (4.8) mean that there is an intersection between the time windows $[t_i^-(m_2), t_i^+(m_2) + \bar{S}_{i,j}]$ and $[t_j^-(n_2), t_j^+(n_2) + \bar{S}_{i,j}]$. If the inequalities (4.9) hold, then the aircraft following flight plan i can arrive first at the beginning of the CFS ($t_i^-(m_1) \leq t_j^+(n_1)$) and can arrive second at the end of the CFS ($t_i^+(m_2) \geq t_j^-(n_2)$). Finally, if the inequalities (4.10) are satisfied, then the aircraft following flight plan j can arrive first at the beginning of the CFS and can arrive second at the end of the CFS.

Each pair in $\bar{E}$ is assigned an index $g \in \{1, 2, ..., |\bar{E}|\}$. The flight plan pair of index g is denoted by $(\bar{i}(g), \bar{j}(g))$, where $\bar{i}(g)$ and $\bar{j}(g)$ are the corresponding flight plan indices. We introduce the simplified notation

$$S_g := \bar{S}_{\bar{i}(g),\bar{j}(g)}.$$

The location of each trailing conflict is given by the indicator matrix $\bar{I}_g^s$ that we define as

$$\bar{I}_g^s = \begin{cases} 1 \text{ if the beginning of the CFS for the } g^{th} \text{ flight plan pair in } \bar{E} \text{ is located in sector } s, \\ 0 \text{ otherwise.} \end{cases}$$

In the preprocessing stage of the model, we determine the flight pairs that share a CFS and then we use (4.4)-(4.10) to determine the pairs that belong to $\bar{E}$ and evaluate $\bar{S}_g$ and $\bar{I}_g^s$.

4.1.2 Variables

In our model, the decision variables are related to trajectory modification manoeuvres. In MSP-SH/CT, these manoeuvres remain the same as in MSP-SH/C. As a result there is no change in the number or the definition of the decision variables in this model in comparison with the MSP-SH/C model. We only need to add a set of dependent variables to detect trailing conflicts.

The detection of a trailing conflict between a pair of trailing aircraft depends on the arrival order of the two aircraft at the beginning of the CFS. We present the arrival order of the aircraft following the g^{th} flight plan pair in $\bar{E}$ at the beginning of the CFS by the indicator

R_g, defined as

$$R_g = \begin{cases} 1 \text{ if the aircraft following flight plan } \bar{i}(g) \text{ arrives to the CFS before the aircraft} \\ \quad \text{following flight plan } \bar{j}(g), \\ 0 \text{ otherwise.} \end{cases}$$

Second, we need two additional variables to determine whether the aircraft following the g^{th} flight plan pair in $\bar{E}$ lose separation along their CFS or not. The first variable that we introduce is C_g^1, defined as

$$C_g^1 = \begin{cases} 1 \text{ if the aircraft following the } g^{th} \text{ plan pair in } \bar{E} \text{ lose separation at the} \\ \quad \text{beginning of the CFS,} \\ 0 \text{ otherwise.} \end{cases}$$

The second variable is C_g^2, defined as

$$C_g^2 = \begin{cases} 1 \text{ if the aircraft following the } g^{th} \text{ plan pair in } \bar{E} \text{ lose separation at the} \\ \quad \text{end of the CFS,} \\ 0 \text{ otherwise.} \end{cases}$$

Finally, we represent a trailing conflict between the g^{th} flight plan pair in $\bar{E}$ by the variable $\bar{C}_g$, defined as

$$\bar{C}_g = \begin{cases} 1 \text{ if a trailing conflict is predicted to happen for the } g^{th} \text{ plan pair in } \bar{E}, \\ 0 \text{ otherwise.} \end{cases}$$

Note that $\bar{C}_g$ takes the value 1 if $C_g^1 = 1$ or $C_g^2 = 1$.

4.1.3 Objective function

We reported the problem of unnecessary trajectory modifications in the testing of the MSP-SH/C model in section 3.5.6. These unnecessary modifications were attributed to the absence of a term representing the number of modified trajectories in the objective function. To avoid this problem, we decided to use a modified objective function in MSP-SH/CT. This function includes a term that represents the percentage of modified trajectories in addition to the number of predicted conflicts.

The new objective function to be minimized in MSP-SH/CT is

$$\bar{Z} = \sum_{p=1}^{|E|} C_p + \sum_{g=1}^{|\bar{E}|} \bar{C}_g + \frac{\sum_{a=1}^{A} \mathcal{I}(a)}{\gamma\, A + 1}. \tag{4.11}$$

The first term in (4.11) is the total number of crossing conflicts in the MSA. The second term is the total number of trailing conflicts. The last term is the total number of modified trajectories divided by the maximum number of modified trajectories plus 1. The last term minimizes the number of modified trajectories.
Since $\sum_{a=1}^{A} \mathcal{I}(a) \leq \gamma\, A$, the last term is always less than one. We chose this formulation so that the model always gives priority to decreasing the number of conflicts over the minimization of the number of modified trajectories. For example, consider a MSA with only two aircraft. Let us assume that it is necessary to modify the trajectories of both aircraft to avoid a conflict. For $\gamma = 1$, the following two solutions are feasible. The first solution implies the modification of both trajectories and avoids the conflict. This solution has an objective value $\bar{Z} = 0 + 0 + \frac{2}{2+1} = 2/3$. The second solution implies using the original trajectories without any modification. This solution has an objective value $\bar{Z} = 1 + 0 + \frac{0}{2+1} = 1$. As a result, the solver will return the first solution as the optimal solution. If we do not add 1 to the denominator of the last term in (4.11), then both solutions will have the same objective value of 1 and the model will return any of them as the optimal solution.
By using (4.11) as the objective function, not all the solutions that share the same number of conflicts are equivalent. The solutions that use a smaller number of modified trajectories are better. This resolves the problem of unnecessary trajectory modifications as it will be shown in section 4.3.2.

4.1.4 Constraints

The constraints related to heading change manoeuvres, speed changes, number of modified trajectories, and crossing conflict prediction remain the same as in MSP-SH/C. We need to introduce a new set of constraints to detect trailing conflicts. We also need to introduce a reformulation of the balancing constraint to include trailing conflicts.

4.1.5 Trailing conflict prediction constraints

A pair of flight plans in $\bar{E}$ leads to a trailing conflict if and only if all the following conditions are satisfied :

1. there exists two aircraft following both flight plans,

2. both flights use the same flight level along the CFS,

3. the difference of the passage times of both aircraft at the beginning or the end of the CFS is less than $\bar{S}_g$, or one of the aircraft following the flight plans arrives first at the CFS but leaves last.

Each of these conditions has to be checked using linear constraints to maintain the model linearity.

First condition : trailing flight plans

Checking if both flight plans are actually used is done by checking the values of $P(i)$ and $P(j)$: if $P(i) = P(j) = 1$, then both flight plans are used.

Second condition : flight level along the CFS

The information regarding the flight levels used along the CFS is given by the indicator $\bar{H}_g(k)$ that we define as

$$\bar{H}_g(k) = \begin{cases} 0 \text{ if both flight plans of the } g^{th} \text{ pair in } \bar{E} \text{ use flight level } k \text{ at the CFS,} \\ 1 \text{ otherwise.} \end{cases}$$

If both flight plans use different flight levels at the CFS, then $\sum_{k=1}^{K} \bar{H}_g(k) = K$. If they use the same flight level, then $\sum_{k=1}^{K} \bar{H}_g(k) = K - 1$.
The evaluation of $\bar{H}_g(k)$ is done as follows. Let let m, n denote the indices of the waypoints at which flight plans $\bar{i}(g)$ and $\bar{j}(g)$ start the CFS respectively. Note that if $L_{\bar{i}(g)}(m,k) = 1$, then an aircraft following flight plan $\bar{i}(g)$ uses flight level k at waypoint m. To have $\bar{H}_g(k) = 0$ if $L_{\bar{i}(g)}(m,k) = L_{\bar{j}(g)}(n,k) = 1$ and $\bar{H}_g(k) = 1$ otherwise, we use the following set of inequalities : for $g \in \{1, 2, ..., |\bar{E}|\}$ and $k \in \{1, 2, ..., K\}$,

$$\begin{cases} L_{\bar{i}(g)}(m,k) + L_{\bar{j}(g)}(n,k) \leq 2 - \bar{H}_g(k), \\ L_{\bar{i}(g)}(m,k) + L_{\bar{j}(g)}(n,k) \geq 1.1 - 2\ \bar{H}_g(k). \end{cases} \tag{4.12}$$

Third condition : passage times on the CFS

For the last condition, we need to check the passage time of each aircraft at the beginning and the end of the CFS and determine the arrival order of the aircraft to the CFS. Note that the beginning and end points of the CFS do not have to be waypoints in the flight plans. For example, Figure 4.7 displays a case where the beginning of the CFS is not a waypoint

for flight plan i and the end of the CFS is not a waypoint for flight plan j. There is no need to add such points to the flight plans as new waypoints. We can calculate the passage time at such points using the passage times at the previous and subsequent waypoints.

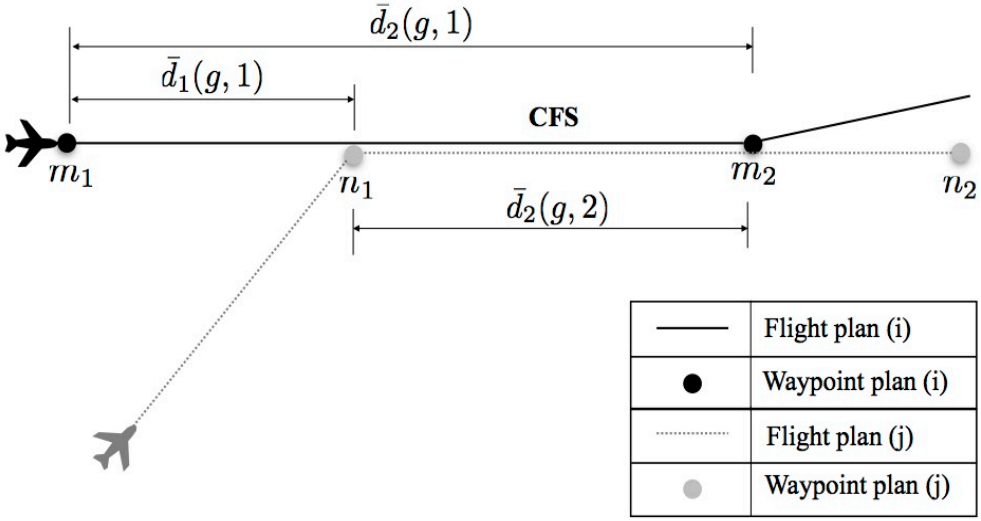

Figure 4.7 A trailing conflict between flight plans i and j.

Let us start with the definition of new variables and new input parameters. First, we denote the passage times at the first and end points of the CFS for the ℓ^{th} flight plan of the g^{th} flight plan pair in $\bar{E}$ as $\bar{t}_1(g,\ell)$ and $\bar{t}_2(g,\ell)$ respectively, $\ell \in \{1,2\}$. We have $\ell = 1$ for the flight plan $\bar{i}(g)$ and $\ell = 2$ for the flight plan $\bar{j}(g)$. For each of these flight plans, we define m as the waypoint at the start of the CFS if the first point of the CFS is a waypoint or as the waypoint that precedes the CFS otherwise. For the example in Figure 4.7, m is the waypoint n_1 for flight plan j and m is the waypoint m_1 for flight plan i. Finally, we define the parameter $\bar{d}_1(g,\ell)$ as the distance between waypoint m and the first point in the CFS and $\bar{d}_2(g,\ell)$ as the distance between waypoint m and the end point in the CFS. For the example in Figure 4.7, $\bar{d}_1(g,1), \bar{d}_2(g,1)$ and $\bar{d}_2(g,2)$ are shown in the figure and $\bar{d}_1(g,2) = 0$.
Using these definitions, we calculate $\bar{t}_1(g,\ell)$ and $\bar{t}_2(g,\ell)$ with

$$\bar{t}_1(g,\ell) = t'_i(m) + \frac{T_i(m)}{D_i(m)}\,\bar{d}_1(g,\ell), \qquad i \in \bar{E}, \tag{4.13}$$

$$\bar{t}_2(g,\ell) = t'_i(m) + \frac{T_i(m)}{D_i(m)}\,\bar{d}_2(g,\ell), \qquad i \in \bar{E}. \tag{4.14}$$

Note that (4.13) and (4.14) hold even if the first or the end points of the CFS are waypoints. Let us consider the example in Figure 4.7. For flight plan j, the first point of the CFS is a

waypoint. Using (4.13) with $m = n_1$ and $\bar{d}_1(g,2) = 0$, the passage time $\bar{t}_1(g,2)$ is given by

$$\bar{t}_1(g,2) = t'_j(n_1) + \frac{T_j(n_1)}{D_j(n_1)} \times 0 = t'_j(n_1).$$

For flight plan i, the last point of the CFS is a waypoint. Using (4.14) with $m = m_1$ and $\bar{d}_2(g,1) = D_i(m_1)$, the passage time $\bar{t}_2(g,1)$ is given by

$$\bar{t}_2(g,1) = t'_i(m_1) + \frac{T_i(m_1)}{D_i(m_1)} \times D_i(m_1) = t'_i(m_1) + T_i(m_1).$$

Note that $T_i(m_1)$ is the flight duration between waypoints m_1 and m_2, hence $T_i(m_1) = t'_i(m_2) - t'_i(m_1)$. Consequently,

$$\bar{t}_2(g,1) = t'_i(m_1) + T_i(m_1) = t'_i(m_1) + t'_i(m_2) - t'_i(m_1) = t'_i(m_2).$$

Using the passage times at the beginning of the CFS, we can determine which aircraft arrives first. To have $R_g = 1$ if the aircraft following flight plan $\bar{i}(g)$ arrives first at the CFS and $R_g = 0$ otherwise, we use the following set of inequalities : for $g \in \{1, 2, ..., |\bar{E}|\}$,

$$\begin{cases} \bar{t}_1(g,1) - \bar{t}_1(g,2) \leq (1 - R_g)\, \bar{M}_g^1, \\ \bar{t}_1(g,1) - \bar{t}_1(g,2) \geq -R_g\, \bar{M}_g^1, \end{cases} \tag{4.15}$$

where $\bar{M}_g^1$ is a large positive number given by

$$\bar{M}_g^1 = \max\{\bar{t}_1^+(g,1) - \bar{t}_1^-(g,2), \bar{t}_1^+(g,2) - \bar{t}_1^-(g,1)\} + \bar{S}_g + 0.1. \tag{4.16}$$

The input parameters $\bar{t}_1^+(g,\ell)$ and $\bar{t}_1^-(g,\ell)$ in (4.16) are the maximum and minimum passage time at the first point in the CFS for the ℓ^{th} flight plan of the g^{th} flight plan pair in $\bar{E}$ respectively.

Verifying safe separation

Having a linear formulation for the three conditions, we can now verify if a pair of aircraft is safely separated along the CFS or not and set the values of C_g^1, C_g^2 and $\bar{C}_g$ accordingly. Note that we want to set $C_g^1 = 1$ if and only if all the following conditions are satisfied :

- both flight plans of the g^{th} flight plan pair in $\bar{E}$ are used, i.e. $P(\bar{i}(g)) = P(\bar{j}(g)) = 1$;
- both flight plans use the same flight level in the CFS, i.e. $\sum_{k=1}^{K} \bar{H}_g(k) = K - 1$;
- The difference between the passage times of the aircraft following the g^{th} flight plan pair at the beginning of the CFS is less than the minimum safe separation time $\bar{S}_g$.

These conditions have to be checked for the two possible arrival orders to the CFS, i.e. for $R_g = 1$ and $R_g = 0$. First, for $R_g = 1$ we check these conditions and set the value of C_g^1 using the following system of inequalities : for $g \in \{1, 2, ..., |\bar{E}|\}$,

$$\begin{aligned} \bar{t}_1(g,2) - \bar{t}_1(g,1) \geq & \bar{S}_g - (1 - R_g)\, \bar{M}_g^1 - (2 - P(\bar{i}(g)) - P(\bar{j}(g)))\, \bar{M}_g^1 \\ & - \left(\sum_{k=1}^{K} \bar{H}_g(k) + 1 - K \right) \bar{M}_g^1 - C_g^1\, \bar{M}_g^1, \end{aligned} \tag{4.17}$$

$$\begin{aligned} \bar{t}_1(g,2) - \bar{t}_1(g,1) \leq & \bar{S}_g + (1 - R_g)\, \bar{M}_g^1 + (2 - P(\bar{i}(g)) - P(\bar{j}(g)))\, \bar{M}_g^1 \\ & + \left(\sum_{k=1}^{K} \bar{H}_g(k) + 1 - K \right) \bar{M}_g^1 + (1 - C_g^1)\, \bar{M}_g^1. \end{aligned} \tag{4.18}$$

If $R_g = 1$ and the first two conditions are satisfied, i.e. $P(\bar{i}(g)) = P(\bar{j}(g)) = 1$ and $\sum_{k=1}^{K} \bar{H}_g(k) = K - 1$, then (4.17) and (4.18) reduce to

$$\begin{cases} \bar{t}_1(g,2) - \bar{t}_1(g,1) \geq \bar{S}_g - C_g^1\, \bar{M}_g^1, \\ \bar{t}_1(g,2) - \bar{t}_1(g,1) \leq \bar{S}_g + (1 - C_g^1)\, \bar{M}_g^1, \end{cases} \tag{4.19}$$

which will set $C_g^1 = 1$ if $\bar{t}_1(g,2) - \bar{t}_1(g,1) < \bar{S}_g$, and set $C_g^1 = 0$ otherwise. If any of the first two conditions are not satisfied or if $R_g = 0$, then the constraints (4.17) and (4.18) are relaxed by adding at least $\bar{M}_g^1$ to the right hand side of the constraint.
Second, for $R_g = 0$ we check the three conditions and set the value of C_g^1 using the following system of inequalities : for $g \in \{1, 2, ..., |\bar{E}|\}$,

$$\begin{aligned} \bar{t}_1(g,1) - \bar{t}_1(g,2) \geq & \bar{S}_g - R_g\, \bar{M}_g^1 - (2 - P(\bar{i}(g)) - P(\bar{j}(g)))\, \bar{M}_g^1 \\ & - \left(\sum_{k=1}^{K} \bar{H}_g(k) + 1 - K \right) \bar{M}_g^1 - C_g^1\, \bar{M}_g^1, \end{aligned} \tag{4.20}$$

$$\begin{aligned} \bar{t}_1(g,2) - \bar{t}_1(g,1) \leq & \bar{S}_g + R_g\, \bar{M}_g^1 + (2 - P(\bar{i}(g)) - P(\bar{j}(g)))\, \bar{M}_g^1 \\ & + \left(\sum_{k=1}^{K} \bar{H}_g(k) + 1 - K \right) \bar{M}_g^1 + (1 - C_g^1)\, \bar{M}_g^1. \end{aligned} \tag{4.21}$$

If any of the first two conditions are not satisfied or if $R_g = 1$, then (4.20) and (4.21) are relaxed by adding at least $\bar{M}_g^1$ to the right hand side of the constraint. If $R_g = 1$, then the constraints (4.20)-(4.21) are relaxed and (4.17)-(4.18) are enforced. If $R_g = 0$, then the constraints (4.17)-(4.18) are relaxed and (4.20)-(4.21) are enforced.
Using the same modelling logic, we verify the aircraft separation at the end of the CFS and

set the value of C_g^2 using the following system of inequalities : for $g \in \{1, 2, ..., |\bar{E}|\}$,

$$\begin{aligned}\bar{t}_2(g,2) - \bar{t}_2(g,1) \geq & \bar{S}_g - (1 - R_g)\,\bar{M}_g^2 - (2 - P(\bar{i}(g)) - P(\bar{j}(g)))\,\bar{M}_g^2 \\ & - \left(\sum_{k=1}^{K} \bar{H}_g(k) + 1 - K\right)\,\bar{M}_g^2 - C_g^2\,\bar{M}_g^2,\end{aligned} \tag{4.22}$$

$$\begin{aligned}\bar{t}_2(g,2) - \bar{t}_2(g,1) \leq & \bar{S}_g + (1 - R_g)\,\bar{M}_g^2 + (2 - P(\bar{i}(g)) - P(\bar{j}(g)))\,\bar{M}_g^2 \\ & + \left(\sum_{k=1}^{K} \bar{H}_g(k) + 1 - K\right)\,\bar{M}_g^2 + (1 - C_g^2)\,\bar{M}_g^2,\end{aligned} \tag{4.23}$$

$$\begin{aligned}\bar{t}_2(g,1) - \bar{t}_2(g,2) \geq & \bar{S}_g - R_g\,\bar{M}_g^2 - (2 - P(\bar{i}(g)) - P(\bar{j}(g)))\,\bar{M}_g^2 \\ & - \left(\sum_{k=1}^{K} \bar{H}_g(k) + 1 - K\right)\,\bar{M}_g^2 - C_g^2\,\bar{M}_g^2,\end{aligned} \tag{4.24}$$

$$\begin{aligned}\bar{t}_2(g,1) - \bar{t}_2(g,2) \leq & \bar{S}_g + R_g\,\bar{M}_g^2 + (2 - P(\bar{i}(g)) - P(\bar{j}(g)))\,\bar{M}_g^2 \\ & + \left(\sum_{k=1}^{K} \bar{H}_g(k) + 1 - K\right)\,\bar{M}_g^2 + (1 - C_g^2)\,\bar{M}_g^2,\end{aligned} \tag{4.25}$$

where $\bar{M}_g^2$ is a large positive number given by

$$\bar{M}_g^2 = \max\{\bar{t}_2^+(g,1) - \bar{t}_2^-(g,2), \bar{t}_2^+(g,2) - \bar{t}_2^-(g,1)\} + \bar{S}_g + 0.1. \tag{4.26}$$

The input parameters $\bar{t}_2^+(g,\ell)$ and $\bar{t}_2^-(g,\ell)$ in (4.16) are the maximum and minimum passage time at the end point in the CFS for the ℓ^{th} flight plan of the g^{th} flight plan pair in $\bar{E}$ respectively.

The constraints (4.17), (4.18) and (4.20)-(4.25) do not only verify the separation at the beginning and the end of the CFS, but also check if the trailing aircraft overtakes the leading aircraft. These constraints set $C_g^2 = 1$ if the trailing aircraft overtakes the leading aircraft even if they are safely separated at the beginning and end of the CFS. For example, let us consider a case where the aircraft following flight plan $\bar{i}(g)$ arrives first at the CFS, i.e. $R_g = 1$. Let us assume that both aircraft are safely separated at the arrival of the trailing aircraft to the beginning the CFS. In such a case, (4.17) and (4.18) set C_g^1 to 0. Now let us assume that the trailing aircraft overtakes the leading aircraft and arrives first at the end of the CFS and that the difference between the passage times is larger than $\bar{S}_g$, i.e. $\bar{t}_2(g,1) - \bar{t}_2(g,2) > \bar{S}_g$. As $R_g = 1$, the inequations (4.24) and (4.25) are relaxed and the inequations (4.22) and (4.23) are reduced to

$$\begin{cases} \bar{t}_2(g,2) - \bar{t}_2(g,1) \geq \bar{S}_g - C_g^2\,\bar{M}_g^2, \\ \bar{t}_2(g,2) - \bar{t}_2(g,1) \leq \bar{S}_g + (1 - C_g^2)\,\bar{M}_g^2. \end{cases} \tag{4.27}$$

Since $\bar{t}_2(g,2) - \bar{t}_2(g,1) < 0$, (4.27) sets $C_g^2 = 1$, which means that there is a trailing conflict predicted to happen.
After setting the values of C_g^1 and C_g^2, the last step in the detection of the trailing conflict is to use these values to determine if each flight pair in $\bar{E}$ caused a conflict or not. Therefore, to have $\bar{C}_g = 1$ if the g^{th} flight plan pair in $\bar{E}$ caused a trailing conflict, i.e. $C_g^1 + C_g^2 \geq 1$, and set $\bar{C}_g = 0$ otherwise, we use : for $g \in \{1, 2, ..., |\bar{E}|\}$,

$$C_g^1 \; + \; C_g^2 \; \leq \; 2\,\bar{C}_g, \tag{4.28}$$

$$C_g^1 \; + \; C_g^2 \; \geq \; -2\,(0.9 - \bar{C}_g). \tag{4.29}$$

4.1.6 Balancing constraint

To include the trailing conflicts in the balancing constraint, we rewrite it as

$$\sum_{p=1}^{|E|} C_p\, I_p^s \; + \; \sum_{g=1}^{|\bar{E}|} \bar{C}_g\, \bar{I}_g^s \; \leq \; \lambda \; \frac{\sum_{p=1}^{|E|} C_p \; + \; \sum_{g=1}^{|\bar{E}|} \bar{C}_g}{|S|}, \qquad s \in \{1, ..., |S|\}. \tag{4.30}$$

This inequality ensures that the sum of the crossing and trailing conflicts predicted to happen in a sector does not surpass λ times the average number of conflicts in all the sectors.

4.1.7 MSP-SH/CT formulation

To be concise, we define $\mathcal{G} := \{1, ..., |\bar{E}|\}$. The complete model takes the following form :

$$\min_{P(i),T_i(m)} \sum_{p=1}^{|E|} C_p + \sum_{g=1}^{|\bar{E}|} \bar{C}_g + \frac{\sum_{a=1}^{A} \mathcal{I}(a)}{\gamma\, A + 1} \tag{4.31}$$

subject to
Speed and heading changes constraints :
(3.7) − (3.15),
Crossing conflict prediction constraints :
(3.16) − (3.17), (3.19), (3.21), (3.23), (3.24),
Common flight segment constraints :
$L_{\bar{i}(g)}(m,k) + L_{\bar{j}(g)}(n,k) \leq 2 - \bar{H}_g(k), \qquad g \in \mathcal{G},\ k \in \mathcal{K},$
$L_{\bar{i}(g)}(m,k) + L_{\bar{j}(g)}(n,k) \geq 1.1 - 2\bar{H}_g(k), \quad g \in \mathcal{G},\ k \in \mathcal{K},$
$\bar{t}_1(g,\ell) = t_i'(m) + \frac{T_i(m)}{D_i(m)}\, \bar{d}_1(g,\ell), \qquad i \in \bar{E},$
$\bar{t}_2(g,\ell) = t_i'(m) + \frac{T_i(m)}{D_i(m)}\, \bar{d}_2(g,\ell), \qquad i \in \bar{E},$

$$\bar{t}_1(g,1) - \bar{t}_1(g,2) \leq (1 - R_g)\,\bar{M}_g^1, \qquad g \in \mathcal{G},$$
$$\bar{t}_1(g,1) - \bar{t}_1(g,2) \geq -R_g\,\bar{M}_g^1, \qquad g \in \mathcal{G},$$

Trailing conflict prediction constraints :

$$\begin{aligned}
\bar{t}_1(g,2) - \bar{t}_1(g,1) \geq & \bar{S}_g - (1 - R_g)\,\bar{M}_g^1 - (2 - P(\bar{i}(g)) - P(\bar{i}(g)))\,\bar{M}_g^1 \\
& - (\sum_{k=1}^{K} \bar{H}_g(k) + 1 - K)\,\bar{M}_g^1 - C_g^1\,\bar{M}_g^1, \qquad g \in \mathcal{G},\\
\bar{t}_1(g,2) - \bar{t}_1(g,1) \leq & \bar{S}_g + (1 - R_g)\,\bar{M}_g^1 + (2 - P(\bar{i}(g)) - P(\bar{j}(g)))\,\bar{M}_g^1 \\
& + (\sum_{k=1}^{K} \bar{H}_g(k) + 1 - K)\,\bar{M}_g^1 + (1 - C_g^1)\,\bar{M}_g^1, \qquad g \in \mathcal{G},\\
\bar{t}_1(g,1) - \bar{t}_1(g,2) \geq & \bar{S}_g - R_g\,\bar{M}_g^1 - (2 - P(\bar{i}(g)) - P(\bar{j}(g)))\,\bar{M}_g^1 \\
& - (\sum_{k=1}^{K} \bar{H}_g(k) + 1 - K)\,\bar{M}_g^1 - C_g^1\,\bar{M}_g^1, \qquad g \in \mathcal{G},\\
\bar{t}_1(g,1) - \bar{t}_1(g,2) \leq & \bar{S}_g + R_g\,\bar{M}_g^1 + (2 - P(\bar{i}(g)) - P(\bar{j}(g)))\,\bar{M}_g^1 \\
& + (\sum_{k=1}^{K} \bar{H}_g(k) + 1 - K)\,\bar{M}_g^1 + (1 - C_g^1)\,\bar{M}_g^1, \qquad g \in \mathcal{G},\\
\bar{t}_2(g,2) - \bar{t}_2(g,1) \geq & \bar{S}_g - (1 - R_g)\,\bar{M}_g^2 - (2 - P(\bar{i}(g)) - P(\bar{j}(g)))\,\bar{M}_g^2 \\
& - (\sum_{k=1}^{K} \bar{H}_g(k) + 1 - K)\,\bar{M}_g^2 - C_g^2\,\bar{M}_g^2, \qquad g \in \mathcal{G},\\
\bar{t}_2(g,2) - \bar{t}_2(g,1) \leq & \bar{S}_g + (1 - R_g)\,\bar{M}_g^2 + (2 - P(\bar{i}(g)) - P(\bar{j}(g)))\,\bar{M}_g^2 \\
& + (\sum_{k=1}^{K} \bar{H}_g(k) + 1 - K)\,\bar{M}_g^2 + (1 - C_g^2)\,\bar{M}_g^2, \qquad g \in \mathcal{G},\\
\bar{t}_2(g,1) - \bar{t}_2(g,2) \geq & \bar{S}_g - R_g\,\bar{M}_g^2 - (2 - P(\bar{i}(g)) - P(\bar{j}(g)))\,\bar{M}_g^2 \\
& - (\sum_{k=1}^{K} \bar{H}_g(k) + 1 - K)\,\bar{M}_g^2 - C_g^2\,\bar{M}_g^2, \qquad g \in \mathcal{G},\\
\bar{t}_2(g,1) - \bar{t}_2(g,2) \leq & \bar{S}_g + R_g\,\bar{M}_g^2 + (2 - P(\bar{i}(g)) - P(\bar{j}(g)))\,\bar{M}_g^2 \\
& + (\sum_{k=1}^{K} \bar{H}_g(k) + 1 - K)\,\bar{M}_g^2 + (1 - C_g^2)\,\bar{M}_g^2, \qquad g \in \mathcal{G},
\end{aligned}$$

$$C_g^1 + C_g^2 \leq 2\,\bar{C}_g, \qquad g \in \mathcal{G},$$
$$C_g^1 + C_g^2 \geq -2\,(0.9 - \bar{C}_g), \qquad g \in \mathcal{G},$$

balancing constraint :

$$\sum_{p=1}^{|E|} C_p I_p^s + \sum_{g=1}^{|\bar{E}|} \bar{C}_g \bar{I}_g^s \leq \lambda\,\frac{\sum_{p=1}^{|E|} C_p + \sum_{g=1}^{|\bar{E}|} \bar{C}_g}{|S|}, \qquad s \in \{1, ..., |S|\},$$

integrality constraints :

$$\bar{H}_g(k),\ R_g,\ C_g^1,\ C_g^2, \bar{C}_g \in \{0,1\}, \qquad g \in \mathcal{G},\ k \in \mathcal{K}.$$

Note that the integrality and non negativity constraints of the MSP-SH/C model (3.26) are also part of the MSP-SH/CT model (4.31). The model MSP-SH/CT is a MILP model which can be solved using a commercial solver. The original trajectories are part of the search space and satisfy the constraints in the case of no balancing, so a feasible solution always exists for this model. The objective function is bounded and has a lower bound of 0 and an upper bound that equals the sum of $|E|$, $|\bar{E}|$ and $\frac{A}{A+1}$.

Similarly to MSP-SH/C, the input data has to pass by a preprocessing stage to generate the input data in a suitable format after which the problem is solved to generate the modified trajectories. An IDEF0 model of the MSP-SH/CT is presented in Figure 4.8, where we see that the preprocessing stage takes as input the flight plans of all aircraft that pass through the MSA over a time horizon of 20 to 90 minutes. It takes also aircraft related data i.e. the cruising, maximum and minimum speeds. Finally, it takes information related to the sectors geometry i.e. the coordinates of the sector boundaries.

In addition to similar output to that of the preprocessing stage of MSP-SH/C (section 3.2.5), the output of the preprocessing stage of the MSP-SH/CT model includes the set $\bar{E}$ of flight plan pairs that are at risk of a trailing conflict, the safe separation time $\bar{S}_g$ for each of these pairs and the sector indicator matrix $\bar{I}_g^s$. The output of the preprocessing stage also includes input parameters regarding the CFS, i.e. $\bar{d}_1(g,\ell), \bar{d}_2(g,\ell), \bar{t}_1^+(g,\ell), \bar{t}_1^-(g,\ell)$, and the values of $\bar{M}_g^1$ and $\bar{M}_g^2$. We programmed the preprocessing stage for this model using MATLAB 8.4. In the solution stage the commercial solver GUROBI 6.5.0 takes the input data from the preprocessing stage with the allowed percentages α, γ of modified trajectories and the balancing factor λ and generates the optimal solution. Following our problem definition in section 3.1, we limit the solution time to 10 minutes. In the following section, we present an example detailing the input and output of each of the two stages of the model.

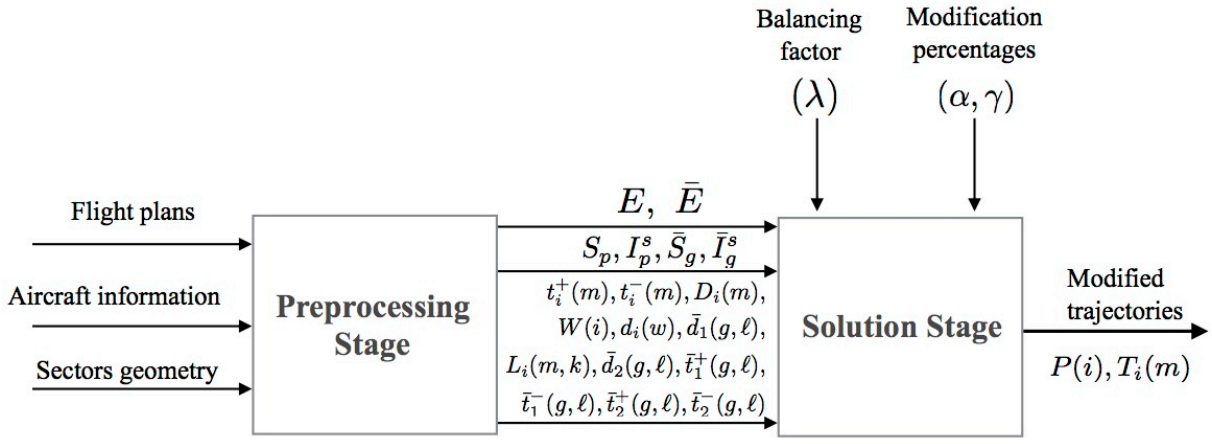

Figure 4.8 IDEF0 for the MSP-SH/CT model.

4.2 Detailed example

We present in this section a detailed example for an air traffic situation that involves a combination of crossing and trailing conflicts. First we present the input data for the preprocessing stage. Second, we present the output of the preprocessing stage, i.e. the input of the solution stage. Finally, we present the optimal solution.

4.2.1 The preprocessing stage input data

The input data for the preprocessing stage are the sectors geometry, aircraft information and flight plans information. For the sectors geometry, we consider in this example a MSA composed of three flight levels and four adjacent square sectors similar to the MSA of the detailed example in section 3.3. Note that the origin (0,0) is the left bottom corner of the MSA.
For the aircraft information, we consider 8 aircraft that are planned to pass through the MSA within a time interval of 20 to 90 minutes. All the aircraft have a minimum speed of 456 knots ($\simeq$ 850 km/hr) and a maximum speed of 513 knots ($\simeq$ 950 km/hr). The cruising speed $\bar{v}_a$ in km/hr of each aircraft is presented in Table 4.1.
The original trajectory of each aircraft detailing the coordinates of each waypoint in km and the passage time in minutes is presented in Table 4.2 and the spatial trajectories are illustrated in Figure 4.9-a. Note that we chose these trajectories and speeds to show the model ability to handle the following cases :

1. Two trailing aircraft are safely separated at the beginning and the end of the CFS but the trailing aircraft overtakes the leading aircraft (aircraft 1 and 2).
2. Two trailing aircraft follow the same spatial trajectory and lose separation along the CFS (aircraft 3 and 4).
3. Two aircraft follow different spatial trajectories up to a point after which their trajectories coincide (aircraft 5 and 6).
4. Two aircraft follow the same spatial trajectory up to a point after which their trajectories separate (aircraft 7 and 8).

If the aircraft use the original trajectories, then there are four crossing conflicts and five trailing conflicts. The crossing conflicts exist for the aircraft pairs (1,4), (2,3), (2,4) and

Table 4.1 Aircraft cruising speed for the detailed example.

Aircraft index a	1	2	3	4	5	6	7	8
$\bar{v}_a$ (km/hr)	850	950	900	920	900	920	900	920

(7,8). The trailing conflicts occur for the aircraft pairs (1,2), (3,4), (5,6) and (7,8). Note that (3,4) lose separation in two different sectors.

4.2.2 The preprocessing stage output data

The preprocessing stage generates the input parameters for the MSP-SH/CT model. First, it generates the alternative flight plans for each aircraft that results from the heading change manoeuvres. The detailed data for the alternative flight plans, including the original trajectories, is presented in Table 4.3 where the waypoints coordinates are in km and the passage times are in minutes. The flight plan indicator matrix $I_a(i)$ is presented in Table 4.4.
In this example, there are 126 pairs of flight plans at risk of a crossing conflict, i.e. that belong to E. The detailed data of E is presented in Appendix C. There are also 28 possible trailing conflicts between the flight plans. The detailed data of the flight plan pairs at risk of a trailing conflict, i.e. that belong to $\bar{E}$, is presented in Table 4.5. This table includes the flight plan pair indices $\bar{i}(g)$ and $\bar{j}(g)$ and the minimum separation time $\bar{S}_g$ in seconds. In this table, we observe that all the flight plan pairs at risk of a trailing conflict have the same minimum separation time $\bar{S}_g = 38.1$ seconds. This is because $\bar{S}_g$ depends solely on the minimum and maximum speeds of the aircraft which are the same for all the aircraft in this example. Note that the parameters $\bar{t}_1^-(g,\ell)$, $\bar{t}_1^+(g,\ell)$, $\bar{t}_2^-(g,\ell)$, $\bar{t}_2^+(g,\ell)$, $\bar{d}_1(g,\ell)$ and $\bar{d}_2(g,\ell)$ are all generated in the preprocessing stage but are not used as an input for the solution stage and they are presented in Appendix C.

4.2.3 The optimal solution

We solved this example optimally in less than 0.1 seconds using Gurobi 6.5.0 on a MacBook pro having 16.0 GB of RAM supported by an Intel® Core i7 running at 2.6GHz with a 6MB cache size, operated with OS X 10.12.1. For this example, the model has 1680 binary variables, 240 continuous variables and 3330 constraints. The example was solved while allowing for

Table 4.2 Original trajectories for the detailed example : (x, y) in km and $t_i(m)$ in minutes.

	Waypoint 1		**Waypoint 2**		**Waypoint 3**	
a	(x,y,z)	$t_i(1)$	(x,y,z)	$t_i(2)$	(x,y,z)	$t_i(3)$
1	(0,100,1)	40.25	(200,100,1)	54.37	(400,100,1)	68.49
2	(0,100,1)	40.9	(200,100,1)	53.53	(400,100,1)	66.16
3	(300,0,1)	53.33	(300,200,1)	66.67	(300,400,1)	80
4	(300,0,1)	54.08	(300,200,1)	67.13	(300,400,1)	80.17
5	(100,0,2)	26.67	(100,200,2)	40	(100,400,2)	53.33
6	(170,0,2)	26.9	(100,200,2)	40.72	(100,400,2)	53.76
7	(0,300,3)	56.67	(200,300,3)	70	(400,370,3)	84.13
8	(0,300,3)	57.5	(200,300,3)	70.54	(400,230,3)	84.36

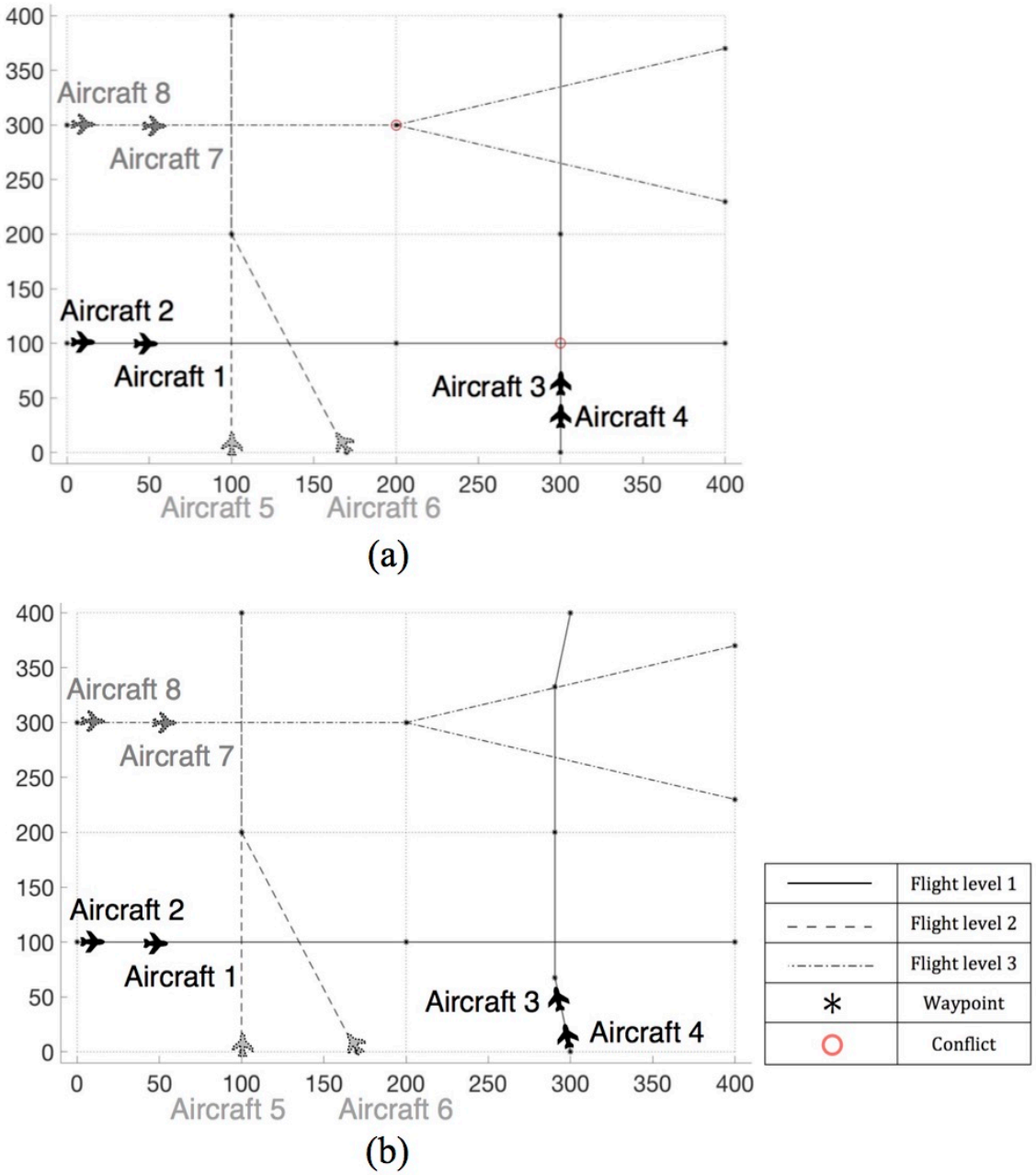

Figure 4.9 Aircraft trajectories for the trailing detailed example : (a) original trajectories ; (b) modified trajectories.

Table 4.3 Alternative flight plans for the detailed example : (x, y) in km and $t_i(m)$ in minutes.

i	**Waypoint 1**		**Waypoint 2**		**Waypoint 3**		**Waypoint 4**		**Waypoint 5**		$N(i)$
	(x,y,z)	$t_i(1)$	(x,y,z)	$t_i(2)$	(x,y,z)	$t_i(3)$	(x,y,z)	$t_i(4)$	(x,y,z)	$t_i(5)$	
1	(0,100,1)	40.25	(200,100,1)	54.37	(400,100,1)	68.49	-	-	-	-	3
2	(0,100,1)	40.25	(67.6,90.5,1)	45.07	(200,90.5,1)	54.41	(332.4,90.5,1)	63.76	(400,100,1)	68.58	5
3	(0,100,1)	40.25	(67.6,109.5,1)	45.07	(200,109.5,1)	54.41	(332.4,109.5,1)	63.76	(400,100,1)	68.58	5
4	(0,100,1)	40.9	(200,100,1)	53.53	(400,100,1)	66.16	-	-	-	-	3
5	(0,100,1)	40.9	(67.6,90.5,1)	45.21	(200,90.5,1)	53.57	(332.4,90.5,1)	61.94	(400,100,1)	66.25	5
6	(0,100,1)	40.9	(67.6,109.5,1)	45.21	(200,109.5,1)	53.57	(332.4,109.5,1)	61.94	(400,100,1)	66.25	5
7	(300,0,1)	53.33	(300,200,1)	66.67	(300,400,1)	80	-	-	-	-	3
8	(300,0,1)	53.33	(309.5,67.6,1)	57.88	(309.5,200,1)	66.71	(309.5,332.4,1)	75.54	(300,400,1)	80.09	5
9	(300,0,1)	53.33	(290.5,67.6,1)	57.88	(290.5,200,1)	66.71	(290.5,332.4,1)	75.54	(300,400,1)	80.09	5
10	(300,0,1)	54.08	(300,200,1)	67.13	(300,400,1)	80.17	-	-	-	-	3
11	(300,0,1)	54.08	(309.5,67.6,1)	58.54	(309.5,200,1)	67.17	(309.5,332.4,1)	75.81	(300,400,1)	80.26	5
12	(300,0,1)	54.08	(290.5,67.6,1)	58.54	(290.5,200,1)	67.17	(290.5,332.4,1)	75.81	(300,400,1)	80.26	5
13	(100,0,2)	26.67	(100,200,2)	40	(100,400,2)	53.33	-	-	-	-	3
14	(100,0,2)	26.67	(109.5,67.6,2)	31.22	(109.5,200,2)	40.04	(109.5,332.4,2)	48.87	(100,400,2)	53.42	5
15	(100,0,2)	26.67	(90.5,67.6,2)	31.22	(90.5,200,2)	40.04	(90.5,332.4,2)	48.87	(100,400,2)	53.42	5
16	(170,0,2)	26.9	(100,200,2)	40.72	(100,400,2)	53.76	-	-	-	-	3
17	(170,0,2)	26.9	(156.64,66.94,2)	31.35	(110.07,200,2)	40.55	(109.5,332.4,2)	49.18	(100,400,2)	53.63	5
18	(170,0,2)	26.9	(138.7,60.66,2)	31.35	(89.93,200,2)	40.98	(90.5,332.4,2)	49.61	(100,400,2)	54.07	5
19	(0,300,3)	56.67	(200,300,3)	70	(400,370,3)	84.13	-	-	-	-	3
20	(0,300,3)	56.67	(67.6,290.5,3)	61.22	(200,290.5,3)	70.04	(339.34,338.7,3)	79.87	(400,370,3)	84.42	5
21	(0,300,3)	56.67	(67.6,309.5,3)	61.22	(200,309.5,3)	70.04	(333.06,356.64,3)	79.46	(400,370,3)	84.01	5
22	(0,300,3)	57.5	(200,300,3)	70.54	(400,230,3)	84.36	-	-	-	-	3
23	(0,300,3)	57.5	(67.6,290.5,3)	61.95	(200,290.5,3)	70.59	(333.06,243.36,3)	79.79	(400,230,3)	84.24	5
24	(0,300,3)	57.5	(67.6,309.5,3)	61.95	(200,309.5,3)	70.59	(339.34,261.3,3)	80.2	(400,230,3)	84.65	5

Table 4.4 The flight plan indicator matrix $I_a(i)$ of the detailed example

a \ i	1	2	3	4	5	6	7	8	9	10	11	12	13	14	15	16	17	18	19	20	21	22	23	24
1	1	1	1	0	0	0	0	0	0	0	0	0	0	0	0	0	0	0	0	0	0	0	0	0
2	0	0	0	1	1	1	0	0	0	0	0	0	0	0	0	0	0	0	0	0	0	0	0	0
3	0	0	0	0	0	0	1	1	1	0	0	0	0	0	0	0	0	0	0	0	0	0	0	0
4	0	0	0	0	0	0	0	0	0	1	1	1	0	0	0	0	0	0	0	0	0	0	0	0
5	0	0	0	0	0	0	0	0	0	0	0	0	1	1	1	0	0	0	0	0	0	0	0	0
6	0	0	0	0	0	0	0	0	0	0	0	0	0	0	0	1	1	1	0	0	0	0	0	0
7	0	0	0	0	0	0	0	0	0	0	0	0	0	0	0	0	0	0	1	1	1	0	0	0
8	0	0	0	0	0	0	0	0	0	0	0	0	0	0	0	0	0	0	0	0	0	1	1	1

100% of the trajectories to be modified, i.e. $\alpha = \gamma = 1$, and with equal balancing among sectors, i.e. $\lambda = 1$.

The MSP-SH/CT model was able to eliminate all the trailing and crossing conflicts, nine conflicts in total, by modifying the trajectories of five out of eight aircraft. Although we did not limit the number of modified trajectories, the optimal solution included the modification of only five trajectories. It is the modified objective function that we introduced in MSP-SH/CT that allowed the model to minimize the number of modified trajectories.

The values of the decision variables $P(i)$ and $T_i(m)$ in the optimal solution are presented in Table 4.6. From this table, we can determine the flight plan used by each aircraft, i.e. heading change manoeuvre, and the waypoints passage times, i.e. speed change. The aircraft spatial trajectories corresponding to the solution are illustrated in Figure 4.9-b. From this figure we see that aircraft 3 and 4 are the only aircraft doing a heading change manoeuvre. The data related to the flight plan used by each aircraft and the change in passage times are presented in Table 4.7. In this table, the column Flight plan (i) gives the index of the flight plan used by each aircraft, the columns $t'_i(m)$ gives the waypoints passage times, the column $\mathcal{I}_s(i)$ indicates if the flight plan i includes a speed change or not, the column $\mathcal{I}_h(a)$ indicates if the aircraft a undergoes a heading change or not and the column $\mathcal{I}(a)$ indicates if the trajectory of aircraft a is modified or not.

These results show the model ability to handle all the different trailing conflicts cases discussed in section 4.2.1. The results also show the model ability to handle a combination of crossing and trailing conflicts. For example, aircraft 1 was involved in a crossing conflict with aircraft 4 and a trailing conflict with aircraft 2, both conflicts were avoided in the solution by modifying both the trajectories of aircraft 1 and 4.

4.3 Numerical experiments

In this section, we conduct four different sets of experiments on the MSP-SH/CT model. In the first set, we solve a set of randomly generated problems twice. The first time we solve

Table 4.5 Flight pairs at risk of a trailing conflict - $\bar{E}$

g	1	2	3	4	5	6	7	8	9	10	11	12	13	14
i(g)	1	1	2	2	2	2	3	3	3	3	7	7	8	8
j(g)	4	4	5	5	5	5	6	6	6	6	10	10	11	11
S_g	38.1	38.1	38.1	38.1	38.1	38.1	38.1	38.1	38.1	38.1	38.1	38.1	38.1	38.1

g	15	16	17	18	19	20	21	22	23	23	25	26	27	28
i(g)	8	8	9	9	9	9	13	14	15	19	20	20	21	21
j(g)	11	11	12	12	12	12	16	17	18	22	23	23	24	24
S_g	38.1	38.1	38.1	38.1	38.1	38.1	38.1	38.1	38.1	38.1	38.1	38.1	38.1	38.1

Table 4.6 The values of the decision variables for the optimal solution of the detailed example- $T_i(m)$ in minutes

i	1	2	3	4	5	6	7	8	9	10	11	12
$\boldsymbol{P(i)}$	1	0	0	1	0	0	0	0	1	0	0	1
$\boldsymbol{T_i(1)}$	12.65	4.82	4.82	12.63	4.31	4.31	13.33	4.55	4.53	13.04	4.45	4.55
$\boldsymbol{T_i(2)}$	12.63	9.35	9.35	12.63	8.36	8.36	13.33	8.83	9.35	13.04	8.64	9.21
$\boldsymbol{T_i(3)}$	0	9.35	9.35	0	8.36	8.36	0	8.83	8.36	0	8.64	8.5
$\boldsymbol{T_i(4)}$	0	4.82	4.82	0	4.31	4.31	0	4.55	4.31	0	4.45	4.31

i	13	14	15	16	17	18	19	20	21	22	23	24
$\boldsymbol{P(i)}$	1	0	0	1	0	0	1	0	0	1	0	0
$\boldsymbol{T_i(1)}$	13.41	4.55	4.55	13.82	4.45	4.45	13.17	4.55	4.55	13.04	4.45	4.45
$\boldsymbol{T_i(2)}$	12.79	8.83	8.83	13.04	9.19	9.63	14.96	8.83	8.83	13.82	8.64	8.64
$\boldsymbol{T_i(3)}$	0	8.83	8.83	0	8.64	8.64	0	9.83	9.41	0	9.21	9.62
$\boldsymbol{T_i(4)}$	0	4.55	4.55	0	4.45	4.45	0	4.55	4.55	0	4.45	4.45

Table 4.7 The modified trajectories in the optimal solution of the detailed example

Aircraft index (a)	**Flight plan (i)**	$t'_i(1)$	$t'_i(2)$	$t'_i(3)$	$t'_i(4)$	$t'_i(5)$	$\mathcal{I}_s(i)$	$\mathcal{I}_h(a)$	$\mathcal{I}(a)$
1	1	40.25	52.9	65.53	-	-	1	0	1
2	4	40.9	53.53	66.16	-	-	0	0	0
3	9	53.33	57.86	67.21	75.57	79.88	1	1	1
4	12	54.08	58.63	67.84	76.34	80.65	1	1	1
5	13	26.67	40.08	52.86	-	-	1	0	1
6	16	26.9	40.72	53.76	-	-	0	0	0
7	19	56.67	69.83	84.79	-	-	1	0	1
8	22	57.5	70.54	84.36	-	-	0	0	0

the problems using an objective function that minimizes only the number of conflicts and the second time using the modified objective function (4.11). We compare the two results to demonstrate the advantages of using the modified objective function. In the second set, we solve a large number of randomly generated problems with varying number of crossing and trailing conflicts. The problems are solved using different combinations of manoeuvres to test and assess the model capacity to solve a large number of crossing and trailing conflicts in a reasonable amount of time. In the third set, we test our model performance with the variation of the allowed percentage γ of modified trajectories. In the fourth set of tests, we solve randomly generated problems with different balancing levels to demonstrate the potential benefits of considering workload balancing in air traffic situations that involve a combination of crossing and trailing conflicts.

4.3.1 Experimental design

Similarly to the tests on the MSP-SH/C model in section 3.5.1, the tests presented in the following sections rely on solving randomly generated problems using four different model variants as follows :

1. MSP-S/CT, which stands for *Multi-Sector Planning support model using Speed changes for Crossing and Trailing conflicts*, using small speed changes, i.e. changes limited to $[-0.06\ \bar{v}_a, 0.03\ \bar{v}_a]$.
2. MSP-S/CT model using large speed changes, i.e. changes limited to $[-0.12\ \bar{v}_a, 0.06\ \bar{v}_a]$.
3. MSP-H/CT which stands for *Multi-Sector Planning support model using Heading changes for Crossing and Trailing conflicts*. This variant uses only heading changes.
4. MSP-SH/CT using small speed changes and heading changes.

The MSP-S/CT model has the same formulation as the MSP-SH/CT model (4.31) with the introduction of (3.27) as an additional constraint, which prevents heading change manoeuvres. To solve the problems using MSP-H/CT, we solve them using MSP-SH/CT while setting the percentage α of speed-modified trajectories to 0.

All the randomly generated problems in this chapter consider a number A of aircraft passing through a MSA composed of four square adjacent sectors of side 300 km. For each problem, we randomly generate a number of $\bar{\mathcal{A}}$ trajectories where the random generation of the spatial coordinates follows the same procedure and distributions used in section 3.5.1. To ensure the occurrence of trailing conflicts, we assign 10 aircraft to each of these trajectories.

The aircraft cruise speeds are randomly generated using the uniform distribution U[458 knots, 506 knots]. The minimum and maximum speed, which are used to evaluate the minimum separation times S_p and $\bar{S}_g$, are set to -12% and $+6\%$ of the cruise speed. The time at which

the aircraft enters the MSA follows the uniform distribution U[20 min, 90 min]. The MSA entry time is generated in such a way that two aircraft following the same spatial trajectory have a MSA entry time difference larger than 1 minute.

The problems are identified by the number $\bar{\mathcal{A}}$ of trajectories. The number A of aircraft is always given by $10\,\bar{\mathcal{A}}$. As in section 3.5.1, the number of conflicts for a given value of $\bar{\mathcal{A}}$ is random. In Figure 4.10, we plotted the average number of conflicts $\bar{\mathcal{N}}$ as a function of the number of generated problems n to determine an appropriate value of n for the tests. We found that for all problem sets, the standard deviation of $\bar{\mathcal{N}}$ is smaller than $0.1\,\bar{\mathcal{N}}$ for $n \geq 50$. In this chapter, we use $n = 50$ as a fair compromise between precision and computation time. We solve the problems using Gurobi 6.5.0 on a MacBook pro having 16.0 GB of RAM supported by an Intel® Core i7 running at 2.6GHz with a 6MB cache size, operated with OS X 10.12.1.

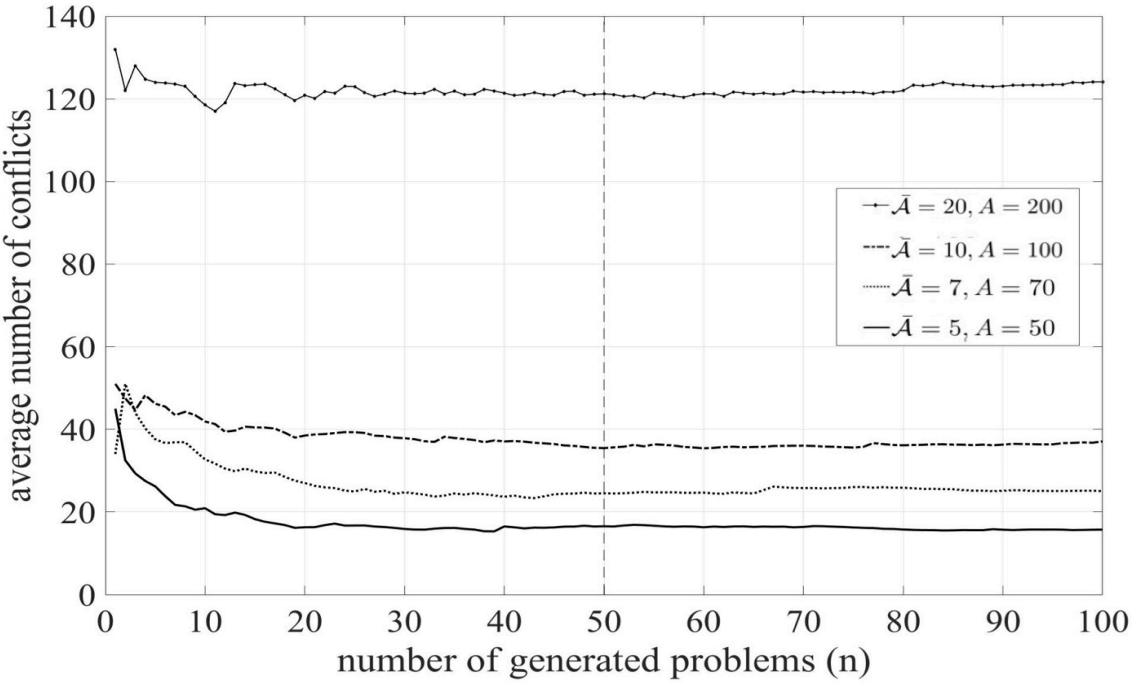

Figure 4.10 Average number of conflicts as a function of the number of problems.

4.3.2 Testing the modified objective function

In section 4.1.3, we proposed the formulation (4.11) for the objective function that minimizes the sum of the crossing conflicts, trailing conflicts and the number of modified trajectories. We chose this formulation to eliminate the problem of unnecessary modifications. In this section, we solve a set of randomly generated problems once using (4.11) and another using

only the first two terms of (4.11), i.e.

$$\bar{Z} = \sum_{p=1}^{|E|} C_p + \sum_{g=1}^{|\bar{E}|} \bar{C}_g. \tag{4.32}$$

Equation (4.32) represents the total number of conflicts. In the following, we refer to (4.32) as the unmodified objective function and to (4.11) as the modified objective function. First, we compare the percentages of modified trajectories obtained with each function for a fixed value of γ. Second, we examine how the solutions vary as a function of γ. Finally, we compare the computational times for solving the model using each of the two functions.

Percentage of modified trajectories

We have four different sets of randomly generated problems, each with a different number $\bar{\mathcal{A}}$ of trajectories. The average number of conflicts $\bar{\mathcal{N}}$ in each set following the original trajectories is presented in Table 4.8. In this table, we can see the average number of crossing and trailing conflicts along with their total.

In this section, the problems are solved using MSP-SH/CT while allowing for the modification of 50% of the trajectories, i.e. $\alpha = \gamma = 0.5$. The average percentage of resolved conflicts using each of the two objective functions is presented in Table 4.9. In this table, we observe that the model eliminated more than 99% of the conflicts on the average in all problem sets. We also see that the number of resolved conflicts is the same using either of the objective functions because both functions prioritize the minimization of the number of conflicts over the minimization of the number of modified trajectories as discussed in section 4.1.3.

The percentage of modified trajectories in the solutions obtained using each objective function is presented in Table 4.10. In this table, the columns avg and SD give the average and standard deviation of the percentage of modified trajectories respectively. In this table, we see that the percentage of modified trajectories is approximately equal to $\gamma = 0.5$ for the unmodified objective function. Using the modified objective function, the average percentage of modified trajectories is reduced by more than 30% for $\bar{\mathcal{A}} \leq 10$ and by approximately 20% for $\bar{\mathcal{A}} = 20$. We conclude that using the modified objective function eliminates the same

Table 4.8 Average number of conflicts per problem.

	$\bar{\mathcal{A}} = 5$	$\bar{\mathcal{A}} = 7$	$\bar{\mathcal{A}} = 10$	$\bar{\mathcal{A}} = 20$
Crossing	10.44	16.26	24.22	95.06
Trailing	6.1	8.26	11.24	26.12
$\bar{\mathcal{N}}$	16.54	24.52	35.46	121.18

Table 4.9 Average percentage of resolved conflicts using the unmodified and modified objective functions (%).

	$\bar{\mathcal{A}} = 5$	$\bar{\mathcal{A}} = 7$	$\bar{\mathcal{A}} = 10$	$\bar{\mathcal{A}} = 20$
Unmodified objective	99.6	99.8	99.2	99.6
Modified objective	99.6	99.8	99.2	99.6

number of conflicts as the unmodified objective function but achieve this with a significant smaller number of modified trajectories.

We plotted the percentage of modified trajectories for each of the 50 problems with $\bar{\mathcal{A}} = 10$ in Figure 4.11. In this figure, we see that the model that uses the modified objective function always returns a solution with a fewer number of modifications than the unmodified objective.

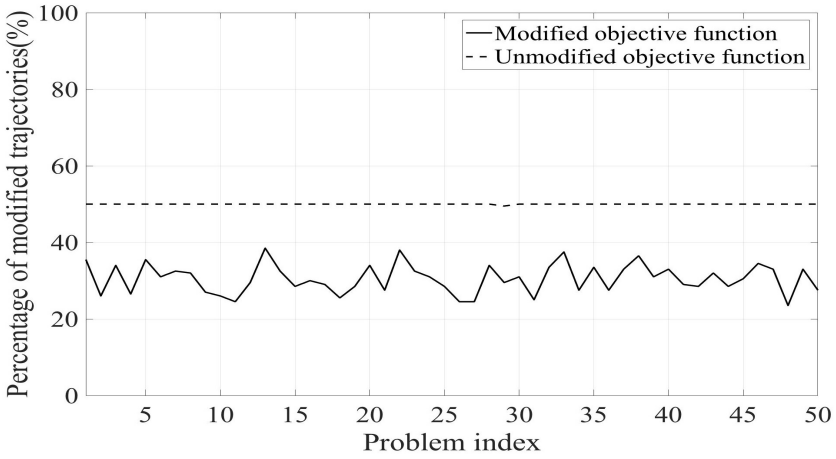

Figure 4.11 The percentage of modified trajectories for the problems with $\bar{\mathcal{A}} = 10$.

Varying the allowed percentage of modified trajectories

In this section, we consider only one of the problems with $\bar{\mathcal{A}} = 10$ that has 31 conflicts. The percentage of modified trajectories and the number of resolved conflicts as a function of γ

Table 4.10 Percentage of modified trajectories using the modified and unmodified objective functions.

	$\bar{\mathcal{A}} = 5$		$\bar{\mathcal{A}} = 7$		$\bar{\mathcal{A}} = 10$		$\bar{\mathcal{A}} = 20$	
	avg (%)	SD (%)	avg (%)	SD (%)	avg (%)	SD (%)	avg (%)	SD (%)
Unmodified objective	49.96	0.28	50	0	50	0	49.99	0.07
Modified objective	13.76	6.9	15.69	5.94	18.02	4.52	30.51	3.81

using the unmodified and the modified objective functions are displayed in the Figures 4.12-a and 4.12-b respectively. In both figures, we see that the modification of 18% of the trajectories is sufficient to eliminate all conflicts. In Figure 4.12-a, we see that by using the unmodified objective function the percentage of modified trajectories increases as γ increases, even after the elimination of all conflicts for $\gamma = 0.18$. We observe in Figure 4.12-b that by using the modified objective function, the percentage of modified trajectories increases as γ increases until the elimination of all conflicts for $\gamma = 0.18$. For $\gamma > 0.18$, the percentage of modified trajectories does not increase and remains constant. Comparing the two figures, we observe that for any value of γ, the modified objective function always eliminates the same number of conflicts as the unmodified objective function ; but with fewer modified trajectories. We conclude that the modified objective function eliminates the problem of the unnecessary trajectory modifications.

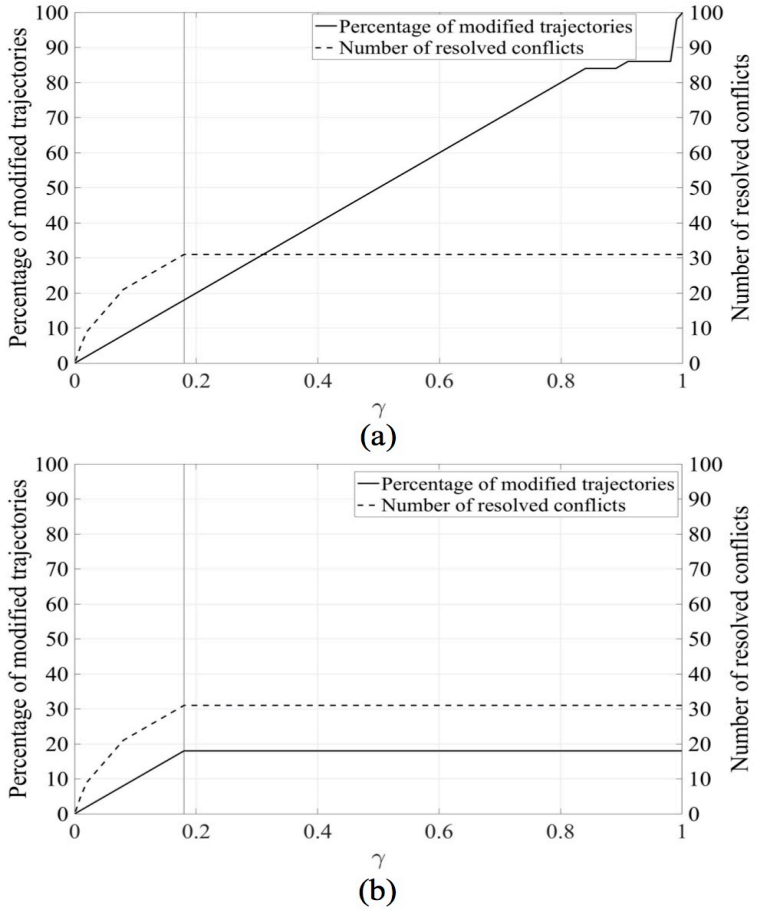

Figure 4.12 A comparison between the percentage of modified trajectories and number of resolved conflicts for a problem with $\bar{\mathcal{A}} = 10$ using : (a) the unmodified objective function, (b) the modified objective function.

Computation time

The average and standard deviation of the computation time using the modified and unmodified objective functions to solve different sets of randomly generated problems is presented in Table 4.11. The problems are solved while allowing for the modification of 50% of the trajectories, i.e. $\alpha = \gamma = 0.5$. We can see in this table that in the case of small size problems, i.e. $\bar{\mathcal{A}} = 5$ and $\bar{\mathcal{A}} = 7$, the computation times using each of the two functions are small (< 2 sec) and comparable. For the problem with $\bar{\mathcal{A}} = 10$, the computation time for the modified objective function is slightly higher than for the unmodified objective function. For the problems with $\bar{\mathcal{A}} = 20$, the computation time for the modified objective function is three times that for the unmodified objective function. We conclude that using the modified objective function increases the computational time on the average in comparison with the unmodified objective function.

Using the modified objective function, the model returned the optimal solution for all the problems with $\bar{\mathcal{A}} = 5, 7$ and 10. For the problems with $\bar{\mathcal{A}} = 20$, there are three problems out of 50 for which the solver did not return the optimal solution or did not determine the optimality of the best solution found in less than 10 minutes.

By further investigating these problems, we found that the times needed to find the solution with the minimum number of conflicts, using either the unmodified or the modified objective, were comparable. For the model that uses the modified objective function, the solver spends most of the computation time to determine the optimal percentage of modified trajectories. We conclude that the modified objective function eliminates the problem of unnecessary modifications, but it can increase significantly the computation time for large size problems, i.e. high traffic situations.

Since the scenario in which our model is applied relies on rerunning the model multiple times, we suggest to use the modified objective function only one time to determine the minimum percentage of modified trajectories. For the remaining times of running the model, we suggest the use of the unmodified objective function while setting γ to the percentage of modified trajectories found by the modified objective function.

Table 4.11 Computational time in seconds using the modified and unmodified objective functions.

	$\bar{\mathcal{A}} = 5$		$\bar{\mathcal{A}} = 7$		$\bar{\mathcal{A}} = 10$		$\bar{\mathcal{A}} = 20$	
	avg	SD	avg	SD	avg	SD	avg	SD
Unmodified objective	0.4	0.2	0.8	0.3	1.9	0.7	42.8	73
Modified objective	0.6	0.5	1.4	0.9	4.2	2.5	120.2	138

4.3.3 Comparison between the performance of each manoeuvre

In this section, we compare the capacity of each of the four model variants to solve a combination of crossing and trailing conflicts. The percentage of resolved conflicts using the four variants in the solution of problems with $\bar{\mathcal{A}}$ up to 20 is displayed in Table 4.12. The problems are solved using the modified objective function (4.11), $\alpha = \gamma = 0.5$ and $\lambda = 4$, i.e. no workload balancing. In Table 4.12, the columns avg and SD give the average and standard deviation of the percentage of resolved conflicts respectively. Note that the average number of conflicts for each problem set is displayed in Table 4.8.

The model solved on the average more than 98.5% of the conflicts using only large speed changes, more than 94% using only small speed changes and more than 77% using only heading changes. These results show that any of the three manoeuvres is efficient in solving most of the conflicts in an air traffic scenario that involves a combination of crossing and trailing conflicts. Although the use of only heading changes solves most conflicts, its capacity to solve conflicts is not comparable to the speed change manoeuvres. This is true even in small size problems contrary to the MSP-SH/C model, where the capacity of heading changes manoeuvres in solving crossing conflicts is comparable to speed changes (see section 3.5.3). This is due to the fact that the average number of conflicts in small size problems ($A \leq 50$) used to test MSP-SH/C was less than 5 conflicts, while the average number of conflicts in small size problem ($\bar{\mathcal{A}} = 5, A = 50$) used to test MSP-SH/CT is 16.54 conflicts. With few conflicts, the capacity of small changes to eliminate most of the conflicts increases.

In Table 4.12, we see that the model MSP-SH/CT that uses a combination of small speed changes and heading changes solved on the average more than 99% of the conflicts in all problem sets. To compare MSP-S/CT (large) and MSP-SH/CT, we plotted the confidence interval of the percentage of resolved conflicts with a confidence level of 95% in Figure 4.13. We observe that the capacity of the two models in solving conflicts is comparable for $\bar{\mathcal{A}} \leq 10$. However, we observe in Figure 4.13-d that for large size problems, $\bar{\mathcal{A}} \geq 20$, the capacity of MSP-SH/CT to solve conflicts is significantly higher than MSP-S/CT (large).

The number of unresolved conflicts for each problem instance for $\bar{\mathcal{A}} = 10$ and $\bar{\mathcal{A}} = 20$ using MSP-S/CT (large) and MSP-SH/CT is presented in Figure 4.14. In this figure, we see that

Table 4.12 Total percentage of resolved conflicts using different model variants.

Number of trajectories $\bar{\mathcal{A}}$	**MSP-S/CT (large)**		**MSP-S/CT (small)**		**MSP-H/CT**		**MSP-SH/CT**	
	avg (%)	SD (%)	avg (%)	SD (%)	avg (%)	SD (%)	avg (%)	SD (%)
5	99.62	2.01	97.86	5.18	84.93	15.95	99.62	2.01
7	99.77	0.79	98.67	2.22	84.7	10.71	99.82	0.71
10	98.69	2.6	95.56	4.88	84.38	7.41	99.19	1.96
20	98.72	1.69	94.05	4.32	77.04	5.14	99.58	0.73

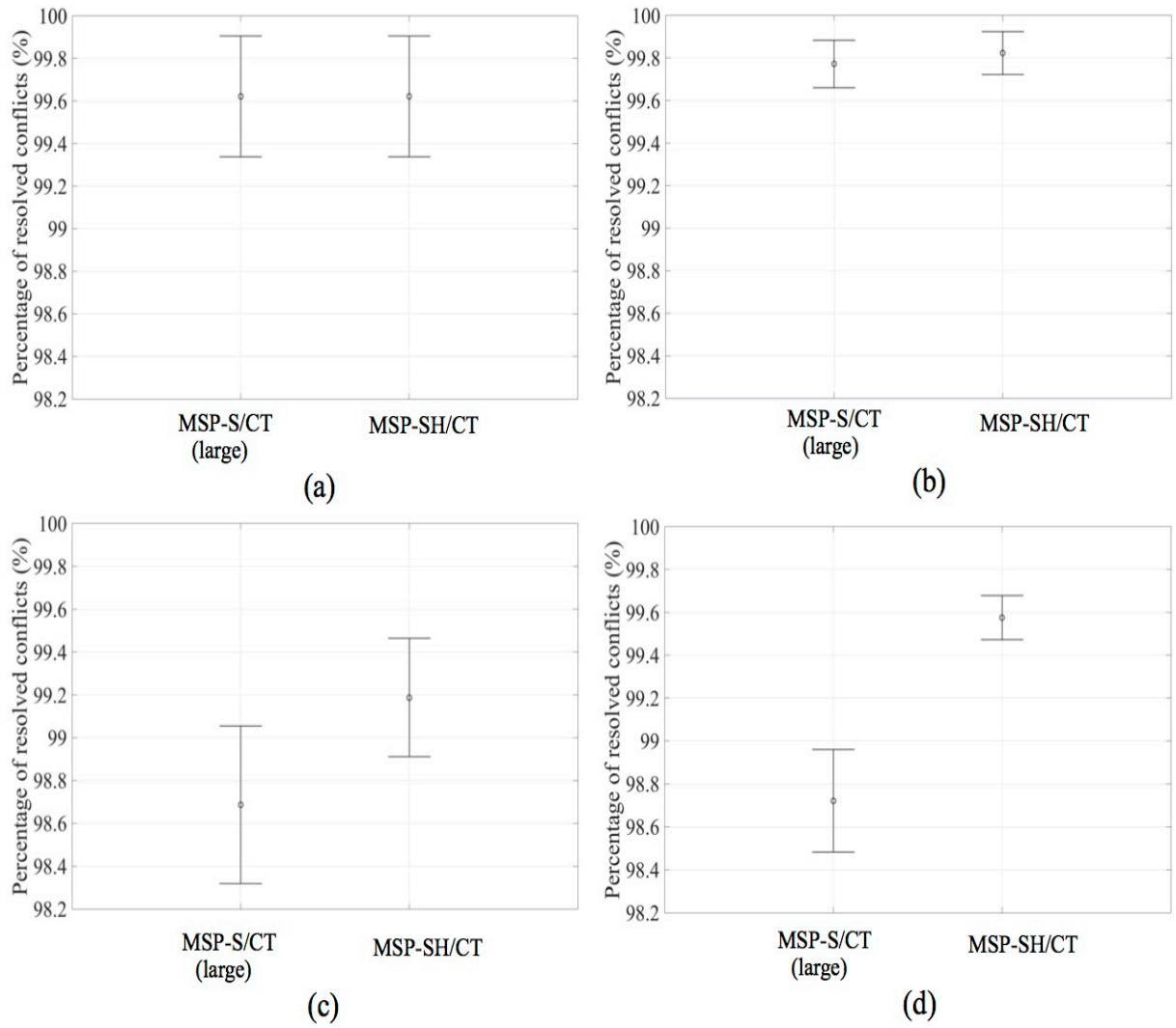

Figure 4.13 Confidence interval of the percentage of resolved conflicts with a confidence level of 95% for problems with : (a) $\bar{\mathcal{A}} = 5$; (b) $\bar{\mathcal{A}} = 7$; (c) $\bar{\mathcal{A}} = 10$; (d) $\bar{\mathcal{A}} = 20$.

MSP-SH/CT gives a solution with the same or a lower number of conflicts than MSP-S/CT (large) for each problem instance and not only on the average.

4.3.4 Travel time results

In this section, we study the change in travel durations for the modified trajectories. This change is measured by the percentage of delay ΔT per modified trajectory evaluated using (3.29). Note that (3.29) calculates ΔT as the sum of the delay percentages divided by the number of modified trajectories. The average delay percentage resulting from using each of the four model variants in solving problems with $\bar{\mathcal{A}}$ up to 20, i.e. 200 aircraft, is displayed in

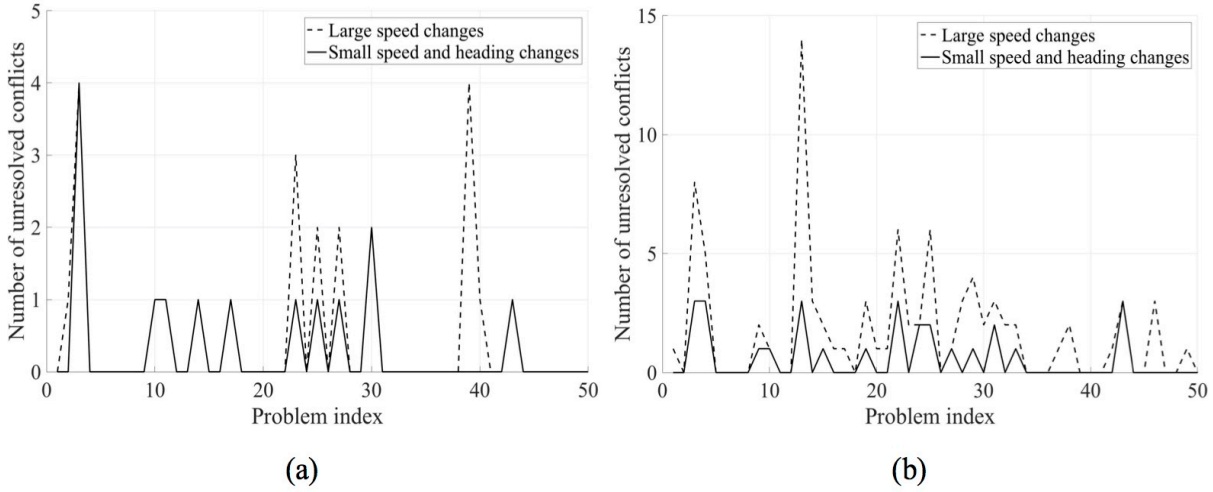

Figure 4.14 Number of unresolved conflicts using MSP-S/CT (large speed) and MSP-SH/CT for problems with : (a) $\bar{\mathcal{A}} = 10$; (b) $\bar{\mathcal{A}} = 20$.

Table 4.13. In this table, the columns avg and max give the average and the maximum value of ΔT for all problem sets.

In Table 4.13, we observe that the largest values of ΔT occur for the large speed change with an average ΔT varying between 3.39% and 4.42%. The heading change manoeuvre has the smallest effect on ΔT with an average ΔT less than 0.77% for all problem sizes. The changes of the travel durations using MSP-S/CT (small) and MSP-SH/CT are comparable. These results show that the model variant MSP-SH/CT reduced the number of conflicts by more than 99% with an average change in the travel duration of the modified trajectories smaller than 2.18%. We conclude that the time delays caused by our trajectory modifications are minimal. We also conclude that using a combination of small speed changes and heading changes eliminates more conflicts than using only large speed changes with less change in the travel durations.

Table 4.13 Percentage of delay per modified trajectory.

	MSP-S/CT (large)		**MSP-S/CT (small)**		**MSP-H/CT**		**MSP-SH/CT**	
$\bar{\mathcal{A}}$	avg	max	avg	max	avg	max	avg	max
5	3.39	7.4	2.61	5.04	0.77	1.35	2.39	5.26
7	3.42	6.18	2.66	4.14	0.68	1.22	2.18	3.27
10	3.63	6.31	2.61	3.52	0.77	1.21	2.2	3.36
20	4.42	5.81	2.68	3.3	0.75	0.99	2.22	2.93

4.3.5 Effect of changing the allowed percentage of modified trajectories

We evaluate our model performance by checking the number of unresolved conflicts, the computation time and the percentage of modified trajectories. In this section, we want to study the effect of varying the allowed percentage γ of modified trajectories on the performance of the MSP-SH/CT model. The Figures 4.15-a and 4.15-b display the average number of unresolved conflicts as a function of γ for problems with $\bar{\mathcal{A}} = 10$ and $\bar{\mathcal{A}} = 20$ respectively. The problems are solved with $\lambda = 4$, i.e. no balancing, to study solely the effect of changing γ.

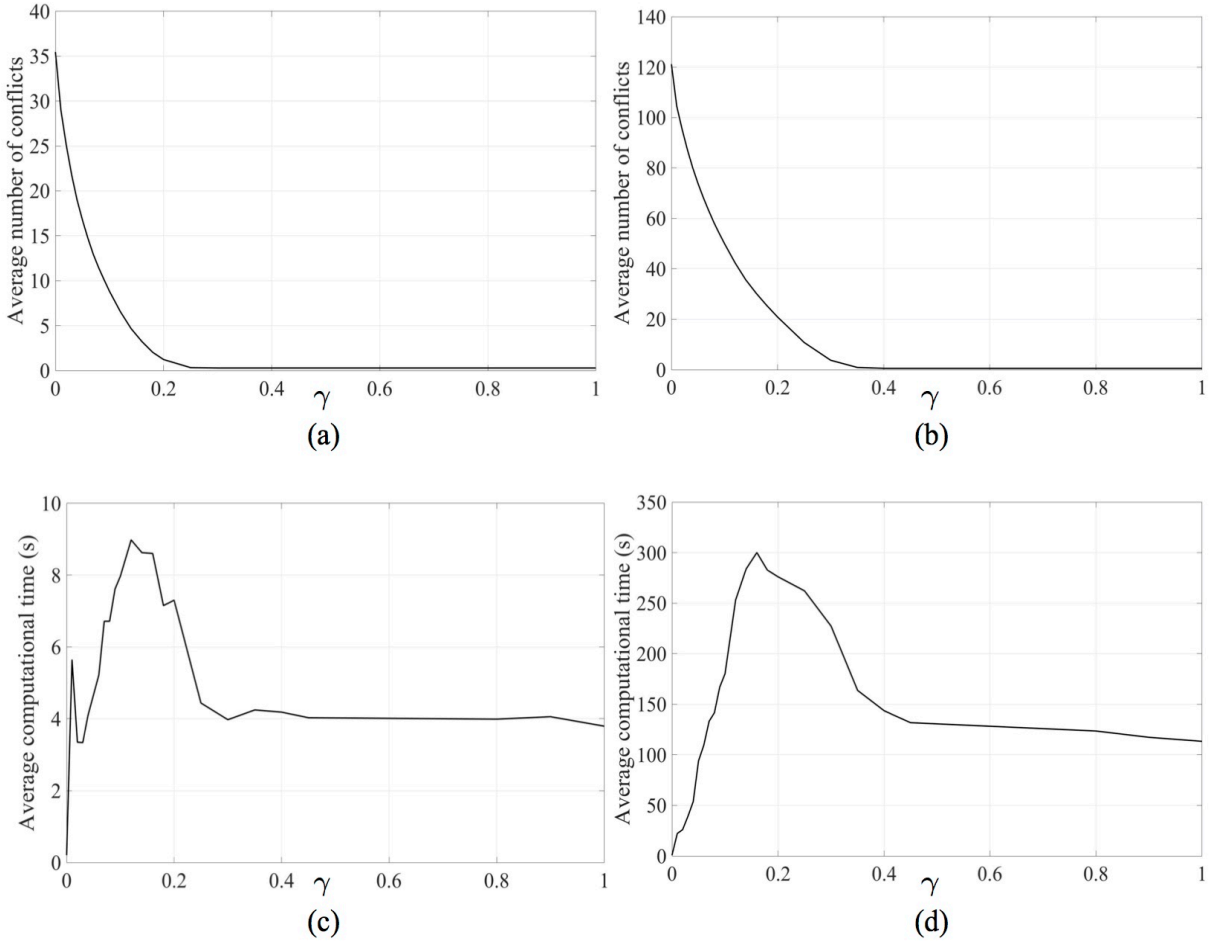

Figure 4.15 Testing the effect of γ on the performance of MSP-SH/CT : (a) number of unresolved conflicts for $\bar{\mathcal{A}} = 10$; (b) number of unresolved conflicts for $\bar{\mathcal{A}} = 20$; (c) average computational time for $\bar{\mathcal{A}} = 10$; (d) average computational time for $\bar{\mathcal{A}} = 20$.

We see in the Figures 4.15-a and 4.15-b that the number of unresolved conflicts decreases as γ increases, and the model converges to a conflict free solution. We also observe that conflict free solutions are obtained by modifying more than 25% and 35% of the trajectories for problems with $\bar{\mathcal{A}} = 10$ and $\bar{\mathcal{A}} = 20$ respectively. In section 3.5.6, we observed that the

minimum value of γ above which the model resolves most conflicts equals to $\gamma = \frac{\mathcal{N}}{A}$. By examining individually the problems solved by MSP-SH/CT, we observed that the minimum value of γ that resolves most conflicts, let us denote it $\bar{\gamma}$, is significantly smaller than $\frac{\mathcal{N}}{A}$. This comes from the fact that in these problems there are many aircraft involved in more than one conflict. Usually the modification of only one trajectory is sufficient to solve more than one conflict.

The average computational times as a function of γ for problems with $\bar{\mathcal{A}} = 10$ and $\bar{\mathcal{A}} = 20$ are displayed in the Figures 4.15-c and 4.15-d respectively. In these figures, we observe that the average computational time is always less than 10 seconds for $\bar{\mathcal{A}} = 10$ and less than 300 seconds for $\bar{\mathcal{A}} = 20$. This difference is explained by the fact that the number of conflicts in the problems with $\bar{\mathcal{A}} = 20$ is three times that in the problems with $\bar{\mathcal{A}} = 10$. Similarly to our observations for MSP-SH/C, the computational time is maximum near $\bar{\gamma}$. Note that $\bar{\gamma} = 0.25$ and 0.35 for $\bar{\mathcal{A}} = 10$ and $\bar{\mathcal{A}} = 20$ respectively.

The actual percentage of modified trajectories as a function of γ for problems with $\bar{\mathcal{A}} = 10$ and $\bar{\mathcal{A}} = 20$ is displayed in the Figures 4.16-a and 4.16-b respectively. In these figures, we observe that the percentage of modified trajectories approximately equals the value of γ for $\gamma < \bar{\gamma}$. For $\gamma > \bar{\gamma}$, the percentage of modified trajectories is the same as for $\gamma = \bar{\gamma}$. This observation confirms that the use of the modified objective function eliminates the unnecessary trajectory modifications.

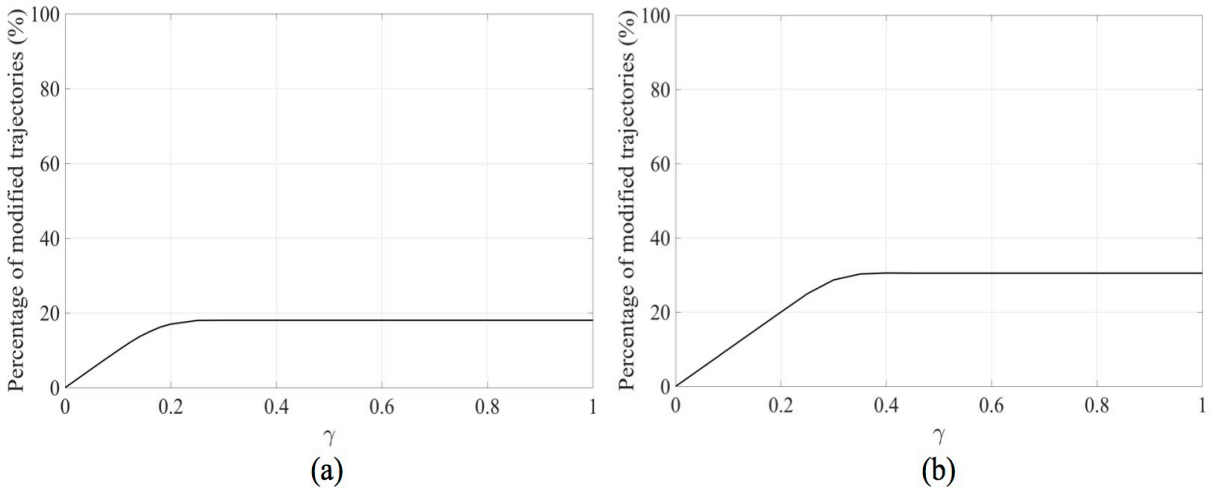

Figure 4.16 Percentage of modified trajectories as a function of γ for problems with : (a) $\bar{\mathcal{A}} = 10$; (b) $\bar{\mathcal{A}} = 20$.

4.3.6 Workload balancing results

In this section, we want to study the effect of varying the balancing factor λ on the solution obtained from MSP-SH/CT for air traffic situations that involves crossing and trailing conflicts. To do so, we solve the problems with $\bar{\mathcal{A}} = 10$ and $\bar{\mathcal{A}} = 20$ using MSP-SH/CT for $\alpha = \gamma = 0.1$ while varying λ between 1 and 4. We chose $\alpha = \gamma = 0.1$ because for these values 25-40% of the conflicts in these problems remain unresolved, which allows us to observe the effect of varying λ.

The average number of unresolved conflicts as a function of λ for $\bar{\mathcal{A}} = 10$ and $\bar{\mathcal{A}} = 20$ is displayed in the Figures 4.17-a and 4.17-b respectively. These figures also display the average number of conflicts per sector, where the sectors are indexed as in section 3.5.7, i.e. sector 1 has the most unresolved conflicts and sector 4 has the least number of unresolved conflicts. Similarly to the problems with only crossing conflicts, we observe in these figures that in the case of no balancing, i.e. $\lambda = 4$, sector 1 has a significantly higher load than the others. As λ decreases, the number of conflicts in this sector decreases by redistributing the conflicts among the sectors and the total number of conflicts increases. While this observation holds on the average, by examining the problems individually we found that in some problems the model equally distributes the conflicts without an increase in the total number of unresolved conflicts.

As discussed in section 3.5.7, minimizing the total number of conflicts and balancing the workload act as competing objectives. Giving priority to one of them depends on the number of conflicts and their distribution among the sectors. For example, if one sector is overloaded to the point that it exceeds controller limit, then the MSPr shall enforce the balancing even if it means increasing the total workload. Our model gives the MSPr the ability to prioritize or deprioritize the workload balancing by changing the value of λ.

The average computation time as a function of λ for problems with $\bar{\mathcal{A}} = 10$ and $\bar{\mathcal{A}} = 20$ is displayed in the Figures 4.17-c and 4.17-d respectively. Comparing both figures, we see that computation time is significantly higher for $\bar{\mathcal{A}} = 20$. This is due to the fact that the number of variables and constraints in our model depends on the number of flight plans and conflicts. The number of flight plans and the number of conflicts in the problems with $\bar{\mathcal{A}} = 20$ are two times and three times that with $\bar{\mathcal{A}} = 10$ respectively.

We also observe in the Figures 4.17-c and 4.17-d that the highest computation time occurs for $\lambda \approx 1$. By examining the solutions for $\lambda \leq 1.25$, we noticed that for 24.7% of the problems with $\bar{\mathcal{A}} = 10$ and 62.7% of the problems with $\bar{\mathcal{A}} = 20$, the model did not reach the optimal solution or determine its optimality in less than 10 minutes. We solved the same problems using the unmodified objective function (4.32) and compared the results. We found that although the model that uses the modified objective did not reach the optimal solution,

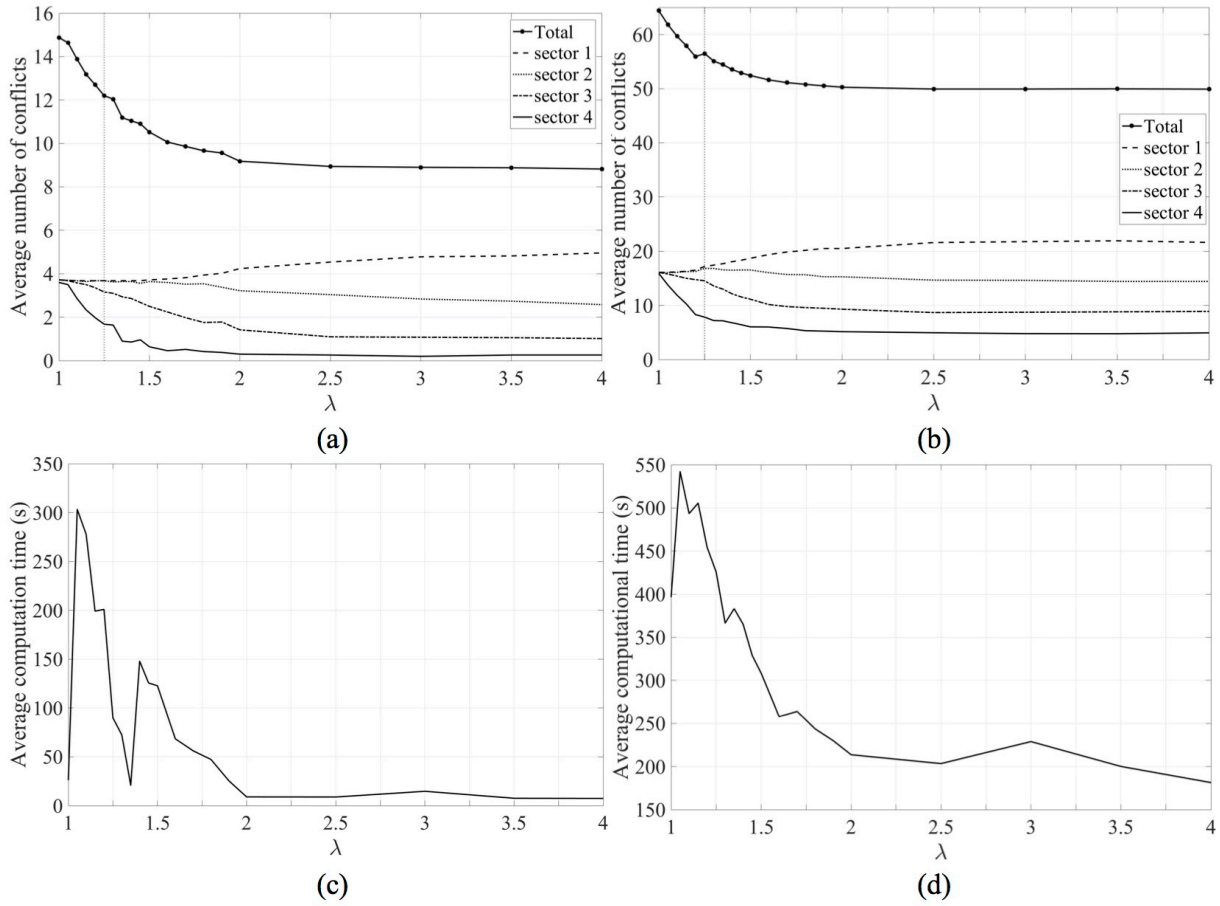

Figure 4.17 Testing the effect of varying λ on the performance of MSP-SH/CT : (a) number of unresolved conflicts for $\bar{\mathcal{A}} = 10$; (b) number of unresolved conflicts for $\bar{\mathcal{A}} = 20$; (c) average computational time for $\bar{\mathcal{A}} = 10$; (d) average computational time for $\bar{\mathcal{A}} = 20$.

it gives a solution with the optimal number of unresolved conflicts. This local maxima in the computation time is due to the use of the modified objective function as discussed in section 4.2. The modified objective did not increase computation time for $\lambda > 1.25$ because for these values the percentage of modified trajectories in the optimal solution equals to the maximum allowed percentage, i.e. γ. This means that when the model reaches a solution with the minimum number of conflicts, it does not take time to minimize the number of modified trajectories. From section 4.3.2 we know that the MSP-SH/CT model takes most of the computation time to minimize the number of modified trajectories.

The average percentage of modified trajectories as a function of λ for problems with $\bar{\mathcal{A}} = 10$ and $\bar{\mathcal{A}} = 20$ is displayed in Figure 4.18. In this figure, we see that for both problems, the percentage of modified trajectories is approximately equal to γ for $\lambda \approx 4$, i.e. no workload balancing. As λ decreases, the percentage of modified trajectories remains close to γ until

the value of λ at which enforcing the balance leads to an increase in the total number of conflicts, i.e. $\lambda \approx 2$ for the two problem sets. For $\lambda < 2$, the optimal solution has a larger number of conflicts than for $\lambda \approx 4$, which generally results in a reduction in the percentage of modified trajectories. This means that for these cases the model minimizes the number of modified trajectories which increases computational time.

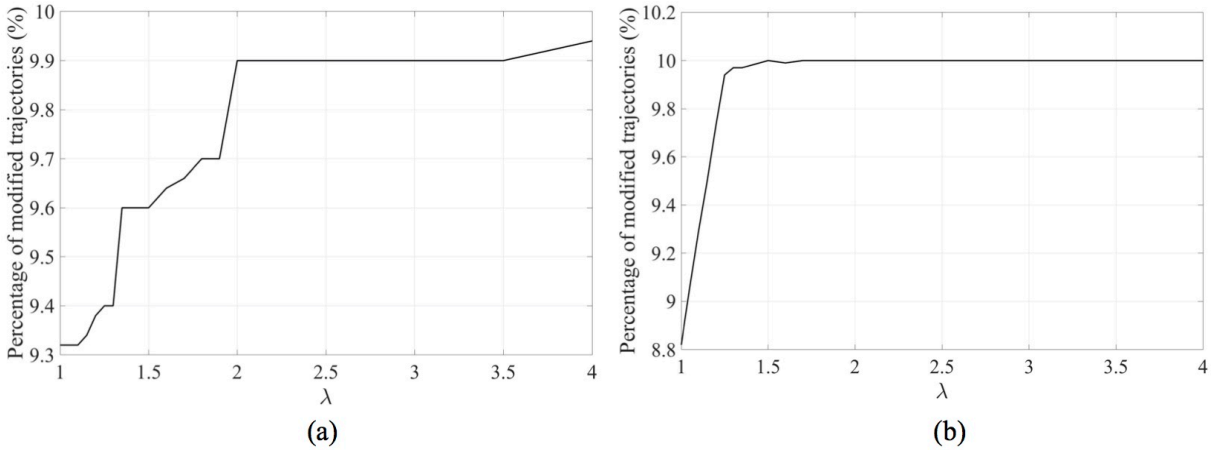

Figure 4.18 Percentage of modified trajectories as a function of λ for problems with : (a) $\bar{\mathcal{A}} = 10$; (b) $\bar{\mathcal{A}} = 20$.

4.4 Concluding remarks

In this chapter, we proposed a MILP model (MSP-SH/CT) to minimize and balance the total number of crossing and trailing conflicts in a MSA, using speed and heading changes. In this model, we introduced a novel linear formulation for the detection and resolution of trailing conflicts. We also introduced a modified objective function that minimizes the number of conflicts and the number of modified trajectories. Our model was able to solve problems that involve a combination of crossing and trailing conflicts while minimizing the number of modified trajectories.

We compared the modified objective function to an objective function that only minimizes the number of conflicts. We found that using the modified objective function gives a solution with the minimum number of conflicts and a significantly smaller number of modified trajectories. Using the modified objective function eliminates the problem of unnecessary trajectory modifications but we found that it may significantly increase the computation time.

In a multi-sector planning environment, the MSP-SH/CT reduces the number of crossing and trailing conflicts significantly while minimizing the number of modified trajectories. For

different sets of randomly generated problems involving up to 200 aircraft, MSP-SH/CT reduced the number of conflicts by 99%. The model also ensures minimal change in the travel duration of the modified trajectories. The average delay per modified trajectory was 2.18%-2.39% of the flight duration in the test problems. The use of a combination of heading changes and small speed changes was proven to outperform the use of only large speed changes. The effect of varying the percentage of modified trajectories γ or the balancing factor λ on the MSP-SH/CT model is qualitatively similar to its effect on the MSP-SH/C model.

In the next chapter, we introduce a reformulation of the MSP-SH/CT model to include altitude modifications as an additional manoeuvre to modify the trajectories.

CHAPTER 5 FLIGHT LEVEL CHANGE MANOEUVRE

In this chapter, we introduce a MILP for multi-sector planning using speed, heading and altitude changes. This model is a reformulation of the MSP-SH/CT model that we introduced in chapter 4. This reformulation aims at introducing altitude modification to the allowed trajectory modifications. Firstly, we introduce the reformulated model, which we call the *Multi-Sector Planning support model using Speed, Heading and Altitude changes for Crossing and Trailing conflicts* (MSP-SHA/CT). Secondly, we solve an example while detailing the new output parameters. Finally, we present various tests using randomly generated problems to show the advantages of considering altitude modifications in a MSP context.

5.1 Multi-sector planning support model using speed, heading and altitude changes for crossing and trailing conflicts

Level capping is a technique used in ATC to increase the ability of controllers to handle high density air traffic. Level capping consists in the separation of flights vertically through the assignment of different flight levels. Such a technique decreases the controllers workload, as vertically separated aircraft do not need close monitoring (Flener et al. (2007a)). A decision support tool for multi-sector planning should be able to model all the possible manoeuvres that a MSPr can use. If it does not, then its solutions may be suboptimal.
In chapter 4, we presented the MSP-SH/CT model for the solution of the complexity resolution problem in a MSP environment using only speed and heading changes. While the MSP-SH/CT can handle aircraft following multiple flight levels along the MSA, it does not allow for altitude modifications. In this section, we introduce the assumptions and formulation, i.e. variables and constraints, for altitude modifications. Note that the input data and the objective function remain unchanged from the MSP-SH/CT model (see sections 4.1.1 and 4.1.3).

5.1.1 Assumptions

In addition to the assumptions in section 3.1.2, the reformulated model MSP-SHA/CT assumes the following :

1. An altitude modification is a change in flight level.
2. An altitude modification is only permitted at the waypoints.

3. Altitude modifications, either for climbing or descending, are limited to only one flight level.
4. The number of flight level changes per aircraft is limited to the maximum between two changes and the number of changes in the original flight plans.

We make assumption 4 to minimize the number of flight level changes. If the original flight plan includes more than one flight level change, then our model does not increase the number of changes but allows to modify the altitude. If the original flight plan includes less than two flight level changes, then the number of flight level changes is limited to two. The first one is used to avoid conflicts and the second one is used to return the aircraft to its original flight level.

At high altitudes, the rate of climb of an aircraft is relatively small and varies depending on various factors such as aircraft type, weight and altitude. For example, the Airbus A-320 family has a rate of climb that varies between 500 feet per minute and 2000 feet per minute. For a small rate of climb and small altitude change, as considered in this thesis, the altitude change has no significant effect on the travel duration of a flight segment. Consequently, we assume that it does not significantly change waypoints passage times. This assumption was also made in the work of Flener et al. (2007a,c).

The assumptions 1-4 are designed to minimize changes in aircraft trajectories. To study the change in fuel consumption due to altitude modifications under these assumptions, we performed a simulation experiment. In this experiment, we used the model presented by Maazoun (2015) for fuel consumption calculation. The simulation included two scenarios involving a Boeing 777-300 with a total mass of 296 tons. In the first scenario, the aircraft flies at FL300 for 80 NM using optimal speed then it undergoes a climb to FL320, maintains this altitude for 80 NM then returns to FL300 and flies for 80 NM. In the second scenario, the aircraft has to fly all the distance at FL300. The aircraft in the first scenario consumed 50 kg of fuel more than the one in the second scenario. For a commercial aircraft using tons of fuel, such a difference is not significant. We conclude that the altitude changes under these assumptions have no significant effect on fuel consumption.

Since we only consider small altitudes changes, we do not consider conflicts between aircraft during altitude changes. We will assume that the change is instantaneous at the waypoints. Following our definition of flight plans and waypoints, the flight level used along a flight segment is determined by the flight level indicated at the waypoint at the beginning of the flight segment. Note that under the assumptions in section 3.1.2, the spatial coordinates of the MSA exit waypoint cannot be modified. Consequently, the aircraft flight level at the MSA exit point has to remain unchanged.

5.1.2 Variables

The decision variables in our model represent trajectory modification manoeuvres. We need to define a new decision variable to represent the altitude modification in the MSP-SHA/CT model. In the models MSP-SH/C and MSP-SH/CT, we used the input parameter $L_i(m,k)$ as an indicator for the flight level used on each flight segment of the flight plans. In both model, the value of $L_i(m,k)$ is determined at the preprocessing stage and remains unmodified in the solution stage. In the new model MSP-SHA/CT, we do not determine the value of $L_i(m,k)$ at the preprocessing stage and we consider it as a binary decision variable that represents the altitude modification.
In our model, we limit the number of flight level changes per flight plan and we also limit the number of modified trajectories. To take into account the number of altitude modifications, we define two additional dependent variables as follows :

$$\mathcal{I}_l(i) = \begin{cases} 1 \text{ if flight plan } i \text{ includes an altitude modification,} \\ 0 \text{ otherwise,} \end{cases}$$

and

$$U_i(m,k) = \begin{cases} 0 \text{ if flight plan } i \text{ uses flight level } k \text{ at the waypoints } m \text{ and } m+1, \\ 1 \text{ otherwise.} \end{cases}$$

Note that if $U_i(m,k) = 0$, then the aircraft following flight plan i uses the same flight level k at two consecutive segments, i.e. between m and $m+1$ and between $m+1$ and $m+2$. The evaluation of these two variables and their use to determine the number of modifications using linear constraints is presented in the following section.

5.1.3 Constraints

All the constraints in the MSP-SH/CT model (4.31) are also part of the formulation of the MSP-SHA/CT model except for constraint (3.14), which determines whether an aircraft trajectory is modified or not. This constraint must be reformulated to include altitude modifications. In addition to these constraints, we need to introduce a new set of constraints to model altitude modifications and the related assumptions.

Flight level assignment constraint

The flight level used on each flight segment is a model variable. To ensure that MSP-SHA/CT assigns a single flight level to each segment in each flight plan, we use the following

constraints : for $m \in \{1, 2, ..., N(i)\}$ and $i \in \{1, 2, ..., J\}$,

$$\sum_{k=1}^{K} L_i(m, k) = 1. \tag{5.1}$$

Flight level constraint

Note that the original flight level for the flight segment between waypoint m and $m + 1$ in flight plan i is given by $z_i(m)$. In the MSP-SHA/CT model, we limit the altitude modification to one flight level up, i.e. ascending, and one flight level down, i.e. descending, from the flight level indicated in the original flight plan. This means that an aircraft following flight plan i cannot be assigned to flight levels other than $z_i(m), z_i(m) + 1$ and $z_i(m) - 1$ on the flight segment between waypoints m and $m + 1$. We formulate this constraint as follows : for $m \in \{1, 2, ..., N(i)\}$, $i \in \{1, 2, ..., J\}$ and $k \in \{1, 2, ..., K\} \setminus \{z_i(m), z_i(m) + 1, z_i(m) - 1\}$,

$$L_i(m, k) = 0. \tag{5.2}$$

Flight level at the MSA exit point

In our model, we do not allow for a change in the spatial coordinates of the MSA exit point to minimize changes for the adjacent MSA. We formulate this constraint as follows : for $i \in \{1, 2, ..., J\}$,

$$L_i(N(i), z_i(N(i))) = 1. \tag{5.3}$$

Note that the index of the MSA exit point equals to the number $N(i)$ of waypoints in flight plan i. The equation (5.3) sets the flight level of the last waypoint to the flight level indicated in the original flight plan, i.e. $z_i(N(i))$.

Number of altitude modifications

The following set of constraints is used to count the aircraft trajectories that include an altitude modification. The variable $\mathcal{I}_l(i)$ indicates whether flight plan i includes an altitude modification, i.e. $\mathcal{I}_l(i) = 1$, or not, i.e. $\mathcal{I}_l(i) = 0$. If flight plan i includes at least one altitude modification, then $\sum_{m=1}^{N(i)} L_i(m, z_i(m)) < N(i)$. To set $\mathcal{I}_l(i) = 1$ if $\sum_{m=1}^{N(i)} L_i(m, z_i(m)) < N(i)$

and set $\mathcal{I}_l(i) = 0$ otherwise, we use the following set of inequalities : for $i \in \{1, 2, ..., J\}$,

$$1 - N(i) + \sum_{m=1}^{N(i)} L_i(m, z_i(m)) \leq (1 - \mathcal{I}_l(i))\ N(i), \tag{5.4}$$

$$1 - N(i) + \sum_{m=1}^{N(i)} L_i(m, z_i(m)) \geq -\mathcal{I}_l(i)\ N(i). \tag{5.5}$$

As for speed modifications, we limit the number of flight plans with an altitude modification using

$$\sum_{i=1}^{J} \mathcal{I}_l(i) \leq \beta\ A, \tag{5.6}$$

where β is the maximum allowed percentage of trajectories with an altitude modification.
Since the constraint (3.14) does not include the altitude modification, we cannot use it in the MSP-SHA/CT model to evaluate $\mathcal{I}(a)$ and indicate whether aircraft a undergoes any type of modification or not. To set $\mathcal{I}(a) = 1$ if the trajectory of aircraft a undergoes a speed change, i.e. $\sum_{i=1}^{J} I_a(i)\ \mathcal{I}_s(i) = 1$, or a heading change, i.e. $\mathcal{I}_h(a) = 1$, or an altitude change, i.e. $\sum_{i=1}^{J} I_a(i)\ \mathcal{I}_l(i) = 1$, we use the following set of inequalities : for $a \in \{1, 2, ..., A\}$,

$$\sum_{i=1}^{J} I_a(i)\ \mathcal{I}_s(i) \leq \mathcal{I}(a), \tag{5.7}$$

$$\mathcal{I}_h(a) \leq \mathcal{I}(a), \tag{5.8}$$

$$\sum_{i=1}^{J} I_a(i)\ \mathcal{I}_l(i) \leq \mathcal{I}(a). \tag{5.9}$$

Note that we did not add constraints to set $\mathcal{I}(a) = 0$ if there is no modification in the trajectory of aircraft a. Indeed, such constraints are not necessary because in the MSP-SHA/CT model we minimize the number of modified trajectories, i.e. $\sum_{a=1}^{A} \mathcal{I}(a)$.

Number of flight level changes per flight plan

Since pilots prefer to avoid flight level changes, we limit the number of flight level changes per aircraft in our model to the maximum between two changes and the number of changes in the original flight plans. This ensures that our model does not increase the number of flight level changes in a flight plan by more than two. To model this constraint we need first to determine the number of flight level changes in the original flight plans. Second, we need a linear formulation to determine the number of flight level changes in the modified flight plans. Finally, we need to limit the flight level changes.
In the first step, we introduce the parameter $L(i)$ defined as the number of the flight level

changes in the original flight plan i. The value of $L(i)$ is determined at the preprocessing stage by checking the values of $z_i(m)$. In the second step, we determine the value of the binary variable $U_i(m,k)$ using linear constraints. To set $U_i(m,k)=0$ if flight plan i uses flight level k at waypoint m and $m+1$, i.e. $L_i(m,k)=L_i(m+1,k)=1$, and set $U_i(m,k)=1$ otherwise, we use the following set of inequalities : for $m \in \{1,2,...,N(i)-1\},\ i \in \{1,2,...,J\}$ and $k \in \{1,2,...,K\}$,

$$L_i(m,k)+L_i(m+1,k) \leq 2-U_i(m,k), \tag{5.10}$$

$$L_i(m,k)+L_i(m+1,k) \geq 1.1-2\ U_i(m,k). \tag{5.11}$$

The variable $U_i(m,k)$ is used to determine the number of flight level changes as follows. For flight plan i, if the aircraft uses the same flight level k^* at the waypoints m and $m+1$, then $U_i(m,k^*)=0$. For $k \in \{1,2,...,K\} \setminus \{k^*\}$, (5.10) and (5.11) set $U_i(m,k)=1$. Consequently, if there is no flight level change at waypoint $m+1$, then $\sum_{k=1}^{K} U_i(m,k)=K-1$. If there is a flight level change at waypoint $m+1$, then $\sum_{k=1}^{K} U_i(m,k)=K$. Using these relations, we observe that

$$1-K+\sum_{k=1}^{K} U_i(m,k) = \begin{cases} 1 \text{ if flight plan } i \text{ changes the flight level at waypoint } m+1 \\ 0 \text{ otherwise.} \end{cases} \tag{5.12}$$

Using (5.12), the number of flight level changes in flight plan i is $\sum_{m=1}^{N(i)-1}\left(1-K+\sum_{k=1}^{K} U_i(m,k)\right)$. In the final step, to limit the number of flight level changes per flight plan, we use the following constraint : for $i \in \{1,2,...,J\}$,

$$\sum_{m=1}^{N(i)-1}\left(1-K+\sum_{k=1}^{K} U_i(m,k)\right) \leq \max\{2, L(i)\}. \tag{5.13}$$

In (5.13), the term $\max\{2,L(i)\}$ is evaluated at the preprocessing stage for each flight plan and consequently (5.13) is linear.

5.1.4 MSP-SHA/CT formulation

To be concise, we define $\bar{\mathcal{K}} := \{1,2,...,K\} \setminus \{z_i(m), z_i(m)+1, z_i(m)-1\}$. The complete model takes the following form :

$$\min_{P(i),T_i(m),L_i(m,k)} \sum_{p=1}^{|E|} C_p + \sum_{g=1}^{|\bar{E}|} \bar{C}_g + \frac{\sum_{a=1}^{A} \mathcal{I}(a)}{\gamma\, A+1} \tag{5.14}$$

subject to

Speed and heading changes constraints :

$(3.7) - (3.13)$, (3.15),

Crossing conflict prediction constraints :

$(3.16), (3.17)$, (3.19), (3.21), (3.23), (3.24),

Trailing conflict prediction constraints :

$(4.12) - (4.15)$, $(4.17), (4.18)$, $(4.20 - 4.25)$, $(4.28) - (4.30)$,

Flight level assignment constraints :

$$\sum_{k=1}^{K} L_i(m,k) = 1, \qquad m \in \mathcal{M}_i,\ i \in \mathcal{J},$$

$$L_i(m,k) = 0, \qquad m \in \mathcal{M}_i,\ i \in \mathcal{J},\ k \in \bar{\mathcal{K}},$$

$$L_i(N(i), z_i(N(i))) = 1 \qquad i \in \mathcal{J},$$

Limiting the number of modifications constraints :

$$1 - N(i) + \sum_{m=1}^{N(i)} L_i(m, z_i(m)) \leq (1 - \mathcal{I}_l(i))\ N(i), \qquad i \in \mathcal{J},$$

$$1 - N(i) + \sum_{m=1}^{N(i)} L_i(m, z_i(m)) \geq -\mathcal{I}_l(i)\ N(i), \qquad i \in \mathcal{J},$$

$$\sum_{i=1}^{J} \mathcal{I}_l(i) \leq \beta\ A,$$

$$\mathcal{I}_h(a) \leq \mathcal{I}(a), \qquad a \in \mathcal{A},$$

$$\sum_{i=1}^{J} I_a(i)\ \mathcal{I}_s(i) \leq \mathcal{I}(a), \qquad a \in \mathcal{A},$$

$$\sum_{i=1}^{J} I_a(i)\ \mathcal{I}_l(i) \leq \mathcal{I}(a), \qquad a \in \mathcal{A},$$

$$L_i(m,k) + L_i(m+1,k) \leq 2 - U_i(m,k), \qquad m \in \mathcal{M}_i,\ i \in \mathcal{J}, k \in \mathcal{K},$$

$$L_i(m,k) + L_i(m+1,k) \geq 1.1 - 2\ U_i(m,k), \qquad m \in \mathcal{M}_i,\ i \in \mathcal{J}, k \in \mathcal{K},$$

$$\sum_{m=1}^{N(i)-1} \left(1 - K + \sum_{k=1}^{K} U_i(m,k)\right) \leq \max\{2, L(i)\}, \qquad i \in \mathcal{J},$$

Integrality and nonnegativity constraints :

$$C_p,\ A_p,\ B_p,\ H_p(k) \in \{0,1\} \qquad p \in \{1, ..., |E|\},\ k \in \mathcal{K},$$

$$P(i),\ \mathcal{I}_s(i),\ \mathcal{I}_a(i),\ \mathcal{I}_h(a),\ \mathcal{I}(a) \in \{0,1\}, \qquad i \in \mathcal{J},\ a \in \mathcal{A},$$

$$T_i(m) \in \mathbb{R}^+, \qquad i \in \mathcal{J},\ m \in \mathcal{M}_i - \{N(i)\},$$

$$t'_i(m),\ \hat{t}_i(w) \in \mathbb{R}^+, \qquad i \in \mathcal{J}, m \in \mathcal{M}_i, w \in \{1, ...W(i)\},$$

$$L_i(m,k) \in \{0,1\}, \qquad i \in \mathcal{J},\ m \in \mathcal{M}_i,\ k \in \mathcal{K},$$

$$\bar{H}_g(k),\ R_g,\ C_g^1,\ C_g^2,\ \bar{C}_g \in \{0,1\}, \qquad g \in \{1, 2, ..., |\bar{E}|\},\ k \in \mathcal{K}.$$

Similarly to the MSP-SH/C and MSP-SH/CT models, the original trajectories are part of the search space and satisfy the constraints in the case of no balancing. Consequently, a feasible solution always exists for this model. As we did not change the formulation of the objective function, it still has a lower bound of 0 and an upper bound that equals the sum of $|E|$, $|\bar{E}|$ and $\frac{A}{A+1}$, hence there exist at least one optimal solution in the case of no balancing.

An IDEF0 model of the MSP-SHA/CT is presented in Figure 5.1. The only difference between the preprocessing stage of this model and that of MSP-SH/CT is that in this model we do

not determine the value of $L_i(m,k)$ at this stage because it is a decision variable. All other input and output of the preprocessing stage remain the same as for the MSP-SH/CT model. The output of the preprocessing stage of the MSP-SHA/CT model includes the set E of flight plan pairs that are at risk of a crossing conflict, the set $\bar{E}$ of flight plan pairs that are at risk of a trailing conflict, the safe separation times S_p and $\bar{S}_g$ and the sector indicator matrices I_p^s and $\bar{I}_g^s$. The output of the preprocessing stage also includes the coordinates of the intersection points and the CFSs.

We programmed the preprocessing stage for this model using MATLAB 8.4. The solution stage relies on providing the formulation along with the output of the preprocessing stage, i.e. the input data, to the commercial solver Gurobi 6.5.0. Using the balancing factor λ and the allowed percentages α, β and γ of modified trajectories, the solver Gurobi generates the optimal solution, i.e. modified trajectories. As for the other models, we limit the solution time to 10 minutes. In the following section, we present an example detailing the output of the solution stage.

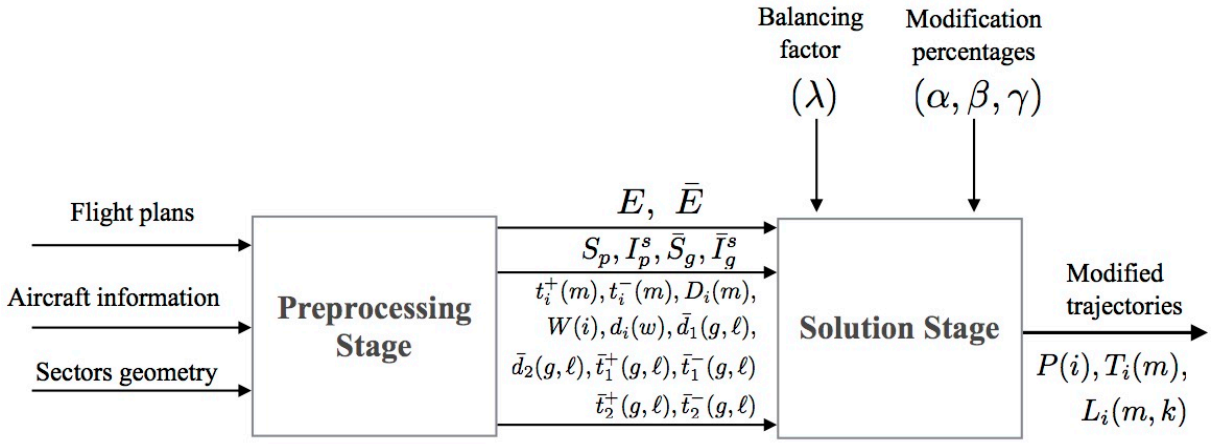

Figure 5.1 IDEF0 for the MSP-SHA/CT model

5.2 Detailed example

In this section, we present an example of seven aircraft that are planned to pass through a MSA with three flight levels and four adjacent square sectors. The geometry of the MSA is the same as in section 3.3. All aircraft have a minimum speed of 456 knots ($\simeq$ 850 km/hr), a maximum speed of 513 knots ($\simeq$ 950 km/hr) and a cruising speed $\bar{v}_a = 485$ knots ($\simeq$ 900 km/hr).

5.2.1 The preprocessing stage input data

The waypoints coordinates in km and the passage times in minutes of the original trajectories are presented in Table 5.1. The spatial trajectories are illustrated in Figure 5.2-a. We chose these trajectories and speeds to create a conflict between multiple aircraft. This conflict cannot be solved using only speed and heading changes. This case allows us to show a solution that involves altitude changes.

If the aircraft use the original trajectories, then we observe in Figure 5.2-a that there are seven crossing conflicts. The crossing conflicts exist for the aircraft pairs (1, 3), (1, 5), (1, 6), (2, 4), (3, 5), (3, 6) and (4, 6). Using original trajectories, there are no trailing conflicts in this example but the aircraft pairs (1, 2), (3, 4) and (5, 6) follow the same spatial trajectories and are at risk of a trailing conflict if they change their speeds.

5.2.2 The preprocessing stage output data

For each aircraft, we have three flight plans representing the original spatial trajectory and the two trajectories with heading changes. The alternative flight plans, including the original trajectories, are presented in Table 5.2. Note that we use the cruising speed to generate the passage times for all flight plans. The flight plan indicator matrix $I_a(i)$ is presented in the Table 5.3. The potential crossing and trailing conflicts are presented in the Tables 5.4 and 5.5 respectively. Note that $(i(p), j(p))$ is the p^{th} flight plan pair in E with a minimum safe separation time S_p and $(\bar{i}(g), \bar{j}(g))$ is the g^{th} flight plan pair in $\bar{E}$ with a minimum safe separation time $\bar{S}_g$. In this example, there are 118 possible crossing conflicts and 26 possible trailing conflicts.

The MSP-SHA/CT considers possible crossing conflicts between a pair of aircraft even if their original flight plans use different flight levels. Although such a pair is vertically separated, the flight levels are model variables and the modified trajectories may use the same flight level. For example, even if the aircraft 6 and 7 use different flight levels (see Figure 5.2-a), we see in Table 5.4 (bottom line) that the flight plans 16, 17 and 18, i.e. aircraft 6, are in possible conflict with the flight plans 19, 20 and 21, i.e. aircraft 7. Note that our model verifies if

Table 5.1 Original trajectories : (x, y) in km and $t_i(m)$ in minutes.

	Waypoint 1		**Waypoint 2**		**Waypoint 3**	
a	(x, y, z)	$t_i(1)$	(x, y, z)	$t_i(2)$	(x, y, z)	$t_i(3)$
1	(50,0,1)	20	(100,200,1)	33.74	(100,400,1)	47.08
2	(50,0,1)	21.8	(100,200,1)	35.54	(100,400,1)	48.88
3	(100,0,1)	20	(50,200,1)	33.74	(50,400,1)	47.08
4	(100,0,1)	21.8	(50,200,1)	35.54	(50,400,1)	48.88
5	(0,100,1)	21.87	(200,100,1)	35.2	(400,100,1)	48.54
6	(0,100,1)	22.67	(200,100,1)	36	(400,100,1)	49.34
7	(300,0,2)	34.37	(300,200,2)	47.7	(300,400,2)	61.04

these flight plans are used and if they use the same flight level at the intersection point. If these two conditions are true, then the model verifies that the passage times difference at the intersection point is larger than the minimum separation time S_p.

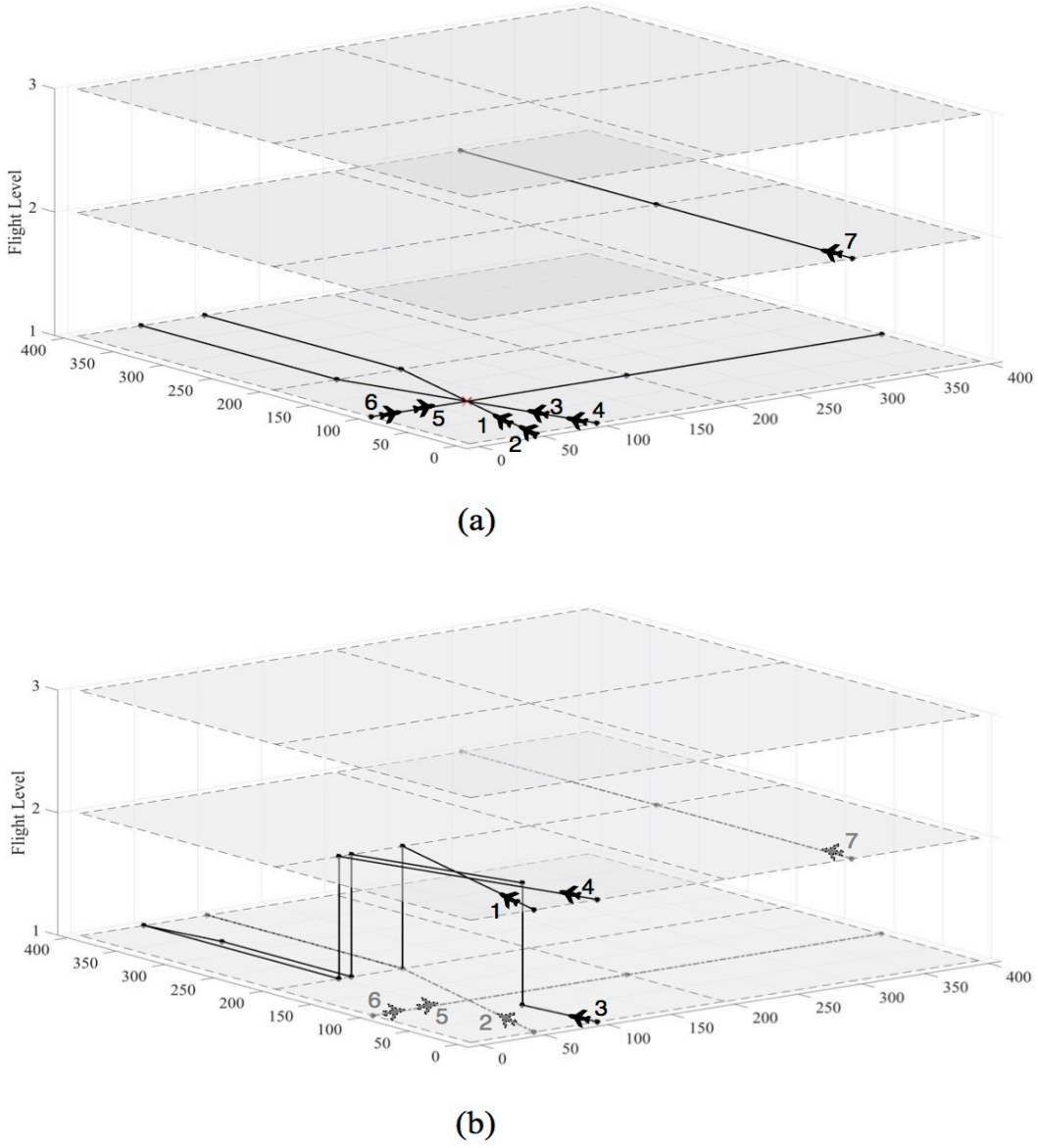

Figure 5.2 Aircraft trajectories for the detailed example with altitude changes : (a) original trajectories ; (b) modified trajectories (the trajectories of the grey-shaded aircraft are not modified).

Table 5.2 Alternative flight plans : (x, y) in km and $t_i(m)$ in minutes.

i	**Waypoint 1**		**Waypoint 2**		**Waypoint 3**		**Waypoint 4**		**Waypoint 5**		$N(i)$
	(x, y, z)	$t_i(1)$	(x, y, z)	$t_i(2)$	(x, y, z)	$t_i(3)$	(x, y, z)	$t_i(4)$	(x, y, z)	$t_i(5)$	
1	(50,0,1)	20	(100,200,1)	33.74	(100,400,1)	47.08	-	-	-	-	3
2	(50,0,1)	20	(75.61,63.27,1)	24.55	(109.79,200,1)	33.95	(109.5,332.4,1)	42.77	(100,400,1)	47.32	5
3	(50,0,1)	20	(57.18,67.88,1)	24.55	(90.21,200,1)	33.63	(90.5,332.4,1)	42.46	(100,400,1)	47.01	5
4	(50,0,1)	21.8	(100,200,1)	35.54	(100,400,1)	48.88	-	-	-	-	3
5	(50,0,1)	21.8	(75.61,63.27,1)	26.35	(109.79,200,1)	35.75	(109.5,332.4,1)	44.57	(100,400,1)	49.12	5
6	(50,0,1)	21.8	(57.18,67.88,1)	26.35	(90.21,200,1)	35.43	(90.5,332.4,1)	44.26	(100,400,1)	48.81	5
7	(100,0,1)	20	(50,200,1)	33.74	(50,400,1)	47.08	-	-	-	-	3
8	(100,0,1)	20	(92.82,67.88,1)	24.55	(59.79,200,1)	33.63	(59.5,332.4,1)	42.46	(50,400,1)	47.01	5
9	(100,0,1)	20	(74.39,63.27,1)	24.55	(40.21,200,1)	33.95	(40.5,332.4,1)	42.77	(50,400,1)	47.32	5
10	(100,0,1)	21.8	(50,200,1)	35.54	(50,400,1)	48.88	-	-	-	-	3
11	(100,0,1)	21.8	(92.82,67.88,1)	26.35	(59.79,200,1)	35.43	(59.5,332.4,1)	44.26	(50,400,1)	48.81	5
12	(100,0,1)	21.8	(74.39,63.27,1)	26.35	(40.21,200,1)	35.75	(40.5,332.4,1)	44.57	(50,400,1)	49.12	5
13	(0,100,1)	21.87	(200,100,1)	35.2	(400,100,1)	48.54	-	-	-	-	3
14	(0,100,1)	21.87	(67.6,90.5,1)	26.42	(200,90.5,1)	35.25	(332.4,90.5,1)	44.07	(400,100,1)	48.63	5
15	(0,100,1)	21.87	(67.6,109.5,1)	26.42	(200,109.5,1)	35.25	(332.4,109.5,1)	44.07	(400,100,1)	48.63	5
16	(0,100,1)	22.67	(200,100,1)	36	(400,100,1)	49.34	-	-	-	-	3
17	(0,100,1)	22.67	(67.6,90.5,1)	27.22	(200,90.5,1)	36.05	(332.4,90.5,1)	44.87	(400,100,1)	49.43	5
18	(0,100,1)	22.67	(67.6,109.5,1)	27.22	(200,109.5,1)	36.05	(332.4,109.5,1)	44.87	(400,100,1)	49.43	5
19	(300,0,2)	34.37	(300,200,2)	47.7	(300,400,2)	61.04	-	-	-	-	3
20	(300,0,2)	34.37	(309.5,67.6,2)	38.92	(309.5,200,2)	47.75	(309.5,332.4,2)	56.57	(300,400,2)	61.13	5
21	(300,0,2)	34.37	(290.5,67.6,2)	38.92	(290.5,200,2)	47.75	(290.5,332.4,2)	56.57	(300,400,2)	61.13	5

Table 5.3 Flight plan indicator matrix $I_a(i)$. Note that $I_a(i) = 1$ if aircraft a can use flight plan i.

a \ i	1	2	3	4	5	6	7	8	9	10	11	12	13	14	15	16	17	18	19	20	21
1	1	1	1	0	0	0	0	0	0	0	0	0	0	0	0	0	0	0	0	0	0
2	0	0	0	1	1	1	0	0	0	0	0	0	0	0	0	0	0	0	0	0	0
3	0	0	0	0	0	0	1	1	1	0	0	0	0	0	0	0	0	0	0	0	0
4	0	0	0	0	0	0	0	0	0	1	1	1	0	0	0	0	0	0	0	0	0
5	0	0	0	0	0	0	0	0	0	0	0	0	1	1	1	0	0	0	0	0	0
6	0	0	0	0	0	0	0	0	0	0	0	0	0	0	0	1	1	1	0	0	0
7	0	0	0	0	0	0	0	0	0	0	0	0	0	0	0	0	0	0	1	1	1

5.2.3 The optimal solution

We solved the problem using the MSP-SHA/CT model while allowing for at most 50% of the trajectories to be modified, i.e. $\alpha = \beta = \gamma = 0.5$, and with equal balancing among sectors, i.e. $\lambda = 1$. Gurobi 6.5.0 found the optimal solution in less than 0.1 seconds on a MacBook pro having 16.0 GB of RAM supported by an Intel® Core i7 running at 2.6GHz with a 6MB cache size, operated with OS X 10.12.1. For this example, the model has 1617 binary variables, 210 continuous variables and 3201 constraints.

The optimal solution found by the MSP-SHA/CT model eliminates all seven crossing conflicts by modifying the trajectories of three out of seven aircraft. The values of the decision variables $P(i)$ and $T_i(m)$ in the optimal solution are presented in Table 5.6, that gives the flight plan used by each aircraft and travel duration along each flight segment. Note that original trajectories have two flight segments and flight plans with heading changes have four flight segments. The value of the decision variable $L_i(m,k)$ for each flight plan that is used, i.e. such that $P(i) = 1$, is presented in Table 5.7.

By comparing the flight levels corresponding to the values of $L_i(m,k)$ in Table 5.7 and the values of $z_i(m)$ in Table 5.2, we can determine the altitude modifications in the solution. For example, let us consider flight plan 1. In Table 5.2, we observe that flight plan 1 originally uses the first flight level at all waypoints, i.e. $z_1(1) = z_1(2) = z_1(3) = 1$. In table 5.7, we see that $L_1(1,2) = 1, L_1(2,1) = 1$ and $L_1(3,1) = 1$. This means that the modified flight plan 1 uses the second flight level at the first waypoint and the first flight level at waypoint 2 and 3. This means that flight plan 1 includes an altitude modification at the first waypoint.

The aircraft spatial trajectories corresponding to the solution are illustrated in Figure 5.2-b. We observe that aircraft 1, 3 and 4 modified their altitude. The model modified the flight levels of aircraft 1 and 3 and ensured their separation by reducing the speed of aircraft 1. The data related to the flight plan used by each aircraft and the change in passage times and flight levels are presented in Table 5.8. In this table, the column i gives the index of the flight plan used by each aircraft, the column $t'_i(m)$ gives the passage time at waypoint m, the column $z'_i(m)$ gives the flight level at waypoint m, the column $\mathcal{I}_s(i)$ indicates if the flight plan i includes a speed change or not, the column $\mathcal{I}_h(a)$ indicates if the aircraft a undergoes a heading change or not, $\mathcal{I}_l(i)$ indicates if flight plan i includes an altitude modification or not and the column $\mathcal{I}(a)$ indicates if the trajectory of aircraft a is modified or not.

We solved the same problem using only speed and heading changes, i.e. using the MSP-SH/CT model. The solution found eliminates five out of the seven crossing conflicts by modifying the trajectories of three out of seven aircraft. Comparing both solutions, we observe that the MSP-SHA/CT model was able to eliminate two additional conflicts using the same number of modified trajectories.

Table 5.4 Flight plan pairs at risk of a crossing conflict.

p	1	2	3	4	5	6	7	8	9	10	11	12	13	14	15	16
$i(p)$	1	1	1	1	1	1	1	1	1	1	1	2	2	2	2	2
$j(p)$	4	7	8	9	13	14	15	16	18	5	6	9	5	7	8	13
S_p	39.9	39.3	39.3	39.3	48.4	48.4	48.4	48.4	48.4	46.2	46.2	41.1	39.9	39.3	39.3	48.4

p	17	18	19	20	21	22	23	24	25	26	27	28	29	30	31	32
$i(p)$	2	2	2	2	2	2	2	3	3	3	3	3	3	3	3	3
$j(p)$	14	15	16	18	5	4	6	6	7	8	9	13	14	15	16	17
S_p	48.4	48.4	48.4	48.4	46.5	46.2	39.2	40	39.3	39.3	39.3	48.4	51.3	46	48.4	51.3

p	33	34	35	36	37	38	39	40	41	42	43	44	45	46	47	48
$i(p)$	3	3	3	3	4	4	4	4	4	4	4	5	5	5	5	5
$j(p)$	18	6	4	5	10	11	12	14	16	17	18	12	10	11	13	14
S_p	46	46.5	46.2	39.2	39.3	39.3	39.3	48.4	48.4	48.4	48.4	41.1	39.3	39.3	48.4	48.4

p	49	50	51	52	53	54	55	56	57	58	59	60	61	62	63	64
$i(p)$	5	5	5	6	6	6	6	6	7	7	7	7	7	7	7	7
$j(p)$	16	17	18	10	11	12	16	17	10	13	14	15	16	18	11	12
S_p	48.4	48.4	48.4	39.3	39.3	39.3	48.4	51.3	39.9	61.9	61.9	61.9	61.9	61.9	46.2	46.2

p	65	66	67	68	69	70	71	72	73	74	75	76	77	78	79	80
$i(p)$	8	8	8	8	8	8	8	8	9	9	9	9	9	9	9	9
$j(p)$	11	13	14	15	18	11	10	12	12	13	14	15	16	17	18	12
S_p	40	61.9	61.9	61.9	61.9	46.5	46.2	39.2	39.9	61.9	68.2	57	61.9	68.2	57	46.5

p	81	82	83	84	85	86	87	88	89	90	91	92	93	94	95	96
$i(p)$	9	9	10	10	10	10	11	11	11	11	11	12	12	13	13	13
$j(p)$	10	11	14	16	17	18	13	14	16	17	18	16	17	17	18	19
S_p	46.2	39.2	61.9	61.9	61.9	61.9	61.9	61.9	61.9	61.9	61.9	61.9	68.2	46.2	46.2	53.9

p	97	98	99	100	101	102	103	104	105	106	107	108	109	110	111	112
$i(p)$	13	13	14	14	14	14	14	14	14	15	15	15	15	15	15	15
$j(p)$	20	21	17	17	19	20	21	16	18	18	18	19	20	21	16	17
S_p	53.9	53.9	46.2	46.2	53.9	53.9	53.9	46.2	39.2	46.2	46.2	53.9	53.9	53.9	46.2	39.2

p	113	114	115	116	117	118
$i(p)$	16	16	17	18	18	18
$j(p)$	19	21	21	19	20	21
S_p	53.9	53.9	53.9	53.9	53.9	53.9

Table 5.5 Flight plan pairs at risk of a trailing conflict.

g	1	2	3	4	5	6	7	8	9	10	11	12	13
$i(g)$	1	1	2	2	2	2	3	3	3	3	7	7	8
$j(g)$	4	4	5	5	5	5	6	6	6	6	10	10	11
S_g	38.1	38.1	38.1	38.1	38.1	38.1	38.1	38.1	38.1	38.1	38.1	38.1	38.1

g	14	15	16	17	18	19	20	21	22	23	23	25	26
$i(g)$	8	8	9	9	9	9	13	14	15	19	20	20	21
$j(g)$	11	11	12	12	12	12	16	17	18	22	23	23	24
S_g	38.1	38.1	38.1	38.1	38.1	38.1	38.1	38.1	38.1	38.1	38.1	38.1	38.1

Table 5.6 Decision variables $P(i)$ and $T_i(m)$ for the optimal solution : $T_i(m)$ in minutes.

i	1	2	3	4	5	6	7	8	9	10	11
$P(i)$	1	0	0	1	0	0	0	1	0	1	0
$T_i(1)$	14.25	4.55	4.55	13.74	4.55	4.55	13.74	4.42	4.55	13.74	4.55
$T_i(2)$	13.78	9.39	9.08	13.33	9.39	9.08	13.33	8.81	9.39	13.33	9.08
$T_i(3)$	-	8.83	8.82	-	8.83	8.83	-	8.57	8.83	-	8.82
$T_i(4)$	-	4.55	4.55	-	4.55	4.55	-	4.42	4.55	-	4.55

i	12	13	14	15	16	17	18	19	20	21
$P(i)$	0	1	0	0	1	0	0	1	0	0
$T_i(1)$	4.55	13.33	4.55	4.55	13.33	4.55	4.55	13.33	4.55	4.55
$T_i(2)$	9.39	13.34	8.82	8.83	13.33	8.82	8.82	13.33	8.82	8.82
$T_i(3)$	8.83	-	8.83	8.82	-	8.83	8.83	-	8.83	8.83
$T_i(4)$	4.55	-	4.55	4.55	-	4.55	4.55	-	4.55	4.55

Table 5.7 The value of $L_i(m,k)$ for the flight plans used in the optimal solution.

	$i=1$			$i=4$			$i=8$					$i=10$			$i=13$			$i=16$			$i=19$		
m	1	2	3	1	2	3	1	2	3	4	5	1	2	3	1	2	3	1	2	3	1	2	3
$L_i(m,1)$	0	1	1	1	1	1	1	0	1	1	1	0	1	1	1	1	1	1	1	1	0	0	0
$L_i(m,2)$	1	0	0	0	0	0	0	1	0	0	0	1	0	0	0	0	0	0	0	0	1	1	1
$L_i(m,3)$	0	0	0	0	0	0	0	0	0	0	0	0	0	0	0	0	0	0	0	0	0	0	0

Table 5.8 The modified trajectories in the optimal solution.

a	i	Waypoint 1		Waypoint 2		Waypoint 3		Waypoint 4		Waypoint 5		$\mathcal{I}_s(i)$	$\mathcal{I}_h(a)$	$\mathcal{I}_l(i)$	$\mathcal{I}(a)$
		$t_i'(1)$	$z_i'(1)$	$t_i'(2)$	$z_i'(2)$	$t_i'(3)$	$z_i'(3)$	$t_i'(4)$	$z_i'(4)$	$t_i'(5)$	$z_i'(5)$				
1	1	20	2	34.25	1	48.04	1	-	-	-	-	1	0	1	1
2	4	21.8	1	35.54	1	48.88	1	-	-	-	-	0	0	0	0
3	8	20	1	24.42	2	33.23	1	41.8	1	46.22	1	1	1	1	1
4	10	21.8	2	35.54	1	48.88	1	-	-	-	-	0	0	1	1
5	13	21.87	1	35.2	1	48.54	1	-	-	-	-	0	0	0	0
6	16	22.67	1	36	1	49.34	1	-	-	-	-	0	0	0	0
7	19	34.37	2	47.7	2	61.04	2	-	-	-	-	0	0	0	0

5.3 Numerical experiments

In this section, we test the effect of introducing the altitude modification as an additional trajectory modification manoeuvre to our model. First we compare the use of altitude modifications to the use of speed changes and heading changes to demonstrate the capacity of altitude modification to solve a combination of crossing and trailing conflicts. Second, we compare the performance of the MSP-SHA/CT model to that of the MSP-SH/CT model to illustrate the advantages of considering altitude modifications. We compare the two models while varying the allowed percentage γ of modified trajectories and the balancing factor λ.
In the first test, we consider solving the problems using only altitude modifications. This can be done by using $\alpha = 0$, i.e. no speed changes, and by adding the constraint (3.27) to the MSP-SHA/CT model. Note that (3.27) prevents the use of heading changes by forcing the aircraft to use the original spatial trajectories (X and Y coordinates). We call the model variant that use only altitude modification, the *Multi-Sector Planning support model using Altitude changes for Crossing and Trailing conflicts* (MSP-A/CT).
We conduct the tests in this section using different sets of randomly generated problems. Since the problems used to test MSP-SH/CT in section 4.3 include multiple flight levels, we use it to test the MSP-SHA/CT model. In this section we use the problem sets used in section 4.3. In these problems we generated a number $\bar{\mathcal{A}}$ of random spatial trajectories and we assigned 10 aircraft to each of these trajectories. The difference in the MSA entry times between any two aircraft following the same spatial trajectory is larger than one minute. We solve the problems using Gurobi 6.5.0 on a MacBook pro having 16.0 GB of RAM supported by an Intel® Core i7 running at 2.6GHz with a 6MB cache size, operated with OS X 10.12.1.

5.3.1 Comparing altitude modifications to speed and heading changes

In this section, we assess the capacity of the altitude modification to resolve a combination of crossing and trailing conflicts. To do so, we compare the performance of the MSP-A/CT model to that of the MSP-S/CT (large), MSP-S/CT (small) and MSP-H/CT models. In this section, we compare the models performance by comparing the percentage of resolved conflicts and the percentage of modified trajectories on randomly generated problems. Using the four model variants, we solved the problems with $\bar{\mathcal{A}} = 5,\ 7,\ 10$ and 20. The problems were solved while allowing for the modification of at most 50% of the trajectories and with no workload balancing, i.e. $\lambda = 4$. Note that for each value of $\bar{\mathcal{A}}$, we solved 50 different randomly generated problems.
The average percentage of resolved conflicts using each of the four model variants is presented in Table 5.9, where the columns avg and SD give the average and standard deviation of the

percentage of resolved conflicts respectively. We observe that using only altitude modifications, our model eliminates more than 95% of conflicts. Comparing the MSP-A/CT model to the MSP-S/CT (large) and MSP-S/CT (small) models, we see that the capacity of the three models to solve conflicts is comparable for $\bar{\mathcal{A}} = 5$ and $\bar{\mathcal{A}} = 7$. For the problems with $\bar{\mathcal{A}} = 10$, the MSP-A/CT and the MSP-S/CT (large) are comparable and both models outperform the MSP-S/CT (small). For $\bar{\mathcal{A}} = 20$, the large speed changes has the largest percentage of resolved conflicts and the altitude modifications outperforms the small speed changes. Comparing the MSP-A/CT and MSP-H/CT models, we observe that using altitude modifications is significantly better than using heading changes in solving conflicts.

The percentage of modified trajectories in the solutions using each model variant is presented in Table 5.10, where the columns avg and SD give the average and standard deviation of the percentage of modified trajectories respectively. We see that on the average the MSP-A/CT has the smallest percentage of modified trajectories. From these results, we conclude that the altitude modification is an effective manoeuvre to eliminate conflicts with the least number of modified trajectories.

5.3.2 Comparison between the performance of MSP-SHA/CT and MSP-SH/CT

In this section, we compare the performance of the MSP-SHA/CT and MSP-SH/CT models. We evaluate the performance of a model by the percentage of resolved conflicts, the percentage of modified trajectories and the computation time in the solution of randomly generated problems. We solve the problems using each of the two models while allowing for the modification of at most 50% of the trajectories, i.e. $\alpha = \beta = \gamma = 0.5$, and with no workload balancing, i.e. $\lambda = 4$.

The percentage of resolved conflicts using each of the two models is presented in Table 5.11, where the columns avg and SD give the average and standard deviation of the percentage of resolved conflicts respectively. We observe that the MSP-SHA/CT model eliminates 100% of the conflicts for all problems. By further investigating the problems, we observe that the difference between the percentage of resolved conflicts in the two models is attributed to the ability of the altitude modification to solve the unsolvable conflicts discussed in section 3.5.4.

Table 5.9 Total percentage of resolved conflicts using different modification manoeuvres.

Number of trajectories $\bar{\mathcal{A}}$	**MSP-S/CT (large)**		**MSP-S/CT (small)**		**MSP-H/CT**		**MSP-A/CT**	
	avg (%)	SD (%)	avg (%)	SD (%)	avg (%)	SD (%)	avg (%)	SD (%)
5	99.62	2.01	97.86	5.18	84.93	15.95	99.22	2.36
7	99.77	0.79	98.67	2.22	84.7	10.71	98.49	2.91
10	98.69	2.6	95.56	4.88	84.38	7.41	98.19	2.41
20	98.72	1.69	94.05	4.32	77.04	5.14	95.93	2.42

Table 5.10 Percentage of modified trajectories using different modification manoeuvres.

	$\bar{\mathcal{A}} = 5$		$\bar{\mathcal{A}} = 7$		$\bar{\mathcal{A}} = 10$		$\bar{\mathcal{A}} = 20$	
	avg (%)	SD (%)	avg (%)	SD (%)	avg (%)	SD (%)	avg (%)	SD (%)
MSP-S/CT (large)	13.4	6.54	15.17	5.4	18.06	5.24	30.68	4.84
MSP-S/CT (small)	14.92	8.12	17.06	6.48	19.78	5.62	35	5.1
MSP-H/CT	18.72	9.48	20.77	8.67	23.94	7	37.35	4.35
MSP-A/CT	12.96	6.33	14.6	5.17	16.82	3.93	28.26	3.13

The unsolvable conflicts are conflicts that have a large minimum separation time, i.e. S_p, that cannot be reached using speed and heading changes. Using altitude modifications, the model can separate vertically the aircraft involved in this type of conflicts.

Both the MSP-SHA/CT and MSP-SH/CT models use an objective function that minimizes the number of modified trajectories. The percentage of modified trajectories in the solutions found by both models is presented in Table 5.12, where the columns avg and SD give the average and standard deviation of the percentage of modified trajectories respectively. In this table, we see that the MSP-SHA/CT model has a smaller percentage of modified trajectories than the MSP-SH/CT model. This difference in the percentage of modified trajectories is due to the fact that the MSP-SHA/CT allows for altitude modifications as an additional trajectory modification manoeuvre. This means that the optimal solution found by the MSP-SH/CT is a feasible solution for the MSP-SHA/CT model. Consequently, the MSP-SHA/CT model can always find a solution as good as MSP-SH/CT and can find a better solution if it exists.

The time taken by the MSP-SHA/CT and MSP-SH/CT models to solve these problems is presented in Table 5.13, where the columns avg and SD give the average and standard deviation of the computation time in seconds respectively. In this table, we observe that the MSP-SHA/CT model has a computation time higher than the MSP-SH/CT model. This difference in the computation time is normal because the MSP-SHA/CT model considers $L_i(m,k)$ as a binary decision variable in addition to the variables in the MSP-SH/CT model. In addition, the MSP-SHA/CT use the binary variables $U_i(m,k)$ and $\mathcal{I}_l(i)$, which are not part of the MSP-SH/CT model.

From these results, we conclude that the introduction of altitude modifications to our model increased the model capacity to solve conflicts while decreasing the percentage of modified

Table 5.11 Percentage of resolved conflicts using MSP-SH/CT and MSP-SHA/CT.

	$\bar{\mathcal{A}} = 5$		$\bar{\mathcal{A}} = 7$		$\bar{\mathcal{A}} = 10$		$\bar{\mathcal{A}} = 20$	
	avg (%)	SD (%)	avg (%)	SD (%)	avg (%)	SD (%)	avg (%)	SD (%)
MSP-SH/CT	99.62	2.01	99.82	0.71	99.19	1.96	99.58	0.73
MSP-SHA/CT	100	0	100	0	100	0	100	0

Table 5.12 Percentage of modified trajectories using MSP-SH/CT and MSP-SHA/CT.

	$\bar{\mathcal{A}} = 5$		$\bar{\mathcal{A}} = 7$		$\bar{\mathcal{A}} = 10$		$\bar{\mathcal{A}} = 20$	
	avg (%)	SD (%)	avg (%)	SD (%)	avg (%)	SD (%)	avg (%)	SD (%)
MSP-SH/CT	13.76	6.9	15.69	5.95	18.02	4.52	30.51	3.81
MSP-SHA/CT	12.64	6.13	14.34	5.17	16.4	3.95	26.03	2.77

Table 5.13 Computation time in seconds using MSP-SH/CT and MSP-SHA/CT.

	$\bar{\mathcal{A}} = 5$		$\bar{\mathcal{A}} = 7$		$\bar{\mathcal{A}} = 10$		$\bar{\mathcal{A}} = 20$	
	avg	SD	avg	SD	avg	SD	avg	SD
MSP-SH/CT	0.63	0.45	1.44	0.86	4.23	2.52	120.21	138.03
MSP-SHA/CT	1.77	1.09	4.27	2.98	12.62	7.08	196.96	80.68

trajectories. We also conclude that the introduction of altitude modifications increases the computation time.

5.3.3 Changing the allowed percentage of modified trajectories

In the previous section, we compared the MSP-SHA/CT and MSP-SH/CT models while allowing for the modification of 50% of the trajectories, i.e. $\gamma = 0.5$. In this section, we compare the two models while varying the value of γ. For this comparison, we solve the problems with $\bar{\mathcal{A}} = 10$ and $\bar{\mathcal{A}} = 20$ while varying γ from 0 to 1 and with no workload balancing, i.e. $\lambda = 4$. We use $\alpha = \beta = \gamma$ so that we do not limit the use of any type of manoeuvres. Similarly to the previous section, we compare the models performance by the percentage of resolved conflicts, percentage of modified trajectories and computation time.

The average percentage of resolved conflicts as a function γ for problems with $\bar{\mathcal{A}} = 10$ and $\bar{\mathcal{A}} = 20$ is displayed in the Figures 5.3-a and 5.3-b respectively. Let $\bar{\gamma}$ be the value of γ beyond which MSP-SH/CT model eliminates most conflicts, i.e. $\bar{\gamma} = 0.25$ for $\bar{\mathcal{A}} = 10$ and $\bar{\gamma} = 0.35$ for $\bar{\mathcal{A}} = 20$. In these figures, we see that for small values of γ, the average percentage of resolved conflicts is the same for both models. As γ increases, the MSP-SHA/CT model resolves more conflicts than the MSP-SH/CT model. The difference between the two models remains significant up to $\gamma = \bar{\gamma}$. For $\gamma > \bar{\gamma}$, the small difference between the percentage of resolved conflicts using the two models is due the unsolvable conflicts. These unsolvable conflicts are solvable using altitude modifications, which is only allowed in the MSP-SHA/CT model. In these figures, we also observe that the MSP-SHA/CT model eliminates 100% of conflicts for a value of γ smaller than $\bar{\gamma}$.

The percentage of modified trajectories as a function of γ for problems with $\bar{\mathcal{A}} = 10$ and $\bar{\mathcal{A}} = 20$ is displayed in the Figures 5.3-c and 5.3-d respectively. In the Figure 5.3-c, we can see the curves as three parts. First for $\gamma \leq 0.18$, the percentage of modified trajectories equals to

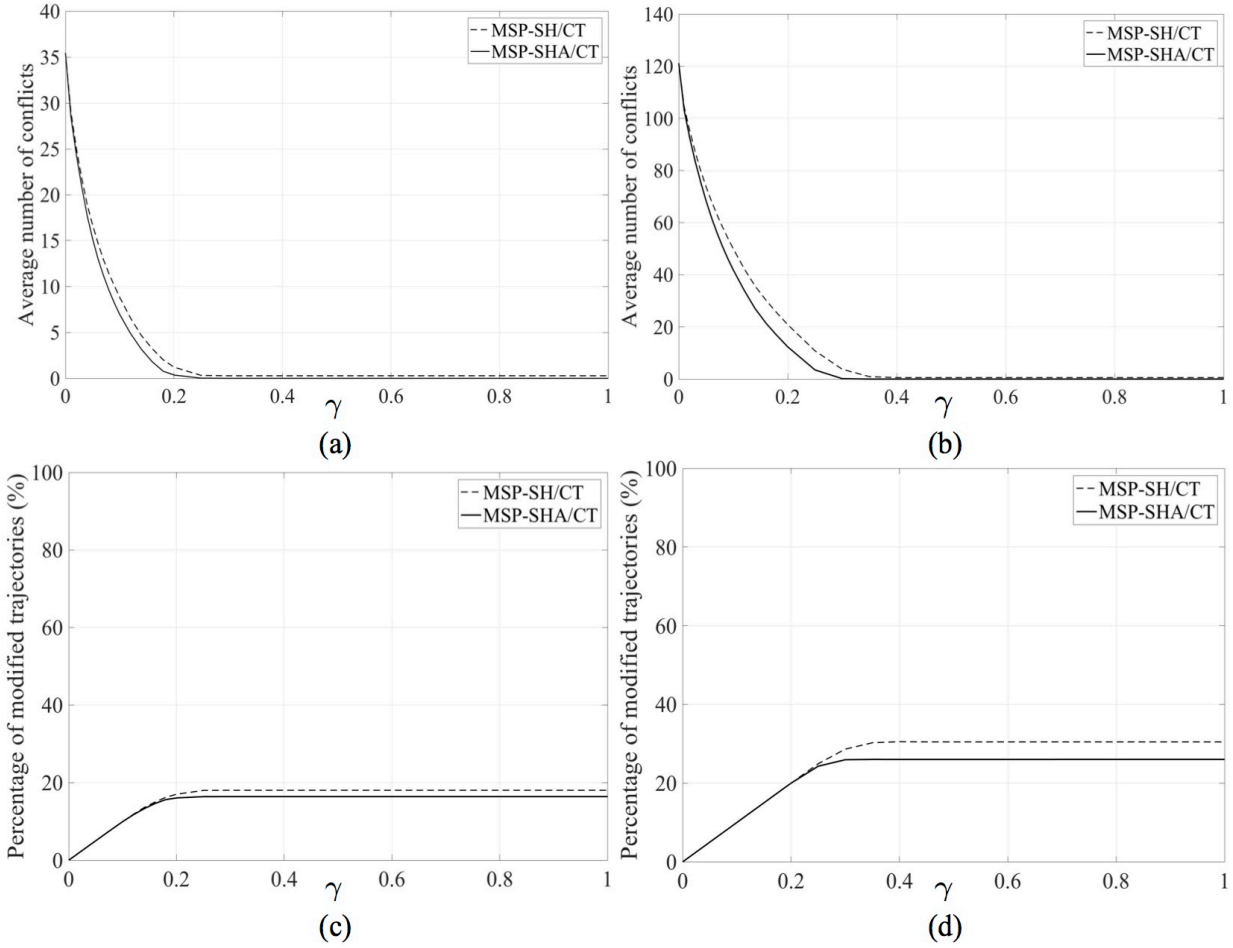

Figure 5.3 Comparing the MSP-SHA/CT and MSP-SH/CT models while varying γ : (a) number of unresolved conflicts for $\bar{\mathcal{A}} = 10$; (b) number of unresolved conflicts for $\bar{\mathcal{A}} = 20$; (c) percentage of modified trajectories for $\bar{\mathcal{A}} = 10$; (d) percentage of modified trajectories for $\bar{\mathcal{A}} = 20$.

γ for both models. For these values of γ, the modification of a trajectory eliminates at least one conflict, so both models modify the maximum allowed number of trajectories. Second for $0.18 < \gamma < 0.25$, as γ increases the percentage of modified trajectories increases but it is less than γ. For these values of γ, the unresolved conflicts requires the modification of more than one trajectory to eliminate a conflict. Consequently, increasing the value of γ does not always lead to an increase in the percentage of modified trajectories. Third for $\gamma \geq 0.25$, both models eliminated all the solvable conflicts and the percentage of modified trajectories remains constant. Note that for $\gamma \geq 0.18$, the MSP-SHA/CT model has a lower percentage of modified trajectories than the MSP-SH/CT model.

Similarly, we observe in the Figure 5.3-d that for $\bar{\mathcal{A}} = 20$, the percentage of modified trajectories equals to γ for $\gamma < 0.25$ using each of the two models. For $\gamma > 0.25$, the MSP-SHA

model modifies a smaller percentage of trajectories than the MSP-SH/CT model.
The average computation time in seconds as a function of γ for problems with $\bar{\mathcal{A}} = 10$ and $\bar{\mathcal{A}} = 20$ is displayed in the Figures 5.4-a and 5.4-b respectively. In Figure 5.4-a, we observe that the computation time using the MSP-SHA/CT model is two to three times that of the MSP-SH/CT model. This difference occurs because the MSP-SHA/CT model has the binary variables $L_i(m,k), U_i(m,k)$ and $\mathcal{I}_l(i)$ in addition to the variables of the MSP-SH/CT model. In Figure 5.4-b, we see that the computation time of the MSP-SHA/CT model is generally larger than that of the MSP-SH/CT model. We also observe that the maximum computation times using for the two models are similar. In both figures, we observe that the maximum computation time occurs near the value of γ that eliminates most conflicts.

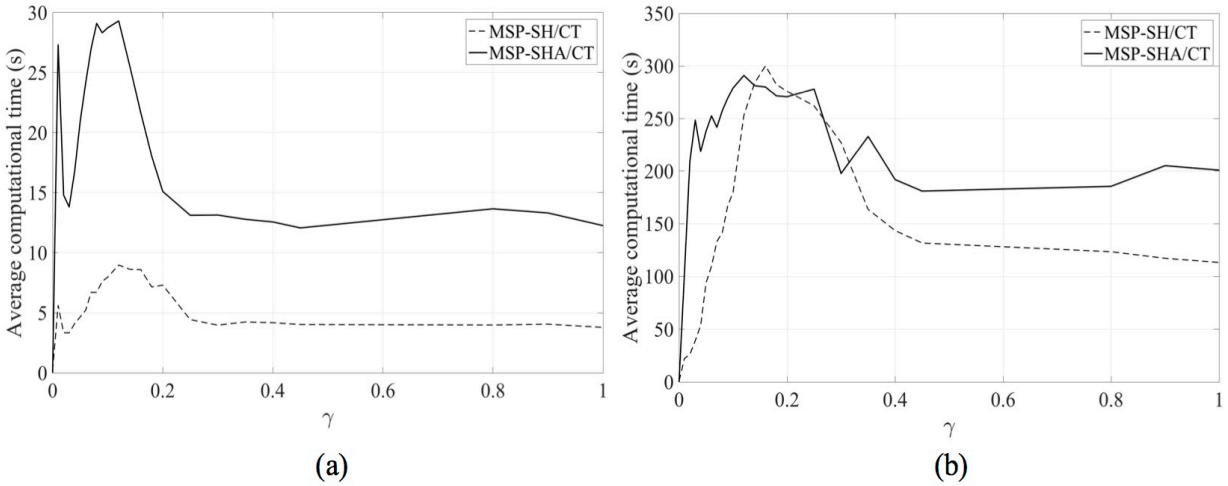

Figure 5.4 Average computation time as a function of γ for problems with : (a) $\bar{\mathcal{A}} = 10$; (b) $\bar{\mathcal{A}} = 20$.

From these results, we conclude that the MSP-SHA/CT and the MSP-SH/CT models have a comparable performance for small values of γ with a smaller computation time for the MSP-SH/CT model. For larger values of γ, the MSP-SHA/CT model solves more conflicts than the MSP-SH/CT model with fewer modified trajectories. We also conclude that the MSP-SHA/CT model has a larger average computation time than the MSP-SH/CT model.

5.3.4 Effect of the workload balancing factor

In this section, we examine the performance of the MSP-SHA/CT model as a function of the balancing factor λ. First, we compare the performance of the MSP-SHA/CT and MSP-SH/CT models. Second, we study the solutions of the MSP-SHA/CT model for a single problem as a function of λ.

Comparison between the MSP-SHA/CT and MSP-SH/CT models

To compare the MSP-SHA/CT and MSP-SH/CT models, we solve the problems with $\bar{\mathcal{A}} = 10$ using each of the two models for $\alpha = \beta = \gamma = 0.1$ while varying λ from 1 to 4. The average number of conflicts as a function of λ using MSP-SHA/CT and MSP-SH/CT is presented in the Figures 5.5-a and 5.5-b respectively. These figures also display the average number of conflicts per sector, where the sectors are indexed in the descending order of the number of conflicts, i.e. sector 1 is the sector with the most unresolved conflicts and sector 4 is the sector with the least number of unresolved conflicts. Comparing these figures, we observe that the MSP-SHA/CT model finds a better solution than the MSP-SH/CT model for all values of λ. We observe that as λ decreases, the sectors become more balanced and the total number of conflicts increases. Using any of the two models, the total number of conflicts increases only for $\lambda \leq 2$ in comparison with the no balancing solution, i.e. $\lambda = 4$. We conclude that the introduction of altitude modifications leads to a decrease in the total number of conflicts with no significant effect on the conflicts distribution among sectors.

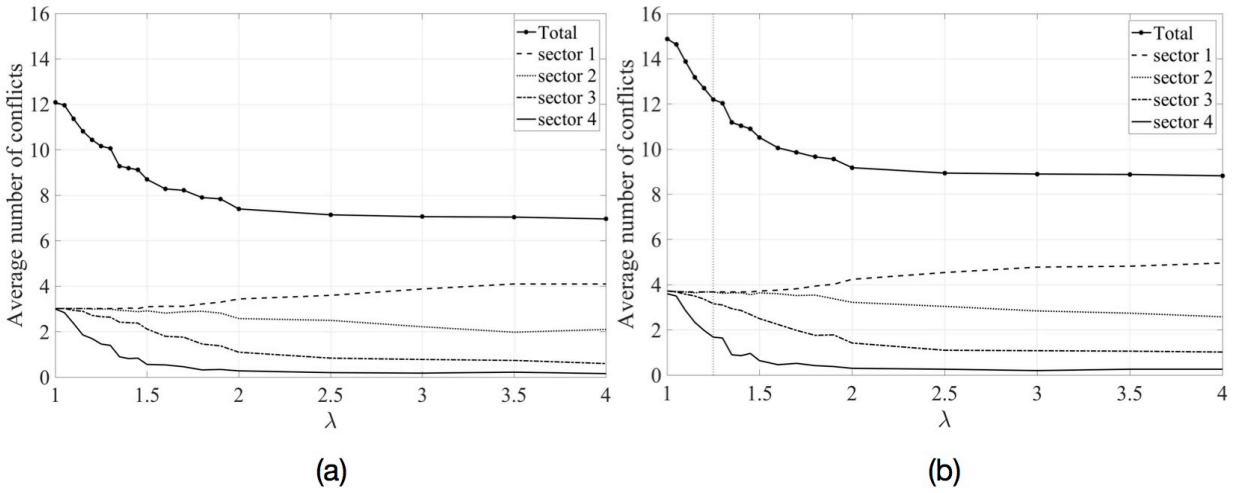

Figure 5.5 Average number of conflicts as a function of λ for problems with $\bar{\mathcal{A}} = 10$ using : (a) MSP-SHA/CT ; (b) MSP-SH/CT.

The average percentage of modified trajectories as a function of λ is displayed in Figure 5.6. We observe that there is no significant difference between the two curves. For $\lambda \leq 2$, enforcing the balancing increases the total number of conflicts, which subsequently decreases the percentage of modified trajectories. In general, the change in the percentage of modified trajectories as a function of λ does not differ significantly between the two models.
The average computation time as a function of λ is displayed in Figure 5.7. We observe that in general the average computation time using MSP-SHA/CT is higher than MSP-SH/CT.

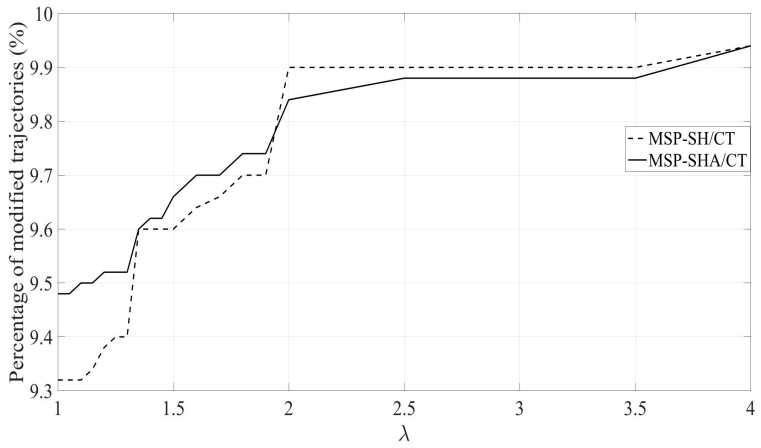

Figure 5.6 Percentage of modified trajectories as a function of λ for problems with $\bar{\mathcal{A}} = 10$.

We also observe that the computation time is higher for $\lambda < 2$ than for $\lambda > 2$ using any of the two models. For $\lambda < 2$, the optimal solution does not modify the maximum allowed percentage of trajectories. Consequently, for $\lambda < 2$, the model takes more time to minimize the percentage of modified trajectories. We observe that the maximum computation time occurs for $\lambda \approx 1$ for the two models. The high computation time for these values of λ was explained in section (4.3.6). We conclude that the introduction of the altitude modification increases the computation time for all values of λ except for $\lambda \approx 1$ where it has no significant effect on the computation time.

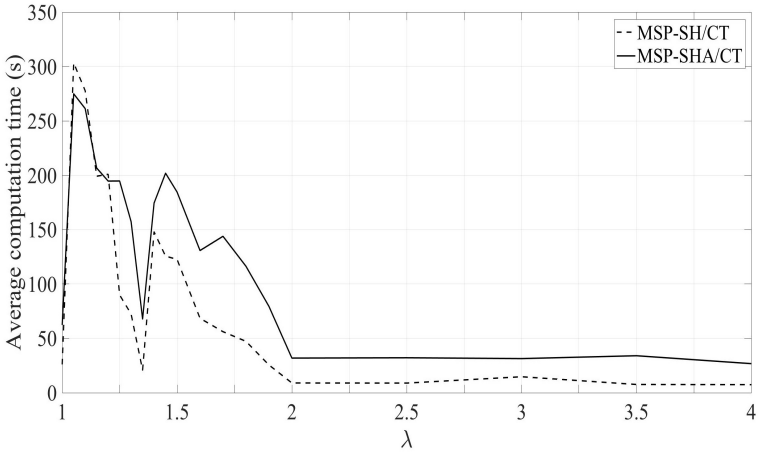

Figure 5.7 Average computation time as a function of λ for problems with $\bar{\mathcal{A}} = 10$.

Performance of the MSP-SHA/CT model for a single problem

In this section, we study the change in the solutions of one problem as a function of λ using the MSP-SHA/CT model. In the previous section, we studied the average performance for 50 problems. Since the problems are randomly generated and do not have the same distribution of aircraft or conflicts, then considering the average performance hides the performance profile for each individual problem. For this section, we solve a problem with $\bar{\mathcal{A}} = 20$ using MSP-SHA/CT for $\alpha = \beta = \gamma = 0.1$ and $\lambda \in [1, 4]$.

The number of conflicts as a function of λ using MSP-SHA/CT is presented in Figure 5.8. We observe that the number of unresolved conflicts in the sector 1 remains constant for $\lambda < 1.35$. The model finds a solution with the minimum number of conflicts in sector 1 for $\lambda = 1.35$. By decreasing λ, i.e. enforcing workload balancing, the model searches for solutions that increase the number of conflicts in the remaining sectors. For this problem, enforcing the workload balancing with $\lambda < 1.35$ increases the total number of conflicts without decreasing the number of conflicts in sector 1, hence using $\lambda < 1.35$ is not beneficial.

The value of λ below which the workload balancing is not beneficial depends on the problem. This is one of the reasons why a problem should be solved using different values of λ. Given these solutions, the MSPr may choose the most appropriate solution.

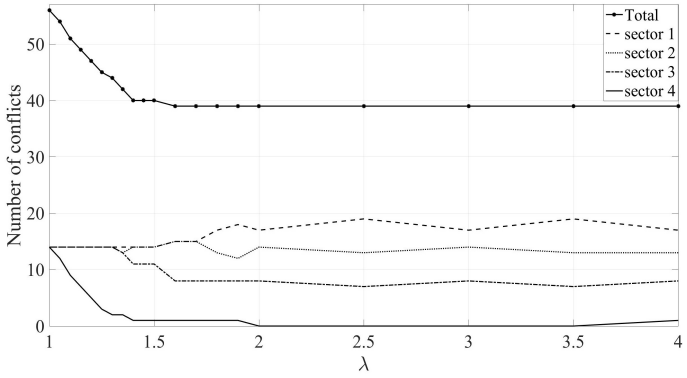

Figure 5.8 Number of conflicts as a function of λ for a problem with $\bar{\mathcal{A}} = 20$ using MSP-SHA/CT.

The percentage of modified trajectories as a function of λ is presented in Figure 5.9. We observe that the percentage of modified trajectories equals $\gamma = 0.1$ for $\lambda \geq 1.35$. The step observed in Figure 5.9 at $\lambda = 1.35$ corresponds to the increase of the total number of conflicts for $\lambda < 1.35$ in Figure 5.8.

The computation time as a function of λ is presented in Figure 5.10. We see that for $\lambda \geq 1.35$, the computation times at different values of λ are comparable and are between 200 and 300 seconds. For $\lambda < 1.35$, the model cannot reach the optimal solution in less than 10 minutes.

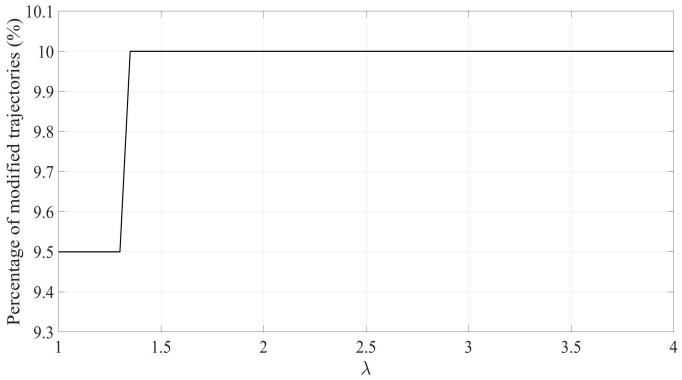

Figure 5.9 Percentage of modified trajectories as a function of λ for a problem with $\bar{\mathcal{A}} = 20$.

By solving the same problem using the unmodified objective function (4.32), we determined the minimum number of conflicts for $1 \leq \lambda \leq 4$. By comparing the solutions, we found that the solution of the MSP-SHA/CT model gives the minimum number of conflicts. For $\lambda < 1.35$, we observed that most of the computation time is used to determine the optimal percentage of modified trajectories.

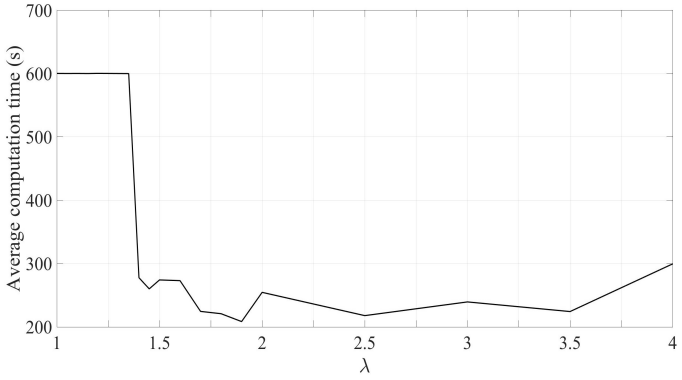

Figure 5.10 Computation time as a function of λ for a problem with $\bar{\mathcal{A}} = 20$.

We conclude that enforcing more balancing is not always beneficial. Decreasing the value of λ beyond a critical value λ_c can increase the total number of conflicts without decreasing the workload in the most charged sector. For $\lambda < \lambda_c$, the percentage of modified trajectories decreases and the computation time increases significantly. The value of λ_c is problem dependent and therefore we should provide the MSPr several solutions at different balancing levels.

5.3.5 Concluding remarks

In this chapter, we introduced altitude modifications as an additional trajectory modification manoeuvre in our model. We formulated altitude modifications and the related assumptions using linear constraints. Using randomly generated problems, the results showed that the altitude modification is an efficient tool to decrease the number of conflicts in a MSP context. Using only altitude modifications, our model eliminated more than 95% of the conflicts in problems involving 200 aircraft. The performance of altitude modifications is comparable to speed changes as it eliminates approximately the same percentage of conflicts with fewer modified trajectories.

For small values of γ, we found that the performance of the MSP-SHA/CT and MSP-SH/CT models is comparable. For larger values of γ, we found that the introduction of altitude modifications as an additional manoeuvre is beneficial. Using different sets of randomly generated problems, we found that the MSP-SHA/CT model eliminates more conflicts than the MSP-SH/CT model with a smaller percentage of modified trajectories. On the average, the introduction of altitude modifications increases computational time.

Comparing the MSP-SHA/CT and MSP-SH/CT models as a function of λ, we found that the use of altitude modifications decreases the total number of conflicts for all values of λ. This decrease is achieved with no significant change in the percentage of modified trajectories. We also found that the introduction of altitude modifications increases the computational time for all values of λ except for $\lambda \approx 1$, i.e. near equal balancing.

CHAPTER 6 CONCLUSION

6.1 Summary

The complexity resolution problem in a MSP context targets the minimization and balancing of controllers workload in a set of adjacent sectors over a medium time horizon. This takes place through the modification of aircraft trajectories. We presented in this work a complete definition for this problem. To solve this problem, we developed a MILP model that considers the use of speed, heading and altitude changes simultaneously. This model considers the detection and resolution of both crossing and trailing conflicts. We defined trajectory modification manoeuvres so that they ensure minimal change on the aircraft travel durations and also ensure spatial trajectory recovery. We use the number of conflicts as the complexity measure to be minimized. Our model also minimizes the number of modified trajectories. We conducted several tests using randomly generated problems. These tests allowed us to assess the performance of our model.

Our model handles efficiently air traffic situations that involve a combination of crossing and trailing conflicts. It decreases the total number of conflicts in a MSA with the minimum number of modified trajectories. In addition, it ensures that the unresolved conflicts are distributed amongst sectors. Since we chose trajectory modification manoeuvres with small magnitude, our model has a minimal effect on the aircraft travel durations. For most cases, our model finds the optimal solution in a reasonable amount of time (less than 10 minutes). We found that in comparison with the use of only speed changes, the introduction of the heading and altitude changes can reduce significantly the number of unresolved conflicts and the number of modified trajectories.

As for the workload balancing, we found that enforcing the balance is advantageous especially in high traffic situations. We also found that enforcing a strict balance, i.e. near equal balancing, is not always useful. It may increase the total number of unresolved conflicts without decreasing the number of conflicts in the sector with the highest workload.

Our model has several solution parameters, i.e. α, β, γ and λ, that can be adjusted to provide different optimal solutions, e.g. only speed changes, only heading changes, different balancing levels. The MSPr should determine the set of solutions that is suitable for each situation. We recommend that this set should include the no balancing and equal balancing solutions as they are important to determine the appropriate balancing level. In the test problems, we found that the computation time depends on the solution parameters. To minimize the computation time, we recommend the use of the modified objective function only once to

determine the minimum percentage of modified trajectories. For the rest of the solutions, we recommend the use of the unmodified objective function and a value of γ that equals to the minimum percentage of modified trajectories.

We solved different set of randomly generated problems that represent low, medium and high traffic situations using different combinations of manoeuvres. We found that for low and medium traffic situations the use of only small speed changes is preferable. It eliminates most of the conflicts in a small computational time. For high traffic situations, the use of a combination of small speed and heading changes or a small speed, heading and altitude changes are preferable. The preference between the two combinations depends on the allowed percentage of modified trajectories. Both combinations decrease the number of unresolved conflicts and the number of modified trajectories.

As a conclusion, we presented in this thesis a support model for the MSPr that evaluates the workload of the controllers by the number of conflicts. This model predicts and solves crossing and trailing conflicts over a medium time horizon. It minimizes and balances the number of conflicts in a MSA. In general, the model returned the optimal solutions for problems involving up to 200 aircraft in a reasonable amount of time.

6.2 Contributions

1. We developed an extension of the work of Vela et al. (2009) on the detection and resolution of crossing conflicts.
2. We developed a novel linear model for the detection and resolution of trailing conflicts. This model relies on the transformation of safe separation distances into safe separation times at the beginning and end of the common flight segments between two trailing aircraft.
3. We developed a MILP model that allows to detect and minimize the number of conflicts in a MSP context using speed, heading and altitude changes.
4. We developed a first linear formulation of the workload balancing in the complexity resolution problem in a MSP context. The workload balancing is a fundamental feature in the MSP concept.
5. We introduced a formulation for the objective function that minimizes the total number of conflicts and the number of modified trajectories. This formulation gives priority to the minimization of the number of conflicts over the number of modified trajectories.

6.3 Future work

— In this thesis, we used the number of conflicts as a measure of controllers workload. A prospective line of work is to use a more comprehensive measure such as the dynamic density (Laudeman et al. (1998)). Such a measure includes other important factors affecting controllers workload, e.g. the number of aircraft with speed, heading or altitude changes, number of conflicts near the borders and the maximum number of simultaneous conflicts. One of the advantages of our model is that such factors can be easily integrated into the model. Our model includes a linear formulation to count the number of aircraft with speed, heading or altitude changes. Also, our model keeps track of the location and time of each conflict in the preprocessing stage. By setting appropriate weights for each of theses factors, our model may be used to balance different comprehensive complexity measures.

— We assumed in this work that the prediction of aircraft positions is deterministic and that there are no errors in the prediction of the MSA arrival times. This assumption was motivated by the future application of 4D FMS and data link communication systems. This means that the application of our model is limited to a future system where the errors in the prediction of aircraft position are insignificant. A future line of work is to consider uncertain aircraft positions and MSA arrival times. First, there is a need to assess the robustness of deterministic solutions for different error levels. Second, there is a need for a stochastic optimization model. A possible model is a two stage stochastic program with fixed recourse. In the first stage, variables will be the same as in the deterministic model. In the second stage, variables will represent corrective manoeuvres to be taken at each possible state.

— In our model, we did not consider conflicts between aircraft during altitude changes. A future extension to our model is to consider this type of conflicts. To formulate this conflict, we may consider that an aircraft occupies two flight levels during altitude changes, i.e. $\sum_{k=1}^{K} L_i(m,k) = 2$. This formulation requires the reformulation of most of the altitude change constraints. It also requires further information regarding the aircraft such as weight to get an estimate of the appropriate rate of climb.

— Our model can be extended to the conflict detection and resolution problem in a single sector. For this problem, the speed and heading changes have a larger magnitude than that assumed in this work. As a result, we cannot assume that aircraft change their speeds and headings instantaneously at waypoints. Note that the formulation of conflict detection in this thesis relies on assuming that the aircraft speeds are constant near intersection points. A possible solution is to assume that the aircraft change their speeds at the beginning of flight segments using constant acceleration. Subsequently,

for each modified trajectory, one should verify that there are enough time and space to reach the desired speed long before the intersection point. A similar assumption was made by Omer (2015) to allow for constant speed around the intersection points.

REFERENCES

M. Al Basman and J. Hu, "Approaches for stochastic safety analysis arising in atm application", in *2012 IEEE 51st IEEE Conference on Decision and Control (CDC)*. IEEE, 2012, pp. 514–519.

A. Alonso-Ayuso, L. F. Escudero, and F. J. Martín-Campo, "Collision avoidance in air traffic management : a mixed-integer linear optimization approach", *IEEE Transactions on Intelligent Transportation Systems*, vol. 12, no. 1, pp. 47–57, 2011.

——, "A mixed 0–1 nonlinear optimization model and algorithmic approach for the collision avoidance in atm : Velocity changes through a time horizon", *Computers & Operations Research*, vol. 39, no. 12, pp. 3136–3146, 2012.

——, "On modeling the air traffic control coordination in the collision avoidance problem by mixed integer linear optimization", *Annals of Operations Research*, vol. 222, no. 1, pp. 89–105, 2014.

——, "An exact multi-objective mixed integer nonlinear optimization approach for aircraft conflict resolution", *TOP*, pp. 1–28, 2015.

——, "Multiobjective optimization for aircraft conflict resolution. a metaheuristic approach", *European Journal of Operational Research*, vol. 248, no. 2, pp. 691–702, 2016.

G. M. Appa, L. S. Pitsoulis, and H. P. Williams, *Handbook on modelling for discrete optimization*. Springer Science & Business Media, 2006, vol. 88, p. 89 :90.

N. Barnier and C. Allignol, "Trajectory deconfliction with constraint programming", *The Knowledge Engineering Review*, vol. 27, no. 3, p. 291, 2012.

A. Bicchi and L. Pallottino, "On optimal cooperative conflict resolution for air traffic management systems", *IEEE Transactions on Intelligent Transportation Systems*, vol. 1, no. 4, pp. 221–231, 2000.

S. Cafieri and N. Durand, "Aircraft deconfliction with speed regulation : new models from mixed-integer optimization", *Journal of Global Optimization*, vol. 58, no. 4, pp. 613–629, 2014.

J. Carlier, V. Duong, D. Nace, and H. H. Nguyen, "Using disjunctive scheduling for optimally

solving en-route conflicts [atc]", in *Digital Avionics Systems Conference, 2002. Proceedings. The 21st*, vol. 1. IEEE, 2002, pp. 1A2–1.

J. Celio, "Performance-based atm : Concept and service provider roles and responsibilities, 7", in *AIAA Aviation Technology, Integration and Operations (ATIO) Conference, Belfast, Northern Ireland*, 2007.

G. Chaloulos, E. Crück, and J. Lygeros, "A simulation based study of subliminal control for air traffic management", *Transportation research part C : Emerging technologies*, vol. 18, no. 6, pp. 963–974, 2010.

J. A. Cobano, D. Alejo, A. Ollero, and A. Viguria, "Efficient conflict resolution method in air traffic management based on the speed assignment", in *Proceedings of the 2nd International Conference on Application and Theory of Automation in Command and Control Systems*. IRIT Press, 2012, pp. 54–61.

S. Constans, B. Fontaine, and R. Fondacci, "Minimizing potential conflicts with speed control", in *International Conference on Research in Air Traffic Transportation, ICRAT*, 2006.

S. Conversy, H. Gaspard-Boulinc, S. Chatty, S. Valès, C. Dupré, and C. Ollagnon, "Supporting air traffic control collaboration with a tabletop system", in *Proceedings of the ACM 2011 conference on Computer supported cooperative work*. ACM, 2011, pp. 425–434.

K. Corker, L. Paul, P. Tom, G. Eromi, M. Lynne, S. Nancy, V. Savvy, J. Homala, and M. Joey, "Analysis of multi-sector planner concepts in us airspace", HAIL Laboratory Report, Tech. Rep., 2006.

D. Delahaye and S. Puechmorel, "Air traffic complexity : towards intrinsic metrics", in *Proceedings of the third USA/Europe Air Traffic Management R & D Seminar*, 2000.

F. Drogoul, P. Averty, and R. Weber, "Erasmus strategic deconfliction to benefit sesar", in *Proceedings of the 8th USA/Europe Air Traffic Management R&D Seminar*, 2009.

N. Durand and J.-M. Alliot, "Ant colony optimization for air traffic conflict resolution", in *ATM Seminar 2009, 8th USA/Europe Air Traffic Management Research and Developpment Seminar*, 2009.

N. Durand, J.-M. Alliot, and J. Noailles, "Automatic aircraft conflict resolution using genetic algorithms", in *Proceedings of the 1996 ACM symposium on Applied Computing*. ACM, 1996, pp. 289–298.

R. Ehrmanntraut and S. McMillan, "Airspace design process for dynamic sectorisation", in *2007 IEEE/AIAA 26th Digital Avionics Systems Conference*. IEEE, 2007, pp. 3–D.

EUROCONTROL, "Gate to gate – journey's end." EUROCONTROL, 2006. [Online]. Available : http://www.eurocontrol.int/eec/public/standard_page/EEC_News_2006_3_G2G.html

——, *Long-Term Forecast, Flight movements 2010-2030*, 2010. [Online]. Available : http://www.eurocontrol.int/publications/eurocontrol-long-term-forecast-flight-movements-2010-2030

——, *Medium-Term Forecast, Flight movements 2011-2017*, 2011. [Online]. Available : https://www.eurocontrol.int/sites/default/files/field_tabs/content/documents/official-documents/forecasts/medium-term-forecast-2011-2017-201102.pdf

——, *Challenges of growth 2013, Task 4 : European Air Traffic in 2035*, 2013. [Online]. Available : https://www.eurocontrol.int/sites/default/files/article/content/documents/official-documents/reports/201306-challenges-of-growth-2013-task-4.pdf

——, *Challenges of growth 2013, Task 7 : European Air Traffic in 2050*, 2013. [Online]. Available : https://www.eurocontrol.int/sites/default/files/article/content/documents/official-documents/reports/201306-challenges-of-growth-2013-task-7.pdf

——, "What is air traffic management ?" EUROCONTROL, 2012. [Online]. Available : https://www.eurocontrol.int/articles/what-air-traffic-management

——, "Air traffic control services", EUROCONTROL, 2014. [Online]. Available : https://www.eurocontrol.int/articles/air-traffic-control-services

P. Flener, J. Pearson, M. Ågren, C. G. Avello, and M. Çeliktin, "Air-traffic complexity resolution in multi-sector planning", Department of Information Technology, Uppsala University, Tech. Rep. 2007-003, Jan. 2007.

P. Flener, J. Pearson, M. Ågren, C. Garcia-Avello, M. Celiktin, and S. Dissing, "Air-traffic complexity resolution in multi-sector planning", *Journal of Air Transport Management*, vol. 13, no. 6, pp. 323–328, 2007.

——, "Air-traffic complexity resolution in multi-sector planning using constraint programming", in *7th USA/Europe Seminar on Air Traffic Management R & D, Barcelona*, 2007. [Online]. Available : `http://atmseminar.eurocontrol.fr/past-seminars/7th-seminar-barcelona-spain-july-2007/papers/paper_023/view`

G. Flynn, A. Benkouar, and R. Christien, "Pessimistic sector capacity estimation", *EEC Note*, vol. 21, no. 03, 2003.

G. Gawinowski, J.-L. Garcia, R. Guerreau, R. Weber, and M. Brochard, "Erasmus : a new path for 4d trajectory-based enablers to reduce the traffic complexity", in *Digital Avionics Systems Conference, 2007. DASC'07. IEEE/AIAA 26th.* IEEE, 2007, pp. 1–A.

S. Herr, M. Teichmann, M. Poppe, and N. Suarez, "The impact of multi sector planning and new working procedures on controller tasks", in *24th Digital Avionics Systems Conference*, vol. 1. IEEE, 2005, pp. 3–B.

B. Hilburn, "Cognitive complexity in air traffic control : A literature review", *EEC note*, vol. 4, no. 04, 2004.

Y. Hong, B. Choi, K. Lee, and Y. Kim, "Conflict management considering a smooth transition of aircraft into adjacent airspace", *IEEE Transactions on Intelligent Transportation Systems*, vol. 17, no. 9, pp. 2490–2501, 2016.

J. Hu, M. Prandini, and S. Sastry, "Optimal coordinated maneuvers for three-dimensional aircraft conflict resolution", *Journal of Guidance, Control, and Dynamics*, vol. 25, no. 5, pp. 888–900, 2002.

ICAO, *Global Operational Data Link Document (GOLD)*, 2nd ed., International Civil Aviation Organization, 2013.

——, *Manual on Implementation of a 300 m (1 000 ft) Vertical Separation Minimum Between FL 290 and FL 410, Inclusive*, 2nd ed., International Civil Aviation Organization, Montreal, Canada, 2002.

R. Irvine, "A geometrical approach to conflict probability estimation." *Air Traffic Control Quarterly*, vol. 10, no. 2, pp. 85–113, 2002.

——, "Target miss distance to achieve a required probability of conflict", in *5th ATM Seminar, Budapest, Hungary*, 2003.

H. Kremer, W. Vertegaal, and R. Jansen, *PHARE Advanced Tools Conflict Probe Final Report, PHARE Document DOC 98-70-18 (Volume 3 of 10)*, EUROCONTROL, 1999.

J. K. Kuchar and L. C. Yang, "A review of conflict detection and resolution modeling methods", *IEEE Transactions on intelligent transportation systems*, vol. 1, no. 4, pp. 179–189, 2000.

——, "A review of conflict detection and resolution modeling methods", *Intelligent Transportation Systems, IEEE Transactions on*, vol. 1, no. 4, pp. 179–189, 2000.

P. Latron, R. McGregor, M. Geissel, E. Wassmer, and A. Mardsen, *PD/3 IOCP PROGRAMME : En-route Multi Sector Planning Procedures, PHARE DOC 97-70-15*, EUROCONTROL, 1997.

I. V. Laudeman, S. Shelden, R. Branstrom, and C. Brasil, "Dynamic density : An air traffic management metric", *Report No. NASA/TM-1998-112226*, 1998.

K. Lee, E. Feron, and A. Pritchett, "Air traffic complexity : an input-output approach", in *American Control Conference*, 2007, pp. 474–479.

P. U. Lee and T. Prevot, "Prediction of traffic complexity and controller workload in mixed equipage nextgen environments", in *Proceedings of the Human Factors and Ergonomics Society Annual Meeting*, vol. 56, no. 1. Sage Publications, 2012, pp. 100–104.

T. Lehouillier, M. I. Nasri, F. Soumis, G. Desaulniers, and J. Omer, "Solving the air conflict resolution problem under uncertainty using an iterative biobjective mixed integer programming approach", *Transportation Science*, 2017.

T. Lehouillier, J. Omer, F. Soumis, and G. Desaulniers, "Two decomposition algorithms for solving a minimum weight maximum clique model for the air conflict resolution problem", *European Journal of Operational Research*, vol. 256, no. 3, pp. 696–712, 2017.

W. Maazoun, "Conception et analyse d'un système d'optimisation de plans de vol pour les avions", Ph.D. dissertation, École Polytechnique de Montréal, 2015.

A. J. Masalonis, M. B. Callaham, and C. R. Wanke, "Dynamic density and complexity metrics for realtime traffic flow management", in *Proceedings of the 5th USA/Europe Air Traffic Management R & D Seminar*, 2003, p. 139.

E. Mueller and L. Sandy, "Experimental evaluation of an integrated datalink and automation-based strategic trajectory concept", in *proceedings of AIAA Aviation Techno-*

logy, Integration and Operations conference, 2007.

H.-H. Nguyen, "Coordination des avions pour la résolution de conflits : Une approche basée sur le graphe pert disjonctif", Ph.D. dissertation, Compiègne, 2004.

M. Nolan, *Fundamentals of air traffic control*. Cengage Learning, 2010.

J. Omer, "A space-discretized mixed-integer linear model for air-conflict resolution with speed and heading maneuvers", *Computers & Operations Research*, vol. 58, pp. 75–86, 2015.

——, "Modèles déterministes et stochastiques pour la résolution numérique du problème de maintien de séparation entre aéronefs", Ph.D. dissertation, Toulouse, ISAE, 2013.

J. Omer and J.-L. Farges, "Automating air traffic control through nonlinear programming", in *5th International Conference on Research in Air Transportation, ICRAT, Berkeley, USA*, 2012.

——, "Hybridization of nonlinear and mixed-integer linear programming for aircraft separation with trajectory recovery", *IEEE Transactions on Intelligent Transportation Systems*, vol. 14, no. 3, pp. 1218–1230, 2013.

P. Orth, S. Yacout, and L. Adjengue, "Accuracy and robustness of decision making techniques in condition based maintenance", *Journal of Intelligent Manufacturing*, vol. 23, no. 2, pp. 255–264, 2012.

L. Pallottino, E. M. Feron, and A. Bicchi, "Conflict resolution problems for air traffic management systems solved with mixed integer programming", *IEEE transactions on intelligent transportation systems*, vol. 3, no. 1, pp. 3–11, 2002.

M. Prandini, J. Hu, J. Lygeros, and S. Sastry, "A probabilistic approach to aircraft conflict detection", *IEEE Transactions on intelligent transportation systems*, vol. 1, no. 4, pp. 199–220, 2000.

M. Prandini, V. Putta, and J. Hu, "A probabilistic measure of air traffic complexity in 3-d airspace", *International Journal of Adaptive Control and Signal Processing*, vol. 24, no. 10, pp. 813–829, 2010.

——, "Air traffic complexity in advanced automated air traffic management systems", in *Proceedings of the 9th Innovative Research Workshop and Exhibition*, 2010.

M. Prandini, L. Piroddi, S. Puechmorel, and S. L. Brázdilová, "Toward air traffic complexity assessment in new generation air traffic management systems", *IEEE Transactions on Intelligent Transportation Systems*, vol. 12, no. 3, pp. 809–818, 2011.

T. Prevot and P. U. Lee, "Trajectory-based complexity (tbx) : A modified aircraft count to predict sector complexity during trajectory-based operations", in *Digital Avionics Systems Conference (DASC), 2011 IEEE/AIAA 30th.* IEEE, 2011, pp. 3A3–1.

T. Prevot, P. Lee, T. Callantine, J. Mercer, J. Homola, N. Smith, and E. Palmer, "Human-in-the-loop evaluation of nextgen concepts in the airspace operations laboratory", in *Proceedings of the AIAA Modeling and Simulation Technologies (MST) Conference, Toronto, Canada*, 2010.

T. Prevot, M. Mainini, and C. Brasil, "Multi sector planning tools for trajectory-based operations", in *10th AIAA Aviation Technology, Integration, and Operations (ATIO) Conference*, 2010, p. 9375.

A. U. Raghunathan, V. Gopal, D. Subramanian, L. T. Biegler, and T. Samad, "Dynamic optimization strategies for three-dimensional conflict resolution of multiple aircraft", *Journal of guidance, control, and dynamics*, vol. 27, no. 4, pp. 586–594, 2004.

D. Rey, C. Rapine, R. Fondacci, and N.-E. El Faouzi, "Minimization of potential air conflicts through speed regulation", *Transportation research record : journal of the transportation research board*, no. 2300, pp. 59–67, 2012.

——, "Subliminal speed control in air traffic management : Optimization and simulation", *Transportation Science*, vol. 50, no. 1, pp. 240–262, 2015.

A. Richards and J. P. How, "Aircraft trajectory planning with collision avoidance using mixed integer linear programming", in *Proceedings of the 2002 American Control Conference (IEEE Cat. No. CH37301)*, vol. 3. IEEE, 2002, pp. 1936–1941.

SESAR, *SESAR definition phase D3 : The ATM target concept*, 2nd ed., The Single European Sky ATM Research project, 2007.

——, *Multi sector planning validation report (VLAR). SESAR DOC Project Number : 04.07.08*, 3rd ed., The Single European Sky ATM Research project, 2013. [Online]. Available : `http://www.sesarju.eu/sesar-solutions/conflict-management-and-automation/multi-sector-planning`

——, *OSED for Controller Team Organisation- Roles and Responsibilities in a Trajectory Based Operation Within En-Route Airspace (including MSP). SESAR DOC Project Number : 04.07.08*, 3rd ed., The Single European Sky ATM Research project, 2013. [Online]. Available : `http://www.sesarju.eu/sesar-solutions/conflict-management-and-automation/multi-sector-planning`

N. Smith, P. Lee, T. Prevot, C. Brasil, J. Homola, A. Kessell, H. Lee, M. Mainini, and J. Mercer, "A human-in-the-loop investigation of multi-sector planning operations for the nextgen mid-term", in *10th AIAA Aviation Technology, Integration, and Operations (ATIO) Conference, September*, 2010, pp. 13–15.

S. Swierstra and S. Green, "Common trajectory prediction capability for decision support tools", in *5th USA/EUROCONTROL ATM R&D Seminar, Budapest, Hungary*, 2003.

M. Türkay and I. E. Grossmann, "Disjunctive programming techniques for the optimization of process systems with discontinuous investment costs- multiple size regions", *Industrial & engineering chemistry research*, vol. 35, no. 8, pp. 2611–2623, 1996.

S. Vales, S. Conversy, J. Lard, and C. Ollagnon, "Mammi phase2-design and evaluation test bed for collaborative practices on en-route control positions", in *CARE-INO 2007, 6th EUROCONTROL Innovative Research Workshop & Exhibition*, 2007, pp. 37–45.

A. Vela, S. Solak, W. Singhose, and J.-P. Clarke, "A mixed integer program for flight-level assignment and speed control for conflict resolution", in *Proceedings of the 48th IEEE Conference on Decision and Control, 2009 held jointly with the 2009 28th Chinese Control Conference. CDC/CCC 2009.* IEEE, 2009, pp. 5219–5226.

A. E. Vela, S. Solak, J.-P. B. Clarke, W. E. Singhose, E. R. Barnes, and E. L. Johnson, "Near real-time fuel-optimal en route conflict resolution", *IEEE Transactions on Intelligent Transportation Systems*, vol. 11, no. 4, pp. 826–837, 2010.

R. Walter, "Flight management systems", in *Digital Avionics Handbook*, C. R. Spitzer, Ed. CRC press, 2000.

M. Whiteley, *PHARE Advanced Tools Tactical Load Smoother Final Report, PHARE Document DOC, 98-70-18 (Volume 9 of 10)*, EUROCONTROL, 1999.

——, *PHARE Advanced Tools Problem Solver Final Report, PHARE Document DOC 98-70-18 (Volume 8 of 10)*, EUROCONTROL, 1999.

K. D. Wichman, G. Carlsson, and L. G. Lindberg, “Flight trials :" runway-to-runway" required time of arrival evaluations for time-based atm environment”, in *Digital Avionics Systems, 2001. DASC. 20th Conference*, vol. 2. IEEE, 2001, pp. 7F6–1.

B. Willems, M. Heiney, and R. Sollenberger, “Study of an atc baseline for the evaluation of team configureations-effects of allocating multisector control functions to a radar associate or airspace coordinator position”, Tech. Rep., 2005.

A. Williams, M. D. Rodgers, S. Mondoloni, and D. Liang, “Improving atc efficiency through an implementation of a multi sector planner position”, in *7th USA/Europe Seminar on Air Traffic Management R & D, Barcelona*, 2007.

W. Yun-sheng, S. Savage, and L. Hang, “The architecture of airborne datalink system in distributed integrated modular avionics”, in *Integrated Communications Navigation and Surveillance (ICNS), 2016*. IEEE, 2016, pp. 2D2–1.

C. Zingale, D. McAnulty, and K. Kerns, “Human factors evaluation of a digital, air-ground communications system”, in *Digital Avionics Systems Conference, 2005. DASC 2005. The 24th*, vol. 1. IEEE, pp. 5–B.

APPENDIX A FORMULATION OF THE SAFE SEPARATION TIME FOR CROSSING CONFLICTS

This appendix presents the formulation of the safe separation time $\dot{S}_{i,j}$ that ensures safe separation between two aircraft with intersecting trajectories. This formulation was first presented in French by Nguyen (2004) to solve air traffic conflicts using disjunctive scheduling. For the sake of completeness, we summarize it in this appendix. This formulation assumes that both aircraft are flying at the same flight level using constant speeds and that their trajectories are linear near the intersection point.

Consider two aircraft i and j flying at the same flight level using constant speeds v_i and v_j respectively. Let us assume that aircraft i is flying along the axis of abscissas and that the trajectory of aircraft j intersects with the axis of abscissas with an angle $\theta_{i,j}$. Let us also assume that at time $t_0 = 0$ the aircraft i is at the intersection point and that the intersection point is at the origin (0,0). At $t_0 = 0$, aircraft j is at a distance d of the origin as shown in Figure A.1.

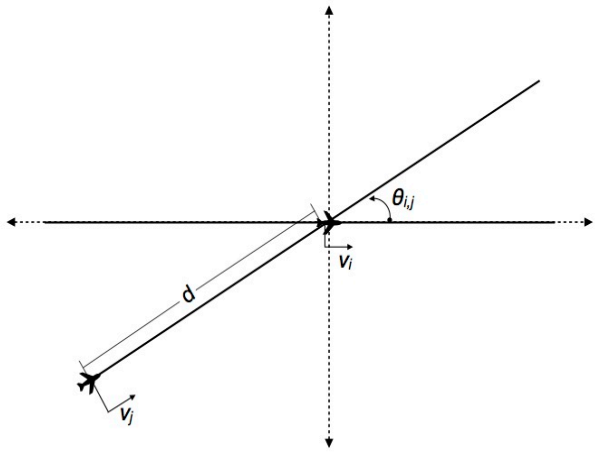

Figure A.1 Two aircraft with an intersection angle $\theta_{i,j}$.

At any time t :

— the position vector of aircraft i is $\vec{r_i} = (v_i\, t, 0)$,

— the position vector of aircraft j is $\vec{r_j} = ((v_j\, t - d)\, \cos(\theta_{i,j}), (v_j\, t - d)\, \sin(\theta_{i,j}))$

Let us denote the distance between the two aircraft i and j at any time t as $d_{i,j}(t)$. This distance is given by

$$\begin{aligned} d_{i,j}^2(t) &= \|\vec{r_i} - \vec{r_j}\|^2 \\ &= \|\vec{r_i}\|^2 + \|\vec{r_j}\|^2 - 2\,\vec{r_i}\,\vec{r_j} \\ &= (v_i\,t)^2 + (v_j\,t - d)^2 - 2\,v_i\,t\,(v_j\,t - d)\cos(\theta_{i,j}) \\ &= (v_j^2 + v_i^2 - 2\,v_i\,v_j\,\cos(\theta_{i,j}))\,t^2 \,+\, 2\,d\,(v_i\,\cos(\theta_{i,j}) - v_j)\,t \,+\, d^2. \end{aligned} \tag{A.1}$$

Let us define the constants :

$$\begin{aligned} A &= v_j^2 + v_i^2 - 2\,v_i\,v_j\,\cos(\theta_{i,j}), \\ B &= d\,(v_i\,\cos(\theta_{i,j}) - v_j), \\ C &= d^2. \end{aligned} \tag{A.2}$$

It follows from (A.2) that (A.1) takes the form

$$d_{i,j}^2(t) = A\,t^2 \,+\, 2\,B\,t \,+\, C. \tag{A.3}$$

To determine the time t^* at which the two aircraft are at the minimum separation distance, we solve $\dfrac{d}{dt}d_{i,j}^2(t) = 2\,A\,t \,+\, 2\,B = 0$, which yields,

$$t^* = \frac{-B}{A}. \tag{A.4}$$

As a result, the minimum value of $d_{i,j}^2(t)$ is

$$d_{i,j}^2(t^*) = \frac{-B^2}{A} + C. \tag{A.5}$$

We want the minimum separation distance between aircraft i and j to be greater than D, i.e. $D^2 \leq d_{i,j}^2(t^*)$, which yields

$$D^2 \leq \frac{-B^2}{A} + C. \tag{A.6}$$

Substituting A, B, and C in (A.6) for their values given in (A.2) and simplifying, we get

$$d \geq \frac{D\,\sqrt{v_i^2 + v_j^2 - 2\,v_i\,v_j\,\cos(\theta_{i,j})}}{v_i\,|\sin(\theta_{i,j})|} \tag{A.7}$$

We define $\dot{S}_{i,j}$ as the difference between the passage times of aircraft i and j at the intersection point given by

$$\dot{S}_{i,j} = \frac{d}{v_j}. \tag{A.8}$$

It follows from (A.7) that

$$\dot{S}_{i,j} \geq \frac{D}{v_i v_j |\sin(\theta_{i,j})|} \sqrt{v_i^2 + v_j^2 - 2v_i v_j \cos(\theta_{i,j})}. \tag{A.9}$$

APPENDIX B THE CROSSING CONFLICT DETECTION CONSTRAINTS

In this appendix, we present a verification for the crossing conflict detection constraints. We formulated these constraints as follows :

$$A_p + B_p + \sum_{k=1}^{K} H_p(k) - P(i(p)) - P(j(p)) + 2 - K \geq -5\ C_p, \qquad p \in \{1, 2, ..., |E|\}, \text{(B.1)}$$

$$A_p + B_p + \sum_{k=1}^{K} H_p(k) - P(i(p)) - P(j(p)) + 2 - K \leq 5\ (1 - C_p), \qquad p \in \{1, 2, ..., |E|\}. \text{(B.2)}$$

The crossing conflict conditions for a flight pair in E are :

1. $P(i(p)) = 1$ and $P(j(p)) = 1$, hence there are two aircraft using flight plans $i(p)$ and $j(p)$,
2. $\sum_{k=1}^{K} H_p(k) = K - 1$, which means that the flight plans i and j use the same flight level at the intersection point,
3. $A_p = B_p = 0$, which means that the difference between the passage times at the intersection point is smaller than S_p.

We want to verify that (B.1) and (B.2) set $C_p = 1$ if these conditions are true for the p^{th} flight plan pair in E, and set $C_p = 0$ otherwise. To do so, we check the constraints for the following two cases. First, we check it for the case where all the conditions are true, i.e. C_p must equal 1. Second, we check it for the case where at least one of the conflict conditions is not true, i.e. C_p must equal 0.

First case : All the conditions are true.
We have

$$\begin{aligned} &P(i(p)) = P(j(p)) = 1, \\ &\textstyle\sum_{k=1}^{K} H_p(k) = K - 1, \\ &A_p = B_p = 0. \end{aligned} \qquad \text{(B.3)}$$

Substituting (B.3) in (B.1) yields,

$$0 + 0 + K - 1 - 1 - 1 + 2 - K \geq -5\ C_p,$$

$$\Rightarrow \quad C_p \geq \frac{1}{5},$$

$$\Rightarrow \quad C_p = 1, \quad \text{because } C_p \in \{0, 1\}. \qquad \text{(B.4)}$$

This means that (B.3) and (B.1) imply that $C_p = 1$.
Substituting (B.3) in (B.2) yields,

$$0 + 0 + K - 1 - 1 - 1 + 2 - K \leq 5\ (1 - C_p)$$

$$\Rightarrow \quad C_p \leq \frac{6}{5},$$

$$\Rightarrow \quad C_p \in \{0, 1\}. \tag{B.5}$$

This means that (B.3) and (B.2) imply that $C_p \in \{0, 1\}$.

From (B.4) and (B.5), if all the crossing conflict conditions are true, then (B.1) and (B.2) set $C_p = 1$.

Second case : At least one of the crossing conflict conditions is not true.
If all the conditions are true as in the first case, then

$$A_p + B_p + \sum_{k=1}^{K} H_p(k) - P(i(p)) - P(j(p)) + 2 - K = -1.$$

If one of the conditions is not true, then $P(i(p)) \neq 1$ or $P(j(p)) \neq 1$ or $\sum_{k=1}^{K} H_p(k) = K$ or $A_p = 0$ or $B_p = 0$. Consequently,

$$A_p + B_p + \sum_{k=1}^{K} H_p(k) - P(i(p)) - P(j(p)) + 2 - K \geq 0.$$

We define $\mathcal{F}$ as follows,

$$\mathcal{F} := A_p + B_p + \sum_{k=1}^{K} H_p(k) - P(i(p)) - P(j(p)) + 2 - K. \tag{B.6}$$

For the case where at least one of the crossing conflict conditions is not true, the possible values of $\mathcal{F}$ are $\{0, 1, 2, 3, 4\}$.
Substituting (B.6) in (B.1) :

$$\mathcal{F} \geq -5\ C_p, \quad \mathcal{F} \in \{0, 1, 2, 3, 4\};$$

$$\Rightarrow C_p \geq 0$$

$$\Rightarrow \quad C_p \in \{0, 1\}. \tag{B.7}$$

This means that for the second case, (B.1) implies that $C_p \in \{0, 1\}$.

Substituting (B.6) in (B.2) :

$$\mathcal{F} \leq 5\ (1 - C_p), \quad \mathcal{F} \in \{0, 1, 2, 3, 4\};$$

$$\Rightarrow 4\ \leq 5\ (1 - C_p)$$

$$\Rightarrow C_p \leq \frac{1}{5}$$

$$\Rightarrow \quad C_p = 0, \quad \text{because } C_p \in \{0, 1\}. \tag{B.8}$$

This means that for the second case, (B.2) implies that $C_p = 0$.

From (B.7) and (B.8), if at least one of the crossing conflict conditions is not true, then (B.1) and (B.2) set $C_p = 0$.

APPENDIX C THE PREPROCESSING STAGE OUTPUT DATA FOR THE DETAILED EXAMPLE

This appendix presents the preprocessing stage output data for the detailed example in section 4.2. Note that some of the preprocessing stage output data was presented in section 4.2.2. The problem in this detailed example consists in 8 aircraft that are planned to pass through the MSA within a time interval of 20 to 90 minutes. All the aircraft have a minimum speed of 456 knots ($\simeq$ 850 km/hr) and a maximum speed of 513 knots ($\simeq$ 950 km/hr). The flight plans pairs at risk of a crossing conflict, i.e. that belong to E, are presented in Table C.1. This table shows the indices $i(p)$ and $j(p)$ of each flight plan pair in E along with the minimum separation time S_p in seconds.

The parameters $\bar{t}_1^-(g,\ell)$, $\bar{t}_1^+(g,\ell)$, $\bar{t}_2^-(g,\ell)$, $\bar{t}_2^+(g,\ell)$, $\bar{d}_1(g,\ell)$ and $\bar{d}_2(g,\ell)$, which define the common flight segments, are presented in Table C.2. In this table, the times are given in minutes and the distances are given in km. Note that if the first point in the common flight segment is the MSA entry waypoint, then the minimum and maximum passage time at this point are the same. For example, $\bar{t}_1^-(g,1) = \bar{t}_1^+(g,1) = 40.25$ minutes (first line).

Table C.1 Flight pairs at risk of a crossing conflict - E.

p	1	2	3	4	5	6	7	8	9	10	11	12	13	14	15	16
$i(p)$	1	1	1	1	1	1	1	1	1	1	2	2	2	2	2	2
$j(p)$	5	6	5	6	7	8	9	10	11	12	4	5	6	5	5	7
S_p	46.2	46.2	46.2	46.2	53.9	53.9	53.9	53.9	53.9	53.9	46.2	46.2	39.2	46.2	46.2	53.9

p	17	18	19	20	21	22	23	24	25	26	27	28	29	30	31	32
$i(p)$	2	2	2	2	2	2	2	2	3	3	3	3	3	3	3	3
$j(p)$	8	9	10	11	12	4	5	6	4	5	6	6	6	7	8	9
S_p	53.9	53.9	53.9	53.9	53.9	46.2	46.2	39.2	46.2	39.2	46.2	46.2	46.2	53.9	53.9	53.9

p	33	34	35	36	37	38	39	40	41	42	43	44	45	46	47	48
$i(p)$	3	3	3	3	3	3	4	4	4	4	4	4	5	5	5	5
$j(p)$	10	11	12	4	5	6	7	8	9	10	11	12	7	8	9	10
S_p	53.9	53.9	53.9	46.2	39.2	46.2	53.9	53.9	53.9	53.9	53.9	53.9	53.9	53.9	53.9	53.9

p	49	50	51	52	53	54	55	56	57	58	59	60	61	62	63	64
$i(p)$	5	5	6	6	6	6	6	6	7	7	7	7	7	7	7	8
$j(p)$	11	12	7	8	9	10	11	12	11	12	11	12	19	20	21	10
S_p	53.9	53.9	53.9	53.9	53.9	53.9	53.9	53.9	46.2	46.2	46.2	46.2	46.7	46.8	46.7	46.2

p	65	66	67	68	69	70	71	72	73	74	75	76	77	78	79	80
$i(p)$	8	8	8	8	8	8	8	8	8	9	9	9	9	9	9	9
$j(p)$	11	11	11	20	10	11	12	19	21	10	12	12	12	19	20	10
S_p	46.2	46.2	46.2	46.8	46.2	46.2	39.2	49.3	49.2	46.2	46.2	46.2	46.2	46.7	46.8	46.2

p	81	82	83	84	85	86	87	88	89	90	91	92	93	94	95	96
$i(p)$	9	9	9	10	10	10	11	11	11	12	12	12	13	13	13	13
$j(p)$	11	12	21	19	20	21	20	19	21	19	20	21	16	18	16	17
S_p	39.2	46.2	44.6	46.7	46.8	46.7	46.8	49.3	49.2	46.7	46.8	44.6	38.7	38.7	38.7	46.2

p	97	98	99	100	101	102	103	104	105	106	107	108	109	110	111	112
$i(p)$	13	14	14	14	14	14	14	14	15	15	15	15	15	15	19	19
$j(p)$	18	16	18	17	17	16	17	18	18	18	18	16	17	18	22	22
S_p	46.2	38.7	38.7	940.9	46.2	46.2	46.8	39.2	38.7	940.9	46.2	46.2	39.2	46.8	38.7	38.7

p	113	114	115	116	117	118	119	120	121	122	123	124	125	126
$i(p)$	19	19	20	20	20	20	20	20	20	21	21	21	21	21
$j(p)$	22	24	23	23	23	22	23	23	24	24	24	24	24	24
S_p	40.4	40.4	46.2	46.2	38.7	40.4	38.7	40.4	40.3	46.2	46.2	38.7	38.7	40.4

Table C.2 Common flight segments parameters.

g	$\bar{t}_1^-(g,1)$	$\bar{t}_1^+(g,1)$	$\bar{t}_2^-(g,1)$	$\bar{t}_2^+(g,1)$	$\bar{t}_1^-(g,2)$	$\bar{t}_1^+(g,2)$	$\bar{t}_2^-(g,2)$	$\bar{t}_2^+(g,2)$	$\bar{d}_1(g,1)$	$\bar{d}_2(g,1)$	$\bar{d}_1(g,2)$	$\bar{d}_2(g,2)$
1	40.25	40.25	52.88	54.37	40.9	40.9	53.53	55.02	0	200	0	200
2	52.88	54.37	65.51	68.49	53.53	55.02	66.16	69.14	0	200	0	200
3	40.25	40.25	44.56	45.07	40.9	40.9	45.21	45.72	0	68.26	0	68.26
4	44.56	45.07	52.92	54.41	45.21	45.72	53.57	55.06	0	132.4	0	132.4
5	52.92	54.41	61.29	63.76	53.57	55.06	61.94	64.41	0	132.4	0	132.4
6	61.29	63.76	65.6	68.58	61.94	64.41	66.25	69.23	0	68.26	0	68.26
7	40.25	40.25	44.56	45.07	40.9	40.9	45.21	45.72	0	68.26	0	68.26
8	44.56	45.07	52.92	54.41	45.21	45.72	53.57	55.06	0	132.4	0	132.4
9	52.92	54.41	61.29	63.76	53.57	55.06	61.94	64.41	0	132.4	0	132.4
10	61.29	63.76	65.6	68.58	61.94	64.41	66.25	69.23	0	68.26	0	68.26
11	53.33	53.33	65.96	67.45	54.08	54.08	66.71	68.2	0	200	0	200
12	65.96	67.45	78.6	81.57	66.71	68.2	79.35	82.32	0	200	0	200
13	53.33	53.33	57.64	58.15	54.08	54.08	58.39	58.9	0	68.26	0	68.26
14	57.64	58.15	66.01	67.5	58.39	58.9	66.76	68.25	0	132.4	0	132.4
15	66.01	67.5	74.37	76.84	66.76	68.25	75.12	77.59	0	132.4	0	132.4
16	74.37	76.84	78.68	81.66	75.12	77.59	79.43	82.41	0	68.26	0	68.26
17	53.33	53.33	57.64	58.15	54.08	54.08	58.39	58.9	0	68.26	0	68.26
18	57.64	58.15	66.01	67.5	58.39	58.9	66.76	68.25	0	132.4	0	132.4
19	66.01	67.5	74.37	76.84	66.76	68.25	75.12	77.59	0	132.4	0	132.4
20	74.37	76.84	78.68	81.66	75.12	77.59	79.43	82.41	0	68.26	0	68.26
21	39.3	40.78	51.93	54.9	40.28	41.86	52.91	55.98	0	200	0	200
22	47.7	50.18	52.01	55	48.48	51.02	52.79	55.83	0	68.26	0	68.26
23	47.7	50.18	52.01	55	48.9	51.49	53.21	56.3	0	68.26	0	68.26
24	56.67	56.67	69.3	70.78	57.5	57.5	70.13	71.62	0	200	0	200
25	56.67	56.67	60.98	61.49	57.5	57.5	61.81	62.32	0	68.26	0	68.26
26	60.98	61.49	69.34	70.83	61.81	62.32	70.17	71.66	0	132.4	0	132.4
27	56.67	56.67	60.98	61.49	57.5	57.5	61.81	62.32	0	68.26	0	68.26
28	60.98	61.49	69.34	70.83	61.81	62.32	70.17	71.66	0	132.4	0	132.4